Chromatin alterations during transformation of B cells by a constitutively active mutant of STAT5

DISSERTATION ZUR ERLANGUNG DES
DOKTORGRADES DER NATURWISSENSCHAFTEN (DR. RER. NAT.)
DER FAKULTÄT FÜR BIOLOGIE UND VORKLINISCHE MEDIZIN
DER UNIVERSITÄT REGENSBURG

vorgelegt von
Samy Unser

aus
Karlsruhe

im Jahr
2018

Das Promotionsgesuch wurde eingereicht am:

Die Arbeit wurde angeleitet von:

PD Dr. Anne Rascle

Unterschrift:

Acknowledgements (Danksagung)

Zuvorderst möchte ich meiner Betreuerin PD Dr. Anne Rascle meinen tiefsten Dank aussprechen. Ich danke ihr für die intensive und persönliche Betreuung – sowohl während der Labor- als auch während der Schreibphase. Ihre wertvollen Anregungen und die kritische Durchsicht meines Manuskripts haben wesentlich zur vorliegenden Arbeit beigetragen. Ich bin ihr dankbar für jede weitere Hilfe und die Ermöglichung dieser Promotion und einer Reihe von Publikationen.

Ich danke Prof. Dr. Joachim Griesenbeck für seine Beratung in wissenschaftlichen Fragen und motivierenden Worte – ebenso wie meinen RIGeL-Mentoren Prof. Dr. Uta-Maria Bauer und Prof. Dr. Michael Rehli.

Ich danke der gesamten 'STAT5 Signaling Research Group' für die Zusammenarbeit. Ich danke Sophia sehr dafür, dass sie mir im Labor immer mit Rat und Tat geholfen hat. Ebenso bin ich Lissy und Susanne für ihre exzellente technische Unterstützung dankbar. Darüber hinaus danke ich dem gesamten 'Institut für Immunologie' und Prof. Dr. Daniela Männel für ihre Unterstützung und die Nutzung ihrer Laborräume.

Mein Dank gilt der 'Deutschen Krebshilfe' und der 'Deutschen Forschungsgemeinschaft, die die vorliegende Arbeit gefördert haben.

Besonders danken möchte ich außerdem meiner Mutter und Schwester für ihre ununterbrochene Unterstützung sowie meinen Freunden Marc und Sonja für ihr offenes Ohr und die zahllosen motivierenden Worte auf diesem Weg

Table of contents

Summary

The transcription factor signal transducer and activator of transcription 5 (STAT5) is activated conditionally and transiently by external stimuli. Thereupon, STAT5 modulates the transcription of its target genes, promoting cell survival and growth. Constitutive STAT5 activity has been shown to be oncogenic in hematopoietic cells. This correlates with the acquisition of cancer hallmarks, such as 'cytokine-independent survival', 'uncontrolled growth' and 'genomic instability'. Chromatin dynamics is of pivotal importance for the regulation of transcriptional activity and DNA damage repair. Accordingly, cancer hallmarks are not only effected by oncogenic 'driver' alterations at the DNA level, but also at the chromatin level. Sustained DNA binding of constitutively active STAT5 might have distinct effects on chromatin, which might lead to 'driver' chromatin alterations and underlie its oncogenicity.

The main goal of the present study was to identify 'driver' chromatin alterations and other 'driver' events during the oncogenesis process induced by constitutively active STAT5. The constitutively active STAT5 mutant STAT5A-1*6 was previously shown to induce oncogenesis in the IL-3-dependent pro-B cell line Ba/F3 by enabling cytokine-independent survival and growth. Specific aims of this study were to characterize the effects of STAT5A-1*6 expression on (i) cell survival and growth, (ii) expression of selected STAT5 target genes and (iii) chromatin rearrangements.

To monitor the oncogenesis process, a stable Ba/F3 cell line – inducibly expressing STAT5A-1*6 upon doxycycline administration (Tet-on expression system) – was generated and validated. Short- and long-term STAT5A-1*6 induction experiments were conducted and STAT5A-1*6 protein levels and activation (Western blot), and cell phenotype in terms of survival, growth and genome stability (cell counting, flow cytometric analysis of cellular DNA content / cell cycle states) were analyzed. Expression of STAT5 target genes including *Cis*, *Osm*, *Spi2.1*, *c-Myc*, *Pim-1*, *Id-1* and *TNFRSF13b* was investigated in parallel using RT-qPCR. As expected, STAT5A-1*6 expression enabled cytokine-independent survival and growth of Ba/F3 cells. Cell viability and proliferation rates increased gradually during the initial phase of induction. Interestingly, after 4–5 weeks of induction cell survival and growth no longer depended on STAT5A-1*6 expression. In addition, in one out of four experiments, STAT5A-1*6-expressing cells accumulated chromosomal aberrations. The correlation patterns of STAT5A-1*6 and STAT5 target gene expression suggested dose-dependent STAT5A-1*6-mediated transcriptional activation of STAT5 target genes, at least within the first few weeks of induction. Later on however, sustained expression of the STAT5 target genes *c-Myc* and *Pim-1* became independent of STAT5A-1*6. Altogether, these observations suggest the acquisition of the 'cytokine-independent survival', 'uncontrolled

growth' and 'genomic instability' cancer hallmarks, possibly due to continually accumulating 'driver' alterations upon sustained expression of STAT5A-1*6.

Interestingly, using chromatin immunoprecipitation STAT5 DNA binding to *Cis*, *Osm*, *Spi2.1*, *Id-1* and *TNFRSF13b* was correlated with a strong decrease in histone H3 occupancy, likely reflecting a loss in nucleosomes. This histone H3 loss was particularly prominent at the STAT5 binding sites, regardless of (i) their location within the gene locus, of (ii) transcriptional activation and of (iii) cytokine supplementation. In addition, sustained STAT5A-1*6 DNA binding patterns were associated with broadened histone H3 loss in regions distant from STAT5 binding sites. Taken together, these data strongly suggest that DNA binding of STAT5 causes a local nucleosome loss, and possibly a global nucleosome loss along its target genes. Accordingly, I propose a general STAT5-mediated chromatin decondensation mechanism leading to a nucleosome loss around STAT5 binding sites, at a step preceding transcriptional activation. The broadened STAT5A-1*6-associated histone H3 loss patterns also raise the possibility of distinct STAT5A-1*6-mediated 'driver' chromatin alterations, which might misregulate chromatin dynamics and, in turn, promote the acquisition of 'driver' DNA alterations (i.e. the 'genomic instability' cancer hallmark). Together, these DNA and chromatin alteration events might underlie the oncogenicity of constitutively active STAT5. Further characterization of these events might contribute to a better understanding of the mechanism of STAT5-mediated oncogenesis and possibly to the identification of novel molecular targets for the development of drugs against STAT5-associated cancers.

Zusammenfassung

Der Transkriptionsfaktor *signal transducer and activator of transcription 5* (STAT5) wird von externen Stimuli zeitlich begrenzt aktiviert. Daraufhin moduliert STAT5 die Transkription seiner Zielgene und vermittelt so eine Zellüberlebens- und Zellwachstumsantwort. Konstitutive STAT5-Aktivität ist onkogen und an der Leukämie- und Lymphomentstehung aus blutbildenden Zellen beteiligt. Diese erwerben dabei Krebsmerkmale wie 'zytokin-unabhängiges Überleben', 'unkontrolliertes Wachstum' und 'Genominstabilität'. Die Chromatindynamik ist von zentraler Wichtigkeit für die Regulierung der Transkriptionsaktivität und die Reparatur von DNA-Schäden. Dementsprechend verursachen nicht nur krebsbedingende sogenannte 'Treiber'-Veränderungen auf DNA-Ebene Krebsmerkmale, sondern auch solche auf Chromatin-Ebene. Daher könnte die dauerhafte DNA-Bindungsaktivität von konstitutiv aktivem STAT5 spezifische Effekte auf das Chromatin haben, die zu 'Treiber'-Chromatinveränderungen führen und so dessen Onkogenität zugrunde liegen.

Das Hauptziel der vorliegenden Arbeit war die Identifizierung von 'Treiber'-Chromatinveränderungen und anderer 'Treiber'-Ereignisse während der von konstitutiv aktivem STAT5 induzierten Onkogenese. Es wurde bereits gezeigt, dass die konstitutiv aktive STAT5-Mutante STAT5A-1*6 in der IL-3-abhängigen pro-B-Zelllinie Ba/F3 Onkogenese induziert, indem sie den Zellen zytokin-unabhängiges Überleben und Wachstum ermöglicht. Die vorliegende Arbeit sollte daher im Einzelnen die Effekte der STAT5A-1*6-Expression auf (i) das Zellüberleben und -wachstum, (ii) die Expression ausgewählter STAT5-Zielgene und (iii) Chromatinumstrukturierungen charakterisieren.

Um die Onkogenese im Zeitverlauf zu beobachten, wurde eine stabile Ba/F3-Zelllinie entwickelt und validiert, die über Doxycyclin-Gabe induzierbar STAT5A-1*6 exprimiert (Tet-on-Expressionssystem). Nach Induktion der STAT5A-1*6-Expression wurden in Zeitkursexperimenten STAT5A-1*6-Proteinlevel und -Aktivierung (*Western blot*) sowie der Überlebens- und Wachstumsphänotyp und die Genomstabilität (Zellzählung, durchflusszytometrische Bestimmung des Zell-DNA-Gehalts und der Zellzyklusphase) und die Gesamt-DNA-Menge (Zellzyklusanalyse) analysiert. Zusätzlich wurde mittels RT-qPCR die Expression von STAT5-Zeilgenen, u.a. *Cis*, *Osm*, *Spi2.1*, *c-Myc*, *Pim-1*, *Id-1* und *TNFRSF13b*, untersucht. Wie erwartet ermöglichte die STAT5A-1*6-Expression Ba/F3-Zellen zytokin-unabhängiges Überleben und Wachstum. Zu Beginn der Zeitkursexperimente nahmen Zellviabiliäts- und Zellproliferationsraten fortlaufend zu. Interessanterweise hingen aber Zellüberleben und -wachstum nach 4–5 Wochen nicht mehr von der STAT5A-1*6-Expression ab. Zudem akkumulierten die Zellen in einem von vier Experimenten Chromosomenaberrationen. Die Expressionsstärke von STAT5A-1*6 korrelierte darüber hinaus mit der von STAT5-Zielgenen – zumindest in den ersten

Wochen. Das wies auf eine dosis-abhängige Transkriptionsaktivierung der STAT5-Zielgene durch STAT5A-1*6 hin. Die STAT5-Zielgene *c-Myc* und *Pim-1* wurden hingegen zu späteren Zeitpunkten zunehmend STAT5A-1*6-unabhängig exprimiert. Zusammengenommen legen diese Beobachtungen den Erwerb der Krebsmerkmale 'zytokin-unabhängiges Überleben', 'unkontrolliertes Wachstum' und 'Genominstabilität' nahe – womöglich aufgrund stetig akkumulierender 'Treiber'-Veränderungen bei langanhaltender STAT5A-1*6-Expression.

Chromatin-Immunpräzipitationsexperimente zeigten, dass die STAT5-DNA-Bindung an den *Cis*, *Osm*, *Spi2.1*, *Id-1* und *TNFRSF13b*-Loci mit einer starken Abnahme im Histon-H3-Gehalt korrelierte. Dies spiegelt wahrscheinlich einen Nukleosomenverlust wider. Besonders ausgeprägt war der Histon-H3-Verlust an STAT5-Bindestellen, ungeachtet (i) deren Lage innerhalb des Genlokus, (ii) von Transkriptionsaktivierung und (iii) von Zytokin-Gabe. Zudem korrelierte die anhaltende STAT5A-1*6-DNA-Bindung mit einer Ausdehnung des Histon-H3-Verlusts. Diese Daten lassen den Schluss zu, dass die Bindung von STAT5 an DNA einen Nukelosomenverlust an dessen Bindestelle und möglicherweise auch überall entlang seiner Zielgene verursacht. Daraus könnte sich ein allgemeiner STAT5-vermittelter Chromatindekondensierungs-Mechanismus ableiten, bei dem es zu Nukleosomenverlust in der Umgebung von STAT5-Bindestellen kommt (an einem Schritt vor STAT5-vermittelter Transkriptionsaktivierung). Aus den Ausdehnungsmustern des STAT5A-1*6-assoziierten Histon-H3-Verlusts lässt sich schlussfolgern, dass STAT5A-1*6 spezifische 'Treiber'-Chromatinveränderungen verursachen könnte. Diese könnten die Chromatindynamik beeinflussen und so wiederum den Erwerb von 'Treiber'-DNA-Veränderungen (d.h. des Krebsmerkmals 'Genominstabilität') begünstigen. Gemeinsam könnten solche DNA- und Chromatin-veränderungsereignisse der Onkogenität von konstitutiv aktivem STAT5 zugrunde liegen. Die weitere Charakterisierung dieser Ereignisse könnte dazu beitragen, den Mechanismus hinter STAT5-vermittelter Onkogenese besser zu verstehen. Das könnte neue molekulare Ansatzpunkte für die Entwicklung von Medikamenten gegen STAT5-assoziierte Krebsformen eröffnen.

1 Introduction

1.1 Cancer

1.1.1 Cancer hallmarks

The term cancer is used for a heterogenous disease with numerous subtypes affecting mammals and other organisms, which originates from normal body cells. For instance, hematologic cancers, i.e. leukemias and lymphomas, derive from hematopoietic cells. In two landmark papers, Hanahan and Weinberg (2000, 2011) argued that all manifestations of mammalian cancer can be unified by ten hallmarks, as uncontrolled growth and other traits underlie their malignant phenotype compared with normal cells (Figure 1). Pathological and molecular evidence suggests that individual (pre-)cancer cells are in competition with each other and that individual cells expand after gaining a selective growth advantage by acquiring cancer hallmark traits (Hanahan and Weinberg, 2000, Merlo *et al.*, 2006), suggesting a clonal evolution process termed oncogenesis, where they pass through benign stages before undergoing [malignant] transformation (Hanahan and Weinberg, 2000).

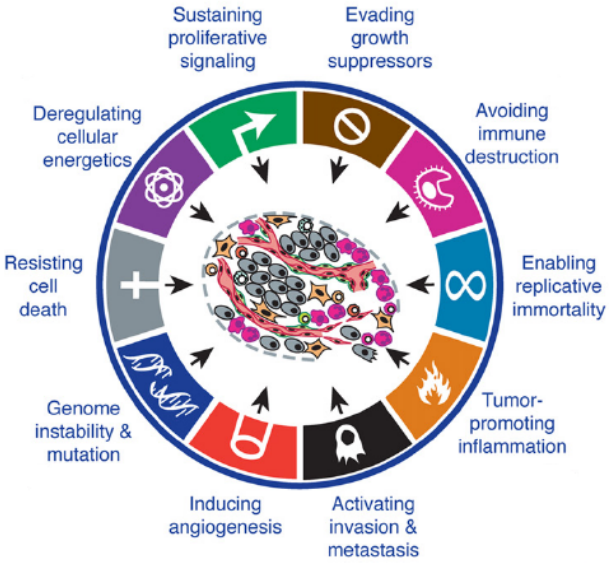

Figure 1: Visualization of ten hallmark traits exhibited by malignant cancers

(adapted from Hanahan and Weinberg, 2011)

This figure visualizes the ten hallmark traits defined by Hanahan and Weinberg (2000, 2011) for malignant cancers, as specified in the figure.

Transformed cells cause the disease cancer, which has a total mortality rate of over 50 % in humans (*Homo sapiens* | Jemal *et al.*, 2011). Their uncontrolled growth has been argued to be caused by four cancer hallmarks acquired during oncogenesis, namely 'resisting cell death', 'evading growth suppressors', 'sustaining proliferative signaling' and 'establishing replicative immortality' (Figure 1 | Hanahan and Weinberg, 2000). After all, normal cells undergo apoptosis after exceeding a certain number of cell divisions or enter a quiescent state termed cell senescence (Hanahan and Weinberg, 2011). Transformed cancer cells often exhibit 'activating invasion and metastasis' hallmark, which enables the spread of cancer to other tissues (Figure 1 | Hanahan and Weinberg,

2000). This is regarded as the leading cause of cancer deaths (Disibio and French, 2008, Hanahan and Weinberg, 2000).

1.1.2 'Driver' DNA and chromatin alterations drive oncogenesis by conferring a selective growth advantage

On the molecular level, the distinct phenotype of cancer cells involves misregulation of all pivotal cellular processes (Hanahan and Weinberg, 2000). In fact, cancer cells have been shown to exhibit numerous chromosomal aberrations and DNA sequence mutations (hereafter collectively referred to as DNA alterations) as well as alterations in DNA methylation and in chromatin composition (Campbell and Turner, 2013, Fraga *et al.*, 2005, Gama-Sosa *et al.*, 1983, Stratton *et al.*, 2009, Weisenberger, 2014). While DNA methylation and chromatin also differ among normal cells with regard to cell differentiation, normal cells all share the same euploid chromosome set and DNA sequence. Strikingly, DNA methylation and chromatin alterations have been found to be tremendously more divergent in cancer cells, when compared with alterations found among normal cells (Gama-Sosa *et al.*, 1983, Shen and Laird, 2013).

In a meta-analysis, Vogelstein *et al.* (2013) statistically evaluated sequencing analyses of multiple human cancers and supported the classification of cancer-associated DNA alterations into 'passenger' and 'driver' DNA alterations. DNA alterations in (pre-)cancer cells are defined as 'drivers', when they confer a selective growth advantage during oncogenesis and cancer progression and, thus, might initiate oncogenesis (Vogelstein *et al.*, 2013). The remaining alterations detected in cancers are defined as 'passengers' and do not (or potentially negatively) impact cell growth (Vogelstein *et al.*, 2013). Functionally, genes targeted by 'driver' alterations (i.e. 'driver' genes) can be subclassified into tumor suppressor and oncogenes, impeding and promoting oncogenesis and cancer progression respectively (Vogelstein *et al.*, 2013). Tumor suppressor genes have been found to be overridden by loss of function mutations, deletions and/or chromatin-dependent silencing (Vogelstein *et al.*, 2013). Oncogenes, on the other hand, have been found to be invigorated by gain-of-function mutations, gene amplifications and/or chromatin-dependent upregulation (Vogelstein *et al.*, 2013).

In their meta-analysis, Vogelstein *et al.* (2013) identified 'driver' genes by the particular types of exhibited DNA alterations. 'Driver' genes are involved in eight key signaling pathways regulating cell survival, growth and differentiation as well as in apoptosis, cell cycle progression and in the maintenance of genomic integrity (Figure 2). Strikingly, the misregulation of these particular cellular processes agrees with the cancer hallmarks proposed by Hanahan and Weinberg (2000, 2011 | Figure 1).

Figure 2: Key cell survival, growth and differentiation pathways and genome maintenance mechanisms are altered during oncogenesis

(adapted from Vogelstein *et al.*, 2013)

This figure illustrates the signaling pathways and cellular components, which are altered during oncogenesis. They were identified by disproportionally frequent somatic DNA mutations in constituent genes, termed 'driver' genes, found in malignant cancers (Vogelstein *et al.*, 2013).

Abbreviations: APC = activated protein C, HH = hedgehog, NOTCH = Notch receptor, MAPK = mitogene-activated protein kinase, PI3K = phosphatidylinositol-4,5-bisphosphate 3-kinase, RAS = rat sarcoma, STAT = signal transducer and activator of transcription, TGF-β = transforming growth factor β.

1.1.3 'Genomic instability' is an enabling hallmark of cancer

'Passenger' DNA alterations are much more frequent than 'driver' DNA alterations, although clonal evolution only favors 'driver' DNA alterations during oncogenesis and cancer progression (Vogelstein *et al.*, 2013). Hanahan and Weinberg, 2011 argued that (prospective) cancer cells with increased mutability (i.e. probability of acquiring 'driver' DNA alterations) possess a selective growth advantage and defined this trait as the enabling 'Genomic instability' cancer hallmark (Figure 1). In line with this, genome maintenance mechanisms are a frequent target of 'driver' DNA alterations (Vogelstein *et al.*, 2013). Thus, 'passenger' DNA alterations might accumulate stochastically during oncogenesis and cancer progression in (pre-)cancer cells and might explain the high degree of genomic heterogeneity among individual (pre-) cancer cells (Vogelstein *et al.*, 2013).

Of note, most 'passenger' DNA alterations are chromosomal aberrations rather than DNA sequence mutations (Vogelstein *et al.*, 2013). Proliferating cells normally progress through four tightly regulated phases (G_1, S, G_2, M) between two cell divisions, forming the cell cycle and passing through three check-points controlling for DNA damage amongst other things (Malumbres and Barbacid, 2009). This prevents the loss of genomic integrity in normal cells. By contrast, uncontrolled growth of (pre-)cancer cells has been reported to involve unscheduled cell cycle progression due to check-point evasion (Hanahan and Weinberg, 2000, Malumbres and Barbacid, 2001). This might cause polyploidization and contribute to structural chromosomal rearrangements (Malumbres and Barbacid, 2009, Vogelstein *et al.*, 2013). Additionally, the frequent misregulation of oxidative phosphorylation in (pre)-cancer cells by 'driver' alterations increases the formation of reactive oxygen species (i.e. oxidative stress), inducing DNA damage as mutagenic agents (Panieri and Santoro, 2016, Pawlowska and Blasiak, 2015). This is accelerated by frequent loss-of-function 'driver' DNA alterations in genome

maintenance mechanisms (i.e. antioxidants intercepting reactive oxygen species and the DNA damage repair machinery | Vogelstein *et al.*, 2013).

1.1.4 'Driver' DNA methylation and chromatin alterations may complement 'driver' DNA alterations

In addition to DNA alterations, alterations in DNA methylation and in chromatin structure participate in oncogenesis by impacting genome maintenance and transcriptional regulation (Vogelstein *et al.*, 2013). This is why Vogelstein *et al.* (2013) proposed that DNA methylation and chromatin alterations exhibited by human cancers may complement DNA alterations and follow their classification into 'drivers' and 'passengers'. The role of chromatin and chromatin-associated *trans*-acting factors in general and in oncogenesis is described in the next chapter. For simplicity, DNA methylation is not mentioned separately hereafter, but included under the term chromatin alterations. In addition, cancer-associated DNA and chromatin alterations are hereafter collectively referred to as 'driver' and/or 'passenger' alterations. Of note, the terms 'driver' and 'passenger' alterations will be used throughout the present study as defined by Vogelstein et al. (2013).

1.2 Chromatin dynamics modulates gene expression

In eukaryotic cells, genetic information is stored in linear DNA molecules called chromosomes. The DNA strands are packaged by histone proteins, forming chromatin together with other associated proteins. The fundamental unit of chromatin is termed nucleosome and is built up by a histone octamer (containing each two histones H2A, H2B, H3 and H4) and 147 bp DNA wrapped around it (Kornberg and Thomas, 1974, Luger *et al.*, 1997). The linker DNA in between nucleosomes is further packaged by the nucleosome-independent linker histone H1 (Thoma *et al.*, 1979). Chromatin can be broadly classified into condensed heterochromatin and decondensed euchromatin (Figure 3). In heterochromatin, the encased DNA strand is generally inaccessible. This precludes the DNA from interacting with most *trans*-acting proteins, which effect pivotal DNA-dependent processes, namely transcription, DNA damage repair, DNA replication and DNA recombination (Han and Grunstein, 1988, Knezetic and Luse, 1986, Li *et al.*, 2007). Therefore, chromatin structure is dynamically remodeled in a spatio-temporal manner to increase accessibility of the DNA strand for *trans*-acting proteins that enable these processes (Li *et al.*, 2007). In doing so, chromatin at a given DNA site has been found to be modulated via (i) the positioning and density of nucleosomes, (ii) the incorporation of non-canonical histone variants and (iii) posttranslational modification of histones (Li *et al.*, 2007). These processes provide a variety of possible chromatin states. Hence, the unique composition of these three chromatin components at a given DNA site is termed chromatin landscape.

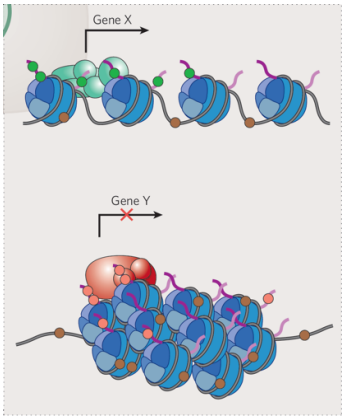

Figure 3: Schematic representation of eu- and heterochromatin
(adapted from Feinberg, 2007)
This figure exemplifies chromatin structure at a transcriptionally active and silent gene, enabling or precluding access of DNA-dependent proteins. The DNA doublestrand is shown in brown and histones in blue. Brown circles denote DNA methylation, which is sparse in active and abundant in silenced genes. Posttranslational histone modifications associated with active genes (active marks) are marked in green and those associated with repressed genes (repressive marks) in red. Two protein complexes involved in the maintenance of the respective eu- or heterochromatic state are shown in green and red.

1.2.1 Transactivation and transrepression

Protein-coding genes are DNA loci, where genetic information is transcribed into mRNA, which, in turn, serves as a template for the pivotal cellular protein production. They consist of the transcribed DNA sequence, the so-called open reading frame (ORF) bordered by a transcription start and termination site (TSS and TTS, respectively), and nearby regulatory sequences located upstream of the TSS, the so-called promoter.

1.2.1.1 Nucleosome positioning at protein-coding genes

Genome-wide analyses of nucleosome positioning revealed that nucleosomes generally display a continuum ranging from mostly fixed to rather unpredictable positioning (Iyer, 2012, Jiang and Pugh, 2009, Yuan *et al.*, 2005). This is why Iyer (2012) as well as Jiang and Pugh (2009) proposed that some nucleosomes are anchored to certain DNA sites based on sequence-affinity or other factors and that other nucleosomes in the vicinity are, in turn, stacked against them in an array by ATP-dependent chromatin remodeling complexes. Intriguingly, most euchromatic protein-coding genes exhibit similar nucleosome positioning and are devoid of nucleosomes at two regions at the 5' and 3' ends of the ORF (Figure 4| Iyer, 2012, Jiang and Pugh, 2009, Yuan *et al.*, 2005). The so-called 5'-nucleosome-free region (5'-NFR) across the promoter is flanked by two nucleosomes (−1 and +1 relative to the TSS) with highly fixed positions (Figure 4). Downstream of the TSS, the first few nucleosomes in the ORF are stacked against the +1 nucleosome, although the following nucleosomes follow no predictable pattern (Figure 4). As heterochromatic protein-coding genes without 5'-NFR are transcriptionally silent, the 5'-NFR might be mandatory for transcription by allowing access of *trans*-acting factors to the promoter. Transcriptional activity, however, must be governed by additional factors, as transcriptionally inactive euchromatic genes also exhibit the 5'-NFR (Bai and Morozov, 2010, Svaren and Horz, 1997).

1.2.1.2 Transcription factors

Indeed, *trans*-acting transcription factor proteins have been argued to be the primary governors of transcriptional activity (The ENCODE Project Consortium, 2012).

Transcription factors access and bind DNA at sequence-specific binding motifs. There, they can effect transcriptional initiation, transactivation and/or transrepression by modulating the recruitment of the transcriptional machinery. Therefore, the conditional activation and/or production of transcription factors enable the precise transcriptional regulation, essential for all forms of life (Maston *et al.*, 2006). The human genome encodes at least 1,400 different transcription factors, illustrating their importance (Latchman, 1997, Vaquerizas *et al.*, 2009).

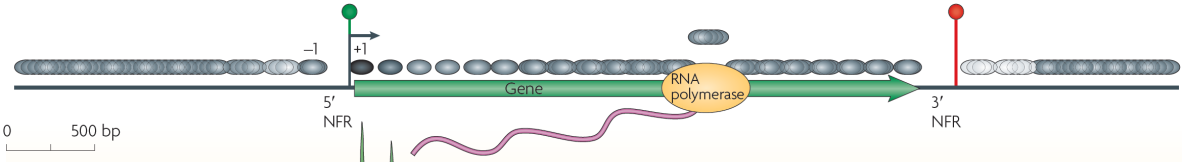

Figure 4: Consensus nucleosome positioning at euchromatic protein-coding genes in eukaryotes
(adapted from Jiang and Pugh, 2009)

This figure illustrates the consensus distribution of nucleosomes along euchromatic genes in budding yeast (*Saccharomyces cerevisiae*), which is mirrored in other eukaryotes. The DNA doublestrand is depicted schematically as a grey line, with the coding open reading frame (ORF) of the gene denoted as a green arrow. Green and red circles mark the transcription start and termination site, respectively. Grey ellipses depict nucleosomes, with the highly positioned + 1 nucleosome at the transcription start site marked in black. An elongating RNA Polymerase, synthesizing a complementary RNA strand (purple), is depicted schematically, showing the temporary eviction of nucleosomes along its way.

Abbreviations: NFR = nucleosome-free region.

Transcription factors have been found to bind their motifs in proximal and distal gene-regulatory elements (i.e. enhancers and silencer, promoting and impeding transcriptional activity, respectively), but also at DNA sites of unknown function (Li *et al.*, 2008, The ENCODE Project Consortium, 2012). Proximal gene-regulatory elements are located in (proximal or distal) promoter sites directly upstream of the TSS. Distal gene-regulatory elements are typically located ± 50 kbp of their target genes – although distal regulatory elements have also been reported farther away and on other chromosomes (Marsman and Horsfield, 2012, Maston *et al.*, 2006) – and are often clustered in so-called super-enhancers (Hnisz *et al.*, 2013). Within the three-dimensional higher order chromatin structure in the nuclei of living cells however, the DNA strand forms loops so that, *in vivo*, distal gene-regulatory elements are found spatially close to the promoter and TSS of their target gene, allowing physical interaction (Carter *et al.*, 2002, The ENCODE Project Consortium, 2012).

Most transcription factor binding motifs in heterochromatin remain unoccupied (Carr and Biggin, 1999, Zaret and Carroll, 2011). In addition, occupied promoter and enhancer binding motifs exhibit high chromatin accessibility, with promoter binding motifs often overlapping the 5'-NFR (Bai *et al.*, 2010, Thurman *et al.*, 2012). This suggests that most transcription factors cannot access nucleosomal DNA with the same efficiency as linker DNA (Figure 3), as supported by *in vitro* assays (Adams and Workman, 1995, Zaret and Carroll, 2011). This is why chromatin accessibility patterns have been proposed to inform DNA binding patterns of transcription factors (Marsman and Horsfield, 2012). In fact, so-

called ‘pioneer’ transcription factors have been shown to efficiently access occluded nucleosomal DNA in condensed chromatin *in vitro* and to initiate chromatin decondensation, providing access to other transcription factors *in vivo* (Cirillo *et al.*, 2002, Zaret and Carroll, 2011).

1.2.1.3 Transcription 'initiation’, ‘elongation’ and ‘termination’

Transcription factors are classified as transactivators, when they promote transcriptional activity, and as transrepressors, when they impede transcriptional activity (Latchman, 1997). Despite their diversity, molecular dynamics of transcription *per se* has been shown to be largely uniform in eukaryotic protein-coding genes with a ‘(pre-)initiation’, ‘elongation’ and ‘termination’ phase involving RNA Polymerase II-mediated pre-mRNA synthesis (Li *et al.*, 2007). In detail, transactivators have been found to recruit auxiliary factors termed co-activators upon binding, which trigger the assembly of a large transcription pre-initiation complex (PIC) in the 5’-NFR, upstream of the TSS in the promoter (Conaway *et al.*, 1990, He *et al.*, 2013, Li *et al.*, 2007). They do so by mediating conducive chromatin alterations and/or by recruiting conducive co-factors such as Mediator or PIC components (Kim *et al.*, 1994, Li *et al.*, 2007, Pokholok *et al.*, 2005). Transrepressors, on the other hand, have been found to recruit so-called co-repressors, which antagonize these processes (Kuzmichev *et al.*, 2002, Li *et al.*, 2007, Pokholok *et al.*, 2005). Strikingly, this dynamic, where the transcription ‘initiation’ phase is either promoted or impeded at gene promoters, has been argued to be the main regulatory step of gene expression (The ENCODE Project Consortium, 2012).

1.2.2 Chromatin alterations

Co-activators/co-repressors promote/impede transcription by establishing, amongst other things, chromatin landscapes conducive or adverse to transcriptional activity, respectively, altering the three chromatin components mentioned above. They do so via their own enzymatic activities or via recruitment of enzymatic co-factors:

1.2.2.1 ATP-dependent chromatin remodeling complexes

Chromatin remodeling enzymes such as brahma-related gene-1 (BRG1) have been found to alter nucleosome positioning by conversing the energy from ATP hydrolysis to move nucleosomes along the DNA strand, evict and/or insert them via a DNA translocase activity (Hargreaves and Crabtree, 2011, Saha *et al.*, 2005, Wang *et al.*, 2007b). In doing so, they can also promote the incorporation of non-canonical histone variants (Hargreaves and Crabtree, 2011, Mizuguchi *et al.*, 2004). As of now, four subfamilies of chromatin remodeling complexes are known (SWI/SNF: switching defective/sucrose non-fermenting; ISWI: imitation SWI; NuRD/Mi-2/CHD: nucleosome remodeling and deacetylation/Mi-2 antigen/chromodomain, helicase, DNA binding;

INO80: inositol-requiring 80), which have been implicated both in transcriptional activation and repression in a context-dependent manner (Ooi *et al.*, 2006, Peterson and Herskowitz, 1992, Wang *et al.*, 2007b, Xu *et al.*, 2007). This may be explained by the fact that the ultimate effects of nucleosome re-positioning depend on the exposed and/or occluded DNA sequences. Besides, chromatin-remodeling enzymes only function in multi-subunit so-called ATP-dependent chromatin remodeling complexes *in vivo*, where non-catalytic subunits may direct the chromatin-remodeling enzymes to certain sites (Dang *et al.*, 2007, Hargreaves and Crabtree, 2011).

1.2.2.2 Histone modifying enzymes

The third chromatin component, namely posttranslational histone modifications, has been found to be altered by histone modifying enzymes (Bannister and Kouzarides, 2011, Black *et al.*, 2012, Brownell *et al.*, 1996, Rea *et al.*, 2000). As of now, a striking plethora of posttranslational histone modifications has been identified, mainly in the easily accessible N-terminal tails of histone proteins protruding from their globular core (Bannister and Kouzarides, 2011, Phillips, 1963). Among these, histone lysine acetylation and methylation are the best characterized, as specified below. The histone modifications discussed and analyzed in the present study are summarized in Table 1. Hereafter they are abbreviated as specified in the legend of Table 1. Based on their catalyzed reaction, histone modifying enzymes can be classified into ‘writers’ or ‘erasers’, adding or removing a given histone modification, respectively (Wang *et al.*, 2007a). The known effects of histone modifications, in turn, can be roughly split into (i) *cis* and (ii) *trans* effects (Wang *et al.*, 2007a).

Cis effects of histone modifications involve the addition/removal of bulky or charged groups to/from histones. This alters the sterical and/or electrostatic composition of the affected nucleosome and influences the local chromatin structure without involving any secondary factors. For instance, histone acetyltransferases (HATs) add acetyl groups to several histone lysine residues (Bannister and Kouzarides, 2011, Brownell *et al.*, 1996). This neutralizes the positive charge of the lysine residues and has been shown to obstruct the interaction between the negatively charged DNA strand and the overall positively charged histone octamer *in vitro* (Hong *et al.*, 1993, Li *et al.*, 2007). This, in turn, increases the accessibility of nucleosomal DNA *in vivo* and has been linked to PIC formation (Li *et al.*, 2007, Verdone *et al.*, 2002). In accordance, genome-wide analyses revealed that histone acetylation is enriched at transcriptionally active enhancers and promoters (Table 1 | Pokholok *et al.*, 2005, The ENCODE Project Consortium, 2012). Of note, histone deacetylases (HDACs) have been found to antagonize HATs (Bannister and Kouzarides, 2011, Taunton *et al.*, 1996). Counterintuitively however, both HATs and HDACs can function as co-activators and co-repressors in a context-dependent manner

(e.g. Lin *et al.*, 2014, Nusinzon and Horvath, 2003, Wang *et al.*, 2009, Zupkovitz *et al.*, 2006). Besides, they have numerous non-histone substrates and, thus, play roles beyond the regulation of histone acetylation (e.g. Choudhary *et al.*, 2009, Iwabata *et al.*, 2005, Shankaranarayanan *et al.*, 2001, Spange *et al.*, 2009).

Table 1: Histone modifications are enriched in relation to transcriptional activity

Based on current literature, this table specifies the estimated relative enrichment of histone modifications discussed and/or analyzed in the present study in mammals at enhancer loci and along gene loci at proximal promoters, transcription start sites (TSS) and open reading frames (ORF) in relation to transcriptional activity. In doing so, hetero-, euchromatin states could be distinguished and correlated with silent and active transcription. Individual histone modifications are abbreviated by the histone name, amino acid residue and the respective modification (ac = acetylation; me1, me2, me3 = mono-, di-, trimethylation). For instance, H3K4me3 designates histone 3 lysine 4 trimethylation. Individual histone lysine acetylation marks are merged under H_K_ac. Based on their relation to transcriptional activity, histone modifications are classified into active and repressive marks. '+++', '++' and '+' specify strong, medium and weak enrichment, respectively. Blank cells specify no detectable enrichment of the respective histone modification.

*Heterochromatin is subdivided into facultative heterochromatin marked by H3K27me3 and constitutive heterochromatin marked by H3K9me3.

References: Ernst and Kellis, 2010, The ENCODE Project Consortium, 2012

Abbreviations: AM = active marks, ORF = open reading frame, RM = repressive marks, TSS = transcription start site.

		silent transcription				active transcription			
		heterochromatin*				euchromatin			
	histone modification	enhancer	promoter	TSS	ORF	enhancer	promoter	TSS	ORF
active marks	H_K_ac					++	+++	+++	++
	H3K4me1					+++	+	+	++
	H3K4me2					+	+	+	+
	H3K3me3						++	+++	+
	H3K9me1								+
	H3K27me1								+
repressive marks	H3K9me3	+++*	+++*	+++*	+++*				
	H3K27me3	+++*	+++*	+++*	+++*				

On the other hand, individual histone modifications are recognized by specific 'reader' proteins that trigger their *trans* effects (Wang *et al.*, 2007a). For instance, bromodomain and extra-terminal domain (BET) family proteins such as BET protein Brd2 (Brd2) have been found to 'read' histone acetylation and to promote transactivation (e.g. Crowley *et al.*, 2002, Dey *et al.*, 2003, LeRoy *et al.*, 2008, Taniguchi, 2016). In addition, mono-, di- and trimethylation of substrate-specific histone lysine residues have been shown to exert such *trans* effects (Bannister and Kouzarides, 2011) and are added/removed by specific histone lysine methyltransferases and demethylases, e.g. the H3K4me1/2 and H3K9me1/2 demethylase lysine-specific demethylase 1 (LSD1 | Black *et al.*, 2012, Shi *et al.*, 2004). Specific roles have been argued for these and other histone modifications in relation to transcription (Bannister and Kouzarides, 2011). In line with this, genome-wide analyses showed that specific histone modifications are correlated positively or negatively with transcriptional activity at protein-coding genes and their enhancer

elements, as specified in (Table 1). In particular, histone modifications primarily associated with transcriptionally active euchromatin have been termed ‘active marks’ (H3K4me1, H3K4me2, H3K4me3 amongst others), whereas the ones primarily associated with transcriptionally silent heterochromatin have been termed ‘repressive marks’ (H3K9me3, H3K27me3 amongst others | Pokholok *et al.*, 2005, The ENCODE Project Consortium, 2012). Taken together, the peculiar distribution of histone modifications gave rise to the ‚histone code hypothesis‘, which proposes that transcriptional activity is at least in part determined by the individual composition of histone modifications at a given gene site (Jenuwein and Allis, 2001, Strahl and Allis, 2000).

1.2.3 Chromatin alterations participate in oncogenesis and cancer progression

As described above (1.1.4), Vogelstein *et al.* (2013) proposed that chromatin alterations complement DNA alterations and can be classified into ‘drivers’ and ‘passengers’, according to chromatin alteration patterns observed both at ‘driver’ genes and globally (Campbell and Turner, 2013, Rideout *et al.*, 1994, Sundarrajan *et al.*, 2002,Fraga *et al.*, 2005 Vogelstein *et al.*, 2013). This presupposes that chromatin alterations are maintained in daughter cells upon replication allowing clonal evolution, as proposed for H3K9me3 and H3K27me3 (Huang *et al.*, 2013). In fact, some chromatin modifiers, e.g. enhancer of zeste homolog 2 (Ezh2), as well as their accessory factors have been identified as targets of ‘driver’ DNA alterations and are hence misregulated in cancer (Figure 2 | Morin *et al.*, 2010, Vogelstein *et al.*, 2013, Wang *et al.*, 2007a, Wang *et al.*, 2007b). This suggests a causal relationship with ‘passenger’ chromatin alterations, reflecting ‘genomic instability’ due to misregulated DNA damage control.

Of note, the misregulation of chromatin modifiers has been found to promote the ‘genomic instability’ cancer hallmark, given the regulation of DNA damage repair and DNA replication by chromatin dynamics (Misteli and Soutoglou, 2009, Mostoslavsky *et al.*, 2006). On the one hand, euchromatin has been found to be more susceptible than heterochromatin to mutagenic agents given the exposed linker DNA (Falk *et al.*, 2008 Cowell *et al.*, 2007, Han *et al.*, 2016, Kim *et al.*, 2007, Lan *et al.*, 2014). On the other hand, euchromatin has been shown to accumulate fewer DNA alterations than heterochromatin, as it is more accessible to the DNA damage repair machinery (Lemaitre and Soutoglou, 2014, Murga *et al.*, 2007, Nair *et al.*, 2017, Schuster-Bockler and Lehner, 2012). Given the loss-of-function ‘driver’ alterations in DNA damage repair components and antioxidants in (pre-)cancer cells (Vogelstein *et al.*, 2013), this proposes that euchromatin is more likely to acquire DNA alterations in response to reactive oxygen species than heterochromatin. In fact, decreasing core histone levels (leading to lower

nucleosome density and more linker DNA) has been correlated with DNA damage during aging (O'Sullivan *et al.*, 2010, Oberdoerffer, 2010), with additional evidence suggesting that DNA damage is a consequence of nucleosome loss (Celona *et al.*, 2011). In addition, decreased core histone levels in yeast (*Saccharomyces cerevisiae*) have been linked with nucleosome loss and chromosomal instability (Hu *et al.*, 2014).

As argued above, transcription factor activities are interrelated with chromatin dynamics. Moreover, transcription factors and signaling pathways regulating transcription factors are significantly overrepresented among 'driver' genes (Figure 2 | Furney *et al.*, 2006, Vogelstein *et al.*, 2013). This suggests that the oncogenicity of misregulated transcription factor activities might involve the mediation of 'driver' chromatin alterations.

1.3 Signal transducer and activator of transcription 5 A/B (STAT5A/B)

The STAT (signal transducer and activator of transcription) pathway is one of the signaling pathways targeted by 'driver' DNA alterations (Figure 2 | Vogelstein *et al.*, 2013). Seven STAT members have been identified in mammals (STAT1, STAT2, STAT3, STAT4, STAT5A, STAT5B and STAT6) and form an important family of intracellular signaling molecules (Fu *et al.*, 1992, Shuai *et al.*, 1992, Stark and Darnell, 2012). They have been found to rapidly transduce extracellular signals from the cell surface into the nucleus, where they function as transcription factors, conditionally impacting gene expression patterns (Paukku and Silvennoinen, 2004). In doing so, they mediate biological responses to various cytokines and hormones, rendering them essential for, amongst others, development, hematopoiesis and immune reactions (Paukku and Silvennoinen, 2004).

1.3.1 Biological roles of the STAT5A and STAT5B paralogs

The present study focused on the paralogous STAT members STAT5A and STAT5B (Azam *et al.*, 1995, Liu *et al.*, 1995, Mui *et al.*, 1995, Wakao *et al.*, 1994). The ancestral *Stat5* gene first separated from *Stat3* and then duplicated into the *Stat5a* and *Stat5b* paralogs, accounting for the adjacent location of these three genes on human chromosome 17 and mouse (*Mus musculus*) chromosome 11 (Copeland *et al.*, 1995, Wang and Levy, 2012). The STAT5A and B paralogs are strongly conserved among mammals, suggesting that findings from mice may be transferable to humans (Liu *et al.*, 1995, Wang and Levy, 2012). The m(urine)/h(uman)STAT5A and B paralogs consist of around 790 amino acids and still exhibit an interspecies as well as a paralog sequence homology of over 90 %. Most divergence between STAT5A and STAT5B is attributed to their C-terminal transactivation domains (Figure 5 | Grimley *et al.*, 1999, Liu *et al.*, 1995).

Interestingly, STAT5A and B single knock-out mice have been reported to survive to adulthood with only mildly impaired phenotypes, whereas *Stat5a/b* double knock-out have severely impaired phenotypes and are not viable due to defective hematopoiesis (Kerenyi *et al.*, 2008, Liu *et al.*, 1997, Teglund *et al.*, 1998, Udy *et al.*, 1997). This indicates functional redundancy between STAT5A and B as well as an essential role in hematopoiesis. Indeed, cell type-specific conditional *Stat5a/b* double knock-out mouse models have confirmed the essential role of STAT5A/B in differentiation, survival and proliferation of hematopoietic cells, for instance during B cell development in interleukin(IL)-7 signaling (Dai *et al.*, 2007, Hoelbl *et al.*, 2006, Malin *et al.*, 2010, Wang and Bunting, 2013, Yao *et al.*, 2006). Nevertheless, *Stat5b* single knock-out mice exhibit male-specific growth retardation amongst other things and female *Stat5a* single knock-out mice fail to lactate after birth, revealing unique biological roles of STAT5A and B (Liu *et al.*, 1997, Teglund *et al.*, 1998, Udy *et al.*, 1997). Overall, STAT5A and B possess both redundant and non-redundant biological roles.

1.3.2 STAT5A/B activation and inactivation dynamics

STAT5A and B have been found to share six characteristic functionally and structurally conserved domains with other STAT family members: a N-terminal oligomerization domain, a coiled-coil domain, a DNA-binding domain, a linker region, a Src Homology 2 (SH2) domain and a C-terminal transactivation domain (TAD | Grimley *et al.*, 1999, Kiu and Nicholson, 2012, Neculai *et al.*, 2005, Wakao *et al.*, 1994). In addition, a conserved tyrosine residue as well as at least one conserved serine residue have been reported to be phosphorylated in STAT family members, as further detailed below for STAT5A/B (Beuvink *et al.*, 2000, Gouilleux *et al.*, 1994, Grimley *et al.*, 1999, Kiu and Nicholson, 2012, Yamashita *et al.*, 1998). This is illustrated in Figure 5 for mSTAT5A and B.

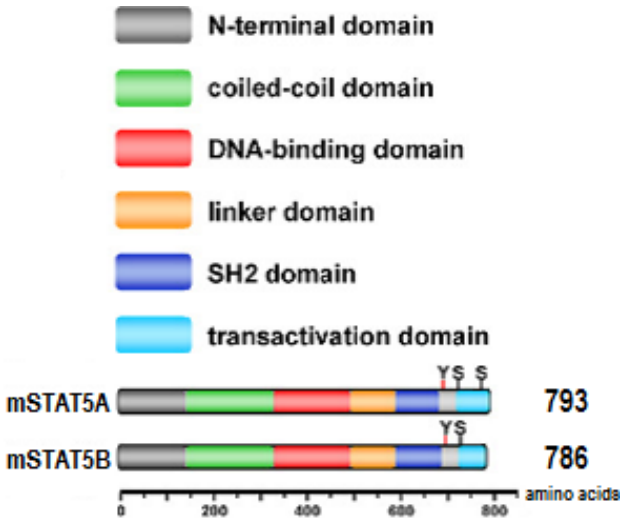

Figure 5: STAT5A and B protein domains

(adapted from Mohr *et al.*, 2012)

This figure schematically illustrates the structural organization of the mammalian STAT5A/B transcription factor proteins into six domains by the example of mSTAT5A/B, as specified in the figure. Domain boundaries are shown to scale within the amino acid sequence from the N- to the C-terminus. The depicted tyrosine and serine residues (Y^{694}, S^{725}, S^{779} in mSTAT5A and Y^{699}, S^{730} in mSTAT5B) have been found to be phosphorylated in multiple contexts with roles in STAT5A/B function, as further detailed in the text.

Abbreviations: m = murine (*Mus musculus*), SH2 = Src Homology 2.

1.3.2.1 Extracellular signals such as interleukin 3 condition STAT5A/B activation

In mammals, extracellular signals are transduced mainly by cytokines and hormones. A myriad of cognate receptors induce specific intracellular responses upon selective binding of their respective ligand cytokine or hormone, activating the STAT5A/B and/or other signaling pathways (reviewed by O'Sullivan *et al.*, 2007, Paukku and Silvennoinen, 2004 for STATs). STAT5A/B activation and inactivation dynamics in response to the cytokine IL-3 is exemplified below, because the murine IL-3-dependent pro-B cell line Ba/F3 served as an experimental system of STAT5 activation in the present study:

The IL-3 cognate transmembrane receptor IL-3 receptor (IL-3R) consists of an IL-3Rα subunit together with either a $\beta_{IL\text{-}3}$ or a common β (β_c) subunit in mice (Broughton *et al.*, 2012, Gorman *et al.*, 1990, Hara and Miyajima, 1992, Itoh *et al.*, 1990). IL-3 binding has been proposed to induce the formation of a duodecameric IL-3-IL-3Rα-β_c/$\beta_{IL\text{-}3}$ complex (Figure 6 | Dey *et al.*, 2009, Hansen *et al.*, 2008, Hara and Miyajima, 1992, Hercus *et al.*, 2012). This has been argued to change substrate specificity of the β_c/$\beta_{IL\text{-}3}$-associated Janus protein tyrosine kinase (JAK) family member JAK2 via *trans*-autophosphorylation, leading to phosphorylation of tyrosine residues in the β_c/$\beta_{IL\text{-}3}$ cytoplasmic domain (Figure 6 | e.g. Feng *et al.*, 1997, Hall *et al.*, 2010, Isfort *et al.*, 1988, Martinez-Moczygemba and Huston, 2003, Sorensen *et al.*, 1989). These residues have been shown to serve as docking sites for STAT5A/B via its SH2 domain (Figure 6 | Chin *et al.*, 1997, Martinez-Moczygemba and Huston, 2003, Sakurai *et al.*, 2000). Upon docking, JAK2 has been shown to phosphorylate the mSTAT5A/B $Tyr^{694/699}$ residue, marking the key event in conditional activation of STAT5A/B activity as a transcription factor (hereafter simply STAT5A/B phosphorylation | Figure 5 | de Groot *et al.*, 1998, Gouilleux *et al.*, 1994, Mui *et al.*, 1995, Watanabe *et al.*, 1996). Apart from the STAT5A/B pathway, IL-3 has been shown to activate the mitogen-activated protein kinase (MAPK) and phosphatidylinositol-4,5-bisphosphate 3-kinase (PI3K) pathways in Ba/F3 cells (Kinoshita *et al.*, 1997, Rosa Santos *et al.*, 2000), which are both likewise targeted by 'driver' alterations in cancer (Figure 2 | Vogelstein *et al.*, 2013) and upregulate STAT5A/B-independent genes such as *c-Fos* (Rascle and Lees, 2003, Watanabe *et al.*, 1997). Interestingly, phosphorylated(p)STAT5A/B has been found to cross-activate the MAPK and PI3K pathways in an IL-3R-independent manner via the adaptor protein Grb2(growth-factor-receptor-bound protein 2)-associated binder-2 (GAB2 | Nyga *et al.*, 2005)

After activation, pSTAT5A/B dimers function as transcription factors and, hence, alter gene expression patterns, mediating the cellular response to upstream cytokine or hormone ligands (Gouilleux *et al.*, 1994, Kang *et al.*, 2013, Wakao *et al.*, 1994). In doing so, STAT5A/B has been argued to mostly play a permissive role for cell survival and

proliferation, but also to have context-dependent instructive roles in cell differentiation (Kang *et al.*, 2013, Paukku and Silvennoinen, 2004).

1.3.2.2 STAT5A/B translocates to the nucleus upon phosphorylation

In the absence of activation, latent unphosphorylated STAT5A has been reported to form antiparallel dimers, putatively through interaction of their DNA-binding domains (Figure 6 | Neculai *et al.*, 2005). Unphosphorylated STAT5A/B has been found to localize in the cytoplasm in Ba/F3 cells (Figure 6 | Kawashima *et al.*, 2006) and in the cytoplasm and to a lesser extent in the nucleus in other cellular contexts (e.g. Herrington *et al.*, 1999, Iyer and Reich, 2008, Shin and Reich, 2013, Zeng *et al.*, 2002). Upon activation however, pSTAT5A/B has been shown to form parallel homo- and heterodimers through the mutual interaction of the phosphorylated tyrosine residues and SH2 domains (Figure 6 | Boehm *et al.*, 2014, Fahrenkamp *et al.*, 2016, Gianti and Zauhar, 2015, Langenfeld *et al.*, 2015), which rapidly accumulate in the nucleus (Figure 6 | Herrington *et al.*, 1999, Iyer and Reich, 2008, Nagy *et al.*, 2002, Shin and Reich, 2013). pSTAT5A/B DNA binding activity might cause their nuclear accumulation, given that DNA binding-deficient STAT5A/B mutants failed to accumulate in the nucleus upon activation (Herrington *et al.*, 1999, Iyer and Reich, 2008).

1.3.2.3 STAT5A/B activation is transient under normal conditions

STAT5A/B activation has been found to be tightly controlled under normal conditions, with regulation of STAT5A/B activation occurring at every step of activation. Protein tyrosine phosphatases (PTPs) and other phosphatases, protein inhibitors of activated STAT (PIASs) and suppressors of cytokine signaling (SOCSs) have been identified as effectors of STAT5A/B pathway inactivation (Chen *et al.*, 2004).

In IL-3-induced STAT5 signaling, amongst others SHP-1 (SH2 domain-containing phosphatase 1) of the PTP family, as well as CIS (cytokine-inducible SH2 domain-containing protein) and SOCS1 of the SOCS family, have been found to negatively impact cell survival and growth (e.g. Nosaka *et al.*, 1999, Xiao *et al.*, 2009, Yi *et al.*, 1993, Yoshimura *et al.*, 1995). SHP-1 dephosphorylates the key tyrosine residues in $\beta_c/\beta_{IL\text{-}3}$, (putatively) JAK2 and STAT5A/B (Figure 6 | e.g. Bone *et al.*, 1997, Wheadon *et al.*, 2002, Xiao *et al.*, 2009, Yi *et al.*, 1993). CIS binds to STAT5A/B docking sites on $\beta_c/\beta_{IL\text{-}3}$, thus competing for STAT5A/B binding and resulting in decreased pSTAT5A/B levels (Matsumoto *et al.*, 1997, Yoshimura *et al.*, 1995) (Figure 6). SOCS1 directly inhibits JAK2 kinase activity (Giordanetto and Kroemer, 2003, Yasukawa *et al.*, 1999) and putatively targets $\beta_{IL\text{-}3}/\beta_c$ and JAK2 for proteasomal degradation (Figure 6 | Bunda *et al.*, 2013, Ungureanu *et al.*, 2002). Accordingly, proteasomal degradation of STAT5A/B pathway components has been found to contribute to STAT5A/B pathway inactivation (Callus and Mathey-Prevot, 1998, Martinez-Moczygemba and Huston, 2001, Mui *et al.*, 1995).

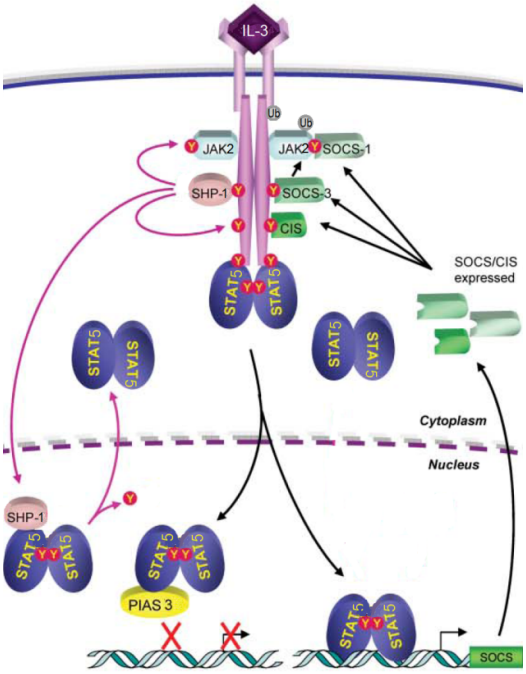

Figure 6: STAT5A/B activation is tightly controlled by negative regulators

(adapted from Lim and Cao, 2006)

This figure schematically illustrates the STAT5A/B pathway activation and inactivation dynamics by the example of the putative response to IL-3. Briefly, IL-3 assembles an IL-3-IL-3 receptor complex, which activates JAK2 kinase activity. JAK2 phosphorylates Y-residues in the IL-3 receptor (Y). This allows inactive antiparallel STAT5A/B dimers to dock in proximity to JAK2. Upon their Y-phosphorylation by JAK2, they form active parallel dimers, which gain DNA binding activity and function as transcription factors in the nucleus. SHP-1, CIS, SOCS1 and 3 plus putatively PIAS3 mediate IL-3-STAT5 pathway inactivation. SHP-1 dephosphorylates the IL-3 receptor, STAT5A/B and putatively JAK2. PIAS3 might interfere with STAT5A/B DNA binding activity. CIS, SOCS1 and 3 expression is induced by STAT5A/B in response to IL-3. CIS inhibits STAT5A/B docking to the IL-3 receptor. SOCS1 and 3 inhibit JAK2 kinase activity and may target JAK2 and the IL-3 receptor for ubiquitination (Ub) and proteasomal degradation. Overall, this constitutes a negative feedback mechanism, leading to a temporary desensitization to IL-3 following STAT5A/B activation.

Abbreviations: CIS = cytokine-inducible Src homology 2 domain-containing protein, IL-3 = interleukin 3, JAK2 = Janus kinase 2, m = murine, PIAS3 = protein inhibitor of activated STAT 3, R = receptor, SHP-1 = Src homology 2 domain-containing phosphatase 1, SOCS = suppressor of cytokine signaling, STAT5 = signal transducer and activator of transcription, Ub = ubiquitin, Y = phosphorylated tyrosine residue.

Of note, *Cis* and *Socs1* are STAT5 target genes transiently induced upon its IL-3-dependent activation (Basham *et al.*, 2008, Nosaka *et al.*, 1999, Yoshimura *et al.*, 1995) and CIS has been found to exhibit low protein stability in response to IL-3, as has been SOCS1 in other contexts (Rico-Bautista *et al.*, 2004, Siewert *et al.*, 1999, Yoshimura *et al.*, 1995), suggesting their prompt degradation after IL-3-dependent production. By contrast, SHP-1 is expressed in an IL-3-independent manner (Paling and Welham, 2002, Yang *et al.*, 1998). Though, the normal conformation of SHP-1 auto-inhibits its tyrosine phosphatase activity, which is activated upon engagement of phosphorylated tyrosine residues (Pao *et al.*, 2007, Pei *et al.*, 1994, Yang *et al.*, 2003), suggesting IL-3-dependent dephosphorylation of $\beta_c/\beta_{IL\text{-}3}$, JAK2 and STAT5A/B by SHP-1. Overall, these observations indicate a *bona fide* negative feedback mechanism in Ba/F3 cells, leading to a temporary desensitization to IL-3 following STAT5A/B activation.

1.3.2.4 Posttranslational modifications modulate STAT5A/B activity

In different cellular contexts, STAT5A/B has been found to be glycosylated at a threonine residue (Freund *et al.*, 2017, Gewinner *et al.*, 2004, Nanashima *et al.*, 2005), acetylated and SUMOylated at lysine residues (Beier *et al.*, 2012, Ma *et al.*, 2010, Van Nguyen *et al.*, 2012) as well as phosphorylated at serine residues (Figure 5 | Beuvink *et al.*, 2000, Clark *et al.*, 2005, Mitra *et al.*, 2012, Yamashita *et al.*, 1998) and at tyrosine residues other than the aforementioned conserved residue (Kabotyanski and Rosen, 2003, Kloth *et al.*, 2002, Olayioye *et al.*, 1999, Schaller-Schönitz *et al.*, 2014). These posttranslational

modifications have been reported to influence STAT5A/B activity by various mechanisms (reviewed by Rani and Murphy, 2016). For instance, STAT5A/B activation and dimerization has been found to be regulated by acetylation (Ma *et al.*, 2010, Van Nguyen *et al.*, 2012). This regulation appears to take place upstream of the signaling pathway, since PD Dr. Anne Rascle's research group has recently shown in Ba/F3 cells that lysine acetylation-mimicking amino acid substitutions in STAT5A did not impact its transcriptional activity (Pinz *et al.*, 2015). In addition, mSTAT5A Ser^{725} and Ser^{779} phosphorylation (hereafter simply STAT5A serine phosphorylation) has been detected in Ba/F3 cells (Cooper *et al.*, 2006, Friedbichler *et al.*, 2010, Haq *et al.*, 2002). Though, disruption of STAT5A serine phosphorylation did not alter the *in vivo* cell survival and proliferation response to cytokine/hormone-activated STAT5A in hematopoietic cells (Friedbichler *et al.*, 2010, Xue *et al.*, 2002), opposing an essential role in Ba/F3 cells.

1.3.3 Phosphorylated STAT5A/B functions as a transcription factor

Since its discovery in the mid-nineties, characteristics of STAT5A/B DNA binding activity and of STAT5A/B-regulated transcriptional activity have been described in numerous studies, taking advantage of technical advances. Specifically, STAT5A/B DNA binding activity has been studied using (i) *in vitro* electronic mobility shift assays (EMSAs) and its *in vivo* DNA binding patterns using (ii) DNA site-specific chromatin immuno-precipitation (ChIP) followed by quantitative PCR (qPCR) and using (iii) genome-wide biased (ChIP-on-chip) and unbiased (ChIP followed by high-throughput sequencing | ChIP-seq) assays. Similarly, STAT5A/B transcriptional activity has been studied using (i) ectopic luciferase reporter assays and by measuring *in vivo* transcript levels using (ii) transcript-specific reverse transcriptase qPCR (RT-qPCR) and using (iii) biased (microarray) and unbiased (RNA high-throughput sequencing | RNA-seq) transcriptome analyses. Similar advances have permitted correlating STAT5A/B-specific findings with DNA site-specific and later genome-wide analyses of histone modifications (using ChIP and ChIP-seq) as well as of chromatin accessibility and nucleosome positioning.

1.3.3.1 STAT5 DNA binding patterns

Upon phosphorylation STAT5A/B dimers gain DNA binding activity and both paralogs have been found to bind to consensus ($TTCN_{3-4}GAA$) and similar non-consensus GAS (interferon γ-activated sequence) motifs – with nearly identical sequence preferences – using *in vitro* EMSAs (Ehret *et al.*, 2001, Soldaini *et al.*, 2000) and by mathematically recovering motifs from DNA sites occupied by either STAT5A or B *in vivo* (hereafter simply STAT5 binding sites), as detected by ChIP-seq (e.g. Liao *et al.*, 2008, Lin *et al.*, 2012, Reid *et al.*, 2010, Yamaji *et al.*, 2012). Nevertheless, STAT5A and B exhibited partially differing, though mostly overlapping, genome-wide DNA binding patterns (Kanai *et al.*, 2014, Liao *et al.*, 2008, Lin *et al.*, 2012, Yamaji *et al.*, 2012), suggesting other

molecular differences. In addition, a minority of STAT5A/B binding sites exhibited only partial or no GAS motifs (e.g. Kanai *et al.*, 2014, Kang *et al.*, 2014, Willi *et al.*, 2016, Zhu *et al.*, 2012). On the one hand, partial adjacent GAS motifs are more easily accessed by STAT5A/B as tetramers, as shown *in vitro* by EMSAs (John *et al.*, 1999, Meyer *et al.*, 2004, Meyer *et al.*, 1997, Soldaini *et al.*, 2000). Accordingly, tetramer-deficient STAT5A/B forms have been found to occupy fewer DNA sites than wild-type STAT5A/B (Lin *et al.*, 2012). Interestingly, considerably more tetramer-specific STAT5B than STAT5A binding sites have been identified *in vivo* (Lin *et al.*, 2012), suggesting paralog-specific differences. On the other hand, STAT5A/B signals at sites lacking GAS motifs may be an artefact of the applied ChIP-seq method (compare Jain *et al.*, 2015) and/or suggest recruitment of STAT5A/B to chromatin by other factors, putatively in a paralog-specific manner.

Of note, STAT5A/B DNA binding patterns differ in a cell type-specific manner (Zeng *et al.*, 2016) with only ~10% of theoretically available GAS motifs occupied (Kang and Hennighausen, 2012). For instance, Nanou *et al.*, 2017 have recently reported ~15,500 STAT5A binding sites in Ba/F3 cells upon synchronized STAT5A/B activation by IL-3, among which ~4,500 overlapped consensus GAS motifs (of altogether ~580,000 theoretically available in the repeat-masked murine genome | Kang and Hennighausen, 2012). In doing so, STAT5A binding sites were mostly located in intergenic (~40 %) and intragenic (predominantly intronic | altogether ~45 %) regions, as opposed to promoters (~15 %), in the Ba/F3 pro-B cell line (Nanou *et al.*, 2017, Theodorou *et al.*, 2013), with similar distributions in other cell types (e.g. Gillinder *et al.*, 2017, Kang *et al.*, 2013, Wan *et al.*, 2013, Zeng *et al.*, 2016).

1.3.3.2 Patterns of STAT5A/B-regulated transcriptional activity

Upon disruption/decrease of STAT5A/B activity numerous gene transcripts are downregulated in a cell type-specific manner with a minority of upregulated transcripts (e.g. Barclay *et al.*, 2011, Legrand *et al.*, 2016, Rowland *et al.*, 2005, Vidal *et al.*, 2007). The reverse pattern is observed upon induction/increase of STAT5A/B activity (e.g. Gass *et al.*, 2003, Kawai *et al.*, 2007, Wierenga *et al.*, 2006, Willi *et al.*, 2016). This identifies STAT5A/B-regulated genes and, in turn, has been correlated with occupied STAT5 binding sites in proximity (up to 100 kB distance) (e.g. Connerney *et al.*, 2017, Kang *et al.*, 2014, Zhang *et al.*, 2012, Zhu *et al.*, 2012), indicating *bona fide* STAT5 target genes. Overall, this suggests that STAT5A/B predominantly functions as transactivator and rarely as transrepressor.

In accordance with this, genome-wide analyses have found that (occupied) STAT5 binding sites exhibit a chromatin landscape conducive to transcriptional activity, i.e. high chromatin accessibility (e.g. Lau-Corona *et al.*, 2017, Siersbaek *et al.*, 2011, Sugathan

and Waxman, 2013, Zeng *et al.*, 2016), enrichment of active marks such as H3K27ac, H3K4me1 and H3K4me3 (e.g. Robinson *et al.*, 2014, Schmidl *et al.*, 2014, Shin *et al.*, 2016, Willi *et al.*, 2016) and depletion of the repressive marks H3K9me3 and H3K27me3 (Mandal *et al.*, 2011, Sugathan and Waxman, 2013, Zhang *et al.*, 2012). Of note, Mandal *et al.* (2011)) have reported enrichment of the repressive mark H3K7me3 at ~10 % of STAT5 binding sites correlating with decreased transcript levels of genes nearby, agreeing with STAT5A/B also functioning as transrepressor. Numerous DNA-site specific analyses, e.g. by PD Anne Rascle's research group for the STAT5 target genes *Cis* and *Osm* in Ba/F3 cells (Pinz *et al.*, 2015, Pinz *et al.*, 2014b, Rascle *et al.*, 2003, Rascle and Lees, 2003), confirm these patterns.

Of note, up to 80 % of occupied STAT5 binding sites could not be linked to STAT5A/B-regulated genes and, in part, were even located in promoter and intragenic regions of genes not regulated by STAT5A/B (e.g. Gillinder *et al.*, 2017, Yamaji *et al.*, 2012, Zhang *et al.*, 2012, Zhu *et al.*, 2012). On the one hand, this suggests that many STAT5 binding sites are transcriptionally silent and might exert independent functions. On the other hand, this suggests that STAT5 binding sites might function as distal regulatory elements in accordance with H3K27ac and H3K4me1 enrichment (see above), marking transcriptionally active enhancers (Table 1). In further support of this, STAT5 binding sites have been identified in established enhancer elements, e.g. in the *c-Myc* super-enhancer in Ba/F3 cells (Nanou *et al.*, 2017, GEO accession number GSE79520; Pinz *et al.*, 2016), and, moreover, in distal enhancers located within or near other genes as identified by enhancer RNA (eRNA) transcription (Gillinder *et al.*, 2017). This offers an explanation for STAT5-bound, but not -regulated, genes. Besides, STAT5-binding enhancer elements have been found to physically interact with promoter regions using 3C chromosome conformation capture assays indicating chromatin looping (Li *et al.*, 2017, Mowel *et al.*, 2017, Wagatsuma *et al.*, 2015), e.g. a *Csn2* enhancer element and the *Csn2* promoter (Kabotyanski *et al.*, 2006, Kabotyanski *et al.*, 2009). Furthermore, disruption of STAT5-binding GAS motifs in several enhancer elements, e.g. of *Wap*, has been shown to impede transactivation (Metser *et al.*, 2016, Shin *et al.*, 2016, Wagatsuma *et al.*, 2015). Taken together, these findings indicate that STAT5A/B transactivates and -represses genes through both promoter and enhancer elements.

Mirroring DNA binding patterns, STAT5A and B paralog-specific knock-down/out experiments have shown that they exhibit partially differing, though mostly overlapping, patterns of transcriptional regulation (e.g. Clodfelter *et al.*, 2006, Clodfelter *et al.*, 2007, Villarino *et al.*, 2016, Yamaji *et al.*, 2012). For instance, ~4 % of the ~7,400 STAT5A target gene transcripts were differentially affected in Ba/F3 cells (Nanou *et al.*, 2017), with e.g. *Bcl-x* mRNA (Bcl-xL isoform) downregulated upon *Stat5b*, but not *Stat5a*, knock-down (Basham *et al.*, 2008, Schaller-Schönitz *et al.*, 2014), despite both STAT5A

and B binding to *Bcl-x* (Nanou *et al.*, 2017, GEO accession number GSE79520; Nelson *et al.*, 2004). This suggests that, given their divergent TADs, STAT5A and B paralog-specific transcriptional regulation depends on selective interaction with other factors.

1.3.3.3 Common and cell type-specific STAT5 target genes

Most STAT5 target genes are differentially regulated depending on the investigated cell type with only a small set of common STAT5A/B-regulated genes (Gillinder *et al.*, 2017, Yamaji *et al.*, 2012, Zeng *et al.*, 2016 and compare above). On the one hand, cell type-specific genes participate in cell differentiation (Zeng *et al.*, 2016), e.g. *Wap* in lactogenesis with up to 1,000-fold transactivation (Shin 2016). On the other hand, common genes participate in the negative feedback mechanisms regulating STAT5A/B transient activity, e.g. *Cis* and *Socs1*, or in cell survival and growth, e.g. *Pim-1* and *Bcl-x*, with lower transactivation levels (Gillinder *et al.*, 2017). Recently, Zeng *et al.* (2016) argued that cell type-specific STAT5 target genes are primarily regulated through enhancers and common genes regulated through promoters, suggesting different molecular transactivation mechanisms.

1.3.3.4 Three parameters inform STAT5 DNA binding and transcriptional regulation patterns

The cell type-specific differences in STAT5A/B DNA binding and transcriptional regulation patterns imply pre-determination by the cellular context.

1.3.3.4.1 The respective STAT5A and B paralog dose informs their DNA binding patterns

The STAT5A and B paralogs exhibit partially differing DNA binding (1.3.3.1) and transcriptional regulation (1.3.3.2) patterns in mammary epithelial cells and in T cells. There, however, STAT5A and B are expressed asymmetrically (Liu *et al.*, 1995, Villarino *et al.*, 2016, Yamaji *et al.*, 2012). Villarino *et al.* (2016) have recently shown that STAT5A only substituted for STAT5B during T cell differentiation, when adjusted for dose. In addition, increasing STAT5A protein levels have been correlated with broadened STAT5A DNA binding patterns, mostly in the number of occupied sites and to a lesser degree in STAT5A chromatin occupancy at a given DNA site (Willi *et al.*, 2016, Yamaji *et al.*, 2012, Zhu *et al.*, 2012). Though, *Stat5a* and *b* overexpression only marginally impacted STAT5 target gene transcript levels (Pham *et al.*, 2018, Zhu *et al.*, 2012), suggesting transcriptionally silent STAT5 binding sites. Taken together, this suggests that the respective pSTAT5A and B dose informs their overlapping and differing DNA binding patterns and to a lower degree differing transcriptional regulation patterns.

1.3.3.4.2 The pre-existent chromatin accessibility informs STAT5 DNA binding patterns

In addition to exhibiting high chromatin accessibility (1.3.3.2), STAT5 binding sites have been found to be co-occupied by cell type-specific pioneer factors (Schmidl *et al.*, 2014, Sugathan and Waxman, 2013). Accordingly, chromatin decondensation has been shown to precede *de novo* STAT5 DNA binding (Rawlings *et al.*, 2011), while cytokine/hormone-inducible heterochromatin formation has been shown to abrogate STAT5 binding to *Foxp3* (O'Malley *et al.*, 2009) and to *Csn2* (Buser *et al.*, 2011). In addition, Zhu *et al.* (2012) have shown that STAT5A does not occupy DNA sites specific to other cell types upon forced *Stat5a* overexpression despite broadened DNA binding patterns. Furthermore, prolactin-induced activation (i.e. deacetylation by HDAC6, Medler *et al.*, 2016) of the linker histone H1 competitor high-mobility group nucleosome-binding chromosomal protein 2 (HMGN2 | e.g. Catez *et al.*, 2002, Martinez de Paz and Ausio, 2016, Rochman *et al.*, 2011, Weisbrod *et al.*, 1980) has been shown to mediate displacement of histone H1 at the *Cis* and putatively other STAT5 binding sites in two human breast cancer cell lines (Schauwecker *et al.*, 2017). Strikingly, this mechanism is a prerequisite for (i) full STAT5 DNA binding to *Cis* and (ii) full transactivation of *Cis* and other STAT5 target genes in response to prolactin, but not for the concurrent core nucleosome loss (i.e. histone H3 and H4) at the *Cis* STAT5 binding site (Fiorillo *et al.*, 2011, Medler *et al.*, 2016, Schauwecker *et al.*, 2017). Therefore, the Clevenger's research group has argued that this is a global mechanism in mammary epithelial cells (in response to prolactin) and proposed that STAT5 DNA binding to *Cis* and putatively other sites is a consequence of prolactin-induced STAT5A/B-independent chromatin decondensation, i.e. both HMGN2-independent nucleosome loss and HMGN2-dependent linker histone H1 displacement (Schauwecker *et al.*, 2017). Overall, these findings suggest that STAT5A/B cannot access nucleosomal DNA and that the pre-existent accessibility of GAS motifs informs STAT5 DNA binding patterns.

1.3.3.4.3 The pre-existent chromatin landscape informs STAT5A/B transcriptional regulation patterns

Gene-specific reports have shown distinct temporal profiles for STAT5 target gene transcripts in response to STAT5A/B activation (e.g. Basham *et al.*, 2008, Chia and Rotwein, 2010, Gillinder *et al.*, 2017, Jegalian and Wu, 2002). In addition, cell type-specific STAT5 target genes can be upregulated much higher than common genes (1.3.3.3). Accordingly, cell type-specific STAT5 target genes have been reported to be poised for transactivation before STAT5 binding in contrast to common STAT5 target genes (e.g. Chia *et al.*, 2010a, Jolivet *et al.*, 2005, Wagatsuma *et al.*, 2015, Wu *et al.*, 2014). For instance, the promoter of the cell type-specific *Igf1* gene was enriched for histone acetylation and occupied by co-activators as well as stalled RNA Polymerase II

prior to STAT5B binding in contrast to common *Cis* and *Socs2*, despite comparable transactivation upon STAT5B binding (Chia and Rotwein, 2010, Chia *et al.*, 2010b). Besides, STAT5A/B has been found to bind and specifically transrepress the *Bcl6* gene in different cell types while consistently transactivating other target genes such as *Cis* (Lau-Corona *et al.*, 2017, Lin *et al.*, 2014, Tran *et al.*, 2010, Ujvari *et al.*, 2018, Walker *et al.*, 2007), whereas it has been argued to transactivate *Bcl6* in a B cell subtype (Scheeren *et al.*, 2005). Strikingly, in a human breast cancer cell line STAT5A (in part) transrepressed *Bcl6* luciferase reporters integrated into the genome upon stable transfection, but transactivated non-integrated ones upon transient transfection (Tran *et al.*, 2010). Overall, this suggests that STAT5A/B may intrinsically function as transactivator of common target genes and that cell type-specific STAT5A/B-mediated transactivation and repression dynamics are informed by the gene-specific chromatin landscape and gene-specific co-factors.

1.3.3.4.4 Synergistic and antagonistic interactions with other factors inform STAT5 DNA binding and transcriptional regulation patterns

A minority of STAT5 binding sites exhibits only partial or no GAS motifs (1.3.3.1). STAT5A/B has been found to access such low-affinity DNA sites by cooperating with other transcription factors (e.g. Bertolino *et al.*, 2005, Robinson *et al.*, 2014, Rusterholz *et al.*, 1999, Tan *et al.*, 2008). For instance, STAT5A/B physically interacts with the glucocorticoid receptor (GR | Baugh *et al.*, 2007, Engblom *et al.*, 2007) and cooperates with GR and CCAAT/enhancer-binding protein β (C/EBPβ) in accessing their *Csn2*-regulating and other binding sites (Jolivet *et al.*, 2005, Kabotyanski *et al.*, 2006, Siersbaek *et al.*, 2011, Wyszomierski and Rosen, 2001, Xu *et al.*, 2007). Of note, GR-STAT5A, but not GR-STAT5B, interaction has been reported in adipocytes (Baugh *et al.*, 2007), showing paralog specificity. By contrast, the *Bcl6* and other STAT5A/B-mediated transrepression mechanisms have been reported to involve the displacement of other transcription factors (e.g. Ono *et al.*, 2007, Rocha-Viegas *et al.*, 2006, Yang *et al.*, 2011), which (putatively) function as transactivators. Strikingly, STAT5A-mediated *Bcl6* transrepression did not require its TAD in a human breast cancer cell line (Tran *et al.*, 2010). This opposes intrinsic STAT5A/B transrepression activity and raises the possibility that competitive binding underlies STAT5A/B-mediated transrepression. Similarly, STAT5A/B has been found to antagonize the transrepressor B cell lymphoma 6 (BCL6) protein and other transcription factors (e.g. Buser *et al.*, 2011, Liao *et al.*, 2014, Lin *et al.*, 2014, Zhang *et al.*, 2012) by competing for their overlapping or adjacent binding sites, promoting transactivation. Taken together, this suggests that synergistic and antagonistic interactions with other transcription factors, including in a paralog-specific manner, inform STAT5 DNA binding and transcriptional regulation patterns.

1.3.3.5 STAT5A/B mediates chromatin alterations by recruiting co-activating and co-repressive chromatin modifiers

STAT5A/B functioning as transcription factor implies STAT5A/B-mediated transient chromatin alterations conducive (as transactivator) or adverse (as transrepressor) to transcriptional activity. Given its biological role in cell differentiation, STAT5A/B might even mediate sustained chromatin alterations, persistently changing transcriptional regulation patterns. Several lines of evidence indicate such STAT5A/B-mediated chromatin alterations:

Firstly, STAT5A/B has been found to physically interact with various chromatin modifiers (and other non-catalytic effectors of chromatin alterations | Table 2A1) and/or to co-occupy regulatory elements with them (Table 2A2). For instance, BRG1, a catalytic subunit of SWI/SNF family ATP-dependent chromatin-remodeling complexes, has been found to co-occupy the *Csn2* promoter and to physically interact with STAT5A/B (Xu *et al.*, 2007). Besides, HDAC3 and LSD1 have been found to physically interact with STAT5A in Ba/F3 cells and to co-occupy ~60 % and ~35 %, respectively, of the ~15,500 STAT5A binding sites (Nanou *et al.*, 2017). Overall, this suggests functional interaction of STAT5A/B and chromatin modifiers.

Secondly, STAT5 DNA binding has been correlated with the recruitment of chromatin modifiers (Table 2B1) and with the chromatin alterations effected by them (Table 2B2) in a dose- and time-dependent manner upon disruption/decrease and upon induction/ increase of STAT5A/B activity. In doing so, these positive and/or negative correlations concurred with STAT5A/B-mediated transactivation or -repression (Table 2B3), suggesting that the effectors contributed positively and/or negatively to STAT5A/B transcriptional activity (Table 2B3). For instance, GAS motif disruption in a *TCRG-Jγ1* STAT5 binding site abrogated the enrichment of H3K4me1/2/3 and histone H4 acetylation as well as the recruitment of BRG1 to *TCRG-Jγ1* (in addition to the abrogation of STAT5 DNA binding and of *TCRγ-Jγ1* transactivation | Wagatsuma *et al.*, 2015). This suggests that STAT5A/B normally mediates chromatin remodeling and the aforementioned histone modifications by recruiting SWI/SNF family complexes, one or more of the HATs interacting with STAT5A/B (Table 2) and unidentified H3K4 methyltransferases, thus creating a chromatin landscape at *TCRγ-Jγ1* conducive to transcriptional activity.

Thirdly, to investigate the functional impact of a given chromatin modifier on STAT5A/B-mediated transactivation and repression, STAT5A/B transcriptional activity has been correlated with disruption/decrease and/or induction/increase of modifier activity (Table 2C). Using luciferase reporter assays (Table 2C1) or by analyzing transcript levels (Table 2C2), chromatin modifiers have been shown to augment and/or to impede STAT5A/B-

mediated transactivation and repression in a dose-dependent manner, indicating both positive and negative roles. For instance, Xu *et al.*, 2007 have shown by RT-qPCR that a dominant-negative BRG1 mutant impeded STAT5A/B-mediated *Csn2* transactivation, suggesting that SWI/SNF complexes function as STAT5A/B co-activators. In addition, transcriptome analyses upon HDAC3 and LSD1 knock-down in Ba/F3 cells suggested that HDAC3 functions as a STAT5A co-activator or co-repressor in a gene-specific manner, whereas LSD1 predominantly functions as a STAT5A co-repressor (Nanou *et al.*, 2017). Of note, the HAT nuclear receptor co-activator 1 (NCoA1) augmented STAT5B-mediated transactivation to a higher degree than STAT5A-mediated transactivation (Litterst *et al.*, 2003), raising the possibility of paralog-specific differences.

Interestingly, HDAC6 inhibition has been shown to impede both STAT5 DNA binding to *Cis* (using the [mostly] HDAC6-specific inhibitor Bufexamac [Bantscheff *et al.*, 2011]) and transactivation of *Cis* (using amongst others the HDAC pan-inhibitor trichostatin A [TSA | Yoshida *et al.*, 1990] and *Hdac6* knock-down) and other STAT5 target genes (using Bufexamac) in response to prolactin in two human breast cancer cell lines (Medler *et al.*, 2016). HDAC6-dependent HMGN2 activation and, in turn, HMGN2-dependent STAT5 DNA binding to and STAT5A/B-mediated transactivation of *Cis* (Fiorillo *et al.*, 2011, Medler *et al.*, 2016, Schauwecker *et al.*, 2017 | compare 1.3.3.4.2) suggest inhibition of STAT5A/B-mediated transactivation through HMGN2 at a step preceding STAT5 DNA binding. By contrast, TSA and other HDAC inhibitors have been found by PD Dr. Anne Rascle's research group to impede STAT5A/B-mediated transactivation of multiple STAT5 target genes such as *Cis* and *Osm* in Ba/F3 cells at a step following STAT5 DNA binding, but before RNA Polymerase II recruitment (Pinz *et al.*, 2015, Pinz *et al.*, 2016, Rascle *et al.*, 2003, Rascle and Lees, 2003). Strikingly, knock-down of various HDACs including HDAC6 did not impact STAT5A/B-mediated transactivation of *Cis* in Ba/F3 cells (Pinz *et al.*, 2015). Taken together, this suggests (i) molecular differences in the *Cis* and putatively other STAT5A/B-mediated transactivation mechanisms in these two cellular contexts, opposing a role for HMGN2 in Ba/F3 cells, and (ii) a mechanism of action for HDAC inhibitors not dependent on a singular function of a specific HDAC in Ba/F3 cells. In fact, PD Dr. Anne Rascle's research group has recently shown that a pan-inhibitor of the BET family equally impedes STAT5A/B-mediated transactivation (of *Cis*, *Osm* and other genes) and that the BET family member Brd2 is recruited to *Cis* upon STAT5 DNA binding in Ba/F3 cells (Pinz *et al.*, 2015). Given that *Brd2* knock-down impeded STAT5A/B-mediated transactivation of *Cis*, but not of *Osm*, in another cellular context (Liu *et al.*, 2014), this suggests the participation of Brd2 in the *Cis* and possibly of another BET family member in the *Osm* transactivation mechanism. Strikingly, PD Dr. Anne Rascle's research group has shown that HDAC inhibitors induce a genome-wide and locus-specific histone hyperacetylation and a concurrent displacement of Brd2 from *Cis*

and, therefore, argued that HDAC inhibitors indirectly inhibit STAT5A/B-mediated transactivation in Ba/F3 cells by decreasing the availability of BET family proteins at STAT5 target genes (Pinz *et al.*, 2015).

Fourthly, the aforementioned augmentation and/or impediment of STAT5A/B transcriptional activity did not depend on cytokine/hormone-induced STAT5A/B activity, as it could be reproduced in the absence of cytokines/hormones using constitutively active (dominant positive) STAT5A/B forms. This excluded the possibility that cytokine/hormone-induced third factors mediated STAT5A/B-associated chromatin alterations. For instance, HDAC3 has been shown to impede transactivation and to augment transrepression by constitutively active STAT5B (Lin *et al.*, 2014).

Table 2 (next page): DNA-bound STAT5 recruits chromatin modifiers to mediate chromatin alterations

STAT5 functions as a transcription factor in response to external stimuli, suggesting STAT5-mediated chromatin alterations by chromatin modifier recruitment. **A:** STAT5 has been found to co-occupy chromatin with chromatin modifiers and/or physically interact with them. These chromatin modifiers are specified and grouped into their respective protein family. Co-occupancy and physical interaction with STAT5 is indicated by '✔'. **B:** STAT5 chromatin occupancy at its target genes has been shown to correlate in dose- and/or time-dependent manner positively (**+**) or negatively (**−**) with modifier recruitment, the chromatin alterations effected by them and up- or downregulated transcript levels, indicating STAT5-mediated transactivation (TA) or transrepression (TR). The (putative) positive (**+**), negative (**−**) or context-dependent positive and negative (**±**) role of a given modifier for STAT5-mediated transactivation (TA) or transrepression (TR) is specified in brackets. **C:** Functional assays using luciferase reporter assays or *in vivo* transcript levels have shown that a given modifier augments (**+**), impedes (**−**) or both augments and impedes (**±**) STAT5-mediated transactivation (TA) or transrepression (TR) by increasing/inducing or decreasing/disrupting of modifier activity. **D:** The (putative) function and role of a given chromatin modifier in transcriptional regulation by STAT5 is briefly summarized. In particular, the effected chromatin alteration and its (putative) role as co-activator (CA) or co-repressor (CR) is specified.

Ⅰ: CTCF and HP1α interact with unphosphorylated, transcriptionally inactive STAT5. Ⅱ: HDAC6-STAT5 chromatin co-occupancy is suggested by circumstantial evidence. Ⅲ: STAT5 co-occupying the same locus as Tet-1/2 has been shown in different studies (50,51).

References: 1: Xu *et al.*, 2007; 2: Wagatsuma *et al.*, 2015; 3: this study, 1.2.2.1; 4: Liu *et al.*, 2014; 5: Pinz *et al.*, 2015; 6: Pinz *et al.*, 2016; 7: Taniguchi, 2016; 8: Park *et al.*, 2016; 9: Merkenschlager and Nora, 2016; 10: Zhu *et al.*, 1999; 11: Gewinner *et al.*, 2004; 12: Masui *et al.*, 2008; 13: Ma *et al.*, 2010; 14: Pfitzner *et al.*, 1998; 15: Ye *et al.*, 2001; 16: Boer *et al.*, 2002; 17: Boer *et al.*, 2003; 18: Garrigan *et al.*, 2013; 19: this study, 1.2.2.2; 20: Peng *et al.*, 2002; 21: Paukku *et al.*, 2003; 22: Litterst *et al.*, 2003; 23: Ling and Lobie, 2004; 24: Kabotyanski *et al.*, 2006; 25: Chia and Rotwein, 2010; 26: Chia *et al.*, 2010a; 27: Chia *et al.*, 2010b; 28: Buser *et al.*, 2011; 29: Yang *et al.*, 2011; 30: Hedrich *et al.*, 2014; 31: Lin *et al.*, 2014; 32: Katerndahl *et al.*, 2017; 33: Sen *et al.*, 2018; 34: Kleinschmidt *et al.*, 2008; 35: Di Lorenzo and Bedford, 2011; 36: Kwon and Workman, 2011; 37: Hu *et al.*, 2013; 38: Fiorillo *et al.*, 2011; 39: Medler *et al.*, 2016; 40: Martinez de Paz and Ausio, 2016; 41: Schauwecker *et al.*, 2017; 42: Xu *et al.*, 2003; 43: Rocha-Viegas *et al.*, 2006; 44: Nanou *et al.*, 2017; 45: Nakajima *et al.*, 2001; 46: Black *et al.*, 2012; 47: Yoo *et al.*, 2015; 48: Mandal *et al.*, 2011; 49: Weng *et al.*, 2014; 50: Feng *et al.*, 2014; 51: Ogawa *et al.*, 2014; 52: Yang *et al.*, 2015; 53: Wu and Zhang, 2017; 54: Pham *et al.*, 2018.

Abbreviations: BET = bromodomain and extra-terminal domain, Brd2 = bromodomain and extra-terminal domain (BET) protein Brd2, BRG1 = brahma-related gene-1, CARM1 = co-activator-associated arginine methyltransferase 1, CTCF = CCCTC-binding factor, CBP = CREB(cAMP response element-binding protein)-binding protein, CPAP = centrosomal P4.1-associated protein, Ezh = enhancer of zeste homolog, HDAC = histone deacetylase, HP1α = heterochromatin protein 1 α, HMGN = high-mobility group nucleosome-binding chromosomal protein, LSD1 = lysine-specific demethylase 1, n/a = not available, NCoA1 = nuclear receptor co-activator 1, NCoR2 = nuclear receptor co-repressor 2, Nmi = n-Myc interactor, occ. = occupancy, p100 = 100 kDa co-activator, p300 = E1A binding protein p300, PIC = pre-initiation complex, PPI = protein-protein-interaction, PRC2 = polycomb repressive complex 2, PRMT1 = protein arginine methyltransferase 1, SMRT = silencing mediator for retinoic acid receptor and thyroid hormone receptor, SWI/SNF = switching defective/sucrose non-fermenting, TA = transactivation, TET = ten-eleven translocation 1 protein, TR = transrepression.

A) Functional/physical interaction				**B)** Correlation of STAT5 DNA binding with:			**C)** Modifier augments/ impedes STAT5-mediated TA/TR:		**D)** (Putative) function and role in transcriptional regulation by STAT5	References
Protein family	Protein	**A1)** co-occ.	**A2)** PPI	**B1)** modifier recruit-ment	**B2)** effected chromatin alteration	**B3)** TA/TR (putative effect)	**C1)** luciferase reporter assays	**C2)** *in vivo* transcript levels		
ATP-dependent chromatin remodelers	**BRG1**	✔	✔	**+**	n/a	**TA(+)**	n/a	**TA+**	catalytic subunit of SWI/SNF complex → chromatin decondensation, CA/CR	1-3
BET reader protein family	**Brd2**	✔	n/a	**+**		**TA(+)**	**TA+**	**TA+**	reader of histone acetylation → histone chaperone, promotes transcriptional activity by facilitating elongation, CA	4–7
CTCF/cohesin complex	**CTCF** [I]	✔	n/a	**+**	n/a	**TR(+)**	n/a	n/a	DNA-binding subunit of CTCF/cohesin complex → mediates long-range chromosomal interactions and informs functional nuclear architecture, CR(?)	8,9
HATs and their recruiters	**CBP**	✔	✔	**+**	**+**	**TA(+)**	**TA+**	**TA+**	HAT activity, recruits PIC components, CA and context-dependent CR	10–19
	CPAP	n/a	✔	n/a	n/a	n/a	**TA+**	n/a	enhances CBP and p300 recruitment, CA and context-dependent CR	19,20
	NCoA1	✔	✔	n/a	n/a	n/a	**TA+**	n/a	HAT activity, CA and context-dependent CR	19,22
	Nmi	n/a	✔	n/a	n/a	n/a	**TA+**	n/a	enhances CBP and p300 recruitment, CA and context-dependent CR	15,19
	p100	n/a	✔	n/a	n/a	n/a	**TA+**	n/a	recruits HATs and PIC components, CA and context-dependent CR	19,21
	p300	✔	✔	**+/−**	**+/−**	**TA(+)/TR(±)**	**TA±/TR+**	**TA+**	HAT activity, recruits PIC components, CA and context-dependent CR	14–19,22–33
histone arginine methyltransferases	**CARM1**	✔	✔	**+/−**	**+/−**	**TA(+)/TR(−)**	**TA+**	**TA+**	H3R17me2 methyltransferase activity (putative active mark), CA	33-35
	PRMT1	✔	✔	**+**	**+**	**TA(+)**	**TA+**	**TA+**	H4R3me2 methyltransferase activity (putative active mark), CA	35,36
Heterochromatin protein 1 family	**HP1α** [I]	✔	✔	**+**		**TR(+)**	n/a	n/a	reader of H3K9me3, promotes heterochromatin formation/maintenance, CR(?)	36,37
HMGN protein family	**HMGN2**	✔	n/a	**+**	**+**	**TA(+)**	**TA+**	**TA+**	competes with linker histone H1 → chromatin decondensation, CA	38–41
HDACs and their recruiters	**HDAC1**	✔	✔	**+**	**+**	**TA(+)**	**TA+**	**TA+**	HDAC activity, CR and context-dependent CA	19,24,42
	HDAC3	✔	✔	**+/−**	**+**	**TA(±)/TR(±)**	**TA−/TR+**	**TA±/TR±**	HDAC activity, CR and context-dependent CA	19,31,43,44
	HDAC6	✔ [II]	n/a	n/a	n/a	n/a	n/a	**TA+/TR+**	HDAC activity, CR and context-dependent CA	19,23,39
	NCoR2/ SMRT	✔	✔	**+**	**+**	**TR(+)**	**TA−**	**TA−**	recruits HDAC3, CR and context-dependent CA	11,19,29 43, 45
histone lysine methylases	**LSD1**	✔	✔	**+/−**	n/a	**TA(±)/TR(±)**	n/a	**TA±/TR±**	H3K4me1/2 and H3K9me1/2 demethylase activity, CR and context-dependent CA	44,46
histone lysine methyltransferases	**Ezh1**	✔	n/a	n/a	n/a	n/a	n/a	n/a	catalytic subunit of PRC2 complex, H3K27me3 methyltransferase activity → mediates heterochromatin formation, CR and context-dependent CA	46,47
	Ezh2	✔	✔	**+/−**	**+/−**	**TA(±)/TR(±)**	**TA+**	**TA±/TR±**		46–49, 54
TET protein family	**Tet1/2**	✔ [III]	✔	**+**	**+**	**TA(+)**	n/a	**TA+**	methylcytosine dioxygenase activity, participate in DNA demethylation, CA	52,53

Taken together, these four lines of evidence consolidate the idea that STAT5A/B can function as a transactivator/repressor by mediating chromatin alterations conducive/ adverse to transcriptional activity. Strikingly, STAT5 DNA binding has been found to be a prerequisite for the binding of other transcription factors (Ogawa *et al.*, 2014, Shi *et al.*, 2008, Shin *et al.*, 2016), raising the possibility that STAT5A/B-mediated chromatin alterations exposed their occluded binding motifs. For instance, disruption of the STAT5 binding sites in the *Wap* super-enhancer abrogated chromatin decondensation (at one of two sites) and the binding of three other transcription factors, which normally synergize with STAT5A/B in *Wap* transactivation (Shin *et al.*, 2016). This suggests that STAT5A/B can function as an anchor for other transcription factors similarly to pioneer factors in some contexts and raises the possibility that sustained STAT5A/B-mediated chromatin alterations underlie its biological role in cell differentiation and oncogenesis.

1.3.3.6 Novel role of unphosphorylated STAT5A/B in chromatin regulation

Unphosphorylated, transcriptionally inactive STAT5A/B has been recently implicated in the regulation of chromatin function and transcriptional repression via interaction with heterochromatin protein 1 α (HP1α) and with CCCTC-binding factor (CTCF | Hu *et al.*, 2013, Park *et al.*, 2016, reviewed by Wingelhofer *et al.*, 2018 | Table 2). Interestingly, unphosphorylated STAT5A has been reported to occupy chromatin in Ba/F3 cells at DNA sites lacking GAS motifs (Nanou *et al.*, 2017), raising the possibility that recruitment of unphosphorylated STAT5A/B participates in chromatin regulation in this cellular context.

1.3.3.7 Summary

In summary, the STAT5A and B paralogs gain DNA binding activity upon phosphorylation and function as transcription factors in both a common and a cell type- and gene-specific manner. In doing so, the mostly overlapping, though partially distinct, DNA binding and transcriptional regulation patterns of the STAT5A and B paralogs are informed by (i) their affinity to access binding motifs as tetramers, (ii) the respective paralog dose, (iii) the pre-existent chromatin landscape (including chromatin accessibility) and (iv) [paralog-specific] synergistic or antagonistic interactions with other transcription factors. STAT5A and B mediate their transcriptional activity by recruiting chromatin modifiers (putatively in a paralog-specific manner), creating a chromatin landscape (more) conducive or (more) adverse to transcriptional activity. Overall these four pre-determining parameters and, both transient and putatively sustained, STAT5A/B-mediated chromatin alterations may underlie the redundant and non-redundant, biological roles of the STAT5A and B paralogs, i.e. their common permissive role in cell survival and growth and their context-dependent instructive role in cell differentiation. The fact, that STAT5A/B function is informed by the pre-existent chromatin landscape and that STAT5A/B can mediate chromatin alterations, implies that STAT5 DNA binding and transcriptional activity can

be principally both a cause for and a consequence of chromatin alterations, stressing the importance of investigating correlative findings.

1.3.4 Misregulated constitutive STAT5A/B activity is oncogenic

1.3.4.1 Hematologic cancers are associated with constitutive STAT5A/B activity

Constitutive instead of transient STAT5A/B activation has been frequently observed in several human cancer subtypes (reviewed by Rani and Murphy, 2016), amongst others in hematologic cancers (i.e. leukemias and lymphomas) such as B cell acute lymphoblastic leukemia (B-ALL | e.g. Gouilleux-Gruart *et al.*, 1997, Heltemes-Harris *et al.*, 2011, Tasian *et al.*, 2012, Weber-Nordt *et al.*, 1996). This has been correlated with DNA alterations of STAT5A/B pathway components in patterns suggesting gain-of-function (constitutively active) variants predominantly of cytokine/hormone receptors and JAKs and rarely of STAT5B, but notably not STAT5A, and loss-of-function variants of negative regulators of STAT5A/B of the SOCS and PTP families (compare 1.3.2 | reviewed by Constantinescu *et al.*, 2008, Shahmarvand *et al.*, 2018). For instance, (putative) gain-of-function missense mutations have been observed in *Csf2rb* (= β_c, $h\beta_c^{R461C}$ | Watanabe-Smith *et al.*, 2016), in *Jak2* (e.g. $hJAK2^{V617F}$ | Levine *et al.*, 2005) and in *Stat5b* (several in the SH2 domain, most often $hSTAT5B^{N642H}$ | e.g. Bandapalli *et al.*, 2014, Kiel *et al.*, 2014, Küçük *et al.*, 2015, Rajala *et al.*, 2013), in addition to gene fusions such as BCR-ABL (de Klein *et al.*, 1982, Nowell P., 1960, Ravandi and Kebriaei, 2009). By contrast, (putative) loss-of-function DNA alterations have been observed in STAT5A/B negative regulators such as *Socs1* (Capello *et al.*, 2013, Melzner *et al.*, 2005) and *Shp-1* (Demosthenous *et al.*, 2015, Vollbrecht *et al.*, 2015) in addition to chromatin alterations (heterochromatic silencing indicated by hypermethylation | e.g.Capello *et al.*, 2013, Chim *et al.*, 2004a, Chim *et al.*, 2004b, Oka *et al.*, 2002, Zhang *et al.*, 2017). This correlative evidence strongly suggests that constitutive STAT5A/B activation is caused by 'driver' DNA alterations in the STAT5A/B pathway *in vivo*. The lack of *de novo Stat5a* mutations raises the possibility of paralog-specific differences in oncogenicity, as supported by other evidence (compare Casetti *et al.*, 2013, Schaller-Schönitz *et al.*, 2014, Zhang *et al.*, 2007).

1.3.4.2 Functional assays have established oncogenicity of constitutively active STAT5A/B

The IL-3-dependent pro-B Ba/F3 cell line, employed in the present study, and other hematopoietic cell lines have served as experimental systems to study the aforementioned gain-of-function variants. In doing so, their forced expression in Ba/F3 cells has been shown to constitutively activate STAT5A/B in an IL-3-independent manner and to enable IL-3-independent cell survival and growth (β_c^{R461C}: Watanabe-Smith *et al.*, 2016; $JAK2^{V617F}$: James *et al.*, 2005; $STAT5B^{N642H}$: Ariyoshi *et al.*, 2000, Bandapalli *et*

al., 2014; BCR-ABL: Ilaria and Van Etten, 1996). This suggested oncogenic uncontrolled growth and, accordingly, mouse models have confirmed the *in vivo* oncogenicity of most of these variants given the development of leukemia or lymphoma upon expression in hematopoietic cells (JAK2^{V617F}: Wernig *et al.*, 2006; STAT5B^{N642H}: Pham *et al.*, 2018; BCR-ABL: Groffen *et al.*, 1993). Of note, increased/decreased doses of constitutively active STAT5A/B have been shown to have both positive and negative effects on cell viability and proliferation at different stages of oncogenesis and cancer progression in models of hematologic cancers (Chen *et al.*, 2013, Hoelbl *et al.*, 2006, Tsuruyama *et al.*, 2002, Wang *et al.*, 2015, Warsch *et al.*, 2011). Accordingly, *in vivo* hematologic cancers have been found to exhibit both decreased and increased levels of STAT5A/B compared to normal cells (Adamaki *et al.*, 2015, Taskinen *et al.*, 2010 Brady *et al.*, 2012, Warsch *et al.*, 2011). This suggests that constitutively active STAT5A/B can have both oncogenic and tumor suppressive effects *in vivo* depending on its dose and the particular cellular context.

Of note, a constitutively active STAT5A form, STAT5A-1*6 (mSTAT5A$^{H298R/S710F}$), has been generated artificially and confers IL-3 independence to Ba/F3 cells (Onishi *et al.*, 1998). The behavior of STAT5A^{N642H} and STAT5A-1*6 agreed with that of its STAT5B paralogs (STAT5B^{N642H} and STAT5B-1*6) in Ba/F3 cells (Ariyoshi *et al.*, 2000, Nosaka *et al.*, 1999, Onishi *et al.*, 1998), with the oncogenicity of both STAT5A-1*6 and STAT5B-1*6 confirmed in mouse models (Funakoshi-Tago *et al.*, 2010, Katerndahl *et al.*, 2017, Nakayama *et al.*, 2009, Schwaller *et al.*, 2000) – albeit neither of the two 1*6 mutations has been found *in vivo* so far. Accordingly, paralog-specific single and double knock-down/out of *Stat5a/b* has been shown to impede/disrupt the effects of oncogenic upstream STAT5 pathway components in Ba/F3 cells (Funakoshi-Tago *et al.*, 2010), in part in a paralog-specific manner (Schaller-Schönitz *et al.*, 2014), and in mouse models (Funakoshi-Tago *et al.*, 2010, Hoelbl *et al.*, 2006, Hoelbl *et al.*, 2010, Walz *et al.*, 2012, Ye *et al.*, 2006). Besides, compounds such as the BCR-ABL-inhibitor imatinib, which inhibit constitutively active STAT5A/B by targeting upstream pathway components, have been clinically approved for treatment of e.g. B-ALL or are undergoing clinical trials (Buchdunger *et al.*, 1996, O'Shea *et al.*, 2015, Schwetz, 2001). Pre-clinical models such as the Ba/F3 cell line have allowed identification of more STAT5A/B-inhibiting compounds, e.g. sulforaphane, by PD Dr. Anne Rascle's research group (Jobst *et al.*, 2016, Pinz *et al.*, 2014a, Pinz *et al.*, 2015, Pinz *et al.*, 2014b). In addition, forced expression of *Socs1* (though not *Cis*) has been shown to induce apoptosis of IL-3-independent Ba/F3 cells expressing STAT5A-1*6 (Nosaka *et al.*, 1999) in accordance with its proposed tumor suppressive role. Strikingly, (T2/Onc Sleeping Beauty transposon) mutagenesis studies have recently shown that STAT5 pathway genes, e.g. *Jak2*, *Stat5a* and *b*, are among the most frequently mutated in Ba/F3 cells selected for

IL-3-independent growth (Guo *et al.*, 2016) as well as in pre-cancer (B-ALL) primary B cells (van der Weyden *et al.*, 2015). Taken together, these findings establish a causal link of constitutive STAT5A/B activity with oncogenesis and cancer progression.

1.3.4.3 Molecular properties of constitutively active STAT5A/B forms

The (putative) gain-of-function *Stat5b* mutations identified *in vivo* are all located within or near the SH2 domain responsible for dimerization (Figure 5), suggesting that a similar molecular mechanism underlies their constitutive activity. Accordingly, the mSTAT5A^{S710F} mutation in STAT5A-1*6, likewise located there, but not the mSTAT5A^{H298R} mutation located in the coiled-coil domain (Figure 5), has been shown to cause constitutive phosphorylation, DNA binding and transcriptional activity (Onishi *et al.*, 1998) and enhanced tetramer formation (Moriggl *et al.*, 2005). In addition, the hSTAT5B^{K694R} and ^{K701R} mutations located in proximity have each been found to decrease/disrupt STAT5B dimerization and transcriptional activity (in addition to acetylation | Ma *et al.*, 2010), while no such effect on transcriptional activity and phosphorylation was observed for the paralogous mutations of mSTAT5A-1*6 (^{K689R} and ^{K696R} | Pinz *et al.*, 2015). Taken together, mSTAT5A^{S710F} and other mutations in the SH2 domain might thus increase the stability of STAT5A/B (parallel) dimerization, tetramerization and/or phosphorylation by changing the conformation of the C-terminal STAT5A/B domains, which include the key mSTAT5A Tyr^{694} residue. In this case, constitutive STAT5A/B-1*6 phosphorylation in IL-3-independent STAT5A/B-1*6 Ba/F3 cell lines might rely on IL-3-independent basal JAK2 tyrosine kinase activity, as supported by the sensitivity of STAT5A-1*6-enabled Ba/F3 cell survival and growth to SOCS1 overexpression (Nosaka *et al.*, 1999), and/or IL-3-independent activity of other tyrosine kinases. On the other hand, the mSTAT5A^{H298R} mutation in STAT5A-1*6, has been shown to prevent interaction with the nuclear receptor co-repressor silencing mediator for retinoid or thyroid-hormone receptors (NCoR2/SMRT | Nakajima *et al.*, 2001, Table 2), suggesting an augmentation of STAT5A/B-1*6 transcriptional activity compared with wild-type STAT5A/B.

1.3.4.4 Mechanisms of STAT5A/B oncogenicity

The frequently oncogenic STAT5 target genes *c-Myc* (Gabay *et al.*, 2014, Hayward *et al.*, 1981), *Pim-1* (Cuypers *et al.*, 1984, Narlik-Grassow *et al.*, 2014) and *Bcl-x* (Ola *et al.*, 2011) have been shown to be upregulated in Ba/F3 cells expressing STAT5A-1*6 and to effect their IL-3-independent survival and growth (Nosaka *et al.*, 1999, Nosaka and Kitamura, 2002), with similar patterns observed in *in vivo* hematologic cancers (e.g. Brault *et al.*, 2012, Katerndahl *et al.*, 2017, Kontro *et al.*, 2014, Pham *et al.*, 2018). This suggests that STAT5A/B, constitutively functioning as a transactivator for oncogenes (i.e. transcriptional misregulation), may inform its oncogenicity. Accordingly, STAT5

glycosylation (Freund *et al.*, 2017), serine phosphorylation (Berger *et al.*, 2014, Friedbichler *et al.*, 2010, Mitra *et al.*, 2012), tetramer formation (Moriggl *et al.*, 2005) have been also found to contribute to or even to be a prerequisite for STAT5A/B oncogenicity, in line with their modulation of STAT5A/B transcriptional regulation patterns (compare 1.3.2.4). Similarly, cross-activation of the PI3K and MAPK pathways via GAB2 has been found to be a prerequisite for STAT5A/B oncogenicity (Harir *et al.*, 2008, Harir *et al.*, 2007, Nyga *et al.*, 2005, Sattler *et al.*, 1999) – with *Gab2* also a frequent target in the aforementioned Ba/F3 mutagenesis study (Guo *et al.*, 2016) – suggesting indirect transcriptional misregulation by constitutively active STAT5A/B through other pathways.

Furthermore, STAT5A/B has been shown to localize in mitochondria and interact with a component of the pyruvate dehydrogenase complex in Ba/F3 cells (Chueh *et al.*, 2010, Chueh *et al.*, 2011). Accordingly, STAT5A/B has been argued to have non-canonical roles in the redox balance in normal and transformed hematopoietic cells, both impeding (Casetti *et al.*, 2013, Cholez *et al.*, 2012) and augmenting oxidative stress (Bourgeais *et al.*, 2017, Moloney *et al.*, 2017, Sallmyr *et al.*, 2008, Warsch *et al.*, 2012), suggesting protective and destructive roles for DNA damage induced by oxidative stress. Of note, Ba/F3 cells expressing STAT5A-1*6 have been recently shown to exhibit increased oxidative stress and downregulation of genes adverse to oxidative stress (Bourgeais *et al.*, 2017), suggesting augmentation of oxidative stress by STAT5A-1*6. By contrast, endogenous STAT5A/B has been shown to transactivate *Rad51*, a DNA damage repair gene, in parental Ba/F3 cells (Heath and Cross, 2004, Slupianek *et al.*, 2002) and to interact with a factor (Kawashima *et al.*, 2006), which augments oxidative stress amongst other things (Acevedo and Gonzalez-Billault, 2018). This proposes a homeostatic role for endogenous STAT5A/B for oxidative stress in parental Ba/F3 cells. Overall, this raises the possibility that STAT5A-1*6 induces oncogenic DNA damage by augmenting oxidative stress.

1.3.4.5 Constitutively active STAT5A/B might mediate ‘driver’ chromatin alterations

The transcriptional misregulation found in cancers exhibiting constitutive STAT5A/B activity (1.3.4.4) proposes that ‘driver’ chromatin alterations up- or down-regulate genes functioning as oncogenes or tumor suppressor genes, respectively. In fact, oncogenic mutations inducing constitutive STAT5A/B activity have been found to concur with mutations of chromatin modifiers (e.g. Atak *et al.*, 2013, Hou *et al.*, 2014, Kiel *et al.*, 2015, Patel *et al.*, 2012) such as the co-repressor Ezh2 (Lopez *et al.*, 2016 Kiel *et al.*, 2014). Accordingly, Ezh2 is a target in the aforementioned Ba/F3 mutagenesis study (Guo *et al.*, 2016). Of note, STAT5A/B has been shown to bind and transcriptionally regulate genes encoding chromatin modifiers in Ba/F3 cells including *Ezh2*, *Dpf3* (a subunit of SWI/SNF ATP-dependent chromatin remodeling complexes) and *Tet2* (Basham *et al.*,

2008, GEO accession number GSE10389; Nanou *et al.*, 2017, GEO accession number GSE79520; Nishioka *et al.*, 2016; Theodorou *et al.*, 2013). Interestingly, *Dpf3*, *Ezh2* and *Tet2* have been found to be transcriptionally misregulated in human hematologic cancers, correlating with increased STAT5 binding to the *Dpf3* promoter (e.g. Hernández-Sánchez *et al.*, 2014, Nishioka *et al.*, 2016, Rabello Ddo *et al.*, 2015, Solary *et al.*, 2014, Theodorou *et al.*, 2013). In addition, forced over-expression of *Tet2* has been correlated with chromosomal aberrations in Ba/F3 cells (Mahfoudhi *et al.*, 2016), indicating the 'genomic instability' cancer hallmark. Overall, this suggests that (i) STAT5A/B-independent loss- and gain-of-function mutations in chromatin modifiers and (ii) STAT5A/B-dependent transcriptional misregulation of chromatin modifiers inform 'driver' chromatin alterations in STAT5A/B-associated cancers.

Though, they may be informed by a third mechanism: 'driver' chromatin alterations of STAT5 target genes might be mediated by DNA-bound constitutively active STAT5A/B itself. In fact, STAT5A/B physically and functionally interacts with Ezh2 and Tet2 (and putatively DPF3 through BRG1 | Table 2). Strikingly, chromatin recruitment of Ezh2 has been shown to be misregulated in the presence of (i.e. putatively because of) constitutively activated STAT5A/B (mediated by $JAK2^{V617F}$) in Ba/F3 cells (Chen *et al.*, 2017). Moreover, the oncogenic STAT5 target gene *Socs2* (compare Laszlo *et al.*, 2014) exhibited increased chromatin accessibility in the presence of constitutive STAT5A/B in primary hematopoietic cells, compared to transient STAT5A/B activity (Viny *et al.*, 2015). Besides, ectopic $STAT5B^{N642H}$, but not wild-type STAT5B, expression has been correlated with the loss of DNA methylation at putative oncogenes and their upregulation in a mouse model of T cell lymphoma (Pham *et al.*, 2018).

The aforementioned hypothesis, in turn, proposes that sustained STAT5 DNA binding, as found in the presence of oncogenic constitutive STAT5A/B activity, can mediate other chromatin alterations than normal transient STAT5 DNA binding. Interestingly, sustained STAT5 DNA binding has been found in two physiological contexts (in both humans and rodents), namely in female livers as opposed to male livers (Choi and Waxman, 1999, Tannenbaum *et al.*, 2001, Zhang *et al.*, 2012) and during lactogenesis (Kang *et al.*, 2014, Liu *et al.*, 1996, Shin *et al.*, 2016, Willi *et al.*, 2016). In doing so, forced sustained STAT5A/B activation in male livers has been shown to cause the almost complete feminization of transcript levels and chromatin accessibility patterns (Lau-Corona *et al.*, 2017, Ling *et al.*, 2010). Moreover, sustained, but not transient, endogenous STAT5A/B activity as well as constitutive STAT5A/B-1*6 activity have been shown to correlate with upregulation of and histone acetylation at *Csn2* in a mammary epithelial cell line (Xu *et al.*, 2009). Taken together, these findings raise the possibility of time-dependent oncogenic effects of sustained STAT5 DNA binding on chromatin. In support of this, a constitutively active, a wild-type, and, strikingly, a dominant negative (i.e. TAD-deficient,

with sustained DNA-binding activity but transcriptionally inactive) STAT5A form have all been found to induce breast tumorigenesis in a mouse model upon ectopic expression in the mammary gland – albeit with decreasing incidence (Iavnilovitch *et al.*, 2004) – suggesting that STAT5A oncogenicity does not exclusively involve its transcriptional activity but also other effects upon DNA binding. In doing so, the lactogenesis-dependent upregulation of a wild-type and constitutively active STAT5A form highly increased the incidence of breast tumors at menopause, when comparing mice experiencing several pregnancies (i.e. cycles of STAT5A upregulation) with virgin mice (Eilon *et al.*, 2007). This suggests that high STAT5A activity levels primed mice for oncogenesis, putatively via STAT5A-mediated chromatin alterations persisting after weaning.

This circumstantial evidence is complemented by molecular differences observed between transiently and constitutively active STAT5. Namely, endogenous STAT5A/B constitutively activated by an upstream mutation has been reported to bind to low-affinity $TTCN_4GAA$ GAS motifs with higher affinity than transiently active endogenous STAT5A/B in Ba/F3 cells (Moucadel and Constantinescu, 2005), suggesting that broadened DNA binding patterns contribute to transcriptional misregulation. Strikingly, STAT5A-1*6 overexpression in hematopoietic cells positively or negatively affected transcript levels of ~400 genes to mostly higher degrees than wild-type STAT5A overexpression, with STAT5A-1*6-specific changes in a few cases (Wierenga *et al.*, 2008). Accordingly, the *miR-28* gene has been found to be strongly upregulated in Ba/F3 cells expressing STAT5A-1*6, BCR-ABL or $JAK2^{V617F}$, but not in parental Ba/F3 cells upon synchronized activation of endogenous STAT5A/B (Girardot *et al.*, 2010), suggesting a transactivation mechanism for *miR-28* specific to constitutive STAT5A/B activity possibly involving distinct chromatin alterations conducive to transcriptional activity. In addition, DNA binding of STAT5B constitutively activated by $JAK2^{V617F}$ in another cell line has been found to be a prerequisite for DNA binding of the transcription factor p53, which physically interacts and synergistically transactivates the *miR-28* gene with STAT5B (Girardot *et al.*, 2015), suggesting that constitutively active STAT5B can function as an anchor for other transcription factors. Strikingly, Brd2 has been shown to co-occupy the *c-Myc* super-enhancer with STAT5A-1*6 in a transformed Ba/F3 cell line, but not with endogenous STAT5A/B in parental Ba/F3 cells, although *c-Myc* transactivation is sensitive to a BET family pan-inhibitor in both cases (Pinz *et al.*, 2016). Accordingly, ectopic STAT5B-1*6 expression in Ba/F3 cells has been correlated with increased histone acetylation at the *c-Myc* (and *Bcl-x*) super-enhancer in addition to *c-Myc* upregulation (albeit not in comparison to wild-type STAT5B activity | Katerndahl *et al.*, 2017). This suggests that STAT5A/B-1*6 specifically mediates (increased) histone acetylation at and Brd2 recruitment to the *c-Myc* super-enhancer (and possibly the *Bcl-x* super-enhancer), thus enhancing gene transactivation.

In summary, these findings raise the possibility that constitutively active STAT5A/B specifically mediates other chromatin alterations than normal transiently active STAT5A/B and that such alterations may constitute 'drivers' for STAT5A/B-associated oncogenesis and cancer progression.

1.1. Objectives

The present study aimed to elucidate effects specific to constitutive STAT5A/B activity as opposed to transient STAT5A/B activity – in particular upon sustained DNA binding on chromatin – underlying its oncogenicity. To do so, a Ba/F3 cell line inducibly expressing constitutively active STAT5A-1*6 was generated as an experimental model system, to allow the monitoring of oncogenic processes induced by STAT5A-1*6 expression.

The main goal of this project was the identification of 'driver' events and alterations characteristic of STAT5-associated cancers. Specific aims of this study were to:

(i) characterize the effects of STAT5A-1*6 on the cell survival and growth phenotypes;
(ii) characterize the effects of STAT5A-1*6 on the molecular phenotype, in terms of STAT5 DNA binding activity and of gene expression of selected STAT5 target genes;
(iii) identify chromatin alterations mediated by endogenous STAT5A/B;
(iv) investigate whether these STAT5A/B-mediated chromatin alterations were misregulated upon sustained DNA-binding of STAT5A-1*6.

Ultimately, these analyses might identify novel molecular targets for drug development against STAT5A/B-associated cancers.

2 Material and Methods

2.1 Material

2.1.1 Purchased chemicals, buffers and reagents

name	product designation	company, registered office	notes
10x qPCR buffer	PCR buffer, 10x	Qiagen GmbH, D - Hilden	
2-mercaptoethanol	2-Mercaptoethanol	Sigma-Aldrich Chemie GmbH D - Taufkirchen	
acetic acid (100 %)	Acetic acid (glacial) 100%	Merck KGaA, D - Darmstadt	
acrylamide-bisacrylamide	Rotiphorese® Gel 30 (37,5:1)	Carl Roth GmbH + Co. KG, D - Karlsruhe	acrylamide : bisacrylamide 37.5 : 1 30 % in H_2O
Agarose	Biozym LE Agarose	Biozym Scientific GmbH, D – Hessisch Oldendorf	
Ampicillin	Ampicillin	Sigma-Aldrich Chemie GmbH D - Taufkirchen	
Aprotinin	Aprotinin	Carl Roth GmbH + Co. KG, D - Karlsruhe	lyophilized reconstituted in H_2O
APS (ammonium persulfate)	Ammonium persulfate	Sigma-Aldrich Chemie GmbH D - Taufkirchen	
Bradford reagent	Roti®-Quant	Carl Roth GmbH + Co. KG, D - Karlsruhe	contains Coomassie Brilliant Blue-G250 5 x concentrate
Brij 97 (polyoxyethylene (10) oleyl ether)	Brij® O10	Sigma-Aldrich Chemie GmbH D - Taufkirchen	
bromophenol blue (3',3",5',5"-tetrabromophenolsulfonphthalein)	Bromophenol Blue sodium salt	Sigma-Aldrich Chemie GmbH D - Taufkirchen	
BSA (bovine serum albumin)	Bovine Serum Albumin (CA#: A9647)	Sigma-Aldrich Chemie GmbH D - Taufkirchen	
BSA (bovine serum albumin), fatty-acid free	Bovine Serum Albumin (CA#: A7511)	Sigma-Aldrich Chemie GmbH D - Taufkirchen	
CutSmart Buffer	CutSmart™ Buffer	New England Biolabs GmbH, D – Frankfurt am Main	
DAPI (4′,6-diamidino-2-phenylindole dihydrochloride)	4′,6-diamidino-2-phenylindole dihydrochloride	Sigma-Aldrich Chemie GmbH D - Taufkirchen	
deoxycholic acid, sodium salt	Sodium Deoxycholate	AppliChem GmbH D - Darmstadt	
DMSO for cryoconservation (dimethyl sulfoxide)	Dimethyl Sulfoxide	AppliChem GmbH D - Darmstadt	
DMSO, cell pre-treatment and SYBR green (dimethyl sulfoxide)	Dimethyl sulfoxide	Sigma-Aldrich Chemie GmbH D - Taufkirchen	
DNA loading dye	Gel Loading Dye, Blue (6X)	New England Biolabs GmbH, D – Frankfurt am Main	
dNTP solution	dNTP Set, PCR Grade, 4 x 250 µl	Qiagen GmbH, D - Hilden	combined before use to: 25 mM dATP, 25 mM dCTP, 25 mM dGTP, 25 mM dTTP
doxycycline	Doxycycline hyclate	Sigma-Aldrich Chemie GmbH D - Taufkirchen	reconstituted in H_2O
dry milk powder	Sucofin skimmed milk powder, easily soluble	TSI GmbH & Co. KG D - Zeven	
ECL Prime detection reagent	Amersham ECL Prime Western Blotting Detection Reagent	GE Healthcare Europe GmbH D - Freiburg	
EDTA (ethylenediaminetetraacetic acid)	EDTA disodium salt dihydrate	AppliChem GmbH D - Darmstadt	
Electroporation buffer	Gene Pulser® Electroporation Buffer	Bio-Rad Laboratories GmbH, D - München	

ethanol (100 %))	Ethanol (CA#: 32205)	Sigma-Aldrich Chemie GmbH D - Taufkirchen	
ethidumbromide	Ethidium Bromide Solution, Molecular Grade	Promega GmbH, D - Mannheim	
FCS (i) (fetal calf serum)	Fötales Rinderserum	PAN Biotech GmbH, D - Aidenbach	heat inactivation before use (30min 50°C)
FCS (ii) (fetal calf serum)	Fetal Bovine Serum	Life Technologies GmbH, D - Darmstadt	heat inactivation before use (30min 50°C)
Femto detection reagent	SuperSignal West Femto Chemiluminescent Substrate	Thermo Fisher Scientific GmbH, D - Dreieich	
Formaldehyde (37% solution)	Formaldehyde solution	Sigma-Aldrich Chemie GmbH D - Taufkirchen	
G418	G418, Geneticin®	PAA Laboratories GmbH, D - Cölbe	
glutamine (cell culture)	L-Glutamin	PAN Biotech GmbH D - Aidenbach	
glycerol	Glycerine	Carl Roth GmbH + Co. KG, D - Karlsruhe	
glycine	Glycine	Merck KGaA, D - Darmstadt	
glycogen solution	Glycogen, 20 mg/ml	Affymetrix GmbH, D - München	
HCl (hydrochloric acid)	Hydrochloric acid fuming 37%	Merck KGaA, D - Darmstadt	
Hotstart Taq Polymerase	HotStarTaq® DNA Polymerase	Qiagen GmbH, D - Hilden	
hygromycin B	Hygromycin B	PAA Laboratories GmbH, D - Cölbe	
IL-3 (recombinant murine interleukin 3)	rmIL-3	ImmunoTools GmbH, D - Friesoythe	lyophilized reconstituted in RPMI medium
iScript RT-qPCR Sample Preparation Reagent	iScript™ RT-qPCR Sample Preparation Reagent	Bio-Rad Laboratories GmbH, D - München	
KCl (potassium chloride)	Potassium chloride	Merck KGaA, D - Darmstadt	
KH_2PO_4 (potassium dihydrogen phosphate)	di-Sodium hydrogen phosphate	Merck KGaA, D - Darmstadt	
leupeptin	Leupeptin	Carl Roth GmbH + Co. KG, D - Karlsruhe	lyophilized reconstituted in H_2O
LiCl	Lithium chloride	Sigma-Aldrich Chemie GmbH D - Taufkirchen	
methanol	Methanol	Merck KGaA, D - Darmstadt	
$MgCl_2$ solution	$MgCl_2$, 25 mM	Qiagen GmbH, D - Hilden	
$MgCl_2$ x $6H_2O$ (magnesium chloride hexahydrate)	Magnesium chloride hexahydrate	Merck KGaA, D - Darmstadt	
Na_3VO_4 (sodium orthovanadate)	Sodium orthovanadate	Sigma-Aldrich Chemie GmbH D - Taufkirchen	
NaAc x $3H_2O$ (sodium acetate trihydrate)	Sodium acetate trihydrate	Merck KGaA, D - Darmstadt	
NaCl (sodium chloride)	Sodium chloride	VWR International GmbH , D - Darmstadt	
NaF (sodium fluoride)	Sodium fluoride	Sigma-Aldrich Chemie GmbH D - Taufkirchen	
$NaHCO_3$ (sodium hydrogen carbonate)	Sodium bicarbonate	Sigma-Aldrich Chemie GmbH D - Taufkirchen	
$NaHPO_4$ (disodium phosphate)	di-Sodium hydrogen phosphate	Merck KGaA, D - Darmstadt	
NaN_3 (sodium azide)	Sodium Azide pure	AppliChem GmbH D - Darmstadt	
NaOH (sodium hydroxide)	Sodium hydroxide	Merck KGaA, D - Darmstadt	pellets
PBS (phosphate buffered saline)	DPBS, without Ca and Mg	PAN Biotech, D - Aidenbach	
Penicillin/ Streptomycin	Penicillin/Streptomycin (CA#: P06-07001)	PAN Biotech GmbH, D - Aidenbach	

Phenol/Chloroform/Isoamyl alcohol	Roti®-Phenol/Chloroform/Isoamyl alcohol	Carl Roth GmbH + Co. KG, D - Karlsruhe	
PIPES [piperazine-N,N′-bis(2-ethanesulfonic acid)]	Pipes	Sigma-Aldrich Chemie GmbH D - Taufkirchen	
PMSF (phenylmethylsulfonyl fluoride)	Phenylmethanesulfonyl fluoride	Sigma-Aldrich Chemie GmbH D - Taufkirchen	reconstituted in ethanol ()
protein A sepharose beads	Protein A Sepharose CL-4B	GE Healthcare Europe GmbH D - Freiburg	
Proteinase K	Proteinase K from *Tritirachium album*	Sigma-Aldrich Chemie GmbH D - Taufkirchen	lyophilized reconstituted in H_2O
RNAse A (ribonuclease A)	Ribonuclease A from bovine pancreas	Sigma-Aldrich Chemie GmbH D - Taufkirchen	
RPMI-1640 medium	RPMI 1640 with L-Glutamine with 2,0 g/l NaHCO3 (CA#: P04-16500)	PAN Biotech, D - Aidenbach	
Salmon sperm DNA solution	UltraPure™ Salmon Sperm DNA Solution	Life Technologies GmbH, D - Darmstadt	sheared to 2.000 bp 10 mg/ml
SDS (sodium dodecyl sulfate)	Dodecylsulfate·Na-salt in Pellets	SERVA Electrophoresis GmbH, D - Heidelberg	
SYBR green	SYBR Green I	Qiagen GmbH, D - Hilden	reconstituted in DMSO
TEMED (tetramethylethylenediamine)	N,N,N′,N′-Tetramethylethylenediamine	Sigma-Aldrich Chemie GmbH D - Taufkirchen	
Tris (tris(hydroxymethyl)aminomethane)	Trizma® base	Sigma-Aldrich Chemie GmbH D - Taufkirchen	
Tris-HCl (tris(hydroxymethyl)aminomethane hydrochloride)	tris(hydroxymethyl)aminomethane hydrochloride	Merck KGaA, D - Darmstadt	
Triton-X 100	Triton® X-100	SERVA Electrophoresis GmbH, D - Heidelberg	
trypan blue solution	Trypan Blue solution	Sigma-Aldrich Chemie GmbH D - Taufkirchen	0.2 % trypan blue in H_2O with 0.9 % NaCl
tryptone	Tryptone	Sigma-Aldrich Chemie GmbH D - Taufkirchen	
TSA (trichostatin A)	Trichostatin A	Sigma-Aldrich Chemie GmbH D - Taufkirchen	
Tween20	TWEEN® 20	Sigma-Aldrich Chemie GmbH D - Taufkirchen	
yeast extract	Yeast Extract	Sigma-Aldrich Chemie GmbH D - Taufkirchen	

2.1.2 Self-made buffers

All buffers were prepared with ultrapure water (filtered by Milli-Q Integral Water Purification System). When the buffers were applied with living cells or native lysates, the buffers where sterilized by autoclaving or supplementation with 0.02 % NaN_3 (sodium azide). If necessary, pH was adjusted using NaOH platelets or HCl.

name	composition	application
0.5x TAE buffer	in H_2O: 20 mM Tris pH 8.0 10 mM acetic acid 500 µM EDTA	Agarose gel electrophoresis
150 mM NaCl wash buffer	in H_2O: 150 mM NaCl 20 mM Tris pH 8.0 5 mM EDTA 1 % Triton X-100 0.2 % SDS	Chromatin immunoprecipitation
500 mM NaCl wash buffer	in H_2O: 500 mM NaCl 20 mM Tris pH 8.0 5 mM EDTA 1 % Triton X-100 0.2 % SDS	Chromatin immunoprecipitation

Brij lysis buffer	in H_2O: 10 mM Tris pH 7.5 150 mM NaCl 2 mM EDTA 0.875 % Brij 0.125 % NP40	Protein isolation
ChIP buffer	in H_2O: 100 mM NaCl 67 mM Tris pH 8.0 5 mM EDTA 0.33 % SDS 1.67 % Triton X-100	Chromatin immunoprecipitation
4x Laemmli buffer	in H_2O: 250 mM Tris-HCl pH 6.8 40 % glycerol 5 % SDS 0.005% bromophenol blue 10% β-Mercaptoethanol	Western blot analysis
LB medium	in H_2O: 10 g/l tryptone 5 g/l yeast extract 10 g/l NaCl adjusted to pH 7.5 autoclaved	Cloning
LiCl wash buffer	in H_2O: 0.5 % deoxycholic acid (sodium salt) 1 mM EDTA 250 mM LiCl 0.5 % NP40 10 mM Tris pH 8.0	Chromatin immunoprecipitation
1x PBST	in H_2O: 1.37 mM NaCl 27 µM KCl 100 µM $NaHPO_4$ x $2H_2O$ 18 µM KH_2PO_4 0.2 % Tween20 adjusted to pH 7.4	Western blot analysis
PIPES buffer	in H_2O: 10 mM PIPES 100 mM NaCl 2 mM $MgCl_2$ x $6H_2O$ 1 % Triton X-100 adjusted to pH 6.8	Flow cytometry
Protein A Sepharose beads slurry buffer	in TE buffer: 1 mg/ml fatty-acid free BSA 400 µg/ml salmon sperm DNA	Chromatin immunoprecipitation
Reverse cross-linking buffer	in H_2O: 1 % SDS 0.2 M $NaHCO_3$	Chromatin immunoprecipitation
PAGE buffer	in H2O: 250 mM Tris 1.92 M glycine 1 % SDS	Western blot analysis
SDS lysis buffer	in H2O: 100 mM NaCl 50 mM Tris pH 8.0 5 mM EDTA 0.5 % SDS	Chromatin immunoprecipitation
2x self-made qPCR mix	2x 10x buffer qiagen 5 mM MgCl2 0.4 mM each dNTP 1:500,000 SYBR green (dATP, dCTP, dGTP, dTTP)	qPCR, RT-qPCR
1x TBST	in H2O: 150 mM NaCl 7,7 mM Tris-HCl 0.2 % Tween20 adjusted to pH 7.5	Western blot analysis
1x TE buffer	in H_2O: 20 mM Tris pH 8.0 1 mM EDTA	miscellaneous

Transfer buffer	in H_2O: 25 mM Tris 0.02 % SDS 192 mM glycine 20 % methanol	Western blot analysis
Triton X-100 dilution buffer	in H_2O: 100 mM NaCl 100 mM Tris pH 8.0 5 mM EDTA 5 % Triton X-100	Chromatin immunoprecipitation

2.1.3 Equipment

name	product designation	company, registered office	application
analytical balance	Sartorius CP224S	Sartorius AG, D - Göttingen	miscellaneous
automatic propipette controller (i)	accu-jet® pro pipette controller	Brand GmbH & Co. KG, D - Wertheim	miscellaneous
automatic propipette controller (ii)	Rainin Pipette-X Lightweight Controller	Mettler-Toledo GmbH, D - Gießen	miscellaneous
balance	PJ400	Mettler-Toledo GmbH, D - Gießen	miscellaneous
CO_2 incubator	Heraeus® BBD6220	Thermo Fisher Scientific GmbH, D - Dreieich	cell culture
electroporator	Gene Pulser Xcell CE Module	Bio-Rad Laboratories GmbH, D - München	transfection
Flow cytometer	BD™ LSR II Flow Cytometer System	Becton Dickinson GmbH, D - Heidelberg	Flow cytometry
Freezer (−20 °C)	Liebherr Premium	Liebherr-International Deutschland GmbH, D - Biberach an der Riß	miscellaneous
Freezer (−80 °C)	Forma 900 Series -86C Upright Freezer	Thermo Fisher Scientific GmbH, D - Dreieich	miscellaneous
gel documentation system	GeneGenius Gel Imaging System	Syngene, UK - Cambridge	agarose gel electrophoresis
heatable magnetic stirrer	MR 2002	Heidolph Instruments GmbH & Co.KG, D - Schwabach	miscellaneous
heating block (72 °C)	Thermomixer 5436	Eppendorf AG, D - Hamburg	chromatin immunoprecipitation
heating block (95 °C)	Bio TDB-100, Dry block thermostat	A. Hartenstein Laborbedarf GmbH, D - Würzburg	Western blot analysis
horizontal, two-dimensional gel system	Sub-Cell® GT Cell	Bio-Rad Laboratories GmbH, D - München	agarose gel electrophoresis
hybridization incubator (37 °C, 55 °C, 65 °C)	hybridization incubator GFL-7601	GFL Gesellschaft für Labortechnik mbH, D - Burgwedel	chromatin immunoprecipitation
ice maker	Scotsman AF80	Scotsman Ice Systems, USA - Vernon Hills	miscellaneous
manual air displacement pipette set: - 0.2 µl – 2 µl - 2 µl – 20 µl - 20 µl – 200 µl - 100 µl – 1.000 µl	Rainin Pipet-Lite XLS+	Mettler-Toledo GmbH, D - Gießen	miscellaneous
incubator, bacteria	WTC binder FD	BINDER GmbH D - Tuttlingen	cloning
incubation shaker, bacteria	MaxQ™ 4000 Benchtop Orbital Shaker	Thermo Fisher Scientific GmbH, D - Dreieich	cloning
live imaging microscpe	TissueFAXSiPLUS	TissueGnostics GmbH, A - Wien	cell culture
microwave	Panasonic inverter	Panasonic Europe GmbH D - Hamburg	agarose gel electrophoresis
ultrapure water system	Milli-Q Integral Water Purification System	Merck KGaA, D – Darmstadt	miscellaneous

nanophotometer	NanoPhotometer® P360	Implen GmbH, D - München	cloning
Neubauer counting chamber	Neubauer-improved (depth 0.1 mm, area 25 μm^2)	Paul Marienfeld GmbH & Co. KG, D - Lauda Königshofen	cell culture
nitrogene tank	MVE 810 Eterne/MVE Euro Cyl	german-cryo® GmbH, D - Jüchen	miscellaneous
optical microscope	Olympus CK2	Olympus Deutschland GmbH, D - Hamburg	cell culture
orbital shaker	GFL Shaker 3015 with Orbital Motion	GFL Gesellschaft für Labortechnik mbH, D - Burgwedel	Western blot analysis
PCR thermal cycler	MyCycler™ PCR Thermal Cycler	Bio-Rad Laboratories GmbH, D - München	Gene expression analysis
pH meter	inoLab® Labor-pH-Meter	WTW GmbH, D - Weilheim	miscellaneous
power supply	Power Pack P25 T	Biometra GmbH, D - Göttingen	Western blot analysis
power supply	PowerPac™ HC High-Current Power Supply	Bio-Rad Laboratories GmbH, D - München	agarose gel electrophoresis
refrigerated centrifuge (1,5 ml and 2 ml tubes)	Microcentrifuge 5417R	Eppendorf AG, D - Hamburg	miscellaneous
refrigerated centrifuge (15 ml and 50 ml tubes)	Centrifuge 5810R	Eppendorf AG, D - Hamburg	miscellaneous
Rotator	BioSan Rotator Multi RS-60	A. Hartenstein Laborbedarf GmbH, D - Würzburg	chromatin immunoprecipitation
Rotor-Gene Q qPCR cycler	Rotor-Gene Q	Qiagen GmbH, D - Hilden	qPCR, RT-qCPR
semi-dry electroblotting cell	Trans-Blot® SD Semi-Dry Transfer Cell	Bio-Rad Laboratories GmbH, D - München	Western blot analysis
sonifier power supply	Branson Sonifier® S-250A analog ultrasonic processor	G. HEINEMANN Ultraschall- und Labortechnik, D - Schwäbisch Gmünd	chromatin immunoprecipitation
sonotrode	5mm tip sonotrode	G. HEINEMANN Ultraschall- und Labortechnik, D - Schwäbisch Gmünd	chromatin immunoprecipitation
sterile laminar flow working bench	Herasafe™ KS (NSF) Class II, Type A2 Biological Safety Cabinet	Thermo Fisher Scientific GmbH, D - Dreieich	cell culture
UV photometer	BioPhotometer®	Eppendorf AG, D - Hamburg	Western blot analysis
vertical, two-dimensional gel system	Mini-PROTEAN® Electrophoresis System	Bio-Rad Laboratories GmbH, D - München	Western blot analysis
vortexer	Vortex-Genie 2, 230V	Scientific Industries, Inc., USA - New York	miscellaneous
water-bath	water-bath TW12	JULABO GmbH, D - Seelbach	miscellaneous
Western blot imaging system	ImageQuant LAS 4000 Mini	GE Healthcare Europe GmbH D - Freiburg	Western blot analysis

2.1.4 Consumables

Standard plastic ware was purchased from Sarstedt AG &Co., D - Nümbrecht.

name	product designation	company, registered office	application
96 well cell culture plates	BD Falcon Zellkulturplatte mit 96 Vertiefungen, Flachboden und Deckel	BD Biosciences USA - Franklin Lakes	
cell culture flasks: 25 cm^2, 75 cm^2 and 175 cm^2	TC flasks with quick-release cap	Sarstedt AG &Co., D - Nümbrecht	Cell culture
cryoconservation tubes	CryoPure 2.0 ml tubes with internal thread and silicone O-ring	Sarstedt AG &Co., D - Nümbrecht	Cell culture
electroporation cuvettes	Gene Pulser/MicroPulser Cuvettes	Bio-Rad Laboratories GmbH, D - München	Transfection
flow cytometry tubes	Tube for flow-cytometer FACSAria, FACSCanto, FACSCalibur, LRS II, FC 500	Sarstedt AG &Co., D - Nümbrecht	Flow cytometry

photometer cuvettes	Semi-micro cuvettes 10 x 4 mm, optical pathway 10mm (CA#: 67.724)	Sarstedt AG &Co., D - Nümbrecht	Bradford assay
pipette tips with filter (i) (2 µl, 20 µl, 200 µl and 1,000 µl)	SafeSeal-Tips® Professional Line	Biozym Scientific GmbH, D – Hessisch Oldendorf	miscellaneous
pipette tips with filter (ii) (20 µl, 200 µl and 1,000 µl)	Rainin Aerosol-resistant Filter Tips	Mettler-Toledo GmbH, D - Gießen	miscellaneous
pipette tips without filter (i) (10 µl, 200 µl and 1,000 µl)	Quality Pipette Tips without filter	Sarstedt AG &Co., D - Nümbrecht	miscellaneous
pipette tips without filter (ii) (20 µl, 200 µl and 1,000 µl)	Rainin SpaceSaver™ Stacked Refill	Mettler-Toledo GmbH, D - Gießen	miscellaneous
pipette tips without filter (ii) (1,000 µl)	Rainin Bulk Tips	Mettler-Toledo GmbH, D - Gießen	miscellaneous
PVDF transfer membrane, 0.45 µm pore size	Immobilon-P Membrane, PVDF, 0.45 µm, 26.5 cm x 3.75 m roll	Merck KGaA, D - Darmstadt	Western blot analysis
qPCR tubes (i)	0,1 ml PCR-Tubes and Caps for Corbett-System	Kisker Biotech GmbH & Co. KG, D - Steinfurt	qPCR, RT-qPCR
qPCR tubes (ii)	Strip Tubes and Caps, 0.1 ml	Qiagen GmbH, D - Hilden	qPCR, RT-qPCR
reaction tubes (15 ml and 50 ml)	Tubes with conical base, screw cap from HD-PE	Sarstedt AG &Co., D - Nümbrecht	miscellaneous
reaction tubes (1.5 ml and 2 ml)	SafeSeal micro tubes, 1.5 ml (or 2.0 ml), PP, with wide hinge	Sarstedt AG &Co., D - Nümbrecht	miscellaneous
serological pipettes (5 ml, 10 ml and 25 ml)	Serological pipettes from clear polystyrene	Sarstedt AG &Co., D - Nümbrecht	miscellaneous
polyamide sieve cloth	polyamide sieve cloth	Reichelt Chemietechnik GmbH, D - Heidelberg	Flow cytometry
stepper pipette tip	Combitips plus 0,5ml	Eppendorf AG, D - Hamburg	miscellaneous
Whatman chromatography paper	Blotting paper Whatman™ 3MM Chr	A. Hartenstein Laborbedarf GmbH, D - Würzburg	Western blot analysis

2.1.5 Kits

name	product designation	company, registered office	application
iScript cDNA synthesis kit	iScript™ cDNA Synthesis Kit	Bio-Rad Laboratories GmbH, D - München	cDNA synthesis
DNA purification kit, NTB buffer	Buffer NTB (for clean-up of SDS-containing samples)	MACHEREY-NAGEL GmbH & Co. KG, D - Düren	DNA purification for qPCR
DNA purification kit (contains NT3 buffer, elution buffer)	NucleoSpin® Gel and PCR Clean-up	MACHEREY-NAGEL GmbH & Co. KG, D - Düren	DNA purification for qPCR
Miniprep kit	Wizard® *Plus* SV Minipreps DNA Purification System	Promega GmbH, D - Mannheim	DNA purification for cloning
Midiprep kit	QIAGEN Plasmid Plus Midi Kit	Qiagen GmbH, D - Hilden	DNA purification for cloning
Agarose gel DNA purification kit	Wizard® SV Gel and PCR Clean-Up System	Promega GmbH, D - Mannheim	DNA purification for cloning

2.1.6 Markers

name	product designation	company, registered office	marker sizes	application
Protein marker	Protein Marker VI (10 - 245) prestained	AppliChem GmbH D - Darmstadt	245 kDa 180 kDa 135 kDa 100 kDa 75 kDa 63 kDa 48 kDa 35 kDa 25 kDa 20 kDa	Western blot analysis

			17 kDa 11 kDa	
100bp DNA ladder	100 bp DNA Ladder	New England Biolabs GmbH, D – Frankfurt am Main	1,517 bp 1,200 bp 1,000 bp 900 bp 800 bp 700 bp 600 bp 500 bp 400 bp 300 bp 200 bp 100 bp	Agarose gel electrophoresis
1 kb DNA Ladder	1 kb DNA Ladder	New England Biolabs GmbH, D – Frankfurt am Main	10,000 bp 8,000 bp 6,000 bp 5,000 bp 4,000 bp 3,000 bp 2,000 bp 1,500 bp 1,000 bp 500 bp	Agarose gel electrophoresis

2.1.7 Primary antibodies (Western blot analysis)

name	product designation	company, registered office	dilution	antibody type, notes
anti-α-Tubulin	α Tubulin (DM1A): sc-32293 (CA#: sc-32293)	Santa Cruz Biotechnology, Inc., D - Heidelberg	1 : 200	monoclonal, raised in mouse
anti-FLAG	Monoclonal ANTI-FLAG® M2, Clone M2 (CA#: F-1804)	Sigma-Aldrich Chemie GmbH D - Taufkirchen	1 : 500	monoclonal, raised in mouse
anti-pSTAT5A/B	Phospho-Stat5 (Tyr694) Antibody (CA#: #9351)	New England Biolabs GmbH, D – Frankfurt am Main	1 : 1,000	polyclonal, raised in rabbit
anti-STAT5A/B	Stat5 (C-17): sc-835 (CA#: sc-835)	Santa Cruz Biotechnology, Inc., D - Heidelberg	1 : 1,000	polyclonal, raised in rabbit,
anti-TetR	TetR Monoclonal Antibody (Clone 9G9) (CA#: 631132)	Takara Bio Europe/Clontech, F - Saint-Germain-en-Laye	1 : 500 to 1 : 1,000	monoclonal, raised in mouse

2.1.8 Secondary antibodies (Western blot analysis)

name	product designation	company, registered office	dilution	antibody type, notes
HRP-conjugated anti-mouse	Anti-Mouse IgG (whole molecule)–Peroxidase antibody produced in goat (CA#: A8924)	Sigma-Aldrich Chemie GmbH D - Taufkirchen	1 : 10,000	polyclonal, raised in goat
HRP-conjugated anti-rabbit	Anti-Rabbit IgG (whole molecule)–Peroxidase antibody produced in goat (CA#: A0545)	Sigma-Aldrich Chemie GmbH D - Taufkirchen	1 : 20,000	polyclonal, raised in goat

2.1.9 Antibodies (ChIP)

ChIP	product designation	company, registered office	per ChIP	antibody type, notes
anti-STAT5A/B	Stat5a (L-20): sc-1081 (CA#: sc-1081) + Stat5 (C-17): sc-835 (CA#: sc-835)	Santa Cruz Biotechnology, Inc., D - Heidelberg	1.2 µg (6 µl) + 1.2 µg (6 µl)	polyclonal, raised in rabbit
anti-RNA Polymerase II	Pol II (N-20): sc-899 (CA#: sc-899)	Santa Cruz Biotechnology, Inc., D - Heidelberg	2 µg (10 µl)	polyclonal, raised in rabbit
anti-histone H3	Anti-Histone H3 antibody - ChIP Grade (CA#: ab1791)	Abcam UK - Cambridge	4 µg (4–13,33 µl)	polyclonal, raised in rabbit
anti-H3K4me1	Anti-Histone H3 (mono methyl K4) - ChIP Grade (CA#: ab8895)	Abcam UK - Cambridge	4 µg (4 µl)	polyclonal, raised in rabbit
anti-H3K4me3	Anti-trimethyl-Histone H3 (Lys4) (CA#: 07-473)	Merck KGaA, D - Darmstadt	4 µg (4 µl)	polyclonal, raised in rabbit

anti-H3K9me1	Anti-Histone H3 (mono methyl K9) - ChIP Grade (CA#: ab8896)	Abcam UK - Cambridge	4 µg (4 µl)	polyclonal, raised in rabbit
anti-H3K9me3	Anti-Histone H3 (tri methyl K9) - ChIP Grade (CA#: ab8898)	Abcam UK - Cambridge	4 µg (4 µl)	polyclonal, raised in rabbit
anti-H3K27me1	Anti-monomethyl-Histone H3 (Lys27) (CA#: 07-448)	Merck KGaA, D - Darmstadt	4 µg (4 µl)	polyclonal, raised in rabbit
anti-H3K27me3	Anti-trimethyl-Histone H3 (Lys27) (CA#: 07-449)	Merck KGaA, D - Darmstadt	4 µg (4 µl)	polyclonal, raised in rabbit
rabbit IgG	IgG from rabbit serum (CA#: I5006)	Sigma-Aldrich Chemie GmbH D - Taufkirchen	2–5 µg (2–5 µl)	polyclonal, raised in rabbit
anti-acetylated histone H3	(CA#: 06-599)	Millipore, D - Darmstadt	3 µg (3 µl)	polyclonal, raised in rabbit
anti-acetylated histone H4	(CA#: 06-866)	Millipore, D - Darmstadt	3 µg (3 µl)	polyclonal, raised in rabbit
anti-BRG1	Brg-1 Antibody (H-88): sc-10768 (CA#: sc-10768)	Santa Cruz Biotechnology, Inc., D - Heidelberg	2–5 µg (10–30 µl)	polyclonal, raised in rabbit

2.1.10 Vectors

product designation	company, registered office	notes
Invitrogen pcDNA™3	Life Technologies GmbH, D - Darmstadt	
pTet-On Advanced	Takara Bio Europe/Clontech, F - Saint-Germain-en-Laye	
pTRE-Tight-BI-AcGFP1	Takara Bio Europe/Clontech, F - Saint-Germain-en-Laye	
pTRE-Tight-BI-Luc2	Takara Bio Europe/Clontech, F - Saint-Germain-en-Laye	
pTK-Hyg	Takara Bio Europe/Clontech, F - Saint-Germain-en-Laye	kind gift from Helen Hoffmeister (Biochemistry III, University of Regensburg, Germany)

2.1.11 Enzymes (Cloning)

name	product designation	company, registered office	application
EcoRI-HF	EcoRI-HF®	New England Biolabs GmbH, D – Frankfurt am Main	restriction enzyme for cloning
NotI-HF	NotI-HF®	New England Biolabs GmbH, D – Frankfurt am Main	restriction enzyme for cloning
T4 DNA Ligase	T4 DNA Ligase	New England Biolabs GmbH, D – Frankfurt am Main	ligation for cloning
KpnI-HF	KpnI-HF®	New England Biolabs GmbH, D – Frankfurt am Main	restriction enzyme for cloning

2.1.12 Oligonucleotides

Oligonucleotides were purchased from Sigma-Aldrich Chemie GmbH (D - Taufkirchen) and/or metabion international AG (D - Planegg) for Sanger sequencing, RT-qPCR and ChIP. Primer design and validation were conducted by PD Dr. Anne Rascle.

2.1.12.1 Primers (Sanger sequencing, expression vector templates)

designation	primer (5'-3')
O21	CGGAAGCAGCAGACCATCATC
O76	ACATCAGCAGCAACCACCTCG
O79	AGCTTCTCACACCAGGACTGC
O94	CAGTGATAGAGAACGTATGTCGAGG
O95	CACTGATAGGGAGTAAACTCGAGTATG
O97	CGCACATTTCCCCGAAAAGT

2.1.12.2 Primers (RT-qPCR, cDNA templates)

designation	forward primer (5'-3')	reverse primer (5'-3')	template mRNA/cDNA
O309, O310	ATGGCAGCAGTGAAGCAAGC	ACGATGCGACCCCAGTTTACTC	*Bcl-x* mRNA
O9, O10	CTGGACTCTAACTGCTTGTC	TAGGCAGCACCGAGTCAC	*Cis* mRNA
O11, O12	AACAGGAACTATGACCTCG	AGCAGCTCGAATTTCTTC	*c-Myc* mRNA
O303, O304	CGACATGAACGGCTGCTACTC	TCTCCACCTTGCTCACTTTGC	*Id-1* mRNA
O182, O183	CATAGTACCCAGTTGTCGGGC	GGCTTTGAATGTGGCATTGG	*IL-2Ra* mRNA
O307, O308	GTGCCTATCACGCTTCTCGG	TGGTTGTCCTCCACAGGGAT	*MKP-1* mRNA
O13, O14	AGATACCTGAGCCCACACAGACAG	AGATACCTGAGCCCACACAGACAG	*Osm* mRNA
O315, O316	TCTTCTGGCAGGTGCTG	GGTAGCGAATCCACTCTG	*Pim-1* mRNA
O48, O49	GGCAGTGCCCTGTTTATTGAA	GCTGGAAATCTGCTGTGAAGG	*Spi2.1* mRNA
O186, O187	CTGCTGTTTCTTGGTGGCCT	AGAGTTTGCTTGTGACCCACG	*TNFRSF13b* mRNA
O15, O16	CGAAGGGAACGGAATAAGATGG	AGACCTCCAGTCAAATCCAGGG	*c-Fos* mRNA
O285, O286	TGATGTCCGACCTGTTCCG	CCGAAGAGACAACGGCACA	*p21* mRNA
O5, O6	GCGTCCTGGCATTGTCTGT	GCCGCAAATGCAGATGG	*36b4* mRNA
O1, O2:	GCAAGATGAAGCTGGATTAC	GGGATGTTCACCACCTG	*S9* mRNA
O81, O168	TTCTCCATTCGGTCCCTGG	GTCATCGTCGTCCTTGTAGTCG	transgenic *mSTAT5A-FLAG* mRNA

2.1.12.3 Primers (ChIP, genomic DNA templates)

designation	forward primer (5'-3')	reverse primer (5'-3')	template genomic DNA (amplicon position, relative to TSS)
O348, O349	AAGCCCAGGATCTGAGTTCCA	CGTGCCACCGTGTTTATATGG	*Bcl-x* gene (-1006/-924)
O346, O347	TTGTACCTGCTTGCTGTCGC	TTTTACTACAACCACCCACCCC	*Bcl-x* gene (+1261/+1385)
O344, O345	ATGGGGGTGACTTTTGGAGAA	GGTCTGAGTCCGGGTTCTAAGG	*Bcl-x* gene (+1325/+1466)
O84, O85	AGGGCTGTCTGGGAGCTGA	TCTCTGAGTGGACCGACAGTTG	*Cis* gene (-831/-755)
O86, O87	CAACTCTAGGAGCTCCCGCC	AACACCTTTGACAGATTTCCAAGAAC	*Cis* gene (-259/-199)
O88, O89	GTCCAAAGCACTAGACGCCTG	TTCCCGGAAGCCTCATCTT	*Cis* gene (-188/-104)
O90, O91	GTTCGCACCACAGCCTTTCAGTCC	GTCCAGGGGTGCGAAGGTCAGG	*Cis* gene (-18/+55)
O261, O262	GCCCCCATTCCTGAGATTTAA	CCCGTCCTGGAGAACCTCTTA	*Cis* gene (+340/+394)
O245, O246	AATTTTCGGACTCTTCGGCA	CACCCAAGAAAGGAAGGCAG	*Cis* gene (+1061/+1112)
O249, O250	GAGGACACTGCCTTCCCTCA	AAGCTTCTACCCACTCCGGC	*Cis* gene (+2236/+2308)
O92, O93	TACCCCTTCCAACTCTGACTGAGC	TTCCCTCCAGGATGTGACTGTG	*Cis* gene (+3963/+4029)
O313, O315	CCTGGCGTCTAACGGTCTG	TGGTTCCTCCTAGTCCTGGTTT	*Id-1* gene (-1048/-979)
O311, O312	GGACCAGGCGCTACTTTCC	TGGTTCCTCCTAGTCCTGGTTT	*Id-1* gene (+5343/+5403)
O324, O325	GCATGATATGATGTGCAGTTTCTTC	TCAGGACTGGTGGTTGGTTG	*ILR2a* gene (-1290/-1170)
O326, O327	AAACACTGCCCACACCTCCT	TTTGCGGTAATTTTTCAAACCA	*ILR2a* gene (-95/-28)
O336, O337	TTCACGGAACACAGGCTCAC	GCCTTCTGGCTGATTTCCAC	*MKP-1* gene (-3431/-3374)
O338, O339	GGCAGCAGTTCCAGCTCTTT	GCTGTGGAGTTCTGCCCTCT	*MKP-1* gene (-1731/-1672)
O136, O137	ATGTTGGCAGTGACCTTGAGGG	CACCTGAGAAAGCGAGAGAGAAAAG	*Osm* gene (-737/-676)
O138, O139	CATCATCCTTGGGCGTGGGGC	CGCTCCTCCTCCCGTTTTCTTCG	*Osm* gene (-184/-122)
O140, O141	GCTGCCAGCCTGCAGGACAC	GTACTCTGGCCCGTGCCTCTCAG	*Osm* gene (+25/+87)
O142, O143	CGGTCCACTACAACACCAGATGTC	TATCCCCAGAGAAAGCCACAGC	*Osm* gene (+2917/+2981)
O328, O329	GCACAGTGGAAGGGAAAAGC	ACCCACCACATCCAACATCA	*Spi2.1* gene (-1767/-1706)
O330, O331	AAATCACCCGGTCTGTCCAT	TGTTGATGCAGATAAGCTGTGC	*Spi2.1* gene (-120/-61)
O332, O333	TAAAGCCCTTGCCTGTGACC	GCTATCCCCGACAGAATGACA	*TNFRSF13b* gene (-562/-489)
O334, O335	GGAACGGCAAGATGGAAGAT	CCATGGACTTCCCAGAAAGC	*TNFRSF13b* gene (+1689/+1765)
O144, O145	GACCATCTCCGAAATCCTACACGC	CACATTTGGGATCTTAGGGGGTCTC	*c-Fos* gene (-259/-200)
O146, O147	GGAAGTCCATCCATTCACAGCG	CAGTCGCGGTTGGAGTAGTAGGC	*c-Fos* gene (-70/-1)
O148, O149	ATCGGCAGAAGGGGCAAAGTAG	CCACAAAGGTCCAGAATCGCTG	*c-Fos* gene (+1260/+1313)
O291, O292	CTAAATCCGAGGAGGAAGACTGG	GCTGTGAGTTCTGACATCTGCTCTC	*p21* gene (-1968/-1891)
O293, O294	GAGGGCGGGCCAGCGAGTC	CTCAGAGGCAGGACCAACCCACTC	*p21* gene (-120/-61)
O295, O296	ATCCAGACATTCAGAGGTGAGAGC	CATTGCTACGGGGAAGAACTATTG	*p21* gene (+75/+136)

O297, O298	AAGGGAGCATCGAAGAGCAGG	CAGCCTTGGTCTTGACTTTCGG	*S16* gene (-307/-247)
O299, O300	CTGAAAAATCGGCTGGGTTGGC	CTCCACACCGCAGCGCCG	*S16* gene (-32/+31)
O301, O302	GAAGTTCATAGTTGCCTGTCACTCC	TGTGCCCATAGAGACCAGAAGAGG	*S16* gene (+1182/+1258)
O201, O202	GGGGAAAGGCTGCTCATAATTCT	GGGAGGAACTGGCAGACTTCAC	*Igk* gene (E_{ki})

2.1.13 Software

Application	product designation	company
Flow cytometry acquisition	BD FACSDiva	BD Biosciences USA - Franklin Lakes,
Flow cytometry analysis	FlowJo 7.6.3 and 10.4.2	Tree Star Inc. USA - Ashland
Western blot imaging	ImageQuant TL 7.0	GE Healthcare Europe GmbH D - Freiburg e healthcare
Table calculation	Microsoft Excel 2010	Microsoft Deutschland GmbH D - Unterschleißheim
(RT-)qPCR acquisition/analysis	Rotorgene Q series software	Qiagen GmbH, D - Hilden
Live microscopy imaging	TissueFAXS -	TissueGnostics GmbH, A - Wien
Cloning	Vector NTI® Software	Thermo Fisher Scientific GmbH, D - Dreieich

2.1.14 Organisms

designation	species	type	source
Ba/F3	*Mus musculus*	immortalized pro-B cell cell line	kind gift from Jacqueline Marvel (IFR 128, BioSciences Gerland-Lyon Sud, France)
human lymphocytes	*Homo sapiens*	primary cells from donor blood	kind gift from Melanie Werner-Klein (Insitute for Immunology, University of Regensburg, Germany)
competent *E. coli*	*Escherichia coli* XL1-blue	host bacteria for cloning	kind gift from Institute for Immunology, University Regensburg, Germany

2.2 Methods

If not specified otherwise, experiments were performed at room temperature. H_2O stands for ultrapure water (filtered by Milli-Q Integral Water Purification System), if not specified otherwise.

2.2.1 Cell culture

2.2.1.1 Cell maintenance and selection of stable cell lines

The immortalized IL-3-dependent murine pro-B cell line Ba/F3, derived from bone marrow (Palacios and Steinmetz, 1985), was obtained from Jacqueline Marvel (IFR 128, BioSciences Gerland-Lyon Sud, France) as a kind gift. From this parental Ba/F3 cell line the following stable cell lines were generated in the present study:

- Ba/F3-wt
- Ba/F3-1*6
- Ba/F3-tet-on
- Ba/F3-tet-on-wt
- Ba/F3-tet-on-1*6

They were kept sterilely in an incubator (Heraeus® BBD6220) at 37 °C with humidified 5 % CO_2 atmosphere. All cell lines grew in suspension in a standard medium with specific additives. They were kept at densities of 0.2 to 0.8 x 10^6 cells/ml. The standard medium consisted of RPMI 1640 medium (containing L-glutamine and 2.0 g/l $NaHCO_3$) supplemented with additional 2 mM L-glutamine, 100 U/ml penicillin, 100 U/ml

streptomycin and 10 % heat-inactivated FCS (i) or FCS (ii). The additives used for culturing the different cell lines are specified in Table 3. All cell lines except Ba/F3-1*6 are dependent on IL-3 and thus were supplemented with 2 ng/ml recombinant murine IL-3. Selective agents were used to select stably transfected Ba/F3 cells, which integrated vectors encoding respective resistance genes as specified in the results section. For selection of clonal stable cell lines higher concentrations of selective agents were used as opposed to later maintenance (Table 3). The concentrations were determined by titration experiments. For maintenance the cells were passaged every two to three days for up to 15 passages by splitting and adding pre-warmed medium. If necessary, the cells were cryoconserved. For cryoconservation 10 to 20 x 10^6 cells per vial were pelleted (300 rcf, 3 min) and resuspended in 1 ml FCS with 10 % DMSO and frozen incrementally at −20 °C, then −80 °C and then in liquid N_2. For thawing, the cryoconserved cells were added to medium and incubated for a few hours before spinning down to remove toxic DMSO.

Table 3: Culture media additives used for Ba/F3 cell lines

The additives to standard medium for culturing the cell lines used in the present study are specified in this table. For selection of clonal stable cell lines higher concentrations of selective agents were used as opposed to maintenance. '✔'specifies use as opposed to '✖'

components:	Ba/F3	Ba/F3-wt and Ba/F3-tet-on		Ba/F3-1*6		Ba/F3-tet-on-wt and Ba/F3-tet-on-1*6	
	main-tenance	selection	main-tenance	selection	main-tenance	selection	main-tenance
standard medium	✔	✔	✔	✔	✔	✔	✔
IL-3	2 ng/ml	2 ng/ml	2 ng/ml	✖	✖	2 ng/ml	2 ng/ml
G418	✖	0.8 mg/ml	0.5 mg/ml	0.8 mg/ml	0.5 mg/ml	0.8 mg/ml	0.5 mg/ml
hygromycin B	✖	✖	✖	✖	✖	1 mg/ml	0.8 mg/ml

2.2.1.2 Stable cell line generation

To generate stable transgenic Ba/F3 cell lines, the expression vector has to integrate into the genome, because non-integrated vectors are not replicated by the cells during proliferation. To introduce vectors into Ba/F3 cells, electroporation was used. A shortly applied electric field temporarily permeabilizes the cell membrane, permitting introduction vector DNA into cells. Thereupon, the integration of the expression vector into the genome is based on stochastic events.

To transfect Ba/F3 cells by electroporation, 1 x 10^6 cells were pelleted (300 rcf, 3 min), washed once with PBS (300 rcf, 3 min) and resuspended in 100 µl electroporation buffer. Beforehand, the electroporation buffer had been supplemented with up to 2 µg vector DNA. The cell suspension was transferred to an electroporation cuvette (Gene Pulser/MicroPulser Cuvettes). Electroporation was performed using an electroporator (Gene Pulser Xcell CE Module) with two successive pulses à 5 ms at 95 V. After electroporation the cells were returned into 3 ml standard medium, optionally supplemented with 2 ng/ml IL-3. The cell suspension was kept in the incubator for 2 days for recovery and then supplemented with a selective agent as specified in Table 3. Only cells, which integrated the vector bearing a resistance gene, survived selection. After one to two weeks of selection, the remaining cells formed a presumably heterogeneous stably transfected bulk culture, whose transgene expression was verified as specified in the results section. To select clonal cell lines, cell density of the bulk culture was determined and the cell suspension was diluted with standard medium (supplemented with respective additives, Table 3) in a limiting dilution. Using 96 well plates the cells were diluted to densities reaching from 50 down to 0.5 cells/ml. After one to two weeks, some wells exhibited proliferating presumably clonal cells, whose transgene expression

was verified as specified in the results section. The limiting dilution was repeated at least once. Thus, stably transfected clonal Ba/F3 cell lines were isolated.

2.2.1.3 Resting and IL-3 stimulation

To turn STAT5A/B activation off in Ba/F3 or Ba/F3-wt cells, they were washed twice (300 rcf, 3 min) with pre-warmed RPMI medium (no additives) and then rested for 9 to 12 h in standard medium lacking IL-3. Optionally, the cells were pre-treated with 0.2 µM trichostatin A (TSA), a HDAC inhibitor, for 30 min to inhibit STAT5A/B transactivation activity. An equal volume of DMSO was used as a vehicle control. To turn STAT5A/B activation on, the rested cells were stimulated with 0.6 ng/ml IL-3 for 30 min. Thus simply put, STAT5A/B activation *per se* and its transcriptional activity specifically could be turned on/off, as specified in Table 4.

Table 4: STAT5A/B activation *per se* and STAT5A/B transcriptional activity was turned on/off

The table illustrates the experimental set-ups used to selectively turn STAT5A/B activation *per se* and STAT5A/B transcriptional activity on/off in Ba/F3 and Ba/F3-wt cells. Resting without IL-3 and IL-3 stimulation turns STAT5A/B activation off/on. Pre-treatment with TSA or the vehicle control DMSO before IL-3 stimulation turns STAT5A/B transactivation activity on/off. Concentrations of additives and further experimental details are specified in the text. '✔' and '✖' specify applied or omitted treatments, respectively. '+' and '−' specify present and absent effects, respectively.

*STAT5A/B transcriptional activity is not inhibited by TSA, but coupled to overall STAT5A/B activation.

Abbreviations: DMSO = dimethyl sulfoxide, TSA = trichostatin A.

treatment			effect		designation
resting (−IL-3, 9–12h)	pre-treatment (45 min)	IL-3 stimulation (+IL-3, 30 min)	STAT5A/B activation *per se*	STAT5A/B transcriptional activity	
✔	✖	✖	−	−*	− IL-3
✔	✖	✔	+	+	+ IL-3
✔	+ DMSO	✖	−	−*	+ vehicle / − IL-3
✔	+ DMSO	✔	+	+	+ vehicle / + IL-3
✔	+ TSA	✖	−	−	+ TSA / − IL-3
✔	+ TSA	✔	+	−	+ TSA / + IL-3

2.2.1.4 Doxycycline induction and removal

Ba/F3-tet-on-wt and Ba/F3-tet-on-1*6 cells inducibly express transgenic STAT5A-wt and STAT5A-1*6 in response to doxycycline administration. A standard induction protocol was established in the present study as specified in the results section. To induce transgene expression, Ba/F3-tet-on-wt and Ba/F3-tet-on-1*6 cells were washed twice (300 rcf, 3 min) with pre-warmed RPMI medium (no additives) and then put into standard medium supplemented with IL-3 or lacking IL-3, respectively. Then, 1 µg/ml doxycycline was administrated to the medium. For sustained induction of transgene expression, 100 ng/ml doxycycline was replenished every two days. Cells that were not administrated with doxycycline were grown in parallel as a control. To halt transgenic STAT5A-wt and STAT5A-1*6 expression in induced cells, cells were washed twice (300 rcf, 3 min) with pre-warmed RPMI medium (no additives) to remove doxycycline and then put into standard medium supplemented with IL-3 or lacking IL-3, respectively.

2.2.1.5 Trypan blue staining-based cell counting

To track absolute cell numbers and to harvest defined amounts of Ba/F3 cells, their density in suspension was determined using a Neubauer counting chamber (Neubauer-improved). Before counting, the cell suspension was diluted 1 : 1 with trypan blue solution, staining dead/dying cells blue due to their increased membrane permeability. With a depth of 0.1 mm and an area 1 mm^2 per larger square, cells counted in one larger square correspond to 1 mm^3 (= 1 µl) of fluid. Hence, cell density was determined with following formula (since 10,000 * 1 mm^3 = 1 ml):

$$average\ count\ per\ larger\ square * dilution\ factor\ 2 * 10{,}000 = cell\ density/ml$$

The cell suspension diluted with trypan blue was loaded in the Neubauer counting chamber and at least four mini-squares were counted using an optical microscope (Olympus CK2). Living and dead/dying cell densities were computed for a given cell suspension with the stated formula. Thus, the percentage of dead/dying cells could be calculated. In addition, absolute living cell numbers could be calculated based on the volume of the given cell suspension. This allowed calculating doubling times using the following formula (Microsoft Office Excel):

$$24h * \log_2\left(\left[\frac{total\ living\ cell\ number\ after\ interval}{total\ living\ cell\ number\ before\ interval}\right]^{\frac{24h}{interval\ in\ h}}\right) = doubling\ time\ in\ h$$

2.2.1.6 Living cell fluorescence microscopy

Ba/F3-tet-on-wt and Ba/F3-tet-on-1*6 cells inducibly express *Aqueorea coerulescens* green fluorescent protein 1 (AcGFP1). Thus, they emitted native GFP fluorescence after induction of transgene expression. To monitor GFP fluorescence and evaluate homogeneity within the cell population, induced living cells were transferred into a 6 well plate and analyzed using TissueFAXSiPLUS system in parallel to AcGFP1-negative cells. Images of the emitted GFP fluorescence were recorded at a 20 x magnification using the manufacturer's software.

2.2.2 Gene expression analyses

Gene expression analysis by relative quantification of mRNA is a standard procedure in molecular biology to determine gene expression levels. For this, mature mRNA is isolated from cells and reverse transcribed into cDNA, which serves as a template in RT-qPCR. The relative quantification is performed on the basis of a housekeeping gene with stable expression level. Thus, this method permits observing changes in gene expression levels under different conditions.

2.2.2.1 Cell harvest

0.4 x 10^5 Ba/F3 cells were harvested into 1 ml ice-cold PBS. Cells were pelleted by centrifugation (2,000 rcf, 1 min, 4 °C). The dry pellet (optionally supplemented with 20 µl of RNA lysis buffer) was processed immediately on ice or flash-frozen in liquid nitrogen and stored at −80 °C for further use.

2.2.2.2 RNA preparation

RNA was prepared with the iScript RT-qPCR Sample Preparation Reagent according the manufacturer's protocol. This reagent is designated to prepare selectively cytoplasmic mRNA for RT-qPCR. It selectively lyses the cytoplasmic membrane, allowing isolation of cytoplasmic RNAs and removal of the nuclear fraction containing the genomic DNA by centrifugation. Constituent RNase inhibitors and RNA stabilizers protect isolated mRNAs. All steps were performed on ice. 100 µl of iScript RNA preparation buffer (80 µl, if 20 µl of it was added before flash-freeze) was added to the dry cell pellet. After vortexing (medium speed, 30 s, room temperature) the lysate was centrifuged (15,000 rcf, 2 min, 4 °C) and 80 µl of the supernatant transferred into a new tube. This RNA lysate was used for cDNA synthesis immediately afterwards and could be stored at −80 °C after flash-freeze with liquid nitrogen for potential re-use.

2.2.2.3 cDNA synthesis

cDNA was synthetized with the iScript cDNA synthesis kit according to the manufacturer's protocol. This kit contains the components needed for cDNA synthesis. In particular, the 5x iScript reaction mix comprises buffer and primers necessary for the

reaction, where the iScript reverse transcriptase transcribes the RNA template into cDNA using the primers as starting points (both oligo(T) and random hexamer primers).

The reaction was set up on ice as follows:

- 1 µl RNA template (prepared RNA lysate)
- 14 µl Nuclease-free water
- 1 µl iScript reverse transcriptase
- 4 µl 5x iScript reaction mix

The components were pipetted into a 50 µl tube and mixed by pipetting up and down. The reverse transcription was performed in a thermal cycler (myCycler) with the following program:

- 5 min 25 °C
- 30 min 42 °C
- 5 min 85 °C

The cDNA samples were stored after the reaction at −20 °C for further use.

2.2.2.4 Reverse transcription quantitative PCR (RT-qPCR)

Accurate relative quantification of cDNA templates can be performed by reverse transcription quantitative PCR (RT-qPCR). As with conventional PCR, DNA is amplified by a thermo-stable DNA polymerase with sequence-specific forward and reverse primers. Though, a DNA-dependent fluorochrome is added to the reaction. SYBR green, used in the present study, binds specifically to dsDNA. After excitation at λ = 494 nm it emits light at λ = 521 nm when bound to dsDNA, but not when in solution. Using SYBR green the amount of DNA in the reaction can be measured in each amplification cycle as a fluorescence signal. Since the sensitive range of the fluorometer is limited, linear changes in fluorescence intensity can only be detected for a certain range of fluorescence intensities and thereby only certain amplification cycles. In the threshold cycle (C_t-value) the fluorescence intensity rises into the sensitive range above background level. Within the sensitive range the fluorescence intensity increases exponentially, eventually reaching a plateau because of the detection limit. The original amount of cDNA (and hence mRNA) can be quantified relatively, by comparing the C_t-values for a stably expressed housekeeping gene with C_t-values for the gene of interest. The relative quantity in this study was calculated with the formula:

$$2^{[C_t(housekeeping\ gene)-C_t(gene\ of\ interest)]} * 10{,}000$$

When using this formula, however, the amplification efficiency for different primers and hence DNA templates must be the same. Primer efficiencies were determined and validated beforehand by PD Dr. Anne Rascle.

Table 5: Set-up of reverse transcription quantitative PCR (RT-qPCR) reaction
The composition of RT-qPCR reactions is specified in this table.

RT-qPCR		
composition per individual reaction:		
reaction component:	**volumes:**	**end concentration:**
self-made qPCR mix (25 mM $MgCl_2$, 25 mM each dNTP)	9.67 µl	2.5 mM $MgCl_2$ 0.2 mM each dNTP
SYBR green I solution	0.25 µl	1:500,000
Hotstart-Taq DNA Polymerase (5 U/µl)	0.08 µl	0.4 U/µl
H_2O	4.6 µl	
cDNA template	0.4 µl	~8 single cells
forward and reverse primer mix (each 1.6 µM) – on top	5 µl	0.4 µM each primer
	20 µl	

The reaction was set up as specified in Table 5. Each reaction was performed in triplicates or duplicates. SYBR green (solved in DMSO) was thawed at room temperature before. All remaining components were thawed and handled at 4 °C. The components

except for the primers were mixed in a master mix and pre-loaded into the qPCR tubes. The primer mix was pipetted on top. The RT-qPCR was performed with the Rotorgene Q qPCR cycler with the following program. The forty amplification cycles included only two temperature steps, 95 °C for denaturation and 60 °C for annealing and elongation:

- 15 min 95 °C activation of Hotstart-Taq DNA Polymerase
- 40 x 15 s 95 °C denaturation
  60 s 60 °C annealing and elongation
- high resolution melting from 60 °C to 95 °C

Fluorescence intensities were acquired at the end of each amplification cycle. SYBR green was excited with $\lambda = 470$ nm and the emitted fluorescence was recorded at $\lambda = 510$ nm. High resolution melting permitted evaluation of fragment sizes, which should be equal for each primer pair. The data were analyzed and the C_t-values were extracted with the Rotorgene Q series software. Gene expression analysis was performed using the stated formula (Microsoft Office Excel). The ribosomal protein gene *S9* was used as housekeeping gene, with another ribosomal protein gene *36B4* serving as an internal control. The obtained gene of interest mRNA levels were expressed as arbitrary units relative to *S9* mRNA level.

2.2.3 Protein analyses

Protein expression analysis by Western blot is a semi-quantitative standard procedure in molecular biology for the detection of proteins. For this, protein is isolated from cells and denatured with SDS allowing separation by size in polyacrylamide gel electrophoresis. After blotting the proteins on a membrane, specific proteins can be detected with antibodies.

2.2.3.1 Cell harvest

1×10^6 to 5×10^6 Ba/F3 cells were harvested by centrifugation (300 rcf, 3 min, 4 °C). The cell pellet was washed once with PBS and the dry pellet was processed immediately on ice or flash-frozen in liquid nitrogen and stored at −80 °C for further use.

2.2.3.2 Protein isolation

Protein was isolated from whole cells with Brij lysis buffer containing Brij, a detergent, which lyses both the cytoplasmic and nuclear membrane and thus allows separation of proteins from other cellular components. All following steps were performed on ice. Directly before use the Brij lysis buffer was supplemented with protease and phosphatase inhibitors (10 µg/µl aprotinin, 10 µg/µl leupeptin, 0.5 mM PMSF, 10 mM Na_3VO_4, 10 mM NaF) to prevent protein degradation and dephosphorylation. If flash-frozen before, the dry cell pellet was thawed on ice. The cell pellet was resuspended in 20 µl to 100 µl Brij lysis buffer (+ inhibitors) according to cell number (20 µl per 1×10^6 cells) and incubated on ice for 20 to 30 min. After centrifugation (maximum speed, 15 min, 4 °C) to remove debris the supernatant was transferred to a new tube. The received protein lysate was processed immediately or flash-frozen in liquid nitrogen and stored at −80 °C for further use.

2.2.3.3 Protein quantification by Bradford assay

Protein quantification was performed according to Bradford (1976) using Bradford reagent containing the dye Coomassie Brilliant Blue-G250. This dye shifts its adsorption maximum to $\lambda = 595$ nm upon forming complexes with proteins. Protein concentration can be calculated by measuring optical density of a protein lysate together with a protein standard curve after incubation with Bradford reagent. In detail, 1 µl protein lysate and a standard curve consisting of 0, 1, 2, 5, 10, 20 µg BSA (bovine serum albumin) were each added to 1 ml 1x Bradford reagent. After mixing and incubation for around 5 min the

optical density was measured at λ = 600 nm with the UV photometer BioPhotometer®. Protein concentration was calculated based on linear regression of the standard curve.

2.2.3.4 SDS-PAGE

Proteins were separated by molecular mass in a denaturing discontinuous polyacrylamide gel electrophoresis (PAGE) as established by Laemmli (1970). Briefly, the protein lysates are treated with Laemmli buffer containing the denaturing agent SDS to mask their intrinsic charge making their (negative) charge dependent on protein size. After denaturation the proteins are separated in a vertical discontinuous polyacrylamide gel by electrophoresis. The proteins are compressed at the boundary of the upper stacking gel (pH 8.8) and then separated by molecular mass in the lower separating gel (pH 6.8). This is achieved with glycine, which functions as trail ion in the stacking gel, but changes to slow ion in the separating gel in response to the lower pH, compressing the proteins at the boundary of the two gel phases.

For SDS-PAGE, equal amounts of proteins were used for each sample. The protein lysates were thawed on ice, if flash frozen before. The protein sample (20 to 50 µg per lane depending on the experiment) was converted to 1x Laemmli buffer, using 4x Laemmli buffer and the lysis buffer for dilution. The samples were denatured for 5 min at 95 °C and spinned down before loading. The discontinuous polyacrylamide gel was poured beforehand using a horizontal, two-dimensional gel system (Sub-Cell® GT Cell). Composition of the gels is specified in Table 6. The polyacrylamide percentage was chosen based on the size of the analyzed protein. The separating gel was overlaid with H_2O for a horizontal upper edge. After polymerization H_2O was removed and the stacking gel poured on top. A protein marker (Protein Marker VI (10 - 245) prestained) was loaded on the gel along with the protein samples. Free lanes were also loaded with 1x Laemmli buffer. PAGE buffer was used both as anode and cathode buffer. The electrophoresis was run at 80 V for the stacking gel and 200 V for the separating gel.

Table 6: Composition of discontinuous polyacrylamide gels for SDS-PAGE
The composition of discontinuous polyacrylamide gels for SDS-PAGE is specified in this table.
Abbreviations: SDS-PAGE = SDS polyacrylamide gel electrophoresis.

gel phase:	stacking gel	separating gel	separating gel
percentage:	**4 %**	**8 %**	**10 %**
H_2O	7,300 µl	2,860 µl	2,200 µl
1 M Tris pH 8.8	-	3,750 µl	3,750 µl
1 M Tris pH 6.8	1,250 µl	-	-
29.2 % acrylamide, 0.8 % bisacrylamide (37.5 : 1 | in H_2O)	1,300 µl	2,660 µl	3,330 µl
glycerol	-	574 µl	574 µl
10 % SDS (in H_2O)	100 µl	100 µl	100 µl
10 % APS (in H_2O)	50 µl	50 µl	50 µl
TEMED	10 µl	10 µl	10 µl

2.2.3.5 Western blot

For Western blot, the proteins separated by molecular mass in SDS-PAGE are blotted on a membrane by applying an electric field. The proteins migrate into fine pores of the membrane, where they bind through intermolecular forces. Specific proteins can be detected immunologically on the membrane. Primary antibodies bind to their epitope in specific proteins on the membrane. They are detected by secondary antibodies (targeting the Fc region of the primary antibodies) conjugated with horseradish peroxidase (HRP). HRP can catalyze chemiluminescence of a substrate allowing optical detection.

After SDS-PAGE the stacking gel was removed and the separating gel was equilibrated in Transfer buffer for 5 min. Beforehand, a PVDF membrane (Immobilon-P Membrane,

PVDF | pore size 0.45 µm) was activated with 100 % methanol for 15 s, washed for 2 min with H_2O and equilibrated in Transfer buffer for 5 min together with Whatman chromatography paper. For blotting, the separating gel was placed on top of the membrane and the stack encased with three Whatman chromatography papers. The proteins were blotted onto the membrane in a semi-dry electroblotting cell (Trans-Blot® SD Semi-Dry Transfer Cell) after removing excess liquid at 24 V for 1 h.

Immunological detection of proteins was performed as follows for all antibodies except for anti-pSTAT5A/B. First, the membrane was blocked for 30 min with 1x PBST plus 5% dry milk to saturate unspecific binding sites. Second, the membrane was incubated for 1 h (or overnight at 4 °C) with 1x PBST plus 3% dry milk and primary antibody in the dilution specified in 2.1.7. Third, after washing three times with 1x PBST for 10 min to remove excess primary antibody, the membrane was incubated with 1x PBST plus 3% dry milk and secondary antibody (against the animal, the primary antibody was raised in) in the dilution specified in 2.1.8. Fourth, after washing three times with 1x PBST for 10 min, antibody binding was detected using the ECL Prime detection reagent or Femto detection reagent (only for very weak signals) according to the respective manufacturer's protocol. The detection reagents emit chemiluminescence dependent on HRP activity, which was detected with a Western blot imaging system (ImageQuant LAS 4000 Mini) using the manufacturer's software (ImageQuant TL 7.0). The membrane could be re-detected with another primary antibody by adding 0.2 % NaN_3 (sodium azide) in the blocking step, which irreversibly inhibits activity of the already bound HRP.

Detection with anti-pSTAT5A/B antibody was performed with a different protocol due to the higher sensitivity of the epitope (phosphorylated $Tyr^{694/699}$ in mSTAT5A/B). First, the membrane was blocked for 30 min with 1x TBST plus 3 % BSA to saturate unspecific binding sites. Second, the membrane was incubated overnight at 4 °C with 1x TBST plus 3% BSA and anti-pSTAT5A/B antibody diluted 1 : 1,000. Third, after washing three times with 1x TBST for 10 min, the membrane was incubated with 1x TBST plus 3 % BSA and anti-rabbit antibody diluted 1 : 20,000. Fourth, after washing three times with 1x TBST for 10 min, antibody binding was detected as specified above.

2.2.4 Chromatin analyses

Chromatin immunoprecipitation (ChIP) is an established method to analyze DNA-protein-interactions in chromatin. To do this, DNA-protein interactions are stabilized by cross-linking. This cross-linked chromatin is fragmented and the obtained fragments containing specific proteins can be immunoprecipitated by antibodies. Co-precipitated DNA fragments can be mapped and quantified by qPCR using sequence-specific primers.

2.2.4.1 Preparation of Protein A sepharose beads

For immunoprecipitation of fragments bound by antibodies, Protein A sepharose beads were used. The Protein A sepharose beads (Protein A Sepharose CL-4B) were reconstituted and washed according to the manufacturer's protocol (in/with H_2O, centrifugation: 500 rcf, 30 s, 4 °C). A 50% Protein A sepharose slurry was prepared by addition of an equal volume of 1x TE buffer supplemented with 1 mg/ml fatty-acid free BSA and 400 µg/ml salmon sperm DNA. To saturate unspecific binding sites for both DNAs and proteins, it was rotated overnight at 4 °C. The Protein A sepharose slurry was stored at 4 °C and homogenized by inverting before use.

2.2.4.2 Cell harvest and cross-linking

Formaldehyde induces covalent, but heat-reversible, cross-linking between proteins and DNA as well as between proteins at a distance of at most 2 Å. It was used in the study to conserve DNA-protein-interactions for ChIP. For cross-linking, 1 % formaldehyde was

added to a Ba/F3 cell suspension and incubated for 10 min at room temperature. Formaldehyde was neutralized by addition of 125 mM glycine and incubation for 5 min. The cell suspension was further processed on ice. After pelleting the cells (2,000 rcf, 3 min, 4 °C) the supernatant was removed. The cell pellet was washed twice with PBS (2,000 rcf, 3 min, 4 °C) and distributed to pellets à 2×10^7 cells. The dry pellets were processed immediately or flash-frozen in liquid nitrogen and stored at −80 °C for further use.

2.2.4.3 Chromatin shearing by sonication

Shearing chromatin by application of ultrasound is a non-biased method to obtain small chromatin fragments. All following steps were performed on ice. Directly before use the SDS lysis buffer and Triton X-100 dilution buffer were supplemented with protease inhibitors to prevent degradation (10 µg/µl aprotinin, 10 µg/µl leupeptin, 0.5 mM PMSF). If flash-frozen before, the dry pellet of 20×10^6 cells was thawed on ice. The pellet was resuspended in 3 ml SDS lysis buffer and sonicated using a sonifier (Branson Sonifier® S-250A analog ultrasonic processor, 5 mm tip sonotrode). Sonication conditions were optimized to shear the chromatin into fragments of around 100–300 bp length (6 pulses à 1 min, 2 min pause, output 5, 60% duty cycle). During and between sonication pulses the lysate was cooled with iced water. After sonication, 1.5 ml Triton X-100 dilution was added to the sonified lysate and debris was removed by centrifugation (4,000 rcf, 10 min, 4 °C). The supernatant was transferred to a new tube and pre-cleared to avoid unspecific binding during ChIP. For pre-clearing, 200 µl Protein A sepharose slurry was added to the lysate and rotated for 1 h at 4°C. The Protein A sepharose beads were removed afterwards (centrifugation: 500 rcf, 30 s, 4 °C). The pre-cleared lysates were processed immediately or flash-frozen in liquid nitrogen and stored at −80 °C for further use.

2.2.4.4 Quality control of chromatin shearing

To ensure comparable results in all ChIP experiments, the chromatin fragments should exhibit similar sizes, as pull-down efficiencies may differ among fragments of different size. Therefore, the DNA encased in the chromatin fragments was purified and their size was evaluated by agarose gel electrophoresis.

The DNA was purified by phenol-chloroform extraction and subsequent ethanol precipitation. 380 µl of pre-cleared sonified lysate was supplemented with 95 ng/µl Proteinase K and 114 ng/µl glycogen. It was incubated for 1 h at 55 °C for protein digest and then overnight at 65 °C to reverse formaldehyde cross-linking. After equilibration to room temperature one volume (400 µl) of phenol/chloroform/isoamyl alcohol was added. The sample was vortexed (maximum speed, 1 min) and centrifuged (maximum speed, 5 min, room temperature). The upper aqueous phase (300 µl) containing DNA was transferred to a new tube and supplemented with 300 mM NaAc, as cations are essential for ethanol precipitation. 1000 µl of chilled 100% ethanol (−20 °C) was added and the sample was incubated for 20 min at −20 °C after mixing. The DNA precipitated and was pelleted by centrifugation (maximum speed, 15 min, 4 °C). After washing the DNA pellet with 700 µl chilled 70% ethanol (−20 °C | maximum speed, 15 min, 4 °C), it was air-dried for 15 min to remove residual ethanol and resuspended in 50 µl 1x TE supplemented with 0.2 µg/µl RNase A for RNA digestion. After incubation for 30 min at 37 °C, the now purified DNA was processed immediately or stored at −20 °C. For agarose gel electrophoresis, 1.5% agarose was added to 0.5 TAE buffer. The mixture was heated until all agarose was dissolved and cooled down to about 50 °C. After adding around 1% ethidium bromide solution, agarose gels were poured using a horizontal, two-dimensional gel system (Sub-Cell® GT Cell). For electrophoresis, 6 µl of purified DNA, corresponding to approximately 0.2×10^6 cells, was supplemented with DNA loading dye and loaded on the agarose gel. Electrophoresis was performed in 0.5 TAE buffer at 100 V

for about 30 min. The DNA bands were evaluated visually using a gel documentation system (GeneGenius Gel Imaging System).

2.2.4.5 Chromatin immunoprecipitation

The pre-cleared sonified lysate contains chromatin fragments of DNA cross-linked with associated proteins. Using specific antibodies, chromatin fragments containing certain proteins can be pulled down by chromatin immunoprecipitation (ChIP). All following steps were performed on ice. If flash-frozen before, the pre-cleared sonified lysate was thawed on ice. 50 µl of lysate was taken as input for later normalization to total DNA amount. 750 µl lysate, corresponding to 3.3×10^6 cells, was supplemented with an antibody and rotated for 3 h at 4 °C to allow antibody binding. The amount of antibody used is specified in 2.1.9. 30 µl Protein A sepharose slurry was added and the lysate was rotated for 2 h at 4 °C to pull down the fragments bound by the antibody. The beads were sedimented by centrifugation (500 rcf, 30 s, 4 °C) and the supernatant was aspirated. Then, the beads were washed to remove non-specifically bound fragments with 900 µl of the respective washing buffer as follows (sedimentation and aspiration as described above):

- ChIP buffer → washed by repeated inverting
- 150 mM NaCl wash buffer → washed by repeated inverting
- 500 mM NaCl wash buffer → washed by rotating for 5 min at 4 °C
- LiCl wash buffer → washed by rotating for 5 min at 4 °C
- 1x TE → washed by repeated inverting

To quantify the co-precipitated chromatin fragments, the DNA was purified. For this, all steps were performed at room temperature. Reverse cross-linking buffer was added to the input samples as well as to the ChIP samples (= Protein A sepharose beads) for a total volume of 120 µl. Both input and ChIP samples were supplemented with 250 mM NaCl, to stabilize DNA with low GC content at higher temperatures. To reverse formaldehyde cross-linking, the samples were incubated overnight at 65 °C. After equilibration to room temperature, they were supplemented with 0.25 µg/µl RNase A and incubated for 1–2 h at 37 °C for RNA digest; and then with 0.4 µg/µl Proteinase K and incubated for 1–2 h at 55 °C for protein digest. The input and ChIP DNA samples were purified using a DNA purification kit (NucleoSpin® Gel and PCR Clean-up) according to the manufacturer's protocol for SDS-containing samples. Briefly, the DNA samples were mixed with 600 µl NTB buffer and loaded on the columns by centrifugation (11,000 rcf, 30 s). They were washed twice with NT3 buffer (centrifugation: 11,00 rcf, 30 s), spinned down to remove excess buffer (11,00 rcf, 2 min) and then air-dried for 5 min at 70 °C to remove residual ethanol. The columns were eluted twice by adding 50 µl pre-warmed elution buffer (70 °C) on the membrane, incubating for 5 min at room temperature and spinning down (11,00 rcf, 1 min). The 100 µl of flow-through contained the purified genomic DNA (gDNA) fragments. As DNA concentrations for relative quantification by qPCR should be in the same range, the ChIP samples were diluted with 200 µl H2O and the input samples with 800 µl H2O. The dilutions have been established previously (Rascle *et al.* (2003)). The purified gDNA ChIP and input samples were processed immediately or stored at −20 °C for further use.

2.2.4.6 qPCR and normalization as input percentage

Relative quantification of the gDNA template was performed by qPCR analogous to RT-qPCR for cDNA (2.2.2.4) using input gDNA as a reference. The reaction was set up as specified in Table 7. Pipetting was performed as described in 2.2.2.4, except that 5 µl gDNA (ChIP or input) was put on top the pre-mixed other components for each reaction. The qPCR was performed with the same program using the Rotorgene Q qPCR cycler.

Purified input and ChIP gDNA were run in parallel in duplicates or triplicates and the C_t-values were extracted and evaluated with the Rotorgene Q series software.

Table 7: Set-up of quantitative PCR (qPCR) reaction
The composition of qPCR reactions for gDNA templates is specified in this table.
Abbreviations: ChIP = chromatin immunoprecipitation.

qPCR composition per individual reaction:		
reaction component:	**volumes:**	**end concentration:**
self-made qPCR mix (25 mM $MgCl_2$, 25 mM each dNTP)	9.67 µl	2.5mM $MgCl_2$ 0.2mM each dNTP
SYBR green I solution	0.25 µl	1:500,000
Hotstart-Taq DNA Polymerase (5 U/µl)	0.08 µl	0.4 U/µl
forward and reverse primer mix (each 1.6 µM)	5 µl	0.4 µM each primer
gDNA template (input or ChIP sample) – on top	5 µl	input gDNA: ~123 single cells ChIP gDNA: ~5,555 single cells
	20 µl	

The relative amount of gDNA encased by the co-precipitated chromatin fragments was expressed relatively to total input gDNA as 'percentage of input' (input %). For this purpose, the volume of pre-cleared lysate corresponding to the 5 µl purified gDNA amplified per reaction was calculated for input and ChIP. The ratio between input and ChIP gDNA was calculated as follows:

$$\frac{\frac{\mu l\ input\ per\ qPCR\ reaction}{\mu l\ input\ purified\ DNA} * \mu l\ sonified\ lysate\ for\ input}{\frac{\mu l\ ChIP\ per\ qPCR\ reaction}{\mu l\ ChIP\ purified\ DNA} * \mu l\ sonified\ lysate\ for\ ChIP} = \frac{\frac{5\ \mu l}{900\ \mu l} * 50\ \mu l}{\frac{5\ \mu l}{300\ \mu l} * 750\ \mu l} = 0.0222$$

This ratio was used to normalize the ChIP C_t-values to input C_t-values. The results were expressed as arbitrary units of percentage of input (input %) using the following formula (Microsoft Office Excel):

$$2^{[C_t(input\ gDNA) - C_t(ChIP\ gDNA)]} * 0.0222 * 100$$

When using this formula, however, the amplification efficiency for different primers and hence DNA templates must be the same. Primer efficiencies were determined and validated beforehand by PD Dr. Anne Rascle applying a gDNA standard.

2.2.5 Flow cytometry

Suspensions of single cells can be analyzed for different parameters by flow cytometry, where the cells are measured individually in a stream of fluid for multiple parameters in real-time (Figure 7). In particular, a light beam is applied towards the stream of fluid/cells and detected by two optical detectors measuring light scattered by a given cell in a forward direction and a sideward direction in an angle of 90° (Figure 7). On the one hand, the light intensity measured by the FSC (forward scatter) detector is proportional to the diameter of a given cell, primarily due to light diffraction around it. On the other hand, the light intensity measured by the SSC (sideward scatter) detector informs about the internal complexity of a given cells, because intracellular structures refract or reflect light to varying degrees. Thus, FCS is a measurement for cell size and SSC a measurement for cell granularity. In addition to these two basic parameters, flow cytometers can excise fluorescent molecules in a given cell and then measure the emitted fluorescence signal intensities using filters for specific wave lengths of light (Figure 7). This permits staining of cells using fluorescent molecules. The employed flow cytometer (BD™ LSR II Flow Cytometer System) can excise at wavelengths of $\lambda = 355$, $\lambda = 495$ nm, $\lambda = 488$ nm, $\lambda = 633$ nm and, thus, measure GFP (FITC-A channel) and DAPI (DAPI channel) signals.

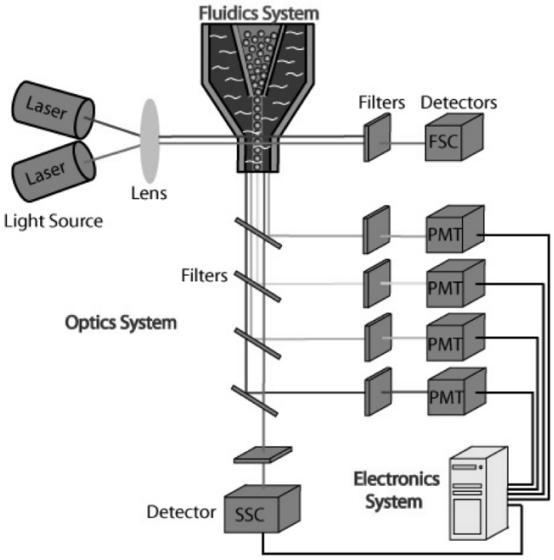

Figure 7: Illustration of a flow cytometer

(adapted from https:// www. flowjo. com/learn/ flowjo-university/flowjo/getting-started-with-flowjo/58, 17.05.18)

The figure schematically illustrates the optical system of a flow cytometer, as further detailed in text.

Abbreviations: FSC = forward scatter, PMT = photomultiplier tube, SSC = sideward scatter.

2.2.5.1 Native GFP fluorescence

Ba/F3-tet-on-wt and Ba/F3-tet-on-1*6 cells inducibly express AcGFP1 (*Aqueorea coerulescens* green fluorescent protein 1). Thus, they emitted native GFP fluorescence after induction of transgene expression, which was analyzed by flow cytometry. For this, 1 x 10^6 cells expected to be GFP-fluorescent were harvested in parallel to 1 x 10^6 control cells not expressing AcGFP1 (centrifugation: 300 rcf, 30 min, 4 °C). The cell pellet was washed once with PBS (centrifugation: 300 rcf, 30 min, 4 °C), resuspended in 2 ml PBS, transferred to a FACS tube and kept on ice for data acquisition.

2.2.5.2 Cell cycle analysis by DAPI staining

Proliferating eukaryotic cells repeatedly transition through four phases, constituting the cell cycle. The cell cycle can be studied using fluorescent dyes staining genomic DNA, with DAPI used in the present study. Hence, fluorescence intensity of a single stained cell is relative to the size of its genome. Proliferating cells double their diploid chromosome set (2 n) during the cell cycle, having 2 n in G_1/G_0 phase, 2–4 n in S phase and 4 n in G_2/M phase. Thus, the distribution of cell phases within Ba/F3 cell populations was determined by analyzing the amount of genomic DNA per cell. This permitted conclusions about their proliferation behavior. In contrast to proliferating cells, dying cells undergoing programmed cell death break down their DNA (Kerr *et al.*, 1972, Prokhorova *et al.*, 2015, Taylor *et al.*, 2008). Hence, hypoploid cells, which have DNA amounts lower than diploid 2 n, could be classified as dead/dying sub-G_1 phase cells. For cell cycle analysis, 1 x 10^6 cells were harvested (centrifugation: 300 rcf, 30 min, 4 °C). The cell pellet was washed once with PBS (centrifugation: 300 rcf, 30 min, 4 °C), resuspended in 2 ml PIPES buffer supplemented with 1 µg/ml DAPI, transferred to a FACS tube and kept for 30 min on ice protected from light before data acquisition. The PIPES buffer permeabilizes membranes, permitting intercalation of DAPI into genomic DNA.

2.2.5.3 Data acquisition and analysis

Theoretically, native GFP could be measured in cells stained with DAPI, but no GFP fluorescence was detectable after application of PIPES buffer. This is why native GFP and DAPI fluorescence were detected separately. Before data acquisition the cell suspensions were filtered with a polyamide sieve cloth and mixed thoroughly by vortexing. The multiparametric data were acquired with the BD FACSDiva software using the flow cytometer BD™ LSR II Flow Cytometer System according to the manufacturer's protocol. 20,000 events were recorded in the stream of fluid at low speed. The data was

analyzed using the FlowJo 7.6.3 software. Data was analyzed in scatter plots plotting two different parameters, where one dot corresponds to one acquired event, or as histograms, where one parameter is plotted against cell number. Cells sticking to each other (doublets) as well as debris (cell fragments) were excluded using SSC and FSC based on their deviations in length and width (doublets) or size (debris). The remaining cells were analyzed for native GFP fluorescence or DAPI staining in histograms. GFP signal from negative control cells was plotted together with the expectedly positive cells, to be able to estimate the degree of unspecific autofluorescence. The DAPI signal was analyzed with the 'Watson Pragmatic' algorithm integrated in the FlowJo 7.6.3 software, offering the percentages of cells in the three different cell phases.

2.2.6 Cloning

For the present study, stable transgenic Ba/F3 cell lines were generated. To do so, expression vectors bearing a given transgene were introduced (see Table 8). The employed expression vectors are listed in Table 8. They all bore an ampicillin resistance gene. Hence, the antibiotic ampicillin was used to select successfully transformed bacteria. The expression vectors bearing mSTAT5A.WT_FLAG and mSTAT5A.1*6_ FLAG cDNAs were generated by cloning, as specified in Table 8 and the results section. Before use, their DNA sequences were validated by Sanger sequencing (by Geneart AG, D - Regensburg). Cloning and sequence validation were conducted by PD Dr. Anne Rascle.

A) Digest with sequence-specific restriction enzymes

Digest with sequence-specific restriction enzymes was performed to excise DNA fragments from a vector and to linearize the target vector for ligation. For this, 10–20 µg vector DNA was mixed with 2 U enzyme per µg DNA and 1x CutSmart Buffer (diluted with H_2O if necessary). The mixture was incubated for 30 min at 37 °C for digest and for 10 min at 65 °C to terminate enzyme activity. The digest was verified by agarose gel electrophoresis (for procedure see 2.2.4.4). The cut DNA could be stored at −20 °C.

B) Isolation of excised DNA fragments

To isolate DNA fragments of a specific size, the DNA was separated in agarose gel electrophoresis. The desired DNA band was cut out of the agarose gel under UV light and DNA was purified using the Wizard® SV Gel and PCR Clean-Up System kit according to the manufacturer's protocol. The isolated DNA could be stored at −20 °C.

C) Ligation

The excised DNA fragments were inserted into the target vector by ligation. The target vector was cut at the same sites to ensure integration in the desired direction. Before ligation, a test agarose electrophoresis was performed to estimate DNA concentrations by comparison with marker bands (of known DNA amount). Ligation was performed with a ratio of 1.5 : 1, 3 : 1 and 6 : 1 for insert DNA : vector DNA. For the ratio 3 : 1 50 µg total DNA was used and accordingly more or less for the other ratios. Additionally, a vector-only control was performed to estimate auto-ligation rate. For ligation 15 µl 1x T4 DNA Ligase buffer was supplemented with the DNAs and 1 µl T4 DNA Ligase. The ligation reaction was incubated overnight at 16 °C.

D) Transformation

The expression vectors employed in this study bore an ampicillin resistance gene allowing selection of transformed bacteria and accurate amplification of a vector with insert. For transformation, 5 µl of ligation reaction was added to 100 µl competent *Escherichia coli* XL1-blue bacteria. The bacteria were incubated for 30 min on ice, shocked for 90 s at 42 °C and put back on ice. The bacteria were mixed with 500 µl LB medium and incubated for 1 h at 37 °C. To concentrate the bacteria, they were pelleted (5,000 rcf, 15 s) and 400 µl of supernatant were discarded. The pelleted bacteria were

resuspended in the remaining medium and plated on pre-warmed agarose plates (15 g/l agarose in LB medium) containing 100 µg/ml ampicillin. The plates were incubated overnight at 37 °C.

E) Miniprep

By comparing the vector-only control with vector-insert samples, the percentage of auto-ligations could be estimated. 5–10 colonies were picked, added to 3 ml LB medium supplemented with 100 µg/ml ampicillin and grown overnight aerobically in an incubation shaker at 37 °C (shaking: 180 rpm). The bacterial cultures were homogenized and DNA from 1,5 ml of bacteria was purified using the Wizard® *Plus* SV Minipreps DNA Purification System according to the manufacturer's protocol. Ligation could then be evaluated by agarose gel electrophoresis, where auto-ligated vectors are distinguished from vectors with insert by size. A control restriction digest was performed for validation by agarose gel electrophoresis. The bacterial cultures were kept at 4 °C for further use.

F) Midiprep

A clone of bacteria containing a vector with successful ligation of vector and insert was chosen for further amplification of the vector. 100 µl of the clonal bacterial culture was added to 50 ml of LB medium supplemented with 100 µg/ml ampicillin. The bacterial culture was grown overnight aerobically in an incubation shaker at 37 °C (shaking: 180 rpm). Vectors were isolated selectively using the QIAGEN Plasmid Plus Midi Kit according to the manufacturer's protocol, yielding 200 µl purified vector DNA. A control restriction digest was performed for validation by agarose gel electrophoresis. DNA concentration and purity were determined with a nanophotometer (NanoPhotometer® P360) with 1 µl sample. For verification of the construct, the vector DNA was sequenced by Sanger sequencing at the GeneArt AG (Thermo Fisher Scientific Inc., Regensburg) and evaluated with the Vector NTI software. The Midiprep procedure to amplify DNA was also used for existing vectors, if necessary. For this, transformed *E. coli* clones were kept in glycerol stocks.

Table 8: Expression vectors employed in the present study

The table lists the expression vectors employed in this study to generate transgenic Ba/F3 cell lines and specifies how they were generated. Cloning and sequence validation were conducted by PD Dr. Anne Rascle, as further specified in the text.

[1]These primers were provided by GeneArt AG (Thermo Fisher Scientific Inc., Regensburg), who performed Sanger sequencing.

Vectors	generation	sequencing primers
pcDNA3.mSTAT5A.WT_FLAG	mSTAT5A.WT_FLAG subcloned into pcDNA3 from pMX.neo.mSTAT5A.wt with EcoRI and NotI	O21, T7[1], SP6[1]
pcDNA3.mSTAT5A.1*6_FLAG	mSTAT5A.1*6_FLAG subcloned into pcDNA3 from pMX.neo.mSTAT5A.1*6 with EcoRI and NotI	O21, T7[1], SP6[1]
pTet-On Advanced	Purchased	
pTRE-Tight-BI-AcGFP1.mSTAT5A.WT_FLAG	mSTAT5A.WT_FLAG subcloned into pTRE-Tight-BI-AcGFP1 from pcDNA3.mSTAT5A.WT_FLAG with EcoRI and KpnI	O76, O79, O94, O95, O97
pTRE-Tight-BI-AcGFP1.mSTAT5A.1*6_FLAG	mSTAT5A.1*6_FLAG subcloned into pTRE-Tight-BI-AcGFP1 from pcDNA3.mSTAT5A.1*6_FLAG with EcoRI and KpnI	O76, O79, O94, O95, O97
pTK-Hyg	Purchased	

3 Results

Constitutive activation of the normally transiently activated transcription factor STAT5A/B has been found to cause oncogenesis. The present study aimed to elucidate the effects of constitutive STAT5A/B activation, which govern its oncogenicity and lead to the acquisition of cancer hallmarks, in particular the role of putative chromatin alterations mediated by sustained STAT5 DNA binding upon constitutive activation.

3.1 Experimental systems

The immortalized murine pro-B cell line Ba/F3 was chosen as an experimental system. The Ba/F3 cell line derives from the murine bone marrow and is dependent on the cytokine IL-3 (Palacios and Steinmetz, 1985). IL-3 mediates Ba/F3 survival and growth via the STAT5A/B, PI3K and MAPK pathways (Kinoshita *et al.*, 1997, Rosa Santos *et al.*, 2000). Non-synchronized Ba/F3 cells growing under IL-3 supplementation form a heterogenous cell population exhibiting successive (non-synchronized) cycles of transient activation of endogenous STAT5A/B. STAT5A/B activation, however, can be turned off/on respectively by temporary IL-3 deprivation (resting) and subsequent IL-3 stimulation to study the effects of endogenous STAT5A/B activation in a synchronized cell population.

The present study aimed to identify the effects of sustained oncogenic constitutive STAT5A-1*6 activation (see 1.3.4) on Ba/F3 cells, with normal transient wild-type STAT5A (hereafter STAT5A-wt) and endogenous STAT5A/B activation serving as controls. The parental Ba/F3 cell line permits identification of the effects of endogenous STAT5A/B activation. Ba/F3 cell lines stably expressing either STAT5A-1*6 or STAT5A-wt permit identification of differences in Ba/F3 cells transformed by STAT5A-1*6. In doing so, ectopic expression of STAT5A-wt permits discerning mere effects of STAT5A over-expression from effects of constitutive STAT5A-1*6 activation. Of note, Ba/F3 cells have been found not to fully survive IL-3 deprivation upon first induction of STAT5A-1*6 expression in contrast to Ba/F3-1*6 cells expressing STAT5A-1*6 long-term (Gesbert and Griffin, 2000, Nosaka *et al.*, 1999). It was hypothesized that surviving Ba/F3 cells gradually acquire cancer hallmarks after first induction of STAT5A-1*6 expression, leading to malignant transformation. Thus, a stable Ba/F3 cell line inducibly expressing STAT5A-1*6 was predicted to permit monitoring this survival and transformation process, allowing identification of time-dependent effects of sustained STAT5A-1*6 DNA binding on STAT5 target genes.

Previously established stable Ba/F3 cell lines constitutively or inducibly expressing STAT5A-1*6 and STAT5A-wt (Gesbert and Griffin, 2000, Nosaka *et al.*, 1999, Onishi *et al.*, 1998) were no longer available for the present study. Of note, the parental Ba/F3 cell

line and stable Ba/F3 cell lines constitutively expressing STAT5A-1*6 (hereafter Ba/F3-1*6) and STAT5A-wt (hereafter Ba/F3-wt) have been studied extensively by a number of research groups, including by the one of PD Dr. Anne Rascle. In particular, the survival and growth phenotype as well as STAT5A/B activation by phosphorylation, STAT5A/B DNA binding and STAT5A/B-mediated transactivation have already been characterized (Nosaka *et al.*, 1999, Onishi *et al.*, 1998, Rascle *et al.*, 2003, Rascle and Lees, 2003). By contrast, Ba/F3 cell lines inducibly expressing STAT5A-1*6 have not been investigated extensively except for their survival and growth phenotype and tumorigenicity *in vivo* in one study (Gesbert and Griffin, 2000). Therefore, stable Ba/F3-1*6 and Ba/F3-wt cell lines were first re-established and validated by verifying their previously published characteristics, with parental Ba/F3 cells serving as a reference. Then, stable Ba/F3 cell lines inducibly expressing either STAT5A-1*6 or as a control STAT5A-wt were established and employed to monitor the transformation process induced by STAT5A-1*6. The consecutive establishment of four separate stable cell lines ensured that the previously established characteristics of Ba/F3-1*6 cells are replicable in the Ba/F3 cell line inducibly expressing STAT5A-1*6, once these cells are transformed.

3.1.1 Ba/F3-wt and Ba/F3-1*6 cell line generation

For the present study, stable Ba/F3-wt and Ba/F3-1*6 cell lines were established from parental Ba/F3 cells received from Jacqueline Marvel (IFR 128, BioSciences Gerland-Lyon Sud, France) as a kind gift. To do so, the expression vectors pcDNA3. mSTAT5A.WT_FLAG and pcDNA3.mSTAT5A.1*6_FLAG expression were generated (Figure 8). They contain mSTAT5A.WT_FLAG and mSTAT5A.1*6_FLAG cDNA inserts, each encoding mSTAT5A-wt and mSTAT5A-1*6 in fusion with a C-terminal FLAG tag (Figure 8 | Hopp *et al.*, 1988). The FLAG tag permits selective detection of transgenic mSTAT5A-wt-FLAG (hereafter simply STAT5A-wt) and mSTAT5A-1*6-FLAG (hereafter simply STAT5A-1*6) production by Western blot (see Figure 9 as an illustration). In Ba/F3-wt and Ba/F3-1*6 cells, the STAT5A-wt and STAT5A-1*6 transgenes are expressed constitutively under the control of the strong viral cytomegalovirus (CMV) promoter (Figure 8). Moreover, a neomycin resistance gene confers resistance to G418, enabling selection of stably transfected cells (Figure 8).

Parental Ba/F3 cells were transfected by electroporation with either pcDNA3. mSTAT5A.WT_FLAG or pcDNA3.mSTAT5A.1*6_FLAG plasmids. Stably transfected cells were selected using G418. Prospective Ba/F3-1*6 cells were grown in the absence of IL-3, because IL-3 induces apoptosis in Ba/F3-1*6 cells (Nosaka *et al.*, 1999). Transgene expression could be demonstrated by Western blot analysis for the selected bulk cultures, using an antibody directed against the FLAG tag (data not shown). Several

Ba/F3-wt and Ba/F3-1*6 single clones were isolated in two rounds of limiting dilution. After evaluating transgene expression by Western blot analysis (data not shown) and the cell survival and growth phenotype by light microscopy and trypan blue staining-based cell counting (data not shown), the single clones Ba/F3-wt A7 and Ba/F3-1*6 F7 (hereafter simply named Ba/F3-wt and Ba/F3-1*6) were chosen for further analyses.

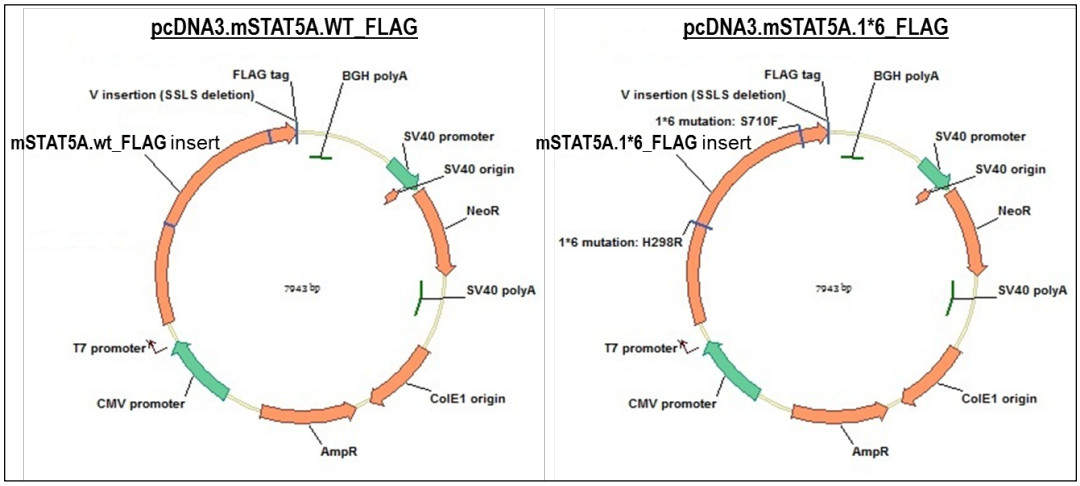

Figure 8: Expression vectors employed to generate stable Ba/F3-wt and Ba/F3-1*6 cell lines

(adapted from PD Dr. Anne Rascle)

The expression vectors pcDNA3.mSTAT5A.WT_FLAG and pcDNA3.mSTAT5A.1*6_FLAG are illustrated schematically. mSTAT5A.WT and mSTAT5A.1*6 cDNAs were inserted into the pcDNA3 expression vector in frame with a FLAG tag sequence and under the control of the CMV promoter.

Abbreviations: AmpR = ampicillin resistance gene, BGH = bovine growth hormone, CMV = cytomegalovirus, ColE1 = colecin E1, NeoR = neomycin resistance gene, polyA = polyadenylation signal, SV40 = simian virus 40, T7 = T7 RNA polymerase.

3.1.2 Parental Ba/F3, Ba/F3-wt and Ba/F3-1*6 cell line validation

The parental Ba/F3 cells as well as the newly established Ba/F3-wt and Ba/F3-1*6 cells were expected to exhibit the characteristics previously reported in the literature. As detailed in the introduction section, upon activation by phosphorylation STAT5A/B translocates to the nucleus, acquires DNA binding and transcriptional activity, and mediates a pro-survival and growth response (see 1.3). Parental Ba/F3, Ba/F3-wt and Ba/F3-1*6 cells have been characterized previously for these parameters (Nosaka *et al.*, 1999, Onishi *et al.*, 1998, Rascle *et al.*, 2003, Rascle and Lees, 2003).

To verify their reported survival and growth phenotype in response to IL-3, parental Ba/F3, Ba/F3-wt and Ba/F3-1*6 cells were cultured in the presence and absence of IL-3 and monitored by living cell microscopy and trypan blue staining-based cell counting. Both parental Ba/F3 and newly established Ba/F3-wt cells grew in the presence of IL-3 and all died upon IL-3 deprivation within a few days, whereas newly established Ba/F3-1*6 cells grew in the absence of IL-3 and all died upon IL-3 supplementation within a few days (data not shown). This pattern is in agreement with previously reported data

and shows the IL-3 independence conferred by STAT5A-1*6 (Nosaka *et al.*, 1999, Onishi *et al.*, 1998).

To verify transgene expression and STAT5A/B activation by phosphorylation as well as STAT5A/B transactivation and DNA binding dynamics, parental Ba/F3 and Ba/F3-wt were rested and IL-3-stimulated to turn STAT5A/B activation off/on and harvested for Western blot analysis, gene expression analysis by RT-qPCR and chromatin immunoprecipitation (ChIP). Ba/F3-1*6 cells growing in the absence of IL-3 were harvested in parallel.

Western blot analysis was performed using antibodies directed against transgenic FLAG-tagged STAT5A-wt/1*6 (FLAG), total STAT5A/B (C-terminal region common to STAT5A and STAT5B) and phosphorylated STAT5A/B (pSTAT5A/B). In doing so, FLAG signals allow identification of transgenic STAT5A-wt/1*6 and total STAT5A/B signals allow assessment of the expression level of STAT5A-wt/1*6 compared with endogenous STAT5A/B. pSTAT5A/B signals allow identification of both IL-3-dependent and -independent STAT5A/B activation. Positive FLAG signals were detected only in Ba/F3-wt and Ba/F3-1*6 cells (Figure 9), demonstrating ectopic STAT5A-wt/1*6 protein production. Slightly higher total STAT5A/B levels in Ba/F3-wt and Ba/F3-1*6 cells compared with parental Ba/F3 cells were observed (Figure 9), indicating a moderate level of overexpression of the respective transgene. Importantly, expression levels of STAT5A-wt and STAT5A-1*6 were comparable (Figure 9). Upon IL-3 stimulation, pSTAT5A/B was detected as expected in parental Ba/F3 and Ba/F3-wt cells, with Ba/F3-wt cells exhibiting higher levels attributed to activation of ectopic STAT5A-wt (Figure 9). On the other hand, pSTAT5A/B was detected in Ba/F3-1*6 in the absence of IL-3 (Figure 9). The observed transgene production and the STAT5A/B activation (i.e. phosphorylation) patterns are in agreement with previously reported data by Onishi *et al.* (1998) and Nosaka *et al.* (1999).

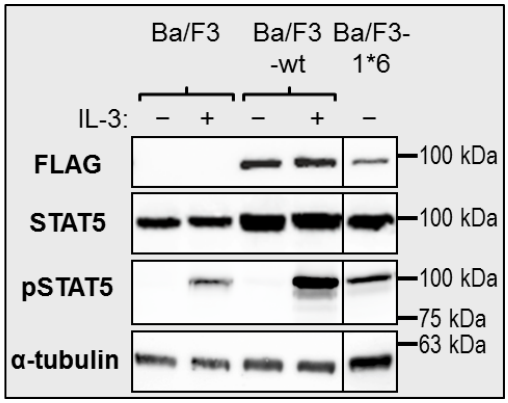

Figure 9: STAT5A-1*6 activation does not depend on IL-3 in contrast to STAT5A-wt activation

Parental Ba/F3 and Ba/F3-wt cells were rested for 12 h without IL-3 and stimulated for 15 min with IL-3 to induce STAT5A/B activation. Ba/F3-1*6 cells were grown in the absence of IL-3. Cells were harvested and Brij protein lysates were prepared. Protein lysates were analyzed by Western blot using antibodies detecting transgenic STAT5A-wt/1*6 (FLAG), total STAT5A/B (STAT5), active STAT5A/B (pSTAT5) and the loading control α-tubulin. Two Western blot analyses were conducted in parallel using (i) anti-STAT5A/B, anti-pSTAT5A/B and anti-α-tubulin as well as using (ii) anti-STAT5A/B, anti-FLAG and anti-α-tubulin antibodies. The two anti-STAT5A/B as well as the two anti-α-tubulin Western blots exhibited similar bands and hence only one representative Western blot is depicted, respectively.

STAT5A/B-mediated transactivation dynamics has been investigated previously using the STAT5 target genes *Cis* and *Osm* and the STAT5A/B-independent MAPK pathway-

controlled *c-Fos* gene as models (Nosaka *et al.*, 1999, Rascle *et al.*, 2003, Rascle and Lees, 2003). Hence, RT-qPCR was performed for *Cis*, *Osm*, *c-Fos* and the housekeeping gene *36b4*. *36b4* mRNA level was expected to be unaffected by treatments applied in the present study and, hence, served as negative control (Rascle *et al.*, 2003). *c-Fos* mRNA level was expected to be upregulated in response to IL-3 but in a STAT5A/B-independent manner and served as positive control for IL-3 stimulation. *36b4* and *c-Fos* were employed as such controls throughout the present study. The STAT5 target genes *Cis* and *Osm* were expected to be upregulated in the presence of transcriptionally active pSTAT5A/B. As expected, the IL-3-independent housekeeping gene *36b4* remained unaffected by IL-3 deprivation and restimulation (Figure 10D), while the IL-3-dependent control gene *c-Fos* was upregulated in the presence of IL-3 (parental Ba/F3 and Ba/F3-wt cells) but not in cells expressing STAT5A-1*6 in the absence of IL-3 (Figure 10C). In parental Ba/F3 and Ba/F3-wt cells, *Cis* and *Osm* expression was likewise upregulated in the presence of IL-3 and, hence, endogenous STAT5A/B and STAT5A-wt activation (Figure 10A and B). In addition, *Cis* and *Osm* expression was upregulated in Ba/F3-1*6 cells despite the absence of IL-3 (compared to baseline level of parental Ba/F3 and Ba/F3-wt cells), correlating with constitutive STAT5A-1*6 activation (Figure 10A and B). The observed pattern is in agreement with previously reported STAT5A/B-mediated transactivation dynamics (Nosaka *et al.*, 1999, Rascle *et al.*, 2003, Rascle and Lees, 2003).

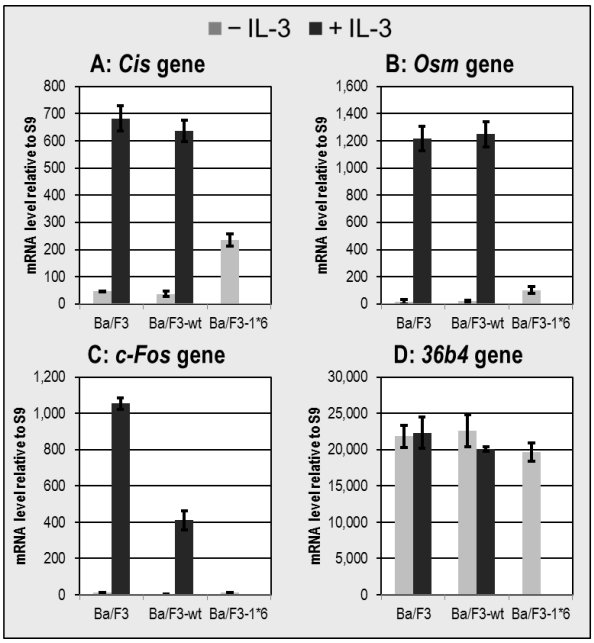

Figure 10: The STAT5A/B-dependent *Cis* and *Osm* genes are induced in IL-3-independent Ba/F3-1*6 cells in contrast to the STAT5A/B-independent *c-Fos* gene

Parental Ba/F3 and Ba/F3-wt cells were rested for 12 h without IL-3 and stimulated for 30 min with IL-3 to induce STAT5A/B activation. Ba/F3-1*6 cells were grown in the absence of IL-3. Cells were harvested, RNA was extracted and reverse transcribed into cDNA. cDNA was analyzed by RT-qPCR using primers specific for transcripts of the STAT5 target genes *Cis* and *Osm* as well as the control genes *c-Fos* and *36b4*. The error bars depict standard deviation among RT-qPCR replicates. The results shown are representative of two independent experiments.

Active STAT5A/B has been shown to bind to GAS motifs in the *Cis* and *Osm* proximal promoters (Verdier *et al.*, 1998, Yoshimura *et al.*, 1996). STAT5 binding at these sites in Ba/F3 cells has been validated by ChIP using antibodies directed against STAT5A/B and primers specific to the *Cis* and *Osm* STAT5 binding sites (Basham *et al.*, 2008, Rascle

et al., 2003, Rascle and Lees, 2003). STAT5 DNA binding has been correlated with transactivation of the *Cis* and *Osm* genes, which involves recruitment of RNA Polymerase II to the *Cis* and *Osm* transcription start sites (TSS | Basham *et al.*, 2008, Rascle *et al.*, 2003, Rascle and Lees, 2003). Recruitment of RNA Polymerase II has been investigated by ChIP using antibodies directed against RNA Polymerase II and primers specific to the *Cis* and *Osm* TSS (Basham *et al.*, 2008, Rascle *et al.*, 2003, Rascle and Lees, 2003). To verify these findings, ChIP was performed on the aforementioned samples using antibodies directed against STAT5A/B and RNA Polymerase II and primers specific to the *Cis* and *Osm* STAT5 binding site and TSS. Primers specific to unrelated sites in *Cis*, *Osm* and *c-Fos* were tested in parallel, as negative controls. Background ChIP signals were evaluated using non-specific IgG antibodies. Only in the presence of IL-3, RNA Polymerase II, but not STAT5A/B, was recruited to the STAT5A/B-independent *c-Fos* gene, correlating with its upregulation (Figures 11A, 11B, 12A and 12B). On the other hand, both STAT5A/B and RNA Polymerase II were recruited to *Cis* and *Osm* upon STAT5A/B activation in IL-3-stimulated parental Ba/F3 and Ba/F3-wt cells as well as in Ba/F3-1*6 cells despite the absence of IL-3 (Figures 11A, 11B, 12A and 12B). These observations demonstrate the IL-3-independent constitutive DNA binding and transcriptional activity of STAT5A-1*6 in Ba/F3-1*6 cells. The observed patterns are in agreement with the previously reported STAT5 DNA binding and RNA Polymerase II recruitment dynamics (Basham *et al.*, 2008, Rascle *et al.*, 2003, Rascle and Lees, 2003).

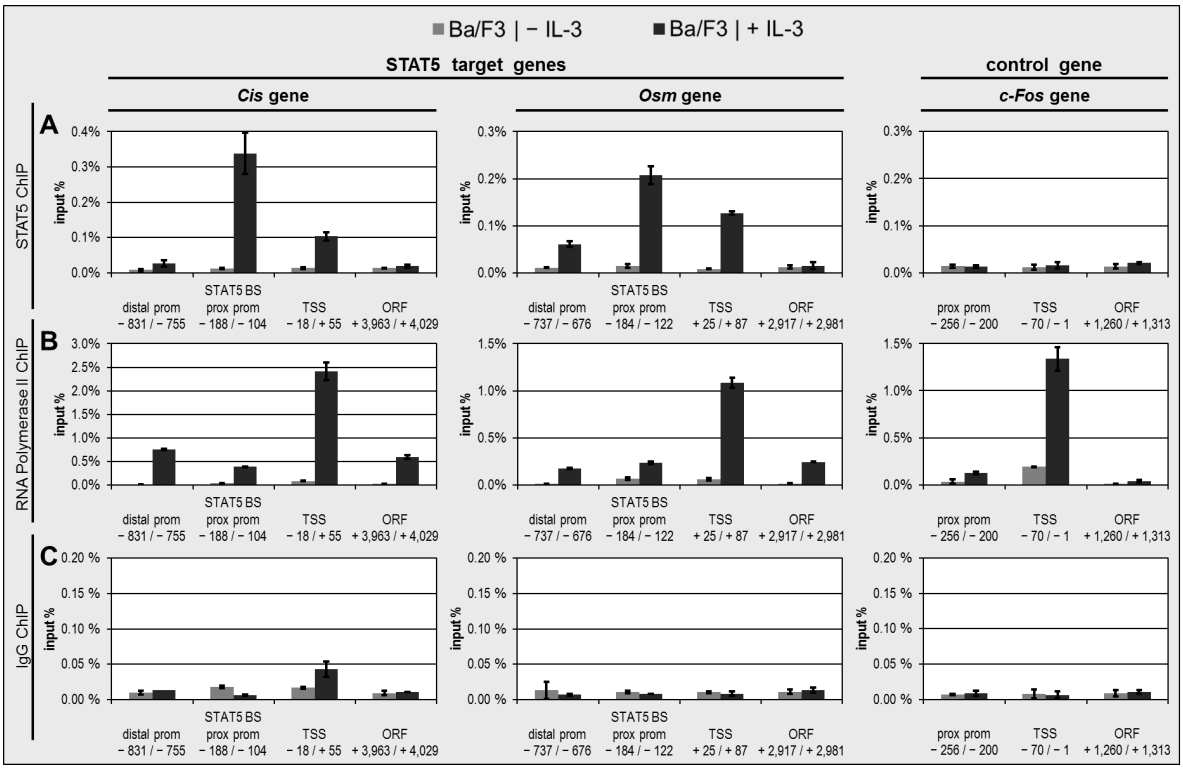

Figure 11 (previous page): STAT5A/B and RNA Polymerase II are recruited to *Cis* and *Osm* upon IL-3-induced STAT5A/B activation

Parental Ba/F3 cells were rested for 12 h without IL-3 and stimulated for 30 min with IL-3 to induce STAT5A/B activation. Cells were harvested and processed for chromatin immunoprecipitation (ChIP) as described in the Material and Methods section. ChIP was performed using antibodies directed against STAT5A/B **(A)**, RNA Polymerase II **(B)** or using Rabbit IgG as a background control **(C)**. Input and co-precipitated genomic DNA were analyzed by quantitative PCR using primers specific for the promoter regions, transcription start sites and open reading frames of the STAT5 target genes *Cis*, *Osm* and the control gene *c-Fos*, as specified further in the figure. *Cis* and *Osm* proximal promoter amplicons overlap their respective STAT5 binding sites. *Cis*, *Osm* and *c-Fos* gene structures as well as amplicon positions are illustrated in Figure 33. The relative quantity of co-precipitated genomic DNA is expressed as percentage of input genomic DNA (input %), denoting chromatin occupancy. The error bars depict standard deviation among qPCR replicates. The results shown are representative of two independent experiments. Nucleotide positions are relative to the transcription start site.

Abbreviations: BS = binding site, ChIP = chromatin immunoprecipitation, ORF = open reading frame, prom = promoter, prox = proximal, TSS = transcription start site

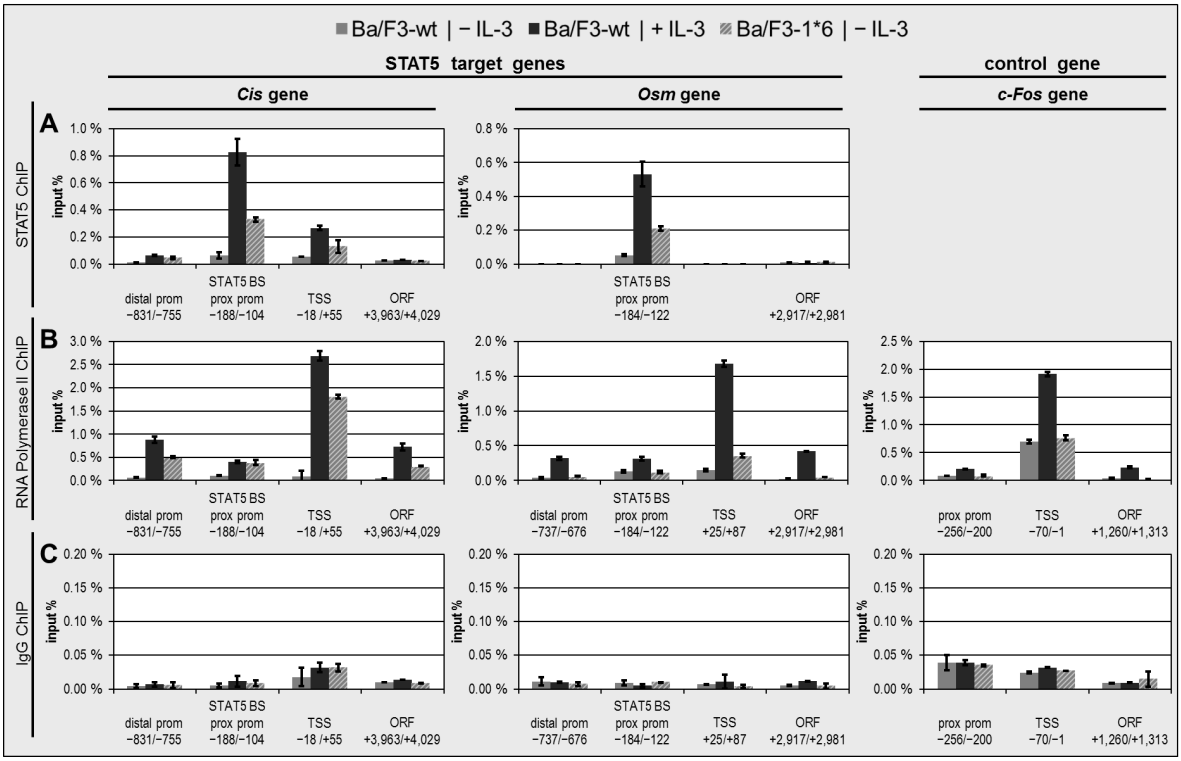

Figure 12: Constitutively active STAT5A-1*6 and RNA Polymerase II are recruited to *Cis* and *Osm* in the absence of IL-3

Ba/F3-wt cells were rested for 13 h without IL-3 and stimulated for 30 min with IL-3 to induce STAT5A/B activation. Ba/F3-1*6 cells were grown in the absence of IL-3. Cells were harvested and processed for chromatin immunoprecipitation (ChIP) as described in the Material and Methods section. ChIP was performed using antibodies directed against STAT5A/B **(A)**, RNA Polymerase II **(B)** or using Rabbit IgG as a background control **(C)**. Input and co-precipitated genomic DNA were analyzed by quantitative PCR using the same primers as in Figure 11, as specified in the figure. *Cis*, *Osm* and *c-Fos* gene structures as well as amplicon positions are illustrated in Figure 33. The relative quantity of co-precipitated genomic DNA is expressed as percentage of input genomic DNA (input %), denoting chromatin occupancy. The error bars depict standard deviation among qPCR replicates. The results shown are representative of two independent experiments. Nucleotide positions are relative to the transcription start site.

Abbreviations: BS = binding site, ChIP = chromatin immunoprecipitation, ORF = open reading frame, prom = promoter, prox = proximal, TSS = transcription start site

Taken together, the newly established Ba/F3-wt and Ba/F3-1*6 cell lines as well as the parental Ba/F3 cells behaved as previously reported (Nosaka *et al.*, 1999, Onishi *et al.*, 1998, Rascle *et al.*, 2003, Rascle and Lees, 2003). In addition, the Ba/F3-wt cell line behaved comparably to the parental Ba/F3 cell line, exhibiting no growth factor

independence and, thus, no oncogenicity despite overexpression of STAT5A-wt. The validation of these stable Ba/F3-wt and Ba/F3-1*6 cell lines justified the generation of stable Ba/F3 cell lines inducibly expressing STAT5A-wt and STAT5A-1*6, to study STAT5A-1*6-mediated cell transformation.

3.1.3 Ba/F3-tet-on-wt and Ba/F3-tet-on-1*6 inducible cell line generation

As detailed above, a Ba/F3 cell line inducibly expressing STAT5A-1*6 was predicted to permit monitoring the transformation process induced by STAT5A-1*6 and a Ba/F3 control cell line inducibly expressing STAT5A-wt was predicted to permit discerning mere effects of STAT5A over-expression from effects of constitutive STAT5A-1*6 activation. These two cell lines had been established previously based on the first generation of the Tet-on inducible expression system (Gesbert and Griffin, 2000), but were not available for the present study. Therefore, Ba/F3 cell lines inducibly expressing STAT5A-1*6 (hereafter Ba/F3-tet-on-1*6) and STAT5A-wt (hereafter Ba/F3-tet-on-wt) were established using the newer and improved second generation of the Tet-on inducible expression system called 'Tet-on Advanced' from Takara Bio Europe/Clontech (Saint-Germain-en-Laye, France | Urlinger *et al.*, 2000). Tet-on (and Tet-off) inducible expression systems were originally developed by Gossen and Bujard (1992) on the basis of a repressor inhibited by tetracycline (tetracycline repressor) targeting a tetracycline resistance gene found in *E. coli*. Specifically, the Tet-on Advanced inducible expression system involves the fusion protein reverse tetracycline-controlled transactivator protein Advanced (rtTA Advanced), which comprises a mutated tetracycline repressor fused to a viral activation domain. rtTA Advanced functions as a doxycycline (dox)-dependent transactivator for sequence-specific tetracycline responsive element (TRE)-promoters. In contrast to Gesbert and Griffin (2000), the present study applied a bidirectional TRE-promoter, where the target gene is co-expressed with a fluorescent protein as an internal control for transgene expression.

The Ba/F3-tet-on-1*6 and Ba/F3-tet-on-wt cell lines were generated using the pTet-on Advanced, pTRE-Tight-BI-AcGFP1.mSTAT5A.1*6_FLAG and pTRE-Tight-BI-AcGFP1. mSTAT5A.WT_FLAG expression vectors. The pTet-on Advanced vector allows constitutive expression of rtTA Advanced thanks to the strong viral CMV promoter, as well as of a neomycin resistance gene conferring resistance to G418 (Figure 13A). The pTRE-Tight-BI-AcGFP1.mSTAT5A.1*6_FLAG and pTRE-Tight-BI-AcGFP1.mSTAT5A. WT_FLAG vectors contain the mSTAT5A.1*6_FLAG and mSTAT5A.WT_FLAG cDNA inserts described above and (in the presence of rtTA Advanced) allow inducible, dox-dependent expression of STAT5A-1*6 and STAT5A-wt, respectively, together with the internal control *Aqueorea coerulescens* green fluorescent protein 1 (AcGFP1, hereafter simply GFP | Figure 13C and D).

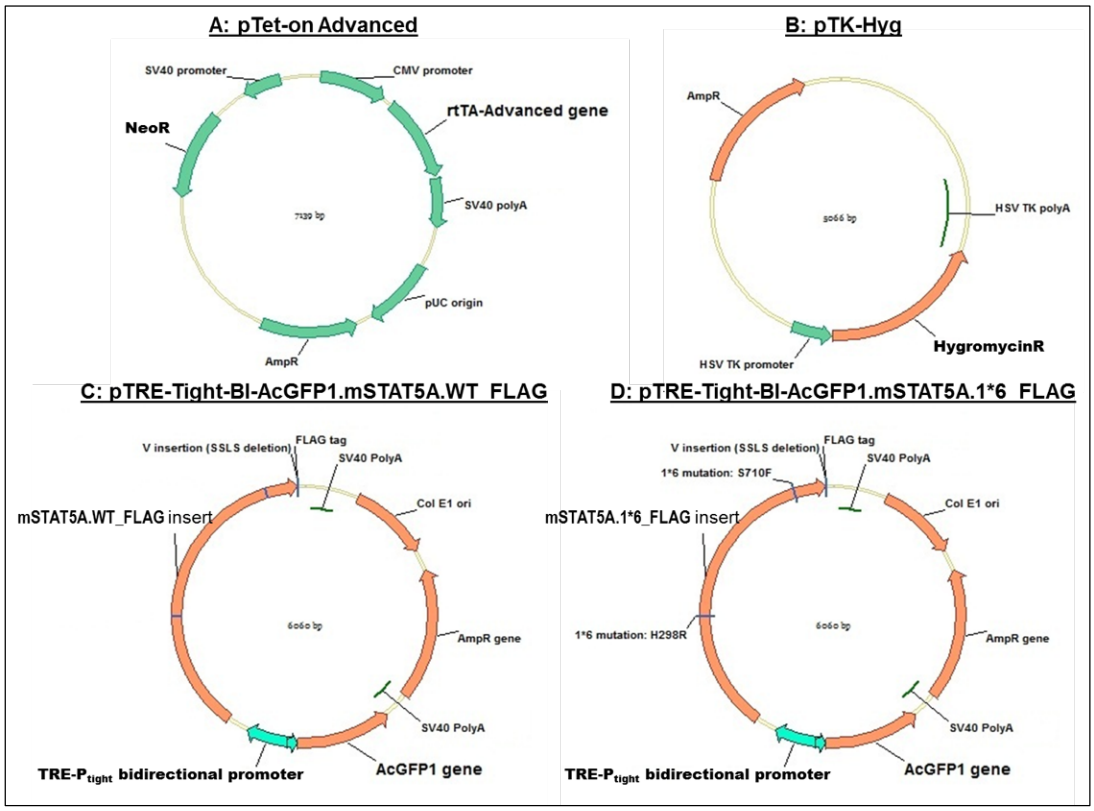

Figure 13: Expression vectors employed to generate stable inducible Ba/F3-tet-on-wt/1*6 cell lines

(adapted from PD Dr. Anne Rascle)

The expression vectors stably transfected in the Ba/F3-tet-on-wt and Ba/F3-tet-on-1*6 cell lines are illustrated. These cell lines were generated using the 'Tet-on Advanced' inducible expression system. pTet-on Advanced **(A)** was employed to generate the Ba/F3-tet-on promoter cell line. pTK-Hyg **(B)** was employed together with pTRE-Tight-BI-AcGFP1.mSTAT5A.wt_FLAG **(C)** and pTRE-Tight-BI-AcGFP1. mSTAT5A.1*6 _FLAG **(D)**, respectively, to generate Ba/F3-tet-on-wt and Ba/F3-tet-on-1*6 responder cell lines from the Ba/F3-tet-on promoter cell line. mSTAT5A.WT and mSTAT5A.1*6 cDNAs in frame with the FLAG tag sequence were inserted into a pTRE-Tight-BI-AcGFP1 backbone, conferring conditional STAT5A-wt-FLAG or STAT5A-1*6-FLAG expression, as well as concomitant GFP expression.

Abbreviations: AmpR = ampicillin resistance gene, CMV = cytomegalovirus, ColE1 ori = colecin E1 origin, HSV TK = Herpes simplex virus thymidine kinase, HygromycinR = hygromycin B resistance gene, NeoR = neomycin resistance gene, polyA = polyadenylation signal, rtTA = reverse tetracycline-controlled transactivator protein, pUC = UC plasmid, TRE = tetracycline responsive element, SV40 = simian virus 40.

The stable Ba/F3-tet-on-1*6 and Ba/F3-tet-on-wt cell lines were generated in two steps. Firstly, Ba/F3 cells were stably transfected with pTet-on Advanced under G418 selection. rtTA Advanced transgene expression was confirmed by RT-qPCR (data not shown). Several single clones were isolated by limiting dilution and evaluated for rtTA Advanced protein production by Western blot, using an antibody directed against rtTA-Advanced (Figure 14A). The Ba/F3-tet-on clone #7.1 was chosen because of its strong rtTA Advanced protein level (Figure 14A, see lane labelled #7). Secondly, Ba/F3-tet-on clone #7.1 was co-transfected with either (i) pTRE-Tight-BI-AcGFP1.mSTAT5A.1*6_FLAG and pTK-Hyg or (ii) pTRE-Tight-BI-AcGFP1.mSTAT5A.WT_FLAG and pTK-Hyg. The pTK-Hyg expression vector confers resistance to hygromycin B (Figure 13B). Stably transfected prospective (i) Ba/F3-tet-on-1*6 and (ii) Ba/F3-tet-on-wt cells were selected using hygromycin B and G418. Using living cell fluorescence microscopy, dox-dependent GFP transgene expression was confirmed on the transfected pool by a

short-term dox induction (1 µg/ml for 24 h according to the manufacturer's protocol, data not shown). Several single clones were isolated by limiting dilution and evaluated for GFP fluorescence (living cell fluorescence microscopy, data not shown; see Figure 16A as an example) and STAT5A-1*6/wt protein production (Western blot anti-FLAG, Figure 14B and C) upon short-term dox induction (1 µg/ml dox for 24 h). The Ba/F3-tet-on-wt clone #3 and Ba/F3-tet-on-1*6 clone #D4.1 (hereafter simply named Ba/F3-tet-on-wt and Ba/F3-tet-on-1*6) were chosen for further analyses, because they exhibited homogenous GFP fluorescence levels (not shown) and the highest STAT5A-1*6/wt protein levels upon dox induction (Figure 14B and C).

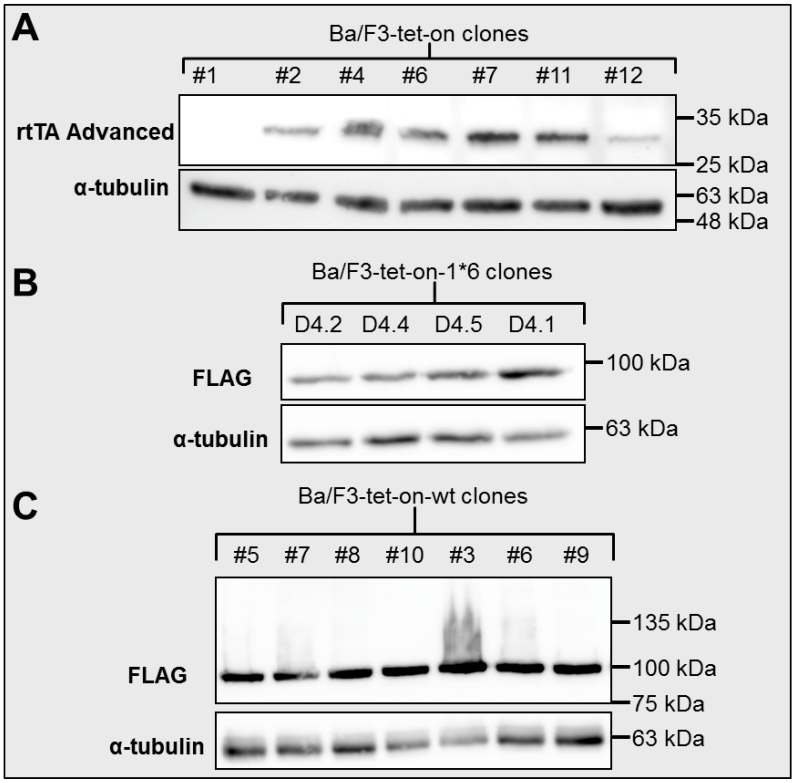

Figure 14: Ba/F3-tet-on, Ba/F3-tet-on-1*6 and Ba/F3-tet-on-wt clone selection

A: Ba/F3-tet-on bulk culture was generated as described in the text. Ba/F3-tet-on bulk culture cells were subjected to limiting dilution and clones #1, #2, #4, #6, #7, #11 and #12 were isolated. Cells were harvested and Brij protein lysates were prepared. Protein lysates were analyzed by Western blot using antibodies detecting rtTA Advanced and the loading control α-tubulin. **B, C:** Ba/F3-tet-on-1*6 and -wt bulk culture was generated as described in the text. Ba/F3-tet-on-1*6 and -wt bulk culture cells were subjected to limiting dilution and clones D4.1, D4.2, D4.4 plus D4.5 and #5, #7, #8, #10, #3, #6 plus #9 were isolated, respectively. Cells were treated with 1 µg/ml dox for 24 h and harvested. Brij protein lysates were prepared and analyzed by Western blot using antibodies detecting FLAG and the loading control α-tubulin.

3.1.4 Conditions for doxycycline-mediated induction of STAT5A-wt and STAT5A-1*6 in Ba/F3-tet-on cell lines

The present study aimed to study the STAT5A-1*6-mediated transformation process during long-term dox induction. Ba/F3-tet-on-1*6 cells were expected to be viable in the absence of IL-3 during long-term dox induction, whereas Ba/F3-tet-on-wt cells were expected to die in the absence of IL-3 (3.1.2, Nosaka *et al.*, 1999, Onishi *et al.*, 1998). Besides, Ba/F3-tet-on-1*6 cells were predicted to die from apoptosis in the presence of IL-3 upon long-term dox induction (Nosaka *et al.*, 1999). Taken together, this meant that dox-induced Ba/F3-tet-on-wt cells could not serve as a long-term control for the transformation process in dox-induced Ba/F3-tet-on-1*6 cells in the absence of IL-3. This is why in the present study Ba/F3-tet-on-wt cells were only employed as a short-term control for the effects of STAT5A-1*6 induction. Hence, non-induced Ba/F3-tet-on-1*6

cells grown in the presence of IL-3 were usually used as a negative control in experiments of dox induction of Ba/F3-tet-on-1*6 cells.

To establish conditions for short-term transgene induction in the newly established Ba/F3-tet-on-1*6 and -wt cell lines, ectopic STAT5A-1*6 production in response to dox was first characterized in a dose-dependent manner. Ba/F3-tet-on-1*6 and -wt cells were induced for 24 h in the presence of 20, 100, 200 and 1,000 ng/ml dox, based on the range recommended by the manufacturer. Non-induced cells served as negative control. For this 24h dox induction, IL-3 was maintained in all conditions, in order to directly compare transgene expression in STAT5A1*6- and STAT5A-wt-expressing cells under identical conditions. Cells were analyzed by Western blot for transgenic STAT5A-1*6/wt protein using an antibody directed against its FLAG tag. STAT5A-1*6/wt protein production was induced in a dose-dependent manner, with strongest induction using 1,000 ng/ml dox (Figure 15A). Thus, this dosage was applied for short-term (24 h) dox induction of Ba/F3-tet-on-1*6 and -wt cells in future experiments.

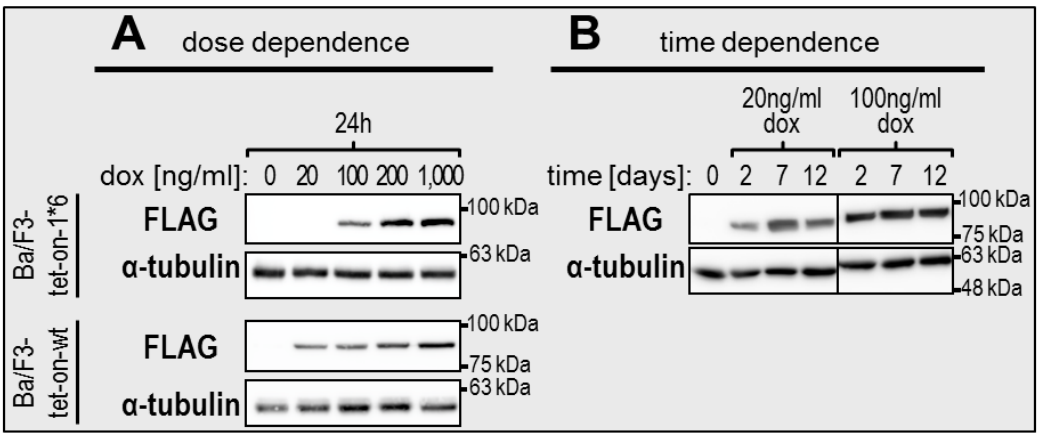

Figure 15: STAT5A-1*6/wt production is induced rapidly, strongly and sustainedly using 1,000 ng/ml doxycycline for short-term and 100 ng/ml doxycycline for long-term induction

A: Ba/F3-tet-on-1*6 (clone #D4.1) and -wt (clone #3) cells were supplemented for 24 h with doxycycline (dox) with dosages from 20–1,000 ng/ml in the presence of IL-3 to induce STAT5A-1*6/wt production, as specified in the figure. Non-induced cells (0) were grown in the presence of IL-3 as a negative control. **B:** Ba/F3-tet-on-1*6 cells (clone #D4.1) were supplemented with 20 or 100 ng/ml dox under gradual IL-3 withdrawal for the indicated times to induce STAT5A-1*6 production. Dox was replenished every two days. Non-induced cells (0) were grown in the presence of IL-3 as a negative control. **A, B:** Cells were harvested and Brij protein lysates were prepared. Protein lysates were analyzed by Western blot using antibodies detecting transgenic STAT5A-1*6/wt (FLAG) and the loading control α-tubulin in three separate experiments (two for **A** and one for **B**).

Abbreviations: dox = doxycycline.

To establish conditions for long-term transgene induction in the newly established Ba/F3-tet-on-1*6 cell line, ectopic STAT5A-1*6 production in response to dox was characterized in a time-dependent manner. For sustained long-term dox induction, dox was replenished every two days because of its short physiological half-life of around 24 h (Agwuh and MacGowan, 2006). To rule out any adverse effects of the high dosage of 1,000 ng/ml dox chosen for short-term dox induction, Ba/F3-tet-on-1*6 cells were deprived of IL-3 and induced with only 20 or 100 ng/ml dox, with non-induced cells

serving as a day 0 control. Cells were harvested after 2, 7 and 12 days of induction and analyzed by Western blot as before. Both 20 ng/ml and 100 ng/ml dox induced ectopic production of STAT5A-1*6 in Ba/F3-tet-on-1*6 cells, with noticeably higher STAT5A-1*6 levels using 100 ng/ml dox (Figure 15B; compare the FLAG to α-tubulin signal ratio). This suggested that a dosage of 100 ng/ml dox sufficed for sustained long-term dox induction. Given that the 24 h time-point was not analyzed and that the 1,000 ng/ml dox dosage had shown a stronger induction of STAT5A-1*6 production than the 100 ng/ml dox dosage (Figure 15A), it could not be ruled out that maximum transgene expression was reached more slowly using 100 ng/ml dox compared with 1,000 ng/ml dox for first induction. To exclude this possibility and for better comparability with short-term dox induction, 1,000 ng/ml dox was applied as first dosage and replenished every two days with 100 ng/ml dox for long-term dox induction in future experiments.

As detailed above, upon dox induction Ba/F3-tet-on-1*6 and -wt cells were expected to co-express GFP and STAT5A-1*6/wt. Given that Ba/F3-tet-on-wt cells were only used as a control for short-term dox induction, GFP co-expression was only investigated for Ba/F3-tet-on-1*6 cells. To confirm co-expression of GFP for both short-term and long-term dox induction, Ba/F3-tet-on-1*6 cells were induced with dox as specified above for up to two weeks in the absence of IL-3 and analyzed regularly for native GFP fluorescence using living cell fluorescence microscopy and flow cytometry. Non-induced cells emitting only autofluorescence served as a negative control. As observed by microscopy, dox-induced cells exhibited elevated levels of GFP fluorescence after 24 h of dox induction (Figure 16A). Similarly, flow cytometry showed that induced cells formed a homogenous cell population emitting elevated levels of GFP fluorescence, when compared to non-induced cells (Figure 16B). The shift in GFP fluorescence was maintained throughout the two-week dox induction (Figure 16B). These findings confirmed rapid and sustained GFP co-expression upon dox induction.

Upon dox induction, Ba/F3-tet-on-1*6 and -wt cells were expected to exhibit patterns of STAT5A protein production and activation by phosphorylation comparable to that of Ba/F3-1*6 and Ba/F3-wt cells, respectively (3.1.2, Onishi *et al.*, 1998). For the reasons stated above, this was only investigated for Ba/F3-tet-on-1*6 cells. Ba/F3-tet-on-1*6 cells were induced for two weeks as specified above and harvested regularly for protein and RNA analysis. Non-induced cells rested without IL-3 served as a negative control. Western blot analysis was performed using antibodies directed against FLAG-tagged STAT5A-1*6, total STAT5A/B and pSTAT5A/B. RT-qPCR analysis was performed using primers specific for the STAT5A-1*6 transgene transcript. As identified by the FLAG tag, maximum STAT5A-1*6 protein level was reached after two days of induction and was maintained thereafter, confirming that dox induced STAT5A-1*6 protein production strongly and sustainedly (Figure 16C). pSTAT5A/B was detected in dox-induced cells,

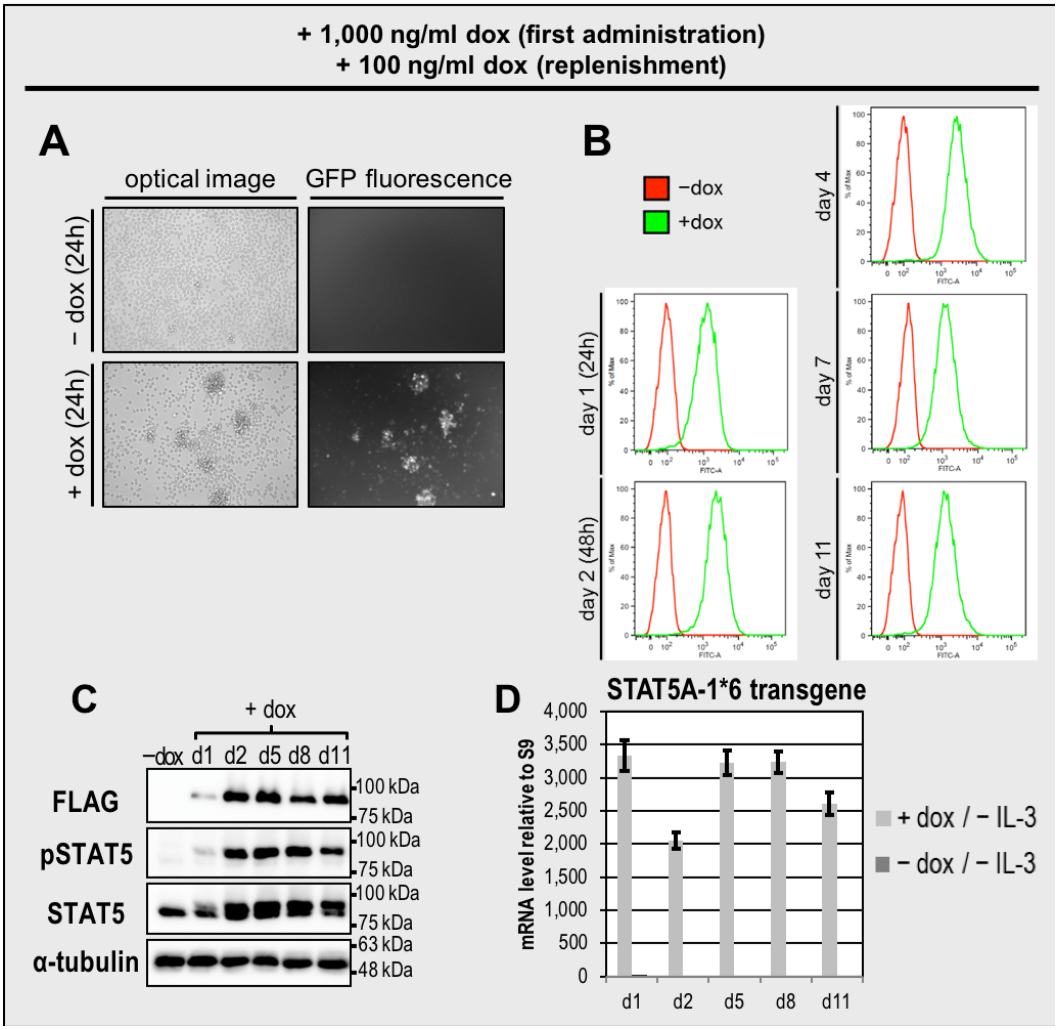

Figure 16 (previous page): Doxycycline induces concomitant STAT5A-1*6 and GFP production in Ba/F3-tet-on-1*6 cells (clone #D4.1) using the standard protocol

Ba/F3-tet-on-1*6 cells (clone #D4.1) were treated with doxycycline (dox) for the indicated times (day 1 for C and D equals 11 h) in the presence **(A)** or absence **(B–D)** of IL-3 to induce STAT5A-1*6 and GFP production in three independent experiments (**A**, **B** and **C/D**). 1,000 ng/ml dox was administrated as first dosage and100 ng/ml dox was replenished every two days. Non-induced cells were grown in the presence of IL-3 **(A,B)** or rested without IL-3 for 11 h **(C, D)** to serve as negative controls. **A:** Living cells were surveyed by light microscopy and fluorescence microscopy specific for wavelengths emitted by GFP after excitation. An exemplary image is shown (20x magnification). **B:** Cells were harvested for flow cytometric analysis of native GFP fluorescence as described in the Material and Methods section. Histograms of GFP fluorescence (FITC-A channel) plotted logarithmically against percentage of maximal cell number (% of Max.) are shown. Induced cells (green) are depicted with the non-induced control (red) as a reference for autofluorescence. **C:** Cells were harvested and Brij protein lysates were prepared. Protein lysates were analyzed by Western blot as described in the legend of Figure 9. **D:** Within the same experiment as in **C**, cells were harvested for RT-qPCR analysis using primers specific for the STAT5A-1*6 transgene mRNA. The error bars depict standard deviation among RT-qPCR replicates.

Abbreviations: d = day, dox = doxycycline.

but not in non-induced cells in the absence of IL-3 (Figure 16C), demonstrating constitutive activation of ectopic STAT5A-1*6. Notably, two total STAT5A/B signals were observed in dox-induced Ba/F3-tet-on-1*6 cells. This resulted from the slower migration of (i) STAT5A-1*6 compared to endogenous STAT5A/B due to the added molecular weight of around 1 kDa from its FLAG tag (Hopp *et al.*, 1988), (ii) STAT5A compared with STAT5B due to its higher molecular weight (Figure 5) and (iii) pSTAT5A/B compared

with unphosphorylated STAT5A/B because of the attached negatively charged phosphate residue (Cooper *et al.*, 2006). Hence, the upper total STAT5A/B signals represent constitutively phosphorylated STAT5A-1*6 and overlap with the FLAG and pSTAT5A/B signals, while the lower signals represent (in the absence of IL-3) unphosphorylated endogenous STAT5A/B. The upper total STAT5A/B signals were approximately two to three times stronger than the lower signals, suggesting a two- to three-fold overexpression of STAT5A-1*6 relative to endogenous STAT5A/B. In accordance with STAT5A-1*6 protein production, STAT5A-1*6 transgene expression was induced strongly and sustainedly upon dox induction (Figure 16D). Maximum mRNA level was already reached after one day of dox induction, exemplifying the very rapid dox-dependent induction of STAT5A-1*6 transgene expression (Figure 16D), and demonstrating a delay in protein production (Figure 17C).

In summary, the newly established Ba/F3-tet-on-1*6 cell line was shown to behave as expected upon dox induction in terms of its STAT5A-1*6 production and activation pattern (see Onishi *et al.*, 1998). Similarly, non-induced Ba/F3-tet-on-1*6 cells behaved as the parental Ba/F3 cells and therefore can be used as reference of choice for the present study. Altogether, this experimental system represents a powerful tool to study STAT5A-1*6-induced cell transformation upon dox induction.

3.2 Characterization of survival and growth phenotype of Ba/F3-tet-on-1*6 cells upon doxycycline induction

The present study aimed to elucidate the effects of sustained constitutive STAT5A-1*6 activation, which govern its oncogenicity, using long-term dox induction of the newly established Ba/F3-tet-on-1*6 cells as an experimental system. STAT5A-1*6 induction was predicted to induce oncogenesis in Ba/F3-tet-on-1*6 cells, leading to the acquisition of cancer hallmarks, in particular ‘cytokine (i.e. IL-3) independence’. As detailed in the introduction section (see 1.1), oncogenesis and cancer progression have been argued to be caused by natural selection, where individual (pre-)cancer cells gain a selective growth advantage by stochastically acquiring cancer hallmark traits (Hanahan and Weinberg, 2000, Merlo *et al.*, 2006). Thus, it was hypothesized that stochastic processes could lead to differences in the events observed among different dox induction experiments. This hypothesis proposes that events shared among different dox induction experiments may be caused by sustained constitutive STAT5A-1*6 activation in a deterministic manner, whereas events unique to one dox induction experiments may have stochastic causes.

To study the effects of sustained constitutive STAT5A-1*6 activation and to distinguish unique from shared events, altogether five independent dox induction experiments (one short-term and four long-term) were conducted (Figure 17A). Dox-induced and control

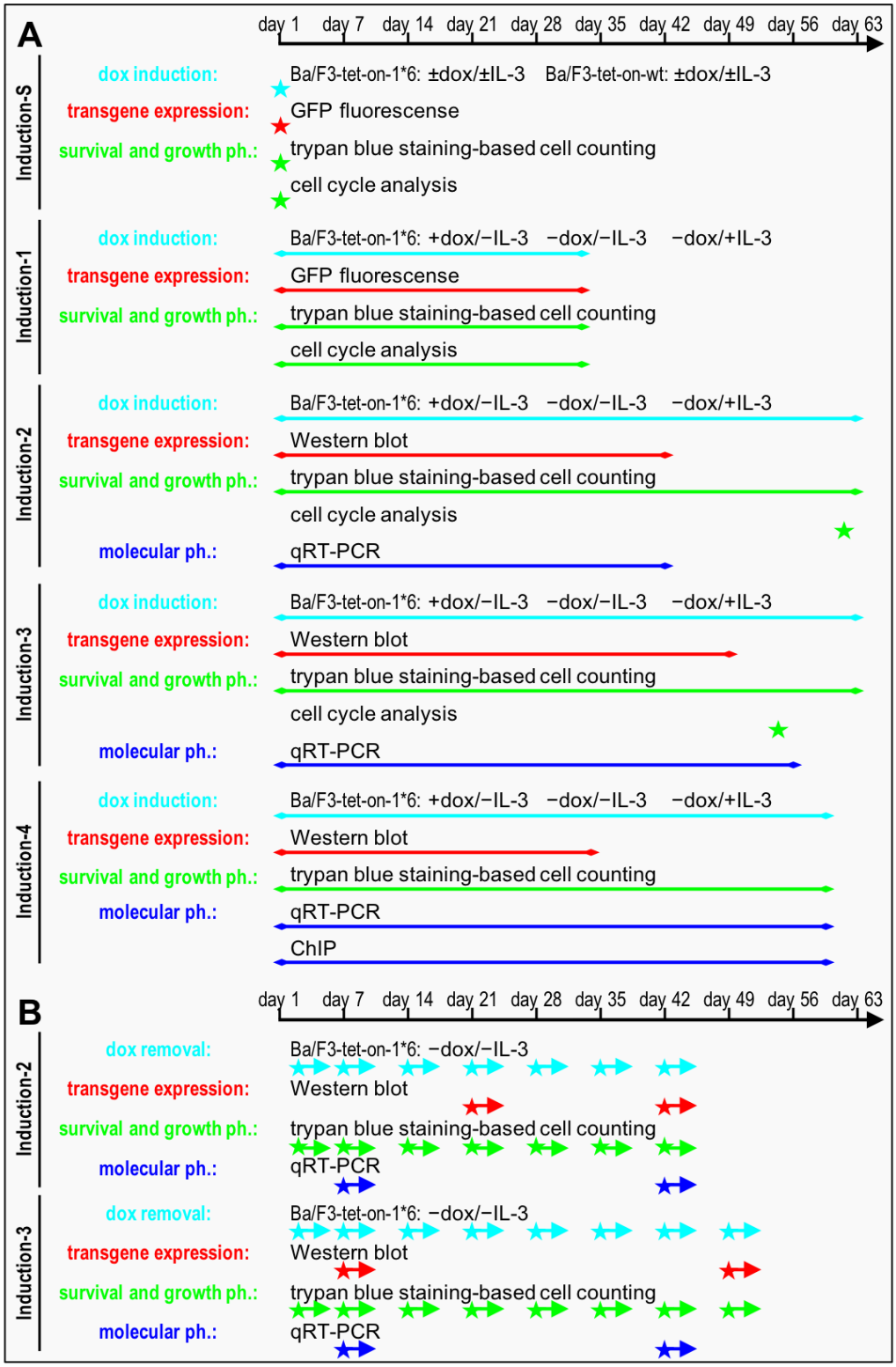

Figure 17: Schematic overview of short- and long-term doxycycline induction as well as doxycycline removal experiments conducted in the present study

One short-term ('Induction-S') and four long-term doxycycline (dox) induction ('Induction-1', '-2', '-3' and '-4') experiments **(A)** and fifteen dox removal (during Induction-2 and -3) experiments **(B)** were conducted as described in the text. The figure schematically illustrates these experiments. The duration of each dox induction experiment **(A)** and the starting point of each dox removal experiment **(B)** is depicted in turquoise. The applied treatment in terms of dox administration and IL-3 deprivation for dox-induced and control cells is detailed in the figure. Transgene expression (red), survival and growth phenotype (green) and optionally molecular phenotype (blue) was monitored in each experiment for the indicated time-points (asterisks indicate single time-points and double-sledged arrows indicate time spans). The applied methods are specified.

Abbreviations: ChIP = chromatin immunoprecipitation, dox = doxycycline, ph. =phenotype.

cells were investigated, in a first step, for their survival and growth phenotype and, in a second step, for their molecular phenotype (gene expression and ChIP profiles | Figure 17A). As explained above, Ba/F3-tet-on-wt cells served as a control for short-term dox induction (Figure 17A). Specifically, Ba/F3-tet-on-1*6 and -wt cells were induced for 14 h with dox both in the presence and absence of IL-3, with non-induced cells serving as a negative control for the effects of STAT5A-1*6/wt (Figure 17A). For long-term dox inductions, Ba/F3-tet-on-1*6 cells were induced with dox for five to eight weeks in the absence of IL-3 (+dox / −IL-3 | Figure 17A), with non-induced cells shortly withdrawn from IL-3 serving as a baseline control for STAT5A-1*6 activation (−dox / −IL-3 | Figure 17A). In addition, non-induced Ba/F3-tet-on-1*6 cells grown in parallel in the presence of IL-3 (−dox / +IL-3 | Figure 17A) served as a control for potential effects of long-term culture. This allowed to discern time-dependent effects of long-term cell culture on Ba/F3 cells of the same clonal background from the long-term effects of STAT5A-1*6 induction *per se.* Hereafter, the short-term (14 h) dox induction experiment is named 'Induction-S' and the long-term dox induction experiments are named 'Induction-1', 'Induction-2', 'Induction-3' and 'Induction-4' (Figure 17A).

3.2.1 STAT5A-1*6 production was continuously induced during short- and long-term doxycycline induction

Dox-induced Ba/F3-tet-on-1*6 and -wt cells were predicted to ectopically produce the transgenic STAT5A-1*6/wt and GFP proteins. In addition, STAT5A/B activation by phosphorylation was expected to occur in the presence of IL-3 and/or STAT5A-1*6 production. To verify transgene expression during Induction-S and -1, GFP fluorescence was analyzed by flow cytometry. To verify transgene expression and investigate STAT5A/B activation by phosphorylation during Induction-2, -3 and -4, Western blot analyses were performed using antibodies directed against FLAG-tagged STAT5A-1*6, total STAT5A/B and pSTAT5A/B, as described before (section 3.1).

As predicted, both Ba/F3-tet-on-1*6 and -wt cells exhibited increased levels of GFP fluorescence in the presence, but not in the absence of dox administration during Induction-S (Figure 18A), indicating ectopic STAT5A-1*6/wt protein production. Likewise, dox-induced Ba/F3-tet-on-1*6 cells of Induction-1 continuously emitted elevated levels of GFP fluorescence, starting as early as 12 h after dox administration, compared to non-induced cells (Figure 18B), indicating continuous ectopic STAT5A-1*6 protein production in the entire cell population. Maximum GFP fluorescence level was observed from day 2 to 4 of induction (Figure 18B). Then, GFP fluorescence level decreased gradually during the monitored time-span of 32 days (Figure 18B). From day 14 to 21 of induction, GFP fluorescence levels in the cell population were not distributed evenly around a mean, but rather around two means (Figure 18B). This suggests

heterogeneity in the cell population and the existence of two distinct ‘lower-GFP’ and ‘higher-GFP’ subpopulations. This observed shift in GFP fluorescence levels suggests that the initially smaller ‘lower-GFP’ subpopulation outgrew and eventually supplanted the ‘higher-GFP subpopulation (Figure 18B), possibly reflecting a selective growth advantage favoring the ‘lower-GFP’ subpopulation (predicted to express lower levels of STAT5A-1*6 protein).

Dox-induced IL-3-deprived Ba/F3-tet-on-1*6 cells continuously exhibited positive FLAG, pSTAT5A/B and total STAT5A/B signals, with IL-3-deprived control (−dox) cells exhibiting only positive total STAT5A/B signals and IL-3-supplemented control (−dox) cells exhibiting only positive pSTAT5A/B and total STAT5A/B signals (Figure 18C–E). This is in agreement with the predicted pattern and indicates specific ectopic STAT5A-1*6 protein production and STAT5A-1*6 activation by phosphorylation throughout long-term (33 to 49 days) dox-induction (Figure 18C–E). Agreeing with GFP fluorescence level during Induction-1, maximum STAT5A-1*6 protein level as identified by the FLAG, upper total STAT5A/B and pSTAT5A/B signals was reached at day 2 of induction and decreased gradually from day 8 to 11 in Induction-2 and -4 (Figure 18C and 18E). Comparison of the upper total STAT5A/B signals (representing STAT5A-1*6) and lower total STAT5A/B signals (representing endogenous STAT5A/B) in dox-induced cells indicated two- to three-fold overexpression of STAT5A-1*6 in the beginning of Induction-2 and -4, which then decreased to an expression level comparable to endogenous STAT5A/B (Figure 18C and E). Disagreeing with the pattern detected during Induction-1, -2 and -4, maximum STAT5A-1*6 protein level as identified by the FLAG and pSTAT5A/B signals detected at day 3 of induction was maintained throughout Induction-3, up to day 49 (Figure 18D). Intriguingly, the FLAG signal detected in Western blot during Induction-3 was broader (Figure 18D) than that detected during Induction-2 and -4 (Figure 18C and E). Additionally, a second pSTAT5A/B signal below the expected signal was detected at day 49 (Figure 18D). This suggests production of at least one aberrant STAT5A-1*6 protein with enhanced migration speed compared to the normal STAT5A-1*6 protein during Induction-3. It cannot be determined whether this aberrant form was also detected by the applied anti-total STAT5A/B antibody, given the overlap with the lower total STAT5A/B signal representing (unphosphorylated) endogenous STAT5A/B (Figure 18D).

In summary, STAT5A-1*6 protein levels were rapidly and continuously induced in all induction experiments and tended to decrease over time in at least four of five experiments. This may hint at deterministic events and/or a selective growth advantage for cells with decreased levels of STAT5A-1*6 protein production. In addition, an aberrant STAT5A-1*6 protein appeared to be produced over time in at least one of three long-term inductions, suggesting the probable existence of stochastic events.

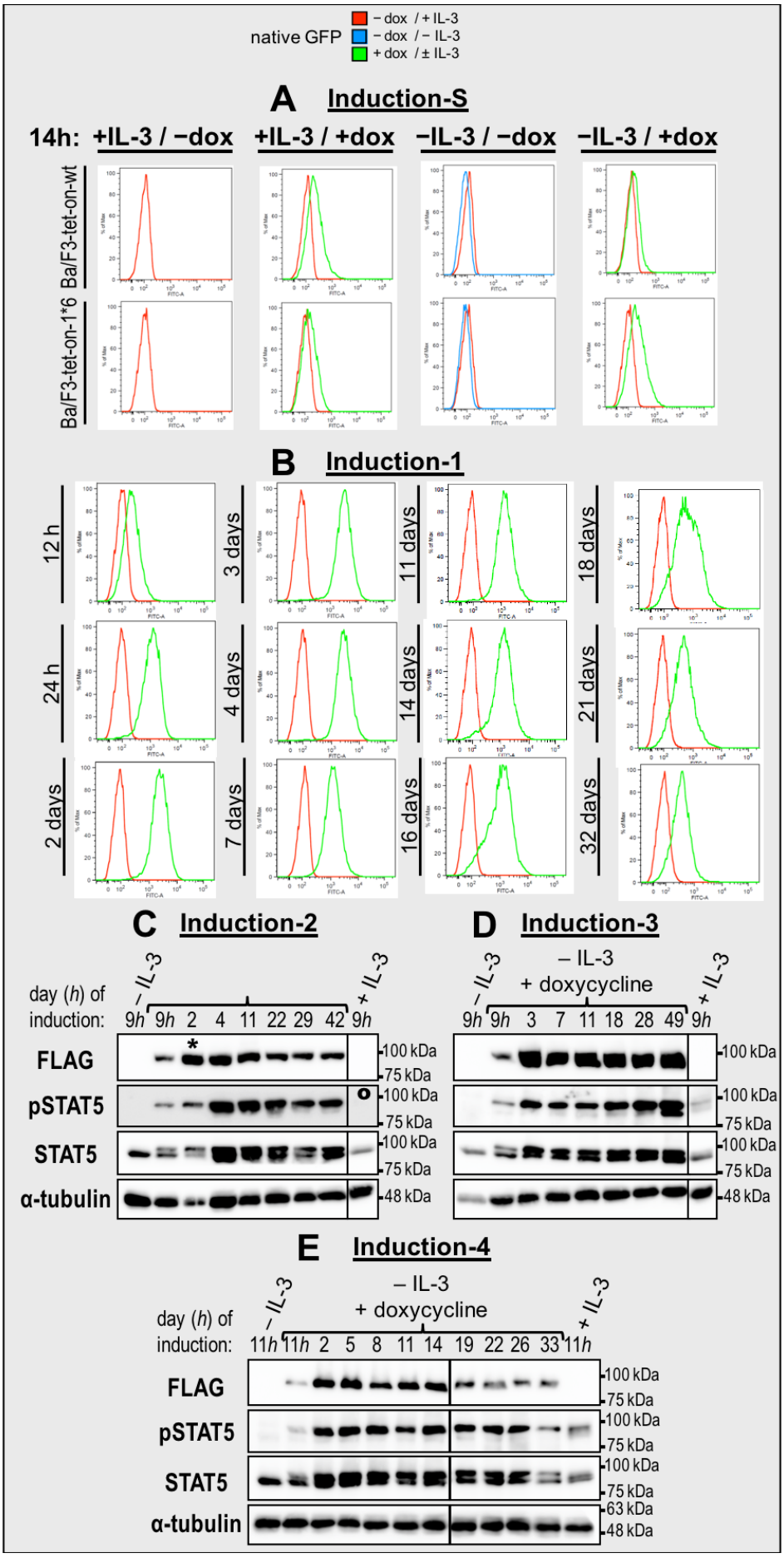
native GFP
– dox / + IL-3
– dox / – IL-3
+ dox / ± IL-3
A Induction-S
14h: +IL-3 / –dox
+IL-3 / +dox
–IL-3 / –dox
–IL-3 / +dox
Ba/F3-tet-on-wt
Ba/F3-tet-on-1*6
B Induction-1
12 h
24 h
2 days
3 days
4 days
7 days
11 days
14 days
16 days
18 days
21 days
32 days
C Induction-2
day (h) of induction:
– IL-3
+ IL-3
9h 9h 2 4 11 22 29 42 9h
FLAG
pSTAT5
STAT5
α-tubulin
100 kDa
75 kDa
48 kDa
D Induction-3
– IL-3
+ doxycycline
9h 9h 3 7 11 18 28 49 9h
E Induction-4
11h 11h 2 5 8 11 14 19 22 26 33 11h
63 kDa

Figure 18 (previous page): Transgenic STAT5A-1*6/wt or GFP protein was continuously detected during short- and long-term doxycycline induction

A: Ba/F3-tet-on-wt and Ba/F3-tet-on-1*6 cells were kept for 14 h in the presence or absence of IL-3 to turn endogenous STAT5A/B and STAT5A-wt activation on/off. They were kept either in the presence or absence of 1,000 ng/ml doxycycline to induce STAT5A-wt/1*6 production and study the effects of constitutive STAT5A-1*6 activation as part of the 'Induction-S' experiment. **B–E:** Ba/F3-tet-on-1*6 cells were grown in the absence of IL-3 and supplemented with doxycycline to induce STAT5A-1*6 production. 1,000 ng/ml dox was administrated as first dosage and100 ng/ml dox was replenished every two days. Cells were kept for up to nine weeks as part of the 'Induction-1', '-2', '-3' and '-4' experiments to study the effects of sustained constitutive STAT5A-1*6 activation. Non-induced cells were grown in the presence of IL-3 as control for the effects of transient endogenous STAT5A/B activation. Non-induced cells were rested without IL-3 for 9–11 h to turn off STAT5A/B activation as a negative control.

A,B:. Cells were harvested at the indicated time-points and analyzed by flow cytometry for native GFP fluorescence, as described in the Material and Methods section. Results are depicted as described in the legend of Figure 16. **C–E:** Cells were harvested at the indicated time-points and Brij protein lysates were prepared. Protein lysates were analyzed by Western blot exactly as described in the legend of Figure 9.

* FLAG-tagged STAT5A-1*6 was detected on a different membrane, where signals of the loading control α-Tubulin were not comparatively weak, as shown here.

º Only a partial faint pSTAT5A/B signal could be detected.

Abbreviations: dox = doxycycline.

3.2.2 STAT5A-1*6, but neither STAT5A-wt nor endogenous STAT5A/B, provides a cell survival and growth signal in the absence of IL-3

Various Ba/F3 cell lines have been shown to be viable and proliferate in the absence of IL-3, when expressing STAT5A-1*6 both continuously and inducibly (Funakoshi-Tago *et al.*, 2010, Gesbert and Griffin, 2000, Nosaka *et al.*, 1999, Onishi *et al.*, 1998). Therefore, dox-induced Ba/F3-tet-on-1*6 cells, but neither non-induced Ba/F3-tet-on-1*6 nor Ba/F3-tet-on-wt cells, were predicted to survive and to exhibit cell growth upon IL-3 deprivation. In addition, Ba/F3 cells have been found to not fully survive IL-3 deprivation upon first induction of STAT5A-1*6 expression in contrast to Ba/F3-1*6 cells expressing STAT5A-1*6 long-term (Gesbert and Griffin, 2000, Nosaka *et al.*, 1999). Therefore, IL-3 deprivation was predicted to initially negatively impact the cell survival and growth phenotype of dox-induced Ba/F3-tet-on-1*6 cells.

To monitor the cell survival and growth phenotype throughout the five independent dox induction experiments, the percentage of living cells and the absolute number of living cells were calculated regularly using trypan blue staining-based cell counting. Increases in the absolute number of living cells indicate the minimum rate of cell proliferation (doubling time). In addition, flow cytometry of DAPI-stained cells was performed during Induction-S and -1. In doing so, forward scatter (FSC) and sideward scatter (SSC) intensities and DAPI fluorescence intensities were measured for individual cells. FSC and SSC are measurements of cell size and granularity, as further detailed in the Material and Methods section (2.2.5, Figure 7). DAPI intercalates into the DNA and, hence, DAPI fluorescence intensity of a single stained cell is relative to the size of its genome. Proliferating eukaryotic cells repeatedly transition through four phases, constituting the cell cycle. They double their diploid chromosome set (2 n) during one cell cycle, having 2 n in G_1/G_0 phase, 2–4 n in S phase and 4 n in G_2/M phase. Given that only proliferating

cells transition through S and G_2 phase before cell division (M phase), high percentages of S and G_2/M phase cells indicate growing cell populations, whereas high percentages of G_1 phase cells indicate a growth arrest. In contrast to proliferating cells, dying cells undergoing programmed cell death break down their DNA (Kerr *et al.*, 1972, Prokhorova *et al.*, 2015, Taylor *et al.*, 2008). Hence, hypoploid cells, which have DNA amounts lower than diploid 2 n, were classified as dead/dying sub-G_1 phase cells.

Throughout Induction-S (Figure 19) and Induction-1 (Figure 20) sub-G1 cells were less granular and smaller than living cells, forming a clearly distinct population of cells in the scatter plot agreeing with the apoptotic breakdown of cells (Kerr *et al.*, 1972, O'Connell and Stenson-Cox, 2007, Prokhorova *et al.*, 2015, Taylor *et al.*, 2008). These differences were also visible upon trypan blue staining, where dead/dying blue-stained cells were smaller than non-stained living cells (data not shown). Living cells, on the other hand, showed size and granularity differences depending on their cell phase. Namely, G_1 phase cells were less granular and smaller than G_2 phase cells, with S phase cells being intermediate (Figures 19 and 20). This suggests that Ba/F3-tet-on-1*6 cells increase in size and granularity while transitioning through the cell cycle.

Both non-induced Ba/F3-tet-on-wt and non-induced Ba/F3-tet-on-1*6 cells as well as dox-induced Ba/F3-tet-on-wt cells showed a comparable survival and growth phenotype in all five dox induction experiments, when supplemented with IL-3. Trypan blue staining-based cell counting continually showed around 5 % dead/dying cells and allowed calculating doubling times of around 12 h for non-induced Ba/F3-tet-on-1*6 cells in the four long-term dox induction experiments (Figure 21 and data not shown). This agreed with around 5 % dead/dying cells detected in cell cycle analysis upon short-term Induction-S (Figure 19A) and during long-term Induction-1 (Figures 20B and 22A). The high percentage of dividing S and G_2/M phase cells of around 50 % confirmed the short doubling times and indicates a high rate of cell proliferation (Figures 19A, 19B, 20B and 22B). Overall, these results agree with previous studies (Funakoshi-Tago *et al.*, 2010, Nosaka *et al.*, 1999, Onishi *et al.*, 1998) and suggest that non-induced Ba/F3-tet-on-1*6 control cells (i.e. cells not expressing STAT5A-1*6) do not undergo time-dependent deterministic or stochastic changes affecting their growth or survival phenotype.

Figure 19 (next page): STAT5A-1*6, but neither STAT5A-wt nor endogenous STAT5A/B, provides a cell survival signal in the absence of IL-3

Ba/F3-tet-on-wt and Ba/F3-tet-on-1*6 cells were kept for 14 h in the presence **(A, B)** or absence of IL-3 **(C, D)** to turn endogenous STAT5A/B and STAT5A-wt activation on/off. They were kept either in the presence **(B, D)** or absence **(A,C)** of 1,000 ng/ml doxycycline to induce STAT5A-wt/1*6 production and study the effects of constitutive STAT5A-1*6 activation. Cells were harvested and analyzed by flow cytometry for cell cycle profiles, as described in the Material and Methods section. Cell cycle profiles were determined by DAPI staining and are depicted as histograms. Cell phases (G_1, S and G_2/M phase) were classified manually based on DNA content, as indicated in the figure. Cells containing DNA contents below the normal diploid chromosome set (2 n) were classified as sub-G_1 phase. This classification is also depicted in a scatter plot (sideward scatter versus forward scatter) to visualize size and granularity differences.

Abbreviations: dox = doxycycline, FSC = forward scatter, n = haploid chromosome set, SSC= sideward scatter.

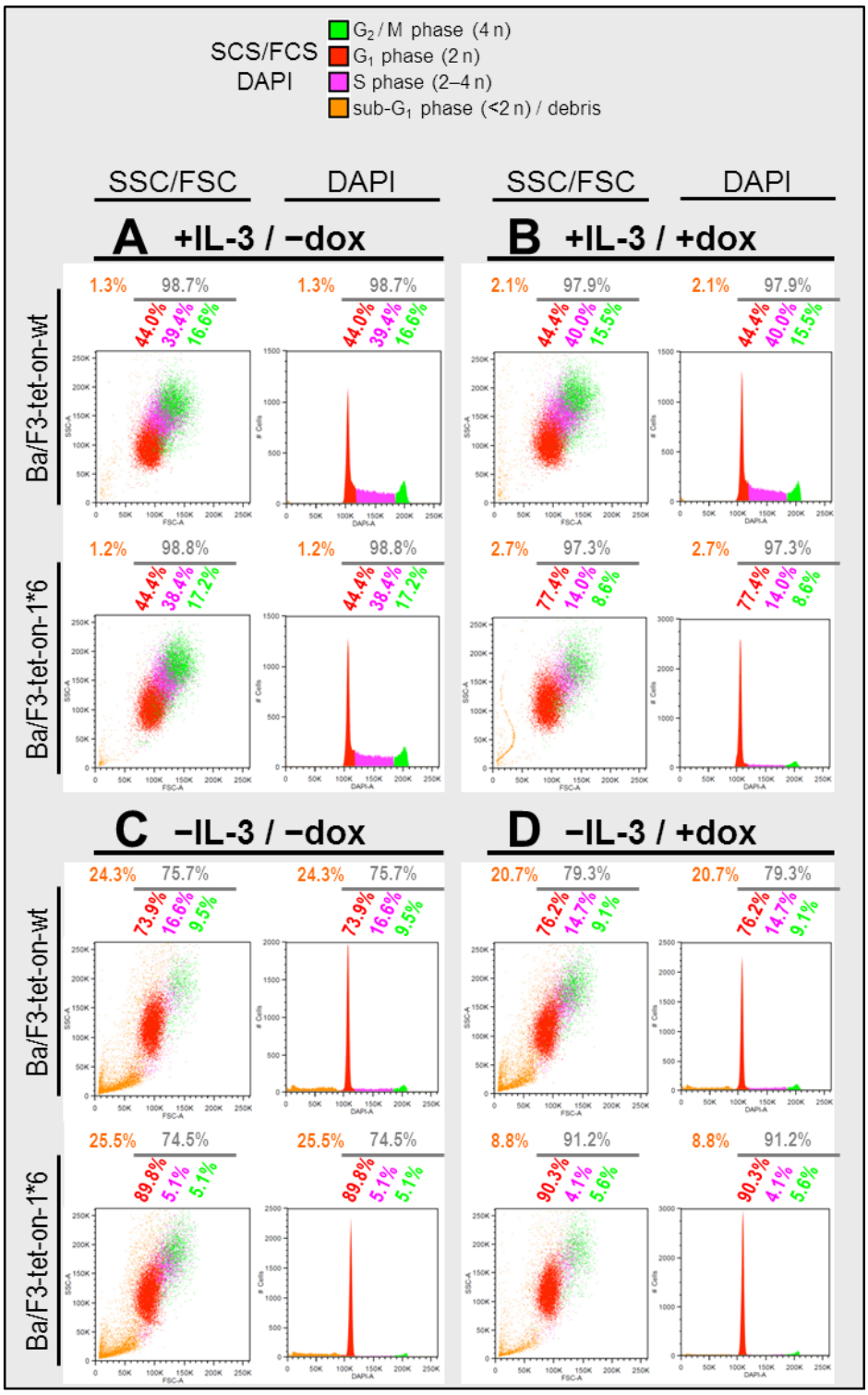

Figure 20 (next page): Ba/F3-tet-on-1*6 cells survive IL-3 deprivation and acquire IL-3-independent growth

Ba/F3-tet-on-1*6 cells were grown in the absence of IL-3 and supplemented with doxycycline to induce STAT5A-1*6 production. Cells were kept for five weeks as part of the 'Induction-1' experiment to study the effects of sustained constitutive STAT5A-1*6 activation **(C)**. Non-induced cells were grown in the presence of IL-3 **(B)** or deprived of IL-3 **(A)**, dying within two days, as controls for the effects of endogenous STAT5A/B activation. Cells were harvested at the indicated time-points and analyzed by flow cytometry for cell cycle profiles, as described in the Material and Methods section. Results are depicted as described in the legend of Figure 19.

Abbreviations: dox = doxycycline, FSC = forward scatter, n = haploid chromosome set, SSC= sideward scatter.

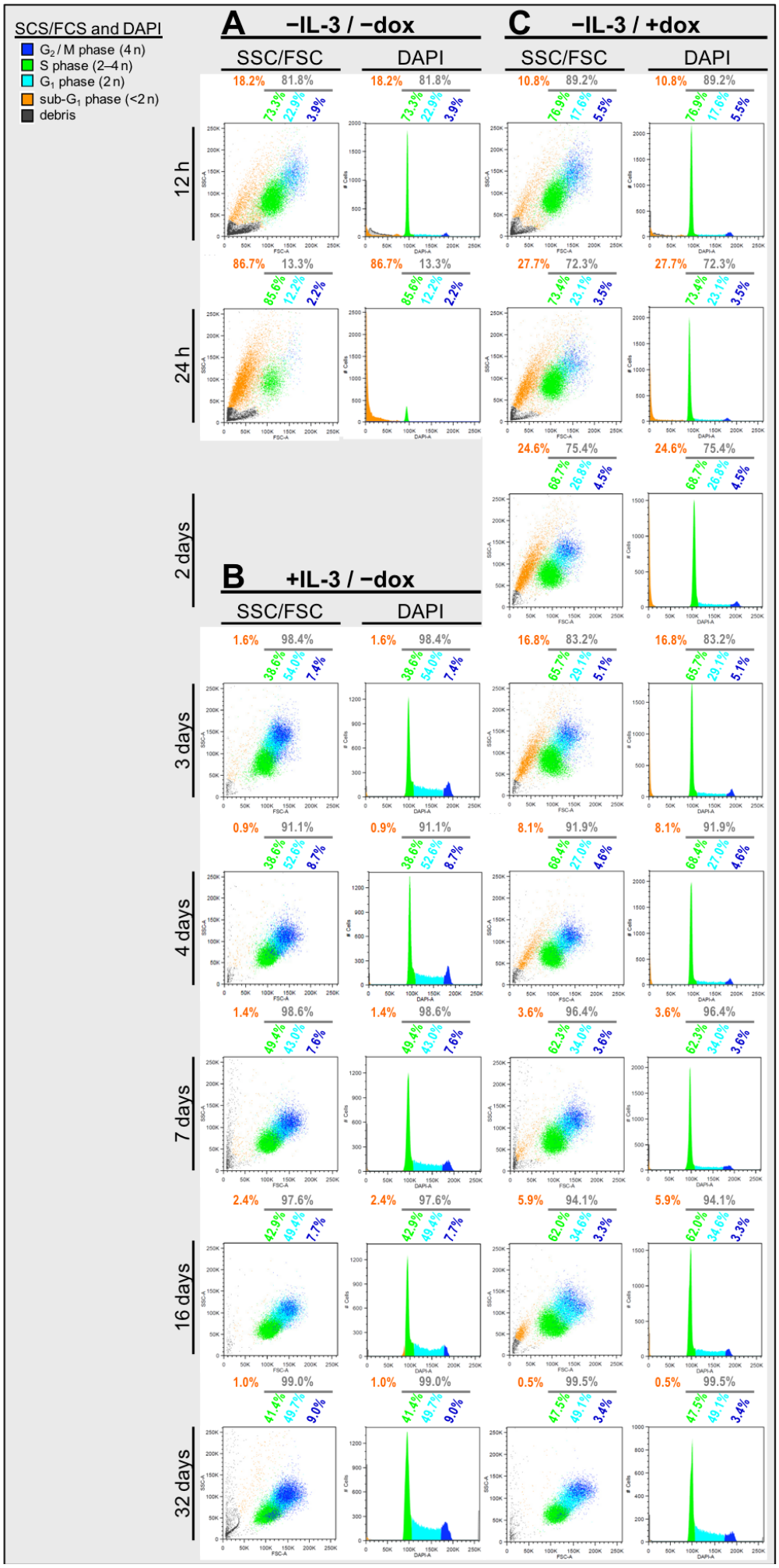
SCS/FCS and DAPI
G2 / M phase (4 n)
S phase (2–4 n)
G1 phase (2 n)
sub-G1 phase (<2 n)
debris
A −IL-3 / −dox
C −IL-3 / +dox
B +IL-3 / −dox
SSC/FSC
DAPI
12 h
24 h
2 days
3 days
4 days
7 days
16 days
32 days

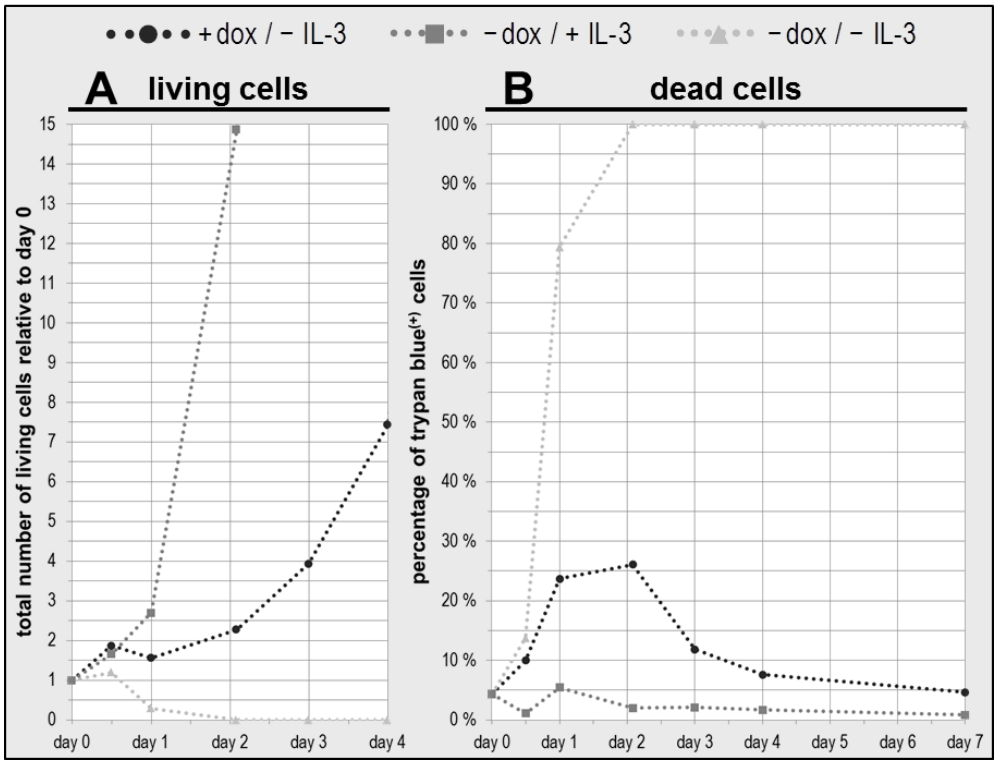

Figure 21: STAT5A-1*6 provides an IL-3-independent survival and growth signal in Ba/F3-tet-on-1*6 cells

Ba/F3-tet-on-1*6 cells were grown in the absence of IL-3 and supplemented with doxycycline to induce STAT5A-1*6 production. Cells were kept for five weeks as part of the 'Induction-1' experiment to study the effects of sustained constitutive STAT5A-1*6 activation. Non-induced cells were grown in the presence of IL-3 or deprived of IL-3, dying within two days, as controls for the effects of endogenous STAT5A/B activation. Cells were counted at indicated time-points after addition of trypan blue, staining selectively dead/dying cells, to determine cell density. **A:** The absolute number of living cells was calculated based on the volume of the cell suspension and plotted relative to the absolute number of living cells at day 0 (= 1). The number of non-induced cells relative to day 0 at day 3 and 4 was beyond the displayed segment of the diagram. The shown results are representative of four independent experiments. **B:** Percentage of dead/dying cells was calculated based on trypan blue staining. The shown results are representative of four independent experiments.

Abbreviations: dox = doxycycline.

In the absence of IL-3, both non-induced and dox-induced Ba/F3-tet-on-wt as well as non-induced Ba/F3-tet-on-1*6 cells died within three days in all induction experiments, as detected using trypan blue staining-based cell counting (Figure 21B and data not shown). Cell cycle analysis during Induction-S (Figure 19C and D) and Induction-1 (Figure 20A) showed that cells accumulated in G_1 phase, indicating a growth arrest, and died rapidly. This shows that neither STAT5A-wt nor endogenous STAT5A/B can provide a cell survival signal in the absence of IL-3, in agreement with previous studies (Funakoshi-Tago *et al.*, 2010, Gesbert and Griffin, 2000, Nosaka *et al.*, 1999, Onishi *et al.*, 1998). Of note, dox-induced Ba/F3-tet-on-1*6 cells expressing STAT5A-1*6 in the presence of IL3 similarly died in the course of several days, but at a slower pace and with longer accumulation in G_1 phase (Figure 19B and data not shown). This likewise agrees with observations reported by Nosaka *et al.* (1999).

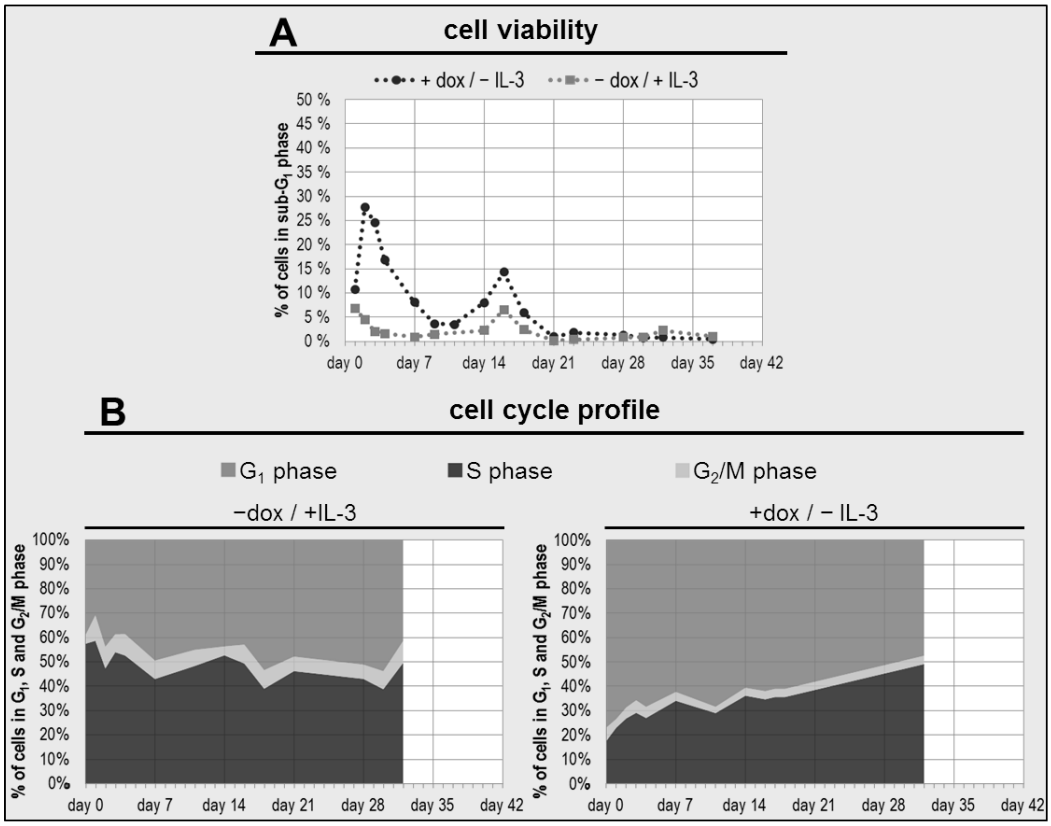

Figure 22: Percentage of dividing cells gradually increases during long-term doxycycline induction

Ba/F3-tet-on-1*6 cells were grown in the absence of IL-3 and supplemented with doxycycline to induce STAT5A-1*6 production. Cells were kept for five weeks as part of the 'Induction-1' experiment to study the effects of sustained constitutive STAT5A-1*6 activation. Non-induced cells were grown in the presence of IL-3 as a control for the effects of endogenous STAT5A/B activation. Cells were harvested regularly and analyzed by flow cytometry for cell cycle profiles, as described in the Material and Methods section. Percentage of dead/dying sub-G_1 phase cells was determined manually using the FlowJo 7.6.3 software at the indicated time-points **(A)**. Percentages of living cells in G_1, S and G_2/M phase were calculated by the 'Watson Pragmatic' algorithm integrated in the FlowJo 7.6.3 software and are depicted as an area diagram **(B)**. For non-induced cells percentages were calculated for day 0, 1, 2, 3, 4, 7, 11, 14, 16, 18, 21, 28, 30 and 32. For doxycycline-induced cells percentages were calculated for day 0, 1, 2, 3, 4, 7, 11, 14, 16 and 32. The day 0 time-point corresponds to 12 h of doxycycline induction and the day 1 time-point to 24 h of doxycycline induction.

Abbreviations: dox = doxycycline.

Overall, Ba/F3-tet-on-1*6 cells treated with dox in the absence of IL-3 exhibited similar changes in their survival and growth phenotype across all induction experiments as detected using trypan blue staining-based cell counting (Figure 21 and data not shown). This is why results from Induction-S and -1 are representative for all induction experiments and described exemplarily. Namely, after 12–14 h of dox induction around 75 % cells accumulated in G_1 phase and exhibited around 10 % dead/dying cells (Figures 19D, 20C and 21B), similarly to non-induced cells deprived of IL-3 (Figures 19C, 20A, and 21B). In sharp contrast however, the absolute number of living dox-induced cells stagnated until 24 h of dox induction and then slowly increased, mirrored by an increase in the percentage of dividing cells (S and G_2/M phase), indicating cell proliferation (Figures 20C, 21A and 22B). The percentage of dead/dying cells increased to 25 % at day 2 of induction and thereafter gradually decreased to 5 % after one week (Figures 20B, 20C, 21B and 22A), suggesting a temporarily impaired cell viability and growth

arrest. In summary, these results suggest that STAT5A-1*6 provides an IL-3-independent (i) survival and (ii) cell growth signal in Ba/F3-tet-on-1*6 cells, as predicted and in accordance with previous studies (Funakoshi-Tago *et al.*, 2010, Gesbert and Griffin, 2000, Nosaka *et al.*, 1999, Onishi *et al.*, 1998).

3.2.3 Doxycycline-induced Ba/F3-tet-on-1*6 cells gradually acquire a survival and growth phenotype

Ba/F3 cells expressing STAT5A-1*6 have been shown to cause progressively worsening tumors after being injected into immunocompromised mice (Funakoshi-Tago *et al.*, 2010, Gesbert and Griffin, 2000). It was thus hypothesized that oncogenicity of Ba/F3-tet-on-1*6 cells in terms of cell survival and growth phenotype progressively increases in the course of long-term dox induction (i.e. in the course of STAT5A-1*6 expression).

As explained above, results of Induction-1 are representative of all induction experiments and described exemplarily. While the percentage of dead/dying cells already reached the 5 % level observed in non-induced cells after only one week of induction (exempting an increase in the third week of dox induction not observed in the other induction experiments, potentially due to an error in cell handling | data not shown, Figures 20C and 22A), the initial percentage of dividing cells of 20 % gradually increased and reached around 55 % at day 30 of induction, comparable to that of non-induced control cells (Figures 20C and 22B). In accordance with this, doubling times gradually decreased and reached around 12 h (comparable to non-induced control cells) at day 30 of induction (data not shown).

3.2.4 Stochastic changes accumulated in Ba/F3-tet-on-1*6 cells transformed by STAT5A-1*6 over time

The fact that the cell survival and growth phenotypes changed in a similar manner in all five induction experiments raises the possibility that these changes occurred in a deterministic manner and are a direct effect of STAT5A-1*6 activity as transcription factor. At the same time, the cells enduring the removal of IL-3 experience a strong selective pressure for survival and growth, as probably do prospective cancer cells during *in vivo* oncogenesis. This may result in stochastic processes, where individual cells with higher viability and/or proliferation rate possess a selective growth advantage and, thus, outgrow other cells.

Flow cytometric analysis of GFP fluorescence levels revealed heterogeneity among dox-induced Ba/F3-tet-on-1*6 cells during Induction-1 and suggested the displacement of most cells by a subpopulation with a selective growth advantage, i.e. clonal evolution (see 3.2.1 and Figure 18B). In addition, their gradual increase in cell survival and growth phenotype (Figures 20–22) likewise pointed to clonal evolution and suggested the acquisition of cancer hallmarks. As detailed in the introduction section (1.1.3), mutability

per se has been argued to confer a selective growth advantage to (pre)-cancer cells, leading to acquisition of the 'genomic instability' cancer hallmark and often involving chromosomal aberrations. STAT5A-1*6 has been linked to oxidative stress in Ba/F3 cells (Bourgeais *et al.*, 2017), which can promote DNA damage and lead to chromosomal aberrations. Therefore, Ba/F3-tet-on-1*6 cells were hypothesized to acquire chromosomal aberrations indicative of 'genomic instability' during long-term dox induction. Numerical chromosomal aberrations lead to changes in the overall DNA content in a given cell. To investigate such potential deviations in DNA content in Ba/F3-tet-on-1*6 cells during long-term dox induction, DAPI-stained dox-induced cells were subjected to cell cycle analysis at day 61 of Induction-2 and at day 54 of Induction-3 together with non-induced cells as control. In parallel, primary human leukocytes were analyzed as a reference for the absolute DNA content, to identify possible deviations from the *in vivo* murine genome.

One haploid murine chromosome set comprises roughly 2.9 Gbp DNA and one such human set roughly 3.1 Gbp DNA (Ensembl database, 27.01.2018). DAPI fluorescence intensity of non-induced Ba/F3-tet-on-1*6 cells (of Induction-2 and -3) in G_1 phase was slightly lower than that of human leukocytes (Figure 23B and data not shown), verifying that the investigated non-induced Ba/F3-tet-on-1*6 cells have roughly the same DNA content as human and murine cells. This suggests an euploid diploid chromosome set for the Ba/F3-tet-on-1*6 cell line (disregarding putative changes during long-term cell culture) and possibly for the parental Ba/F3 cell line (disregarding putative changes during establishment of the Ba/F3-tet-on-1*6 cell line) employed in the present study.

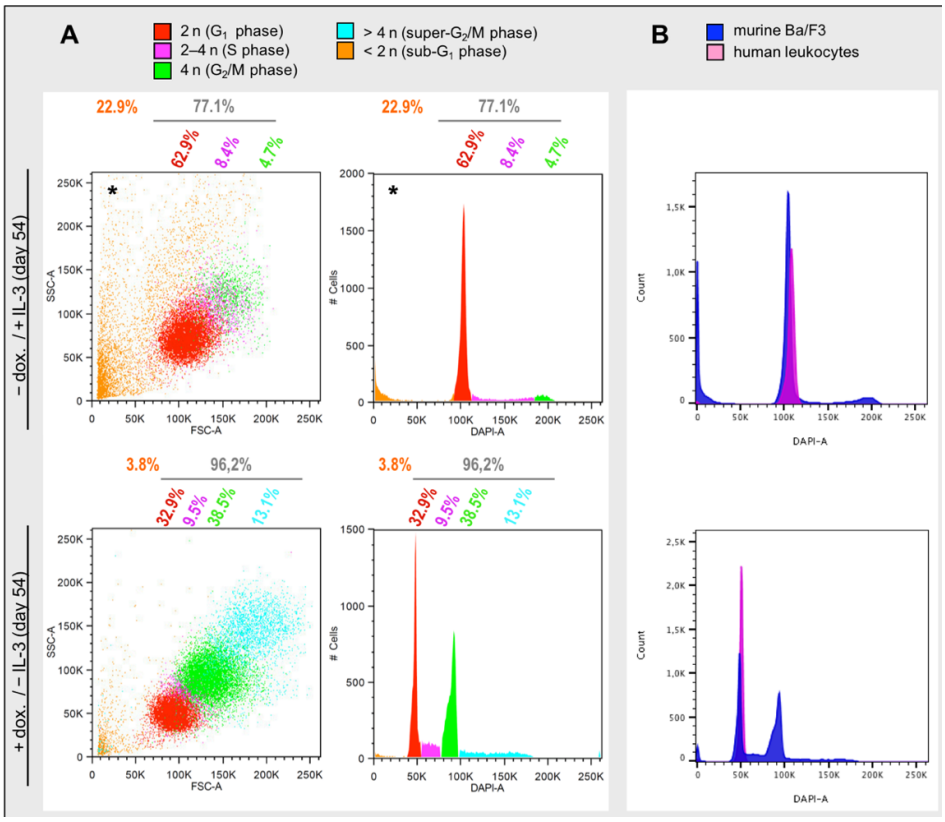

Figure 23 (previous page): An aneuploid Ba/F3-tet-on-1*6 subpopulation emerged during long-term doxycycline induction

A, B: Ba/F3-tet-on-1*6 cells were grown in the absence of IL-3 and supplemented with doxycycline as part of the 'Induction-3' experiment to induce STAT5A-1*6 production in order to study the effects of sustained constitutive STAT5A-1*6 activation. Non-induced cells were grown in the presence of IL-3 as a control for the effects of endogenous STAT5A/B activation. Doxycycline-induced and non-induced cells were harvested after 54 days. **A:** Cells were analyzed by flow cytometry for cell cycle profiles as described in the Material and Methods section. Results are depicted as described in the legend of Figure 19. **B:** Leukocytes were extracted from human blood as a reference for genome size (kind donation from Dr. Melanie Werner-Klein). Cell cycle profiles of Ba/F3-tet-on-1*6 cells and human blood leukocytes are depicted together as histograms. **A, B:** The scale depicting DAPI fluorescence intensities was adjusted to fit the data of doxycycline-induced cells into the shown window. Both non-induced and doxycycline-induced cells exhibited equal DAPI fluorescence intensities for the depicted 2–4 n cell (sub)population.

*An error in cell handling (cell density too high) caused increased cell death in non-induced cells.

Abbreviations: dox = doxycycline, n = haploid chromosome set.

The cell cycle profile of dox-induced cells from Induction-2 was similar to that of non-induced cells (data not shown), indicating no acquisition of numerical chromosomal aberrations in Induction-2 cells. Strikingly though, dox-induced cells from Induction-3 exhibited an aneuploid subpopulation of cells in addition to a 2 n–4 n subpopulation, as observed in non-induced cells (Figure 23A, > 4 n cell population). The DNA content of this aneuploid subpopulation ranged from roughly 4 n to roughly 8 n (Figure 23B), suggesting tetraploidy and ongoing cell proliferation. This finding implies that a tetraploidization event probably occurred in at least one cell during Induction-3. This therefore points to a possible clonal evolution of cancer hallmarks during long-term dox induction and strongly suggests acquisition of the 'genomic instability' cancer hallmark during Induction-3. Besides, the heterogeneity within the cell population detected in Induction-1 (Figure 18B) and Induction-3 (Figure 23) agrees with the heterogeneity found in cancers *in vivo* (Vogelstein *et al.*, 2013).

3.3 Characterization of the growth and survival phenotypes of induced Ba/F3-tet-on-1*6 cells upon doxycycline removal

Three previous findings, namely (i) the heterogeneity detected during Induction-1 and -3 (Figures 18B and 23), (ii) the gradual change in cell survival and growth phenotype during all induction experiments (Figures 20–22) and (iii) the putatively tetraploid subpopulation detected during Induction-3 (Figure 23), may indicate that individual Ba/F3-tet-on-1*6 cells acquired 'driver' alterations in a stochastic manner during long-term dox induction, potentially mirroring *in vivo* oncogenesis. These 'driver' alterations are predicted to spread and establish themselves by clonal evolution, leading to an incremental increase in oncogenicity. In particular, these findings potentially point to the acquisition of the 'resisting cell death', 'sustaining proliferative signaling' and 'genomic instability' cancer hallmarks during long-term dox induction. Acquisition of the 'Resisting cell death' and 'Sustaining proliferative signaling' cancer hallmarks implies that Ba/F3-tet-on-1*6 cells do not rely on survival and growth signals, including constitutive STAT5A-1*6 activation in place of IL-3 signaling.

To investigate this hypothesis, dox was removed at different stages of dox induction, to halt STAT5A-1*6 production and, thus, to uncover the effects that are dependent and independent of constitutive STAT5A-1*6 activation. Dox was removed weekly during Induction-2 and -3, as depicted schematically in Figure 17B, and cells were thereafter investigated, in a first step, for their survival and growth phenotype and, in a second step, for their gene expression profile.

3.3.1 STAT5A-1*6 production halted upon dox removal

The employed 'Tet-on advanced' inducible expression system has been shown to be tight and reversible (Urlinger *et al.*, 2000). Hence, dox removal was predicted to result in a rapid halt of STAT5A-1*6 transgene expression and, accordingly, a persisting absence of STAT5A/B activation by phosphorylation given the absence of IL-3. To verify this, Western blot analysis was performed using antibodies directed against FLAG-tagged STAT5A-1*6, total STAT5A/B and pSTAT5A/B during selected dox removal experiments, namely dox removal from day 21 and day 42 of Induction-2 as well as from day 7 and day 49 of Induction-3 (see Figure 17B). Non-induced cells rested without IL-3 served as a negative (baseline) control for STAT5A/B activation.

As predicted, FLAG and the upper total STAT5A/B protein signals disappeared after two days of dox removal, evidencing the halt in ectopic STAT5A-1*6 protein production (Figure 24). pSTAT5A/B levels concurrently dropped upon dox removal, although faint pSTAT5A/B signals remained in dox-removed cells later than day 2 of dox removal, albeit not in the negative control (Figure 24). It is unclear, whether the residual pSTAT5A/B signals constitute *bona fide* signals or merely artefacts.

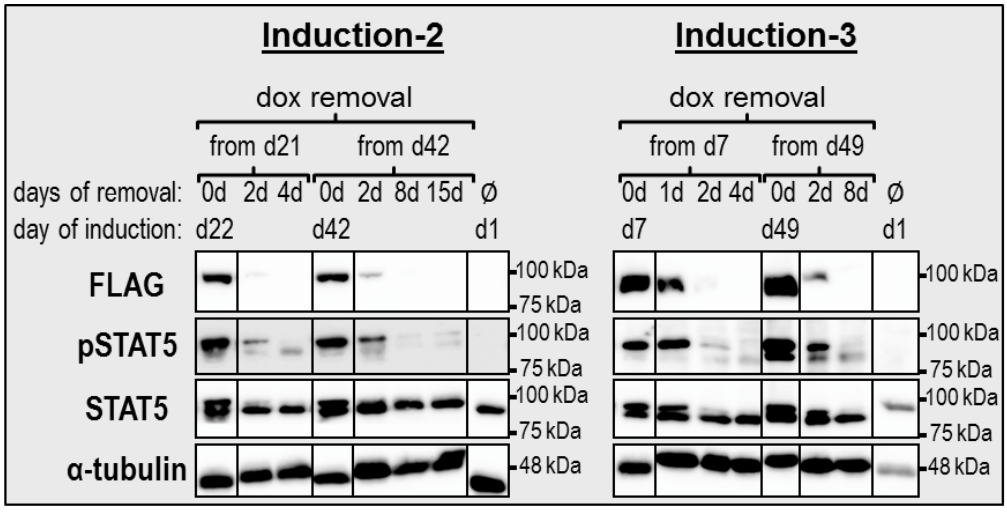

Figure 24: STAT5A-1*6 protein production halts upon doxycycline removal

Ba/F3-tet-on-1*6 cells were supplemented with doxycycline to induce STAT5A-1*6 production and grown in the absence of IL-3. Cells were kept for seven weeks as part of the 'Induction-2' and 'Induction-3' experiments to study the effects of sustained constitutive STAT5A-1*6 activation. At the indicated time-points, a subset of cells was washed and removed from doxycycline and kept in the absence of IL-3 to halt STAT5A-1*6 production in order to uncover the effect of constitutive STAT5A-1*6 activation. Non-induced cells were rested for 9 h without IL-3 to turn off STAT5A/B activation as a negative control (Ø). Cells were harvested at the indicated time-points and Brij protein lysates were prepared. Protein lysates were analyzed by Western blot exactly as described in the legend of Figure 9.

Abbreviations: Ø = rested without IL-3, d = day(s), dox = doxycycline.

3.3.2 STAT5A-1*6 function as survival and growth signal decreases over time

As detailed above, Ba/F3-tet-on-1*6 cells were hypothesized to acquire the 'Resisting cell death' and 'Sustaining proliferative signaling' cancer hallmarks during long-term dox induction. Accordingly, they would be expected to survive and proliferate despite dox removal upon acquisition of these cancer hallmarks. To investigate their cell survival and growth phenotype upon dox removal, dox-removed cells were monitored by light microscopy and trypan blue staining-based cell counting, as described above.

Interestingly, all dox-induced cells ultimately died when dox removal was initiated within the first two weeks of Induction-2 and within the first four weeks of Induction-3 (Table 9). In doing so, the absolute number of living cells decreased slowly, the culture showing > 90 % dead/dying cells after 4–7 days of dox removal (Table 9 and data not shown). At the latest 11 days after dox removal, no living cells remained (Table 9). In later weeks (4 to 5) of induction however, dox-induced cells were less susceptible to dox removal. Specifically, first only scattered morphologically aberrant cells survived dox removal in the long term (Table 9). After that however, higher percentages of cells managed to survive dox removal, with up to 25 % living cells observed after one week of dox removal (Table 9 and data not shown). The absolute number of living cells increased over time, albeit with longer doubling times than for dox-induced cells, indicating ongoing cell proliferation (Table 9 and data not shown). Overall, these results indicate that a cell survival and proliferation effect independent of STAT5A-1*6 was acquired over time, allowing survival and growth despite the loss of STAT5A-1*6 expression (Table 9).

Table 9: STAT5A-1*6 function as survival and growth signal decreases over time

Ba/F3-tet-on-1*6 cells were supplemented with doxycycline to induce STAT5A-1*6 production and grown in the absence of IL-3. Cells were kept for seven weeks as part of the 'Induction-2' and 'Induction-3' experiments to study the effects of sustained constitutive STAT5A-1*6 activation. At the indicated time-points, a subset of cells was washed and removed from doxycycline and kept in the absence of IL-3 to halt STAT5A-1*6 production in order to uncover the effect of constitutive STAT5A-1*6 activation. Doxycycline-removed cells were monitored by trypan blue staining-based cell counting exactly as described in the legend of Figure 21. The table specifies the percentage of dead/dying cells following doxycycline removal at the indicated time-points and the change (Δ) in absolute living cell number within the first four days of doxycycline removal. '−' specifies decrease, '+' increase and '0' no change. Doubled '−' signified ≥ 50% decrease, doubled '+' ≥ 100 % increase and tripled '+' ≥ 200 % increase.

* Only scattered morphologically aberrant cells survived.

doxycycline removal	Induction-2		Induction-3	
	% cell death	Δ absolute living cell number (4 days)	% cell death	Δ absolute living cell number (4 days)
week 1 (day 3)	100 % after 6 days	−−	100 % after 11 days	−−
week 1 (day 7)	100 % after 7 days	−−	100 % after 9 days	−−
week 2 (day 14)	100 % after 10 days	−−	100 % after 10 days	−−
week 3 (day 21)	> 90 % after 7 days*	**0**	100 % after 10 days	−
week 4 (day 28)	~70 % after 7 days	++	> 90 % after 16 days*	−
week 5 (day 35)	~75 % after 8 days	+	> 90 % after 23 days*	++
week 6 (day 42)	~40 % after 18 days	+++	~50 % after 11 days	+++
week 7 (day 49)	no experiment		~50 % after 9 days	++

Intriguingly, this was noticeably occurring earlier in case of Induction-2 compared to Induction-3 (Table 9).

In summary, these observations suggest that STAT5A-1*6 function as a survival and growth factor is essential in the first few weeks of dox induction, while it appears to be progressively lost thereafter. These findings support the hypothesized acquisition of 'resisting cell death' and 'sustaining proliferative signaling' cancer hallmarks during Induction-2 and -3.

3.4 Characterization of the molecular phenotype of Ba/F3-tet-on-1*6 cells upon dox induction and dox removal

3.4.1 STAT5 target gene expression was induced throughout long-term doxycycline induction and aborted upon doxycycline removal

STAT5A/B has been found to be a potent transactivator of tumor suppressor and oncogenes as well as of genes, which have no known role in oncogenesis (Kang *et al.*, 2013). This raises the question as to how constitutive STAT5A-1*6 activation relates to STAT5 target gene expression during long-term dox induction. STAT5A-1*6 protein levels declined during Induction-2 and -4, but remained stable during Induction-3 (Figure 18C–E). STAT5A-1*6 protein levels were hypothesized to correlate with STAT5A-1*6 transcriptional activity and, accordingly, mRNA levels of its target genes. Additionally, the progressive increase in cell survival and proliferation during long-term dox induction (Figures 20 and 22) raises the possibility that expression of STAT5-controlled tumor suppressor and oncogenes might be subjected to negative and positive selection pressures, respectively. Hence, it was hypothesized that Ba/F3-tet-on-1*6 cells accumulated 'driver' alterations during long-term dox induction that affected the mRNA levels of tumor suppressor and of oncogenes in an opposite manner. Moreover, the importance of STAT5A-1*6 function as survival and growth signal decreased over time (Table 9), raising the possibility of an acquired upregulation of oncogenes independent of STAT5A-1*6 transcriptional activity, allowing survival and growth of dox-induced cells upon dox removal.

To investigate these three hypotheses, samples taken during the long-term dox induction experiments Induction-2, -3 and -4 and selected dox removal experiments (Induction-2: dox removal from day 7 and day 42; Induction-3: dox removal from day 7 and day 49) were analyzed by RT-qPCR (as depicted in Figure 17). In doing so, samples from rested non-induced cells served as baseline control, allowing calculation of fold-induction, and samples from non-induced cells growing with IL-3 (exhibiting non-synchronized cycles of transient endogenous STAT5A/B activity) as reference. Using RT-qPCR, STAT5A-1*6 transgene mRNA levels were analyzed and compared to STAT5A-1*6 protein levels. *36b4* housekeeping gene mRNA levels were monitored as internal control, in addition to

mRNA levels of a panel of STAT5 target genes (*Cis*, *Spi2.1*, *c-Myc*, *Pim-1*, *Bcl-x* and *Osm* [only Induction-4]). Of note, Nosaka *et al.* (1999), Nosaka and Kitamura (2002) and Funakoshi-Tago *et al.* (2013) have shown that *c-Myc*, *Pim-1* and *Bcl-x* effect IL-3-independent survival of Ba/F3 cells expressing STAT5A-1*6, suggesting essential roles of these genes in STAT5A-1*6-induced oncogenesis.

As expected, STAT5A-1*6 transgene mRNA levels were at the detection limit in non-induced cells (Figure 25A). Upon dox induction, STAT5A-1*6 transgene mRNA levels were strongly induced (Figure 25A). Subsequently, the STAT5A-1*6 mRNA levels decreased to around 30 % of the maximal level during Induction-2, -3 and -4, albeit less rapidly during Induction-4 (Figure 25A). This decrease in mRNA levels thus correlated with decreasing protein levels observed in Induction-2 and -4 (Figure 18C and E). Interestingly, the considerable decrease in STAT5A-1*6 mRNA level during Induction-3 was not reflected at the protein level (Figure 18D), suggesting a possible difference at a regulation step of STAT5A-1*6 protein production or stability following mRNA synthesis in Induction-3, compared to Induction-2 and -4. In contrast to Induction-2 and -4, STAT5A-1*6 mRNA levels in Induction-3 increased again to the level of initial induction after seven weeks of dox treatment (Figure 25A). Intriguingly, this renewed peak of mRNA level correlated with the detection of a putatively tetraploid subpopulation and was followed by another decrease after eight weeks of dox treatment (Figure 23). As opposed to STAT5A-1*6 mRNA levels, mRNA levels of the housekeeping gene *36b4* remained stable in non-induced and dox-induced cells throughout long-term dox induction (Figure 25H).

In non-induced cells, *Cis* mRNA was stably detected in cells grown in the presence of IL-3, at levels ten- to twenty-fold above those observed in non-induced rested cells (Figure 25B). *Cis* mRNA levels were likewise sustainedly upregulated during dox induction and correlated closely with STAT5A-1*6 mRNA levels, (Figure 25A and B). *Spi2.1* mRNA levels, on the other hand, were near detection limit in non-induced rested cells and not detectably expressed in IL-3-growing cells (Figure 25C). This suggests a transient IL-3-mediated induction of *Spi2.1* mRNAs, resulting in overall low mRNA levels in non-synchronized non-induced cells grown in IL-3, in agreement with past observations by Rascle *et al.* (2003). Strikingly, however, *Spi2.1* mRNA levels were strongly upregulated in dox-induced cells (Figure 25C). In particular, *Spi2.1* mRNA levels increased progressively upon dox induction during Induction-2 and -4, reaching thirty-fold induction relative to non-induced rested cells in the second week of dox treatment (Figure 25C). This tremendous upregulation suggests a STAT5A-1*6-specific effect. Accordingly, *Spi2.1* mRNA levels subsequently decreased, correlating with the decrease in STAT5A-1*6 mRNA levels (Figure 25A and C). By contrast, during Induction-3, *Spi2.1* expression was only induced around eight-fold above the respective levels of

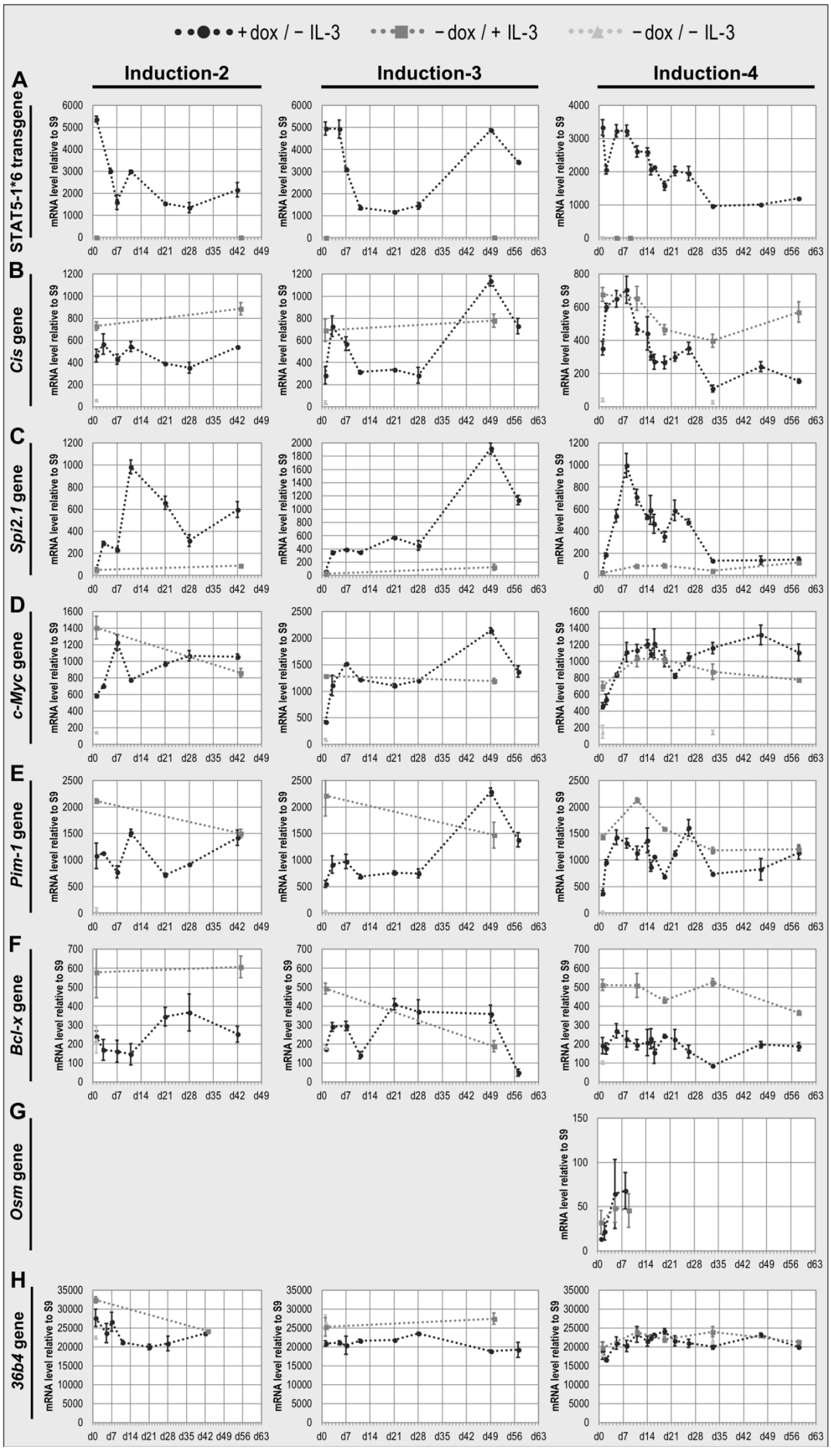
+dox / − IL-3
−dox / + IL-3
−dox / − IL-3
Induction-2
Induction-3
Induction-4
A STAT5-1*6 transgene
B Cis gene
C Spi2.1 gene
D c-Myc gene
E Pim-1 gene
F Bcl-x gene
G Osm gene
H 36b4 gene
mRNA level relative to S9
d0 d7 d14 d21 d28 d35 d42 d49 d56 d63

Figure 25 (previous page): Expression of STAT5 target genes *Cis*, *Spi2.1*, *c-Myc* and *Pim-1* is induced throughout long-term STAT5A-1*6 induction

Ba/F3-tet-on-1*6 cells were grown in the absence of IL-3 and supplemented with dox (doxycycline) to induce STAT5A-1*6 production. Cells were kept for six to nine weeks as part of the 'Induction-2', '-3' and '-4' experiments to study the effects of sustained constitutive STAT5A-1*6 activation. Non-induced cells were grown in the presence of IL-3 as control for the effects of endogenous STAT5A/B activation or rested without IL-3 for 9–14 h as a baseline control for the absence of STAT5A/B activation. Cells were harvested at the indicated time-points. RNA was extracted and reverse transcribed into cDNA. cDNA was analyzed by RT-qPCR using primers specific for the transcripts of the STAT5A-1*6 transgene, the STAT5 target genes *Cis*, *Spi2.1*, *c-Myc*, *Pim-1*, *Bcl-x* (Bcl-xL isoform) and the control gene *36b4*. The error bars depict standard deviation among RT-qPCR replicates. The dotted lines connect single data points for dox-induced cells and non-induced cells, growing in the presence of IL-3.

Abbreviations: d = day, dox = doxycycline.

non-induced rested cells in the first four weeks of induction (Figure 25C). Then, *Spi2.1* mRNA levels increased tremendously correlating with that of STAT5A-1*6 (Figure 25A and C). Taken together, these results suggest that STAT5A-1*6 protein transactivated both *Cis* and *Spi2.1* in a dose-dependent manner throughout long-term dox induction.

In non-induced cells, *c-Myc* and *Pim-1* mRNA levels were stably detected, around four- to twelve-fold and around twenty- to fifty-fold above the respective levels observed in rested cells, in cells grown in IL-3 (Figure 25D and E). Upon dox induction, *c-Myc* and *Pim-1* mRNA levels were upregulated at least four(*c-Myc*)/eight(*Pim-1*)-fold relative to non-induced rested cells initially and then increased steadily to at least seven (*c-Myc*)/ twenty(*Pim-1*)-fold above the level of non-induced rested cells during the first week of induction (though to a lesser extent for *Pim-1* in Induction-2 | Figure 25D and E). This pattern correlated with those of STAT5A-1*6, *Cis* and *Spi2.1* mRNA levels (Figure 25A–C). This suggests that STAT5A-1*6 likewise mediated *c-Myc* and *Pim-1* transactivation in a dose-dependent manner. Moreover, the increase in *c-Myc* and *Pim-1* mRNA levels (Figure 25D and E) correlated with the increase in cell survival and proliferation (Figures 20 and 21) observed during the first week of induction, suggesting a dose-dependent effect of *c-Myc* and *Pim-1* expression on cell survival and growth. Subsequently, *c-Myc* and *Pim-1* mRNA levels only correlated partially with STAT5A-1*6 mRNA levels (Figure 25A, D and E) and, in sharp contrast to *Cis* and *Spi2.1*, did not follow the strong decrease in STAT5A-1*6 mRNA level (Figure 25A–E). This suggests that *c-Myc* and *Pim-1* expression became less dependent on transactivation by STAT5A-1*6 over time.

In non-induced cells grown in the presence of IL-3, *Bcl-x* mRNA levels were three- to four-fold above those of rested cells (Figure 25F). Similarly, *Bcl-x* mRNA levels were only upregulated maximally two-fold in dox-induced cells relative to rested cells (Figure 25F). The patterns of *Bcl-x* and STAT5A-1*6 mRNA levels did not correlate with each other (Figure 25A and F). This was unexpected given the upregulation of *Bcl-x* in Ba/F3-1*6 cells reported by Nosaka *et al.* (1999), and the description of *Bcl-x* as a *bona fide* STAT5 target gene in parental Ba/F3 cells by Dumon *et al.*, 1999 (confirmed by Nelson *et al.*,

2004 and Basham *et al.*, 2008). On the other hand, *Osm* mRNA levels were at the limit of detection in both dox-induced and non-induced cells during Induction-4 (Figure 25G), and were therefore not further analyzed. The transient IL-3-mediated induction pattern reported for *Osm* mRNAs (Nosaka *et al.*, 1999, Rascle *et al.*, 2003, Yoshimura *et al.*, 1996) might explain the overall low mRNA levels detected in these experiments. Taken together, these findings indicate that neither *Bcl-x* nor *Osm* were transactivated by STAT5A-1*6 during long-term dox induction and that *Bcl-x* expression was regulated in a STAT5A-1*6-independent manner.

To further investigate their dependence to STAT5A-1*6, gene expression was also analyzed following withdrawal of dox treatment. As expected, STAT5A-1*6 transgene mRNA levels rapidly decreased upon dox removal (Figure 26A). Though, low levels of STAT5A-1*6 transgene mRNA were observed above the background level observed in non-induced rested cells throughout all investigated dox removal experiments (Figure 26A), with slightly higher levels detected during dox removal from day 42/49 than from day 7 of induction (Figure 26A, data not shown). This suggests some level of sustained expression of the STAT5A-1*6 transgene and/or persistence of its mRNA and suggests that the faint pSTAT5A/B signals detected by Western blot (Figure 24) were not artefacts, but rather represented residual constitutive STAT5A-1*6 activation. As expected, dox removal did not affect mRNA levels of the housekeeping gene *36b4* (Figure 26G). Interestingly, *Cis* and *Spi2.1* mRNA levels decreased gradually upon dox removal and then remained above the baseline level (Figure 26B and C). Given that their mRNA profiles during dox induction suggested STAT5A-1*6-controlled expression (Figure 25A–C), this further suggests that *Cis* and *Spi2.1* remained transactivated by residual STAT5A-1*6 proteins.

Strikingly, *c-Myc* and *Pim-1* mRNA levels were differentially affected by dox removal depending on the duration of the preceding dox induction (Figure 26D and E). Specifically, *c-Myc* and *Pim-1* mRNA levels gradually decreased to 20–30 % of their initial level upon early dox removal after one week of induction, still exhibiting three- to five-fold change relative to rested non-induced cells after four days of dox removal (Figure 26D and E). By contrast, *c-Myc* and *Pim-1* mRNA levels were not markedly impacted by late dox removal after six weeks of induction (Figure 26D and E). This corroborates the suggestion that late expression of *c-Myc* and *Pim-1* was STAT5A-1*6-independent. In addition, their STAT5A-1*6 independence as transactivator correlated with the improved cell survival and growth phenotype observed in later dox removal experiments. On the other hand, dox removal did not impact *Bcl-x* mRNA levels (Figure 26F), further corroborating its STAT5A-1*6-independent transactivation pattern.

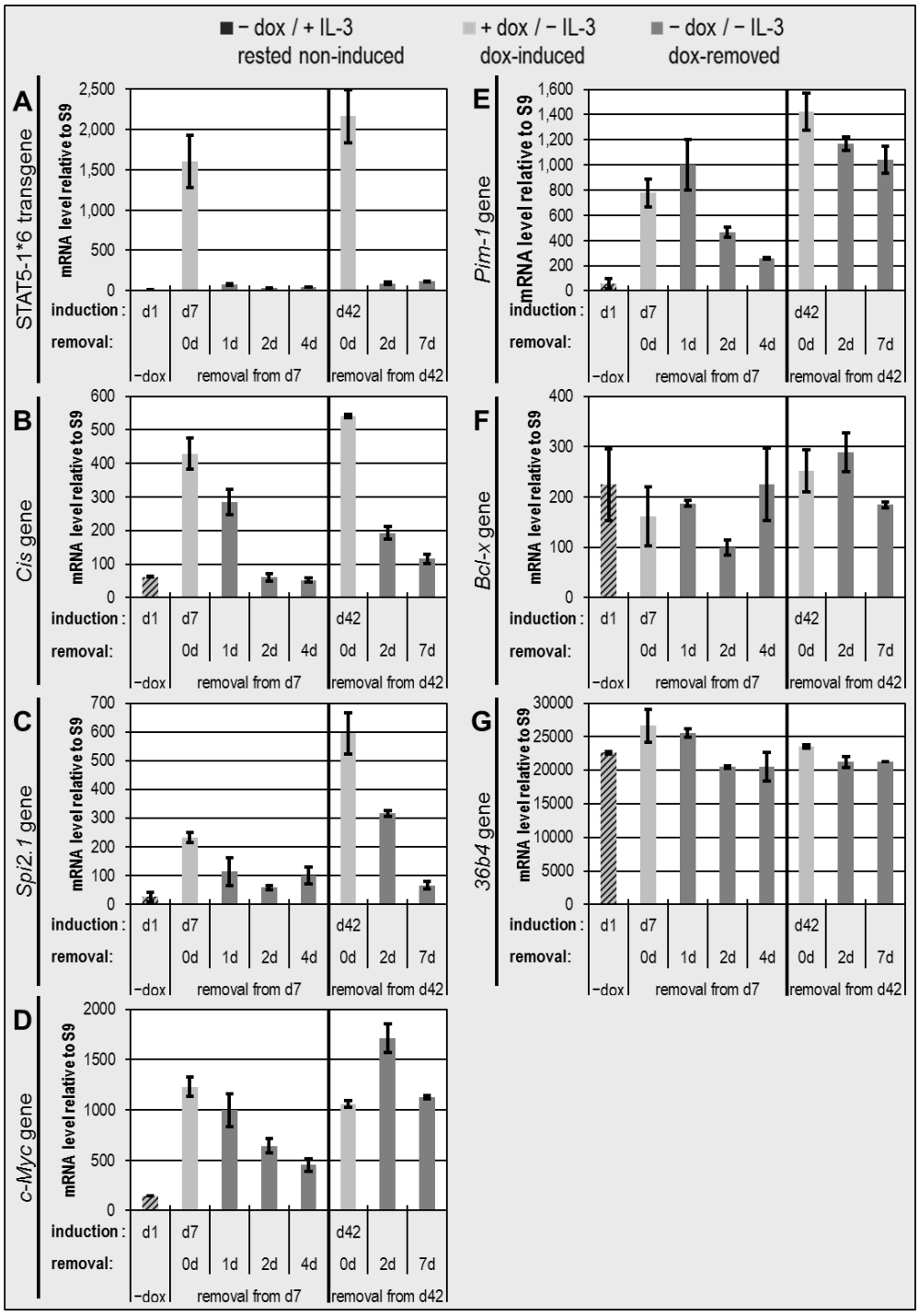

Figure 26: *Cis* and *Spi2.1* expression, but not *c-Myc* and *Pim-1* expression, is exclusively controlled by constitutively active STAT5A-1*6

Ba/F3-tet-on-1*6 cells were supplemented with doxycycline to induce STAT5A-1*6 production and grown in the absence of IL-3. Cells were kept for seven weeks as part of the 'Induction-2' experiment to study the effects of sustained constitutive STAT5A-1*6 activation. At the indicated time-points, a subset of cells was washed, removed from doxycycline and kept in the absence of IL-3 to halt STAT5A-1*6 production in order to uncover the effect of constitutive STAT5A-1*6 activation. Non-induced cells were rested without IL-3 for 9 h as baseline control for the absence of STAT5A/B activation. Cells were harvested at the indicated time-points. RNA was extracted and reverse transcribed into cDNA. cDNA was analyzed by RT-qPCR using primers specific for the transcripts of the STAT5A-1*6 transgene, the STAT5 target genes *Cis*, *Spi2.1*, *c-Myc*, *Pim-1*, *Bcl-x* (Bcl-xL isoform) and the control gene *36b4*. The error bars depict standard deviation among RT-qPCR replicates. The results shown are also representative of doxycycline removal experiments conducted during the 'Induction-3' experiment.

Abbreviations: d = day(s), dox = doxycycline.

3.4.2 STAT5 binding to the promoter elements of *Spi2.1*, but not to those of *Cis* and *Osm*, correlated with STAT5A-1*6 transgene expression and transactivation activity

Cis and *Spi2.1* mRNA profiles during long-term dox induction (Figure 25A–C) suggested a dose-dependent transactivation by STAT5A-1*6. In particular, the decline in available STAT5A-1*6 proteins during Induction-2 and -4 (Figure 18C and E) was hypothesized to impact the DNA binding and, thus, transcriptional activity of STAT5A-1*6 on the *Cis* and *Spi2.1* genes. Besides, the *Osm* gene was not detectably upregulated during long-term dox induction and therefore expected to exhibit weak binding of STAT5A-1*6 to its promoter.

To test these hypotheses, samples taken during Induction-4 were analyzed for their STAT5 occupancy at its binding sites in the *Cis*, *Spi2.1* and *Osm* genes using ChIP (Figure 17A | Basham *et al.*, 2008). Of note, STAT5 binding sites regulating *c-Myc* and *Pim-1* expression would have been an interesting target of research given the hypothesized time-dependent decrease in STAT5A-1*6-dependent regulation. Though, they could not be investigated in the present study, because STAT5 binding sites (putatively) regulating *c-Myc* in the *c-Myc* super-enhancer had not yet been identified (Pinz *et al.*, 2016; confirmed by Nanou *et al.*, 2017, GEO accession number GSE79520) and STAT5 binding sites (putatively) regulating *Pim-1* through promoter and enhancer elements (Katerndahl *et al.*, 2017, Kieffer-Kwon *et al.*, 2013, Matikainen *et al.*, 1999 and others) had not yet been identified and validated in Ba/F3 cells (Nanou *et al.*, 2017, GEO accession number GSE79520). In addition, RNA Polymerase II occupancy at the TSS of the *Cis* gene was analyzed using ChIP, as a measure of active transcription (Li *et al.*, 2007, Rascle *et al.*, 2003, Rascle and Lees, 2003). As before, non-induced cells (rested and growing with IL-3) served as controls.

As expected, RNA Polymerase II occupancy at the *Cis* TSS correlated closely with Cis mRNA level in both non-induced and dox-induced cells (Figures 25B and 27B). In accordance with *Cis* transactivation (Figure 25B), STAT5 DNA binding activity to *Cis* was detected continuously in non-induced cells in the presence of IL-3 and in dox-induced cells in the absence of IL-3 (Figure 27A), confirming IL-3-dependent DNA binding activity of endogenous STAT5A/B and IL-3-independent DNA binding activity of constitutively active STAT5A-1*6, respectively (Nagata and Todokoro, 1996, Onishi *et al.*, 1998). Conspicuously however, the detected STAT5 occupancy at *Cis* did not correlate well with *Cis* mRNA level in the course of dox induction, neither in non-induced nor in dox-induced cells (Figures 25B and 27A). Instead, STAT5 occupancy fluctuated randomly between 0.2 and 0.7 % input DNA (Figure 27A).

In line with its background expression level (Figure 25C), STAT5 DNA binding activity to *Spi2.1* was near the detection limit in non-induced cells despite the presence of IL-3 (Figure 27C). In dox-induced cells, however, STAT5 was bound to the STAT5 binding site of the *Spi2.1* gene (Figure 27C) in accordance with its transactivation (Figure 25C). Strikingly, STAT5 occupancy nearly tripled in the second week of induction correlating with the tremendous thirty-fold upregulation of the *Spi2.1* mRNA level (relative to the level of non-induced rested cells | Figure 25C) and with the increase in STAT5A-1*6 mRNA levels (Figure 25A). This suggests more effective recruitment of STAT5A-1*6 and possibly of the transcription machinery to the *Spi2.1* locus at this time-point.

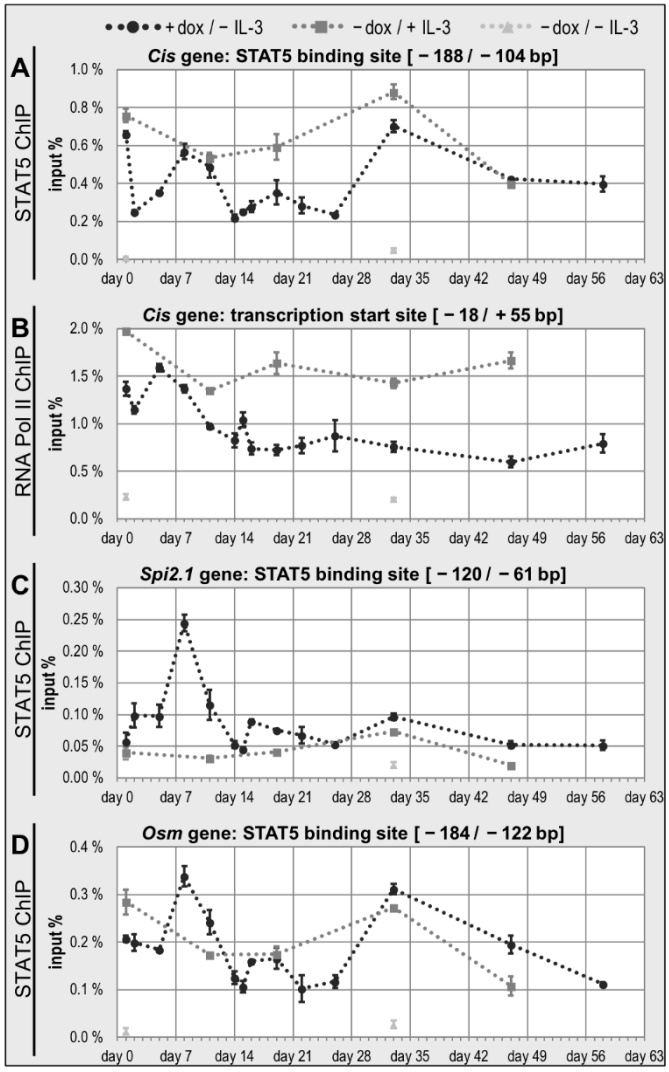

Figure 27: STAT5A-1*6 bound to its *Cis*, *Spi2.1* and *Osm* binding sites throughout long-term doxycycline induction

Ba/F3-tet-on-1*6 cells were grown in the absence of IL-3 and supplemented with doxycycline to induce STAT5A-1*6 production. Cells were kept for nine weeks as part of the 'Induction-4' experiment to study the effects of sustained constitutive STAT5A-1*6 activation. Non-induced cells were grown in the presence of IL-3 as control for the effects of endogenous STAT5A/B activation or rested without IL-3 for 11 h as baseline control for the absence of STAT5A/B activation. Cells were harvested at the indicated time-points and processed for chromatin immunoprecipitation (ChIP) as described in the Material and Methods section. ChIP was performed using antibodies directed against STAT5A/B **(A, C, D)** and RNA Polymerase II **(B)**. Input and co-precipitated genomic DNA were analyzed by quantitative PCR using primers specific for the promoter regions of the STAT5 target genes *Cis*, *Osm* and *Spi2.1* (STAT5) and the *Cis* transcription start site (RNA Polymerase II), as specified further in the figure. *Cis*, *Osm* and *Spi2.1* proximal promoter amplicons overlap their respective STAT5 binding sites. *Cis*, *Osm* and *Spi2.1* gene structure as well as amplicon positions are illustrated in Figure 33. The relative quantity of co-precipitated genomic DNA is expressed as percentage of input genomic DNA (input %), denoting chromatin occupancy. The error bars depict standard deviation among qPCR replicates. Nucleotide positions are relative to the transcription start site. The dotted lines connect single data points for dox-induced cells and non-induced cells, growing in the presence of IL-3.

Abbreviations: ChIP = chromatin immunoprecipitation, dox = doxycycline, Pol = Polymerase.

Intriguingly, STAT5 DNA binding to the *Osm* promoter was detected in both non-induced (+IL-3) and dox-induced (−IL-3) cells (Figure 27D), although *Osm* was not upregulated in these conditions (Figure 25G). STAT5 occupancy at *Osm* STAT5 binding sites fluctuated between 0.1 and 0.3 % input DNA in dox-induced cells (Figure 27D), following a pattern similar to that found at the STAT5 binding sites of the *Cis* gene (Figure 27A). Importantly, this refutes a hypothesized lack of STAT5A-1*6 DNA binding as a cause for

the undetectable *Osm* transactivation (Figure 25G). This, in turn, suggests that either missing co-factors, the *Osm*-specific chromatin context or high *Osm* mRNA instability impeded the detection of *Osm* mRNAs in STAT5A-1*6-induced cells. On the other hand, it cannot be excluded that the region overlapping the applied quantitative PCR primers was altered in Ba/F3-1*6 cells, impeding *Osm* mRNA detection in our assay.

Altogether, these findings confirm the STAT5A-1*6-dependent regulation of the STAT5 target genes *Cis* and *Spi2.1*. They also suggest that the gene-specific chromatin context (e.g. at *Osm*) might play a significant role in transcriptional regulation by STAT5A-1*6 and, ultimately, hint at the acquisition of 'driver' and/or 'passenger' chromatin alterations during long-term dox induction.

3.5 Chromatin regulation by transiently- and constitutively-active STAT5A/B forms

The present study aimed to elucidate whether constitutively active STAT5A-1*6 mediates sustained chromatin alterations as opposed to transient alterations mediated by wild-type active STAT5A/B. It was hypothesized that STAT5A-1*6 can mediate different chromatin modifications than endogenous STAT5A/B and that this may play a role in its oncogenicity.

3.5.1 The STAT5 target genes *Cis* and *Osm* are enriched for active, but not for repressive histone marks upon STAT5 binding

To uncover which particular chromatin alterations may be impacted by STAT5A-1*6 DNA binding, a panel including common active and repressive histone modifications (The ENCODE Project Consortium, 2012) was investigated and correlated with changes mediated by IL-3 stimulation in parental Ba/F3 cells. Specifically, STAT5A/B activation in parental Ba/F3 cells was turned off/on by IL-3 removal/stimulation and cells were analyzed by ChIP using antibodies targeting histone H3 bearing the H3K4me1, H3K4me3, H3K9me1, H3K9me3, H3K27me1 and H3K27me3 marks. H3K4me1 and H3K4me3 constitute active marks, whereas H3K9me3 and H3K27me3 constitute repressive marks (Table 1). In addition, ChIP was conducted in parallel using antibodies against total histone H3 as a reference for changes in total histone occupancy and using IgG as background control. ChIP signal relative to total input DNA was analyzed by qPCR for sites in the *Cis* and *Osm* gene, namely the distal promoter, the proximal promoter overlapping STAT5 binding sites, the TSS and the open reading frame (ORF). As a negative control, ChIPed DNA was analyzed for sites in the distal promoter, at the TSS and in the ORF of the STAT5A/B-independent gene *c-Fos*. These three genes have been previously studied by the PD Dr. Anne Rascle's research group for their STAT5 and RNA Polymerase II occupancy as well as for histone acetylation at the afore-mentioned sites in Ba/F3 cells (Rascle *et al.*, 2003, Rascle and Lees, 2003). *Cis*, *Osm*

and *c-Fos* expression is induced upon IL-3 stimulation, correlating with increased occupation of RNA Polymerase II at their TSS and of STAT5 proteins at the *Cis* and *Osm* STAT5 binding sites (Rascle *et al.*, 2003, Rascle and Lees, 2003 | verified in the present study, Figures 10 and 11).

H3K9me1, H3K9me3, H3K27me1 and H3K27me3 enrichment was at or near the background level (ranging from ~0.01 % to ~0.06 % of input DNA) at the tested sites in the *Cis*, *Osm* and *c-Fos* genes both in the presence and absence of IL-3 (Figure 28), with the exception of the *Osm* ORF (H3K9me3, H3K27me1, ~0.09 % to 0.15 % input DNA; Figure 28B and C) and the *c-Fos* ORF (H3K27me1, H3K27me3, ~0.08 % input DNA; Figure 28C). This indicates no or negligible mono- and trimethylation of both H3K9 and H3K27. Though, it could not be ruled out that the lack of positive signals was caused

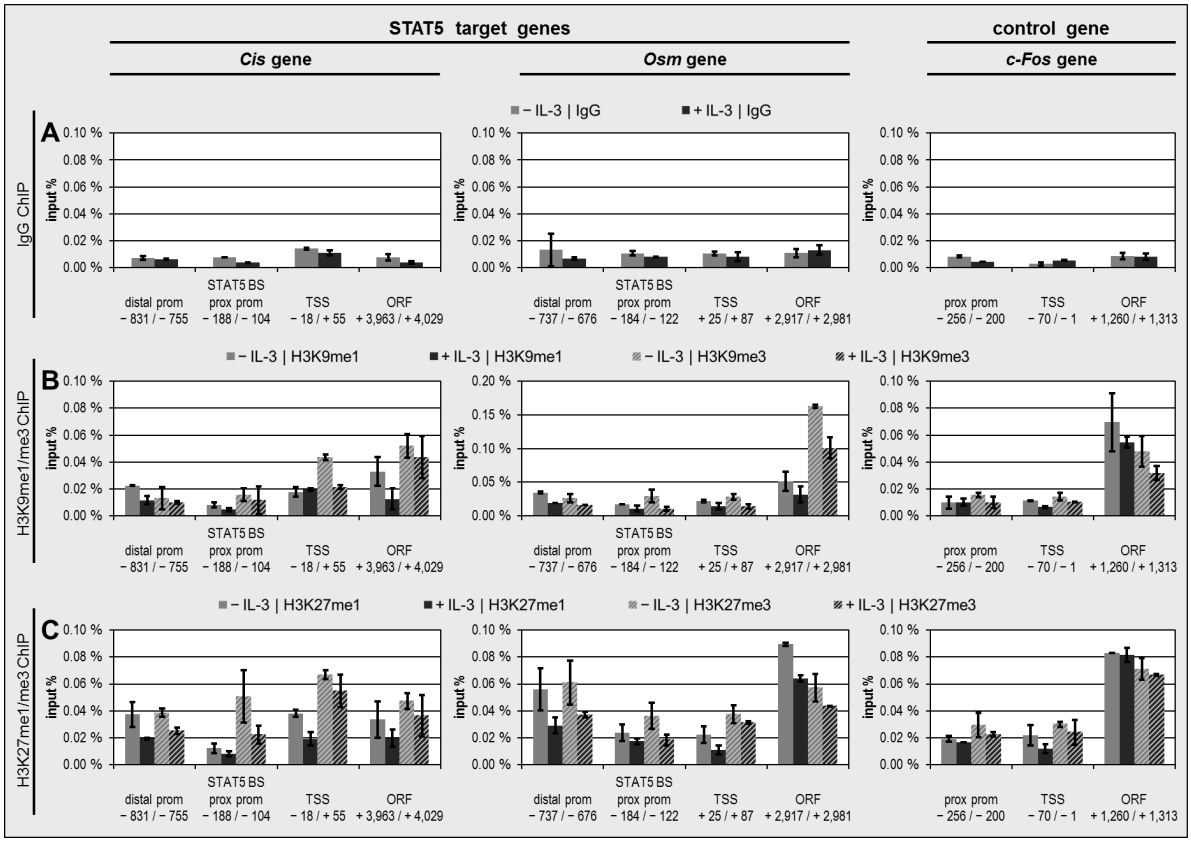

Figure 28: Repressive histone marks H3K9me3 and H3K27me3 were not enriched at *Cis*, *Osm* and *c-Fos*

Parental Ba/F3 cells were rested for 12 h without IL-3 and stimulated for 30 min with IL-3 to turn STAT5A/B activation off/on. Cells were harvested and processed for chromatin immunoprecipitation (ChIP) as described in the Material and Methods section. ChIP was performed using antibodies directed against the modified histones H3K9me1 **(B)**, H3K9me3 **(B)**, H3K27me1 **(C)** and H3K27me3 **(C)** or using Rabbit IgG as a background control **(A)**. Input and co-precipitated genomic DNA was analyzed by quantitative PCR using the same primers for *Cis*, *Osm* and *c-Fos* as in Figure 11 and as specified further in the figure. *Cis*, *Osm* and *c-Fos* gene structure as well as amplicon positions are illustrated in Figure 33. The relative quantity of co-precipitated genomic DNA is expressed as percentage of input genomic DNA (input %), denoting chromatin enrichment. The error bars depict standard deviation among qPCR replicates. Nucleotide positions are relative to the transcription start site.

Abbreviations: BS = binding site, ChIP = chromatin immunoprecipitation, ORF = open reading frame, prom = promoter, prox = proximal, TSS = transcription start site.

by non-functioning antibodies. To verify the functionality of the anti-H3K27me3 antibody, H3K27me3 enrichment was analyzed by qPCR at the *Igk*-$E_{\kappa i}$ DNA site, where H3K27me3 marks have been described previously in murine B cells (Mandal *et al.*, 2011). H3K27me3 was enriched at this site, with 1–1.5 % of input DNA (Figure 29), validating the functionality of the anti-H3K27me3 antibody, and thus confirming the absence of this repressive histone mark at the *Cis, Osm* and *c-Fos* genes. Such control sites were not readily available for the anti-H3K9me1, anti-H3K9me3 and anti-H3K27me1 antibodies, whose functionality hence could not be confirmed. At any rate, the absence or marginal enrichment of H3K9me1, H3K9me3, H3K27me1 and H3K27me3 along *Cis*, *Osm* and *c-Fos* agrees with their distributions reported for actively transcribed euchromatic genes (Table 1).

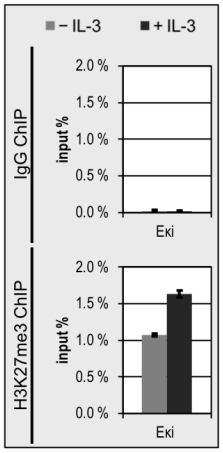

Figure 29: The histone mark H3K27me3 is enriched at the *Igk*-$E_{\kappa i}$ site, used in the present study as a positive control for the H3K27me3-specific antibodies

Parental Ba/F3 cells were rested for 12 h without IL-3 and stimulated for 30 min with IL-3 to turn STAT5A/B activation off/on, respectively. Cells were harvested and processed for chromatin immunoprecipitation (ChIP) as described in the Material and Methods section. ChIP was performed using antibodies directed against the modified histone H3K27me3 or using Rabbit IgG as a background control. Input and co-precipitated genomic DNA was analyzed by quantitative PCR using primers specific for the $E_{\kappa i}$ site in the *Igk* gene. The relative quantity of co-precipitated genomic DNA is expressed as percentage of input genomic DNA (input %), denoting chromatin enrichment. The error bars depict standard deviation among qPCR replicates.

Abbreviations: ChIP = chromatin immunoprecipitation.

The active marks H3K4me1 and H3K4me3 were enriched at the tested sites along *Cis*, *Osm* and *c-Fos* both in the absence and presence of IL-3 (Figure 30A). Interestingly, total histone H3 occupancy decreased upon IL-3 stimulation along *Cis* and *Osm*, in particular within their promoter and TSS regions, but not along *c-Fos* (Figure 30C). Strikingly, this decrease was most pronounced at the STAT5 binding sites in the *Cis* and *Osm* proximal promoters (Figure 30C). Given that a change in total histone H3 occupancy will impact the interpretation of detected H3K4me1 and H3K4me3 signals, H3K4me1 and H3K4me3 ChIP results were normalized to total histone H3 occupancy (Figure 30B), to better reflect true histone mark enrichment. Upon normalization to histone H3 occupancy, H3K4me3 was tremendously enriched in the proximal promoter and at the TSS, both in the absence and presence of IL-3 (Figure 30B). H3K4me3 was also detected at the *Cis* and *Osm* distal promoter, but was comparatively low in the *Cis*, *Osm* and *c-Fos* ORF (Figure 30B). Upon IL-3 stimulation, H3K4me3 level increased slightly at the transcription start site of all three genes (Figure 30B), correlating with the increased transcriptional activity (Figure 10). H3K4me3 level around the STAT5 binding sites in the *Osm* and *Cis* proximal promoters, as well as within the *c-Fos* proximal promoter, remained mainly unchanged upon IL-3 stimulation (Figure 30B). On the other

hand, H3K4me1 exhibited considerably lower signal than H3K4me3, indicative of lower enrichment, and remained unaffected by IL-3 stimulation (Figure 30B). Altogether, the distribution of mono- and trimethylation of H3K4 agreed with previous reports for actively transcribed euchromatic genes (Table 1).

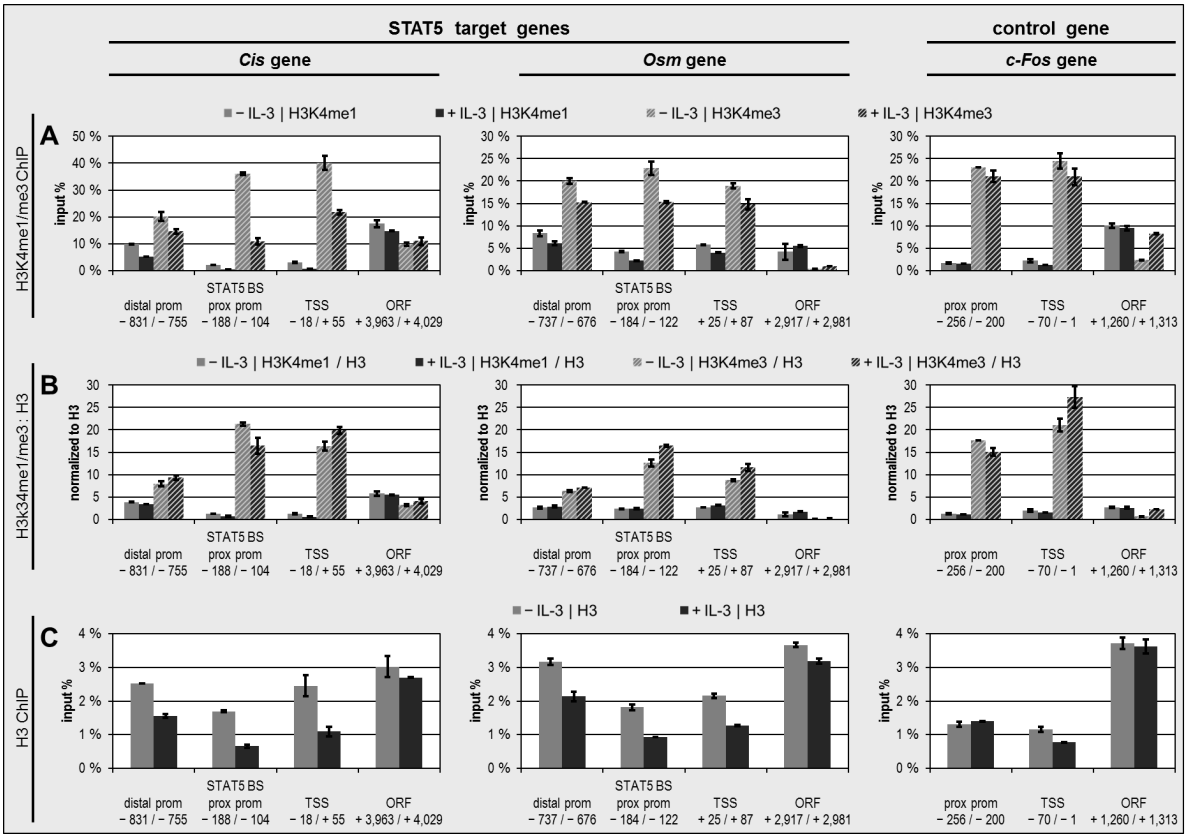

Figure 30: Active mark H3K4me3 is enriched at the transcription start site upon transactivation of *Cis*, *Osm* and *c-Fos*

Parental Ba/F3 cells were rested for 12 h without IL-3 and stimulated for 30 min with IL-3 to turn STAT5A/B activation off/on. Cells were harvested and processed for chromatin immunoprecipitation (ChIP) as described in the Material and Methods section. ChIP was performed using antibodies directed against the modified histones H3K4me1 **(A)**, H3K4me3 **(A)** as well as total histone H3 **(C)**. Input and co-precipitated genomic DNA was analyzed by quantitative PCR using the same primers for *Cis*, *Osm* and *c-Fos* as in Figure 11, as specified further in the figure. *Cis*, *Osm* and *c-Fos* gene structures as well as amplicon positions are illustrated in Figure 33. The relative quantity of co-precipitated genomic DNA is expressed as percentage of input genomic DNA (input %), denoting chromatin occupancy/enrichment. H3K4me1 and H3K4me3 occupancy was normalized to total histone H3 occupancy **(B)**. The error bars depict standard deviation among qPCR replicates. The shown results are representative of two independent experiments. Nucleotide positions are relative to the transcription start site.

Abbreviations: BS = binding site, ChIP = chromatin immunoprecipitation, ORF = open reading frame, prom = promoter, prox = proximal, TSS = transcription start site.

The fact that relative H3K4me1 and H3K4me3 enrichment did not change in a manner specific to the investigated STAT5 target genes opposes STAT5A/B-specific effects on these marks. Therefore, H3K4me1 and H3K4me3 were not further investigated in the present study. However, the striking decrease in total histone H3 occupancy correlating with STAT5 binding to *Cis* and *Osm* suggests a chromatin remodeling event that either mediates or is mediated by STAT5 binding. This chromatin remodeling event was therefore investigated in detail in the remaining part of the present study.

It should be noted that, due to a lack of time, the histone marks investigated above in IL-3-stimulated Ba/F3 cells were not assessed in cells expressing STAT5A-1*6 and therefore that the question of how these marks might be altered during STAT5A-1*6-induced oncogenesis was not addressed.

3.5.2 STAT5 DNA binding correlates with a histone H3 decrease in parental Ba/F3 cells

3.5.2.1 STAT5 DNA binding correlates with a histone H3 decrease all along the *Cis* gene

The most pronounced decrease in histone H3 occupancy upon STAT5 DNA binding and transactivation of *Cis* was observed at its STAT5 binding site. To further investigate whether this decrease was also detected at other sites along the *Cis* locus, histone H3 occupancy in Ba/F3 cells was analyzed by qPCR using the same ChIP samples as before (3.5.1). Primers specific for multiple representative sites all along the *Cis* gene between position −831 bp and +4029 bp relative to the TSS were employed for the qPCR, in parallel to control sites within the *c-Fos* gene, as illustrated in Figure 33.

Both in the presence and absence of IL-3, histone H3 occupancy along the *Cis* and *c-Fos* gene was lower at the TSS and in the proximal promoter compared with the ORF and the distal promoter region (Figure 31). This pattern follows the nucleosome distribution reported for euchromatic protein-coding genes with a 5' nucleosome-free region (5'-NFR) upstream of the TSS (Figure 4| Iyer, 2012, Jiang and Pugh, 2009, Yuan *et al.*, 2005). Of note, the comparatively low histone H3 occupancy within the *Cis* promoter agrees with the 5'-NFR encompassing the STAT5 binding sites. Strikingly, histone H3 occupancy decreased all along the *Cis* gene upon IL-3 stimulation, but only negligibly along the *c-Fos* gene (Figure 31A). The decrease in histone H3 occupancy thus correlates with STAT5 DNA binding and transactivation (Figures 10A, 11A and 31A). Although the decrease in histone H3 occupancy was observed all along the *Cis* locus in response to IL-3, it was strongest around the STAT5 binding sites, down to 10 % of the histone H3 occupancy detected in rested cells (Figure 31B). Overall, these findings raise the possibility that the decrease in histone H3 occupancy around the STAT5 binding region is a consequence of STAT5 DNA binding, suggesting a possible STAT5A/B-mediated nucleosome loss (although STAT5A/B-independent nucleosome loss cannot be excluded at this point). This is in agreement with the increased chromatin accessibility reported for the *Cis* STAT5 binding site upon STAT5 binding by Rascle and Lees (2003). These observations also raise the question as to whether the decrease in histone H3 content along the entire *Cis* locus reflects a global increase in chromatin accessibility at this locus as a consequence of (or alternatively in preparation for) STAT5 binding and/or transcriptional activation.

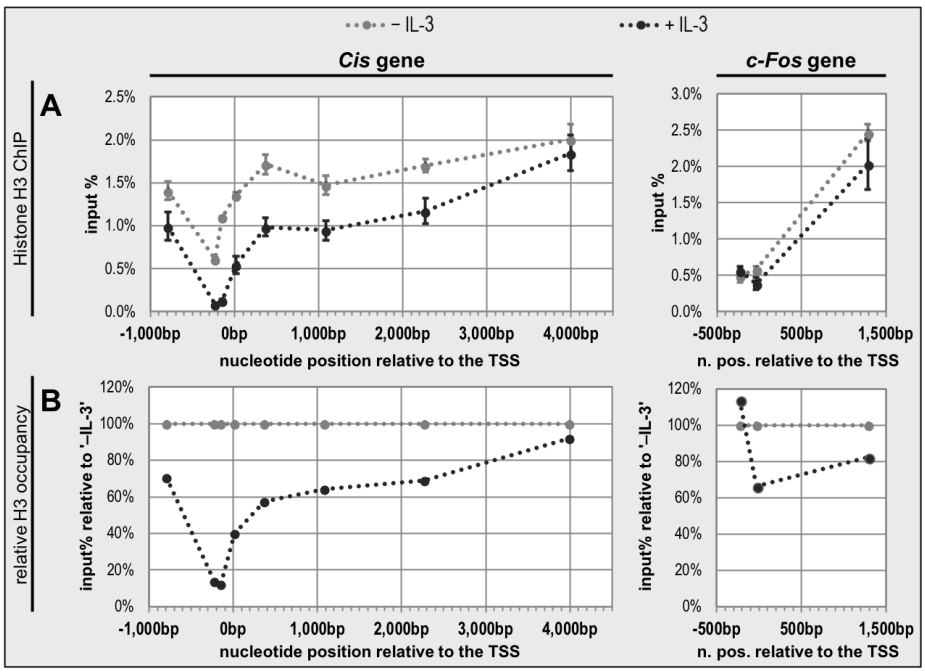

Figure 31: Upon IL-3 stimulation, histone H3 occupancy decreases along the STAT5 target gene *Cis,* but is strongest in the proximal promoter, around the STAT5 binding site

Parental Ba/F3 cells were rested for 9 h without IL-3 and stimulated for 30 min with IL-3 to turn STAT5A/B activation off/on. Cells were harvested and processed for chromatin immunoprecipitation (ChIP) as described in the Material and Methods section. ChIP was performed using antibodies directed against histone H3 **(A)**. Input and co-precipitated genomic DNA were analyzed by quantitative PCR using primers specific for sites all along the STAT5 target gene *Cis* and for the proximal promoter, transcription start site and open reading frame of the control gene *c-Fos*, as specified further in the figure. The relative quantity of co-precipitated genomic DNA is expressed as percentage of input genomic DNA (input %), denoting histone H3 occupancy **(A)**. Histone H3 occupancy relative to '−IL-3' was calculated **(B)**. *Cis*, *Osm* and *c-Fos* gene structures as well as amplicon positions are illustrated in Figure 33. The error bars depict standard deviation among qPCR replicates. The shown results are representative of three independent experiments. Nucleotide positions are relative to the transcription start site.

Abbreviations: ChIP = chromatin immunoprecipitation, n. = nucleotide, pos. = position, TSS = transcription start site.

3.5.2.2 STAT5A/B-associated histone H3 decrease does not correlate with enriched histone acetylation at the *Cis* STAT5 binding site

The detected decrease in histone H3 occupancy indicates a decrease in nucleosome density along *Cis* and *Osm* (Figures 30C and 31). As detailed in the introduction section, two main mechanisms have been found to govern nucleosome density: (i) ATP-dependent chromatin remodeling complexes, and (ii) HATs and HDACs (1.2). ATP-dependent chromatin remodeling complexes dislocate and/or eject nucleosomes, leading to local nucleosome loss (1.2). HATs acetylate various histone lysine residues, which impedes nucleosome-DNA interaction and, thus, leads to a local decrease in nucleosome density (1.2). Of note, STAT5A/B has been argued to recruit HATs as well as ATP-dependent chromatin remodeling complexes (1.3.3.5, Table 2). Therefore, it was hypothesized that both mechanisms might contribute to the observed histone H3 decrease along *Cis* and *Osm*. Hence, histone acetylation was predicted to be enriched in parallel to the histone H3 decrease in the *Cis* and *Osm* gene upon STAT5 binding to DNA. To investigate this, the parental Ba/F3 samples used before (3.5.1, 3.5.2.1) were

analyzed by ChIP using antibodies targeting acetylated histone H3 (acH3) and H4 (acH4). acH3 and acH4 enrichment was analyzed by qPCR at the previously investigated sites in *Cis* and *Osm,* as well as in *c-Fos* as a control, and normalized to total histone H3 occupancy as before (3.5.1).

Interestingly, acH3 and acH4 was enriched upon IL-3 stimulation in the *Cis* and *Osm* distal promoter region, in the *c-Fos* proximal promoter region and at the *Cis*, *Osm* and *c-Fos* TSS (Figure 32B). Though, acH3 and acH4 was only slightly or not enriched in the *Cis*, *Osm* and *c-Fos* ORF, slightly enriched at the *Osm* STAT5 binding site and not enriched at the *Cis* STAT5 binding site upon IL-3 stimulation (Figure 32B). This agrees with the reported distribution for actively transcribed euchromatic genes, with the exception of the *Cis* (and to a lesser extent *Osm*) STAT5 binding site lacking the expected enrichment in histone acetylation (Figure 32B, Table 1). This opposes the hypothesis that HAT activity contributed to the decrease in histone H3 occupancy, i.e. nucleosome density, at the *Cis* STAT5 binding site (Figures 30C and 31). Though, this does not exclude that HAT activity contributed to the histone H3 decrease detected at other investigated sites (Figure 30C). Overall, these findings suggest that the

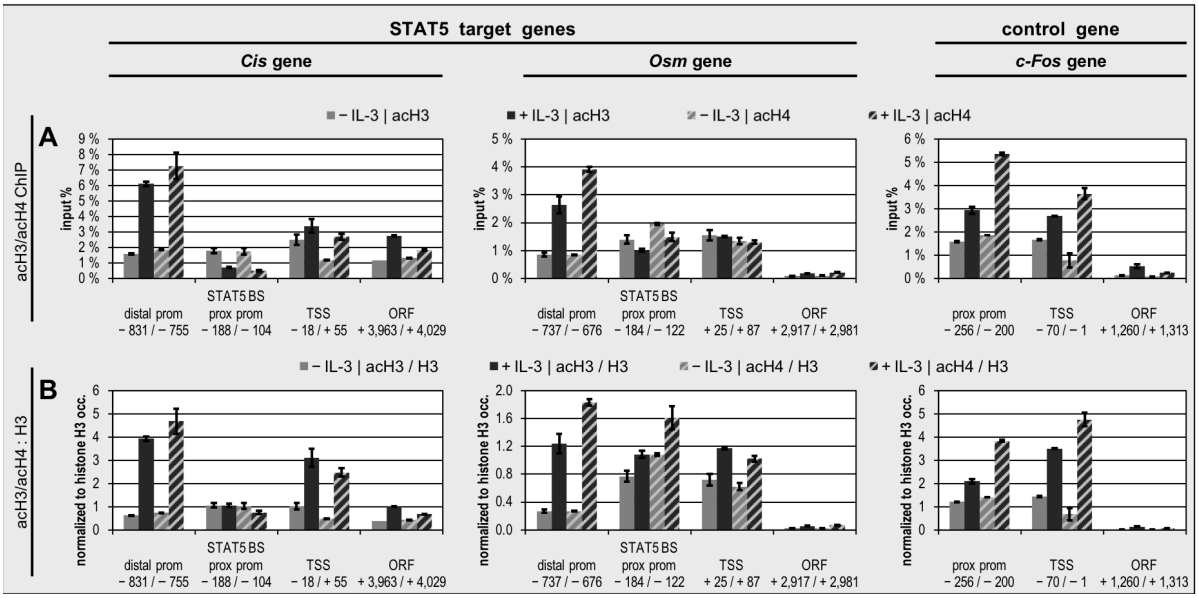

Figure 32: Acetylated histones H3 and H4 are not enriched upon IL-3 stimulation at the *Cis* STAT5 binding site

Parental Ba/F3 cells were rested for 12 h without IL-3 and stimulated for 30 min with IL-3 to turn STAT5A/B activation off/on. Cells were harvested and processed for chromatin immunoprecipitation (ChIP) as described in the Material and Methods section. ChIP was performed using antibodies directed against acetylated histone H3 (acH3) and acetylated histone H4 (acH4) **(A)** as well as total histone H3 (data shown in Figure 30C). Input and co-precipitated genomic DNA was analyzed by quantitative PCR using the same primers for *Cis*, *Osm* and *c-Fos* as in Figure 11, as specified further in the figure. *Cis*, *Osm* and *c-Fos* gene structures as well as amplicon positions are illustrated in Figure 33. The relative quantity of co-precipitated genomic DNA is expressed as percentage of input genomic DNA (input %), denoting chromatin enrichment. acH3 and acH4 enrichment was normalized to total H3 occupancy **(B)**. The error bars depict standard deviation among qPCR replicates. The shown results are representative of three independent experiments. Nucleotide positions are relative to the transcription start site.

Abbreviations: BS = binding site, ChIP = chromatin immunoprecipitation, ORF = open reading frame, prom = promoter, prox = proximal, TSS = transcription start site.

nucleosome loss at the *Cis* STAT5 binding site might be dependent on the recruitment of ATP-dependent chromatin remodeling complexes, but not on HATs. They also suggest that different mechanisms might be involved in the nucleosome loss at the STAT5 binding sites of *Cis* (likely HAT-independent) and at upstream and downstream regions along these gene loci (likely HAT-dependent).

3.5.2.3 BRG1 co-recruitment with STAT5A/B was not detected at the *Cis* STAT5 binding site

STAT5A/B has been shown to functionally and physically interact with BRG1, a catalytic subunit of SWI/SNF family ATP-dependent chromatin remodeling complexes, in mediating chromatin alterations conducive to transcriptional activity (Wagatsuma *et al.*, 2015, Xu *et al.*, 2007 | 1.3.3.5, Table 2). Given this, the putatively HAT-independent H3 decrease at the *Cis* STAT5 binding site (Figures 30C, 31 and 32B) was hypothesized to be catalyzed by a BRG1-containing SWI/SNF family complex. This proposes co-recruitment of BRG1 with STAT5A/B to the *Cis* STAT5 binding site upon IL-3 stimulation. To investigate this, Ba/F3-wt cells (shown to be comparable to parental Ba/F3 cells in the present study, 3.1.2) were subjected to IL-3-stimulation and analyzed by ChIP using an antibody targeting BRG1 (5 µg and 2 µg) and using IgG (5 µg) as background control. Occupancy relative to total input DNA was analyzed by qPCR at the previously investigated *Cis* STAT5 binding site and at the *Cis* TSS as a control.

At the tested sites, BRG1 occupancy was at or near the background level both in presence and absence of IL-3 (≤ 0.04 % of input DNA, data not shown). This indicates no or negligible recruitment of BRG1 to the *Cis* STAT5 binding site and proposes that the histone H3 decrease at these sites (Figure 35C) was not catalyzed by a BRG1-containing SWI/SNF complex. However, given that primers specific to a control DNA site with a known positive BRG1 signal in Ba/F3 cells were not tested, it cannot be totally ruled out that the lack of positive signals was caused by occlusion of the BRG1 epitope or by a non-functioning antibody.

3.5.2.4 Histone H3 decrease is not restricted to STAT5 binding sites located in the proximal promoter region

STAT5 binding to the *Cis* and *Osm* proximal promoters correlated with a decrease in histone H3 occupancy. STAT5 binding sites mediating transcriptional activation are not always located within proximal promoters, but are also found in other locations relative to the ORF (1.3.3.1, Kang *et al.*, 2013). This raises the question as to whether the detected nucleosome loss upon STAT5 binding depends on the location of the STAT5 binding sites within the gene locus. A decrease in histone H3 occupancy at STAT5 binding sites regardless of their location would support the hypothesis of a STAT5A/B-mediated nucleosome loss.

To investigate this hypothesis, a panel of STAT5 target genes with different STAT5 binding site locations validated by Basham *et al.*, (2008 | *Spi2.1*, *Id-1*, *TNFRSF13b*, *Bcl-x*, *MKP-1* and *IL2Ra*) as well as control regions from the IL-3-inducible STAT5-regulated *p21* gene and from the IL-3-independent housekeeper *S16* as additional controls were selected and studied using the same parental Ba/F3 cell samples employed before (cDNA, STAT5-co-precipitated DNA and histone H3-co-precipitated DNA | 3.5.1, 3.5.2.1). Even though IL-3-inducible *p21* transactivation is impeded upon STAT5A and/or STAT5B knock-down and as such defined *p21* as a STAT5 target gene (Basham *et al.*, 2008), STAT5A/B was not found to bind to two GAS motifs identified in the *p21* promoter (PD Dr. Anne Rascle, personal communication), suggesting that STAT5A/B transactivates *p21* through distinct element(s) (two such candidate STAT5 binding sites [overlapping previously not investigated GAS motifs] have been recently identified within promoter/enhancer regions located ~4 kb upstream and ~11 kb downstream of the *p21* ORF | Nanou *et al.*, 2017, GEO accession number GSE79520). Given previous reports in Ba/F3 cells, the IL-3-dependent *Spi2.1*, *Id-1*, *TNFRSF13b*, *Bcl-x*, *MKP-1*, *IL2Ra* and *p21* genes were expected to be transactivated upon IL-3 stimulation and were analyzed by RT-qPCR for their mRNA levels (Basham *et al.*, 2008, Dumon *et al.*, 1999, Nelson *et al.*, 2004, Rascle *et al.*, 2003, Xu *et al.*, 2003 Lecine *et al.*, 1996). mRNA levels for the IL-3-independent control gene *S16* were not analyzed, as they were expected to remain unchanged, comparatively to those of the housekeeping gene *36b4* (Figure 10D). STAT5 binding sites of the investigated genes are located in the proximal promoter (*Spi2.1*) and distal promoter (*MKP-1* and *IL2Ra*) regions, within an intron (*TNFRSF13b* and *Bcl-x*) or farther downstream the ORF (*Id-1*), as illustrated in Figure 33. They were expected to be occupied by STAT5 upon IL-3 stimulation, and were analyzed by ChIP-qPCR. Histone H3 occupancy was expected to decrease at the investigated STAT5 binding sites, and was analyzed by ChIP-qPCR in parallel to at least one control site for each investigated gene (Figure 33). Moreover, various sites in the *p21* and *S16* genes were analyzed for their histone H3 occupancy as an additional control for the effects of the presence and absence of IL-3-inducible transactivation (Figure 33).

Figure 33 (next page): Structure of the investigated gene loci and depiction of amplicon positions analyzed by ChIP

Ba/F3 cells were harvested, processed and analyzed by chromatin immunoprecipitation, as described in the Material and Methods section, to quantify protein-DNA interactions in chromatin at specific loci using antibodies targeting the desired protein. The obtained genomic DNA co-precipitated by the antibody and input genomic DNA was quantified relatively by qPCR using sequence-specific primers. The relative quantity of co-precipitated genomic DNA expressed as percentage of input genomic DNA denotes the occupancy of the desired protein in the chromatin at a specific DNA site. This figure illustrates the DNA sites targeted by the employed sequence-specific primers. The primers amplified amplicons in the STAT5 target genes *Cis*, *Osm*, *Spi2.1*, *Id-1*, *TNFRSF13b*, *Bcl-x*, *MKP-1, IL2Ra* and *p21* as well as the IL-3-inducible STAT5-independent gene *c-Fos* and the IL-3-independent housekeeping gene *S16* as controls. Their loci are depicted schematically, with exons and introns in the open reading frame marked in dark grey and light grey, respectively. When the ORF extended beyond the shown section, this is indicated by an arrow. The position and number of STAT5 binding sites is denoted, as validated by Basham *et al.* (2008) for Ba/F3 cells. Position of the qPCR amplicons are marked by rectangles. Red rectangles signify amplicons at STAT5 binding sites and green rectangles amplicons at control sites. Annotations are relative to the transcription start site (0 bp) and were extracted from the Ensembl database (https://www.ensembl.org, 26.02.2015).

Abbreviations: BS = binding site, ChIP = chromatin immunoprecipitation.

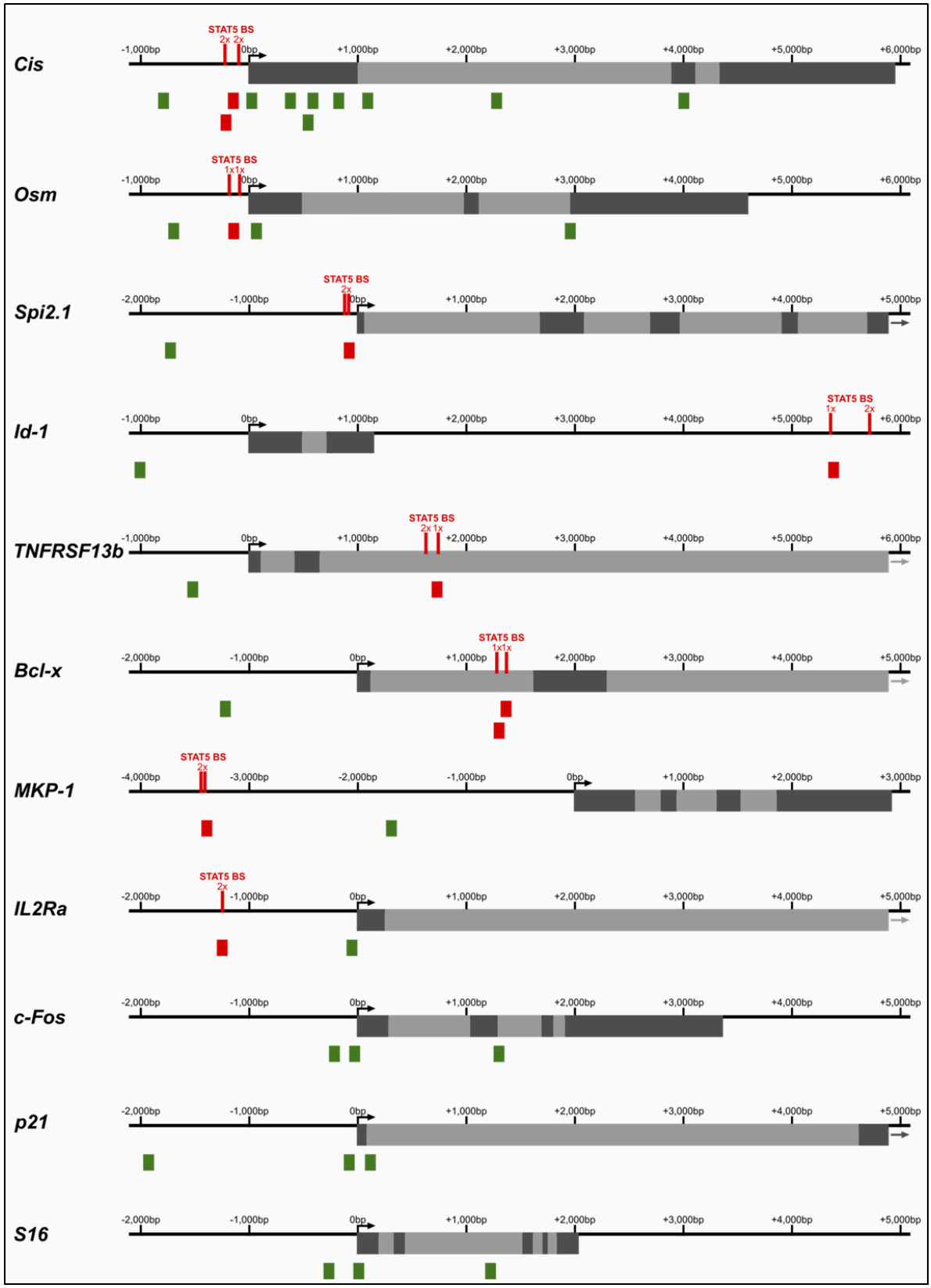

It should be noted that upon 30-minute IL-3 stimulation, the early-responsive genes *p21*, *MKP-1* and *Id-1* were expected to show a stronger upregulation than the late-responsive genes *Spi2.1*, *IL2Ra*, *TNFRSF13b* and *Bcl-x* (Basham *et al.*, 2008, Rascle *et al.*, 2003).

In agreement with these reports, mRNA levels of the STAT5-regulated genes *p21*, *Spi2.1*, *Id-1*, *TNFRSF13b*, *Bcl-x* and *MKP-1* were upregulated upon IL-3 stimulation to various extents (Figure 34A). The *IL2Ra* mRNA level, however, was at the detection limit both in the presence and absence of IL-3 (Figure 34A), disagreeing with the *IL2Ra* mRNA levels slightly above the detection limit detected by Basham *et al.* (2008) and with the description of *IL2Ra* as STAT5 target gene in Ba/F3 cells (Basham *et al.*, 2008, Lecine *et al.*, 1996, Rascle *et al.*, 2003) and in other hematopoietic cells (e.g. Imada *et al.*, 1998, John *et al.*, 1996, Lin *et al.*, 2012, Matikainen *et al.*, 1999, Meyer *et al.*, 1997, Nakajima *et al.*, 1997, Rusterholz *et al.*, 1999). This suggests differences between the parental Ba/F3 cell line employed in the present study, the one employed previously (Basham *et al.*, 2008, Rascle *et al.*, 2003) and by others (Lecine *et al.*, 1996), possibly involving a DNA and/or chromatin alteration at the *IL2Ra* locus. Further agreeing with Basham *et al.* (2008), STAT5 occupancy increased upon IL-3 stimulation at the *Spi2.1*, *Id-1*, and *TNFRSF13b* STAT5 binding sites, and at the *Bcl-x* STAT5 binding site to a lesser extent, indicating STAT5A/B-mediated transactivation (Figure 34B). The STAT5 target genes *MKP-1* and *IL2Ra*, however, exhibited no detectable STAT5 binding upon IL-3 stimulation (Figure 34B), disagreeing with Basham *et al.* (2008). This may oppose STAT5A/B-mediated transactivation for these genes and, thus, suggests further differences between the parental Ba/F3 cell line employed in the present study and the one employed by Basham *et al.* (2008). The absence of STAT5 binding to the *IL2Ra* promoter, however, is in line with the absence of regulation of this gene at the mRNA level (Figure 36A), and further suggests the acquisition of a DNA and/or chromatin alteration preventing the recruitment of STAT5 to the *IL2Ra* promoter.

Figure 34 (next page): STAT5 DNA binding activity correlates with histone H3 decrease in *Spi2.1*, *Id-1* and *TNFRSF13b* gene

Parental Ba/F3 cells were rested for 9–12 h without IL-3 and stimulated for 30 min with IL-3 to turn STAT5A/B activation off/on. Cells were harvested and processed for RT-qPCR or chromatin immunoprecipitation (ChIP) as described in the Material and Methods section.

A: RNA was extracted and reverse transcribed into cDNA. cDNA was analyzed by RT-qPCR using primers specific for the transcripts of the STAT5 target genes *Spi2.1*, *Id-1*, *TNFRSF13b*, *Bcl-x* (Bcl-xL isoform), *MKP-1*, *IL2Ra* and *p21*.

B–D: ChIP was performed using antibodies directed against STAT5A/B **(B)** and total histone H3 **(C)**. Input and co-precipitated genomic DNA were analyzed by quantitative PCR using primers specific for the STAT5 binding sites of the *Spi2.1*, *Id-1*, *TNFRSF13b*, *Bcl-x*, *MKP-1* and *IL2Ra* genes (STAT5, H3) as well as control sites in the latter genes (H3) and the *p21* and *S16* genes (H3), as specified further in the figure. The relative quantity of co-precipitated genomic DNA is expressed as percentage of input genomic DNA (input %), denoting chromatin occupancy. Histone H3 occupancy relative to '−IL-3' was calculated **(D)**. Structures of the studied genes as well as amplicon positions are illustrated in Figure 33.

A–D: The error bars depict standard deviation among (RT-)qPCR replicates. The results shown in **A** and **B** derive from another experiment than **C** and **D**. The two depicted independent experiments are nonetheless representative of each other (data not shown). Nucleotide positions are relative to the transcription start site.

Abbreviations: ChIP = chromatin immunoprecipitation, BS = binding site, ORF = open reading frame, prom = promoter, prox = proximal, TSS = transcription start site

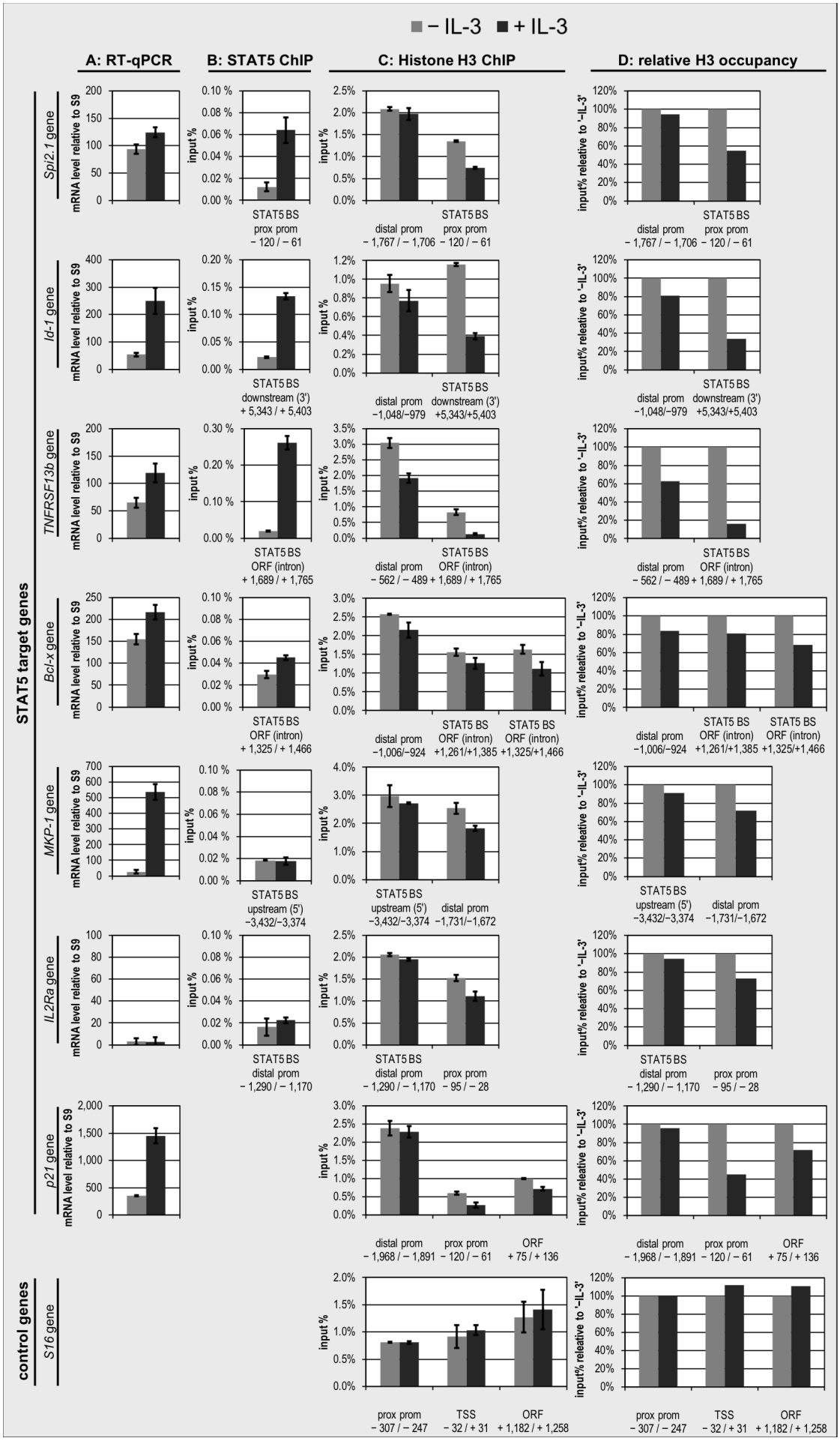
− IL-3 + IL-3
A: RT-qPCR
B: STAT5 ChIP
C: Histone H3 ChIP
D: relative H3 occupancy
STAT5 target genes
control genes
Spi2.1 gene
Id-1 gene
TNFRSF13b gene
Bcl-x gene
MKP-1 gene
IL2Ra gene
p21 gene
S16 gene
mRNA level relative to S9
input %
input% releative to '−IL-3'
STAT5 BS
prox prom − 120 / − 61
distal prom − 1,767 / − 1,706
downstream (3') + 5,343 / + 5,403
distal prom −1,048/−979
+5,343/+5,403
ORF (intron) + 1,689 / + 1,765
distal prom − 562 / − 489
+ 1,689 / + 1,765
ORF (intron) + 1,325 / + 1,466
distal prom −1,006/−924
+1,261/+1,385
+1,325/+1,466
upstream (5') −3,432/−3,374
distal prom −1,731/−1,672
distal prom − 1,290 / − 1,170
prox prom − 95 / − 28
distal prom − 1,968 / − 1,891
ORF + 75 / + 136
prox prom − 307 / − 247
TSS − 32 / + 31
ORF + 1,182 / + 1,258

Histone H3 occupancy did not change in response to IL-3 in the housekeeping gene *S16,* correlating with its predicted constitutive expression pattern (Figure 34C). On the other hand, histone H3 occupancy, which was very low in the proximal promoter of the *p21* gene before IL-3 stimulation (~0.5 % input DNA), further decreased in response to IL-3, down to 40 % of the histone H3 occupancy level of rested cells, correlating with transactivation (Figure 34C and D). However, changes in histone H3 occupancy at other sites along the *p21* gene were negligible upon IL-3 stimulation (Figure 34C and D). *Bcl-x*, *MKP-1* and *IL2Ra*, which showed no or low STAT5 binding (Figure 34B), exhibited a low decrease in histone H3 occupancy at STAT5 binding and control sites upon IL-3 stimulation, with levels remaining at 70–95 % of that of rested cells (Figure 34C and D). Strikingly, a strong decrease in histone H3 occupancy down to 15–55 % of that of rested cells, was observed at the STAT5 binding sites of *Spi2.1*, *Id-1* and *TNFRSF13b* upon IL-3 stimulation (Figure 34C and D), correlating with the stronger binding of STAT5 observed at these sites (Figure 34B). This correlation between STAT5 binding and reduced histone H3 occupancy is in line with the strong decrease of histone H3 occupancy to 10% of that of rested cells observed at the *Cis* STAT5 binding site (Figure 31). These results therefore confirm a strong association between STAT5 binding and reduced histone H3 occupancy at STAT5 binding sites, and this regardless of the location of the STAT5 binding sites within the gene. These observations thus support the hypothesized STAT5A/B-mediated nucleosome loss, although an event consequential to STAT5 DNA binding cannot be ruled out yet.

Of note, the decrease in histone H3 occupancy was also observed to a lesser extent at control sites in the *TNFRSF13b* proximal and *Spi2.1* as well as *Id-1* distal promoter regions (Figure 34C and D), suggesting a global decrease in histone H3 occupancy along these genes, as observed for the *Cis* and *Osm* genes (Figures 30C and 31).

3.5.3 The STAT5A/B-associated histone H3 decrease does not depend on the upregulation of transcriptional activity *per se*

The absence of detectable STAT5 binding to *Bcl-x* and *MKP-1* despite the IL-3-inducible transactivation and histone H3 decrease (Figure 34) might suggest a STAT5A/B-independent transactivation and chromatin remodeling mechanism. Besides, the IL-3-inducible genes *p21* and *c-Fos* exhibited some degree of histone H3 loss within their proximal promoter correlating with their transactivation, in contrast to IL-3-independent *S16* (Figures 31, 34A, 34C and 34D), possibly indicating transactivation-associated chromatin remodeling. Taken together, this raises the possibility that the upregulation of transcriptional activity *per se,* rather than STAT5 DNA binding*,* may be responsible for the histone H3 decrease in a gene-specific manner. The HDAC inhibitor trichostatin A (TSA) has been found by PD Dr. Anne Rascle's research group to inhibit STAT5A/B-

mediated transactivation at a step following STAT5 binding to DNA but preceding the recruitment of RNA polymerase II, a prerequisite for transcriptional activation (Rascle *et al.*, 2003, Rascle and Lees, 2003). Given the hypothesized STAT5A/B-mediated nucleosome loss, TSA was predicted to inhibit STAT5A/B-mediated transactivation, but not the STAT5A/B-associated histone H3 decrease.

To investigate the effect of TSA-induced inhibition, rested Ba/F3-wt cells were pre-treated with TSA or a vehicle control and subjected to IL-3 stimulation. Ba/F3-wt cells have been shown to be comparable to parental Ba/F3 cells in the present study (3.1.2). The previously investigated STAT5 target genes *(Cis*, *Osm*, *Spi2.1*, *Id-1*, *TNFRSF13b*, *IL2Ra* and *p21*) and the IL-3-inducible STAT5A/B-independent gene *c-Fos* were analyzed for their mRNA levels (RT-qPCR), and for STAT5 and histone H3 occupancy (ChIP), as before.

As expected from Rascle *et al.* (2003) and Rascle and Lees (2003), TSA inhibited IL-3-induced transactivation of the STAT5 target genes *Cis*, *Osm*, *Spi2.1*, *Id-1* and *p21* to varying degrees while not impacting transactivation of the IL-3-inducible STAT5A/B-independent gene *c-Fos* (Figure 35A). Of note, induction of the late-responsive STAT5 target gene *TNFRSF13b* was not detectable after 30 minutes of IL-3 stimulation in the Ba/F3-wt cells (Figure 35A), as opposed to the weak induction detected in parental Ba/F3 cells in similar conditions (Figure 34A), despite strong STAT5 binding at its STAT5 binding site (Figure 35B). *IL2Ra* expression was at the detection limit regardless of treatment (Figure 35A), as observed before in parental Ba/F3 cells (Figure 34A). Thus, the inhibitory effect of TSA could not be evaluated for these two genes. The slightly increased mRNA levels in rested Ba/F3-wt cells pre-treated with TSA, as observed in *Cis*, *Spi2.1* and *Id-1* (Figure 35A), have been proposed by PD Dr. Anne Rascle's research group to be caused by genome-wide hyperacetylation (Pinz *et al.*, 2014b, Figure 6 and Pinz *et al.*, 2015, Figure 5) and/or locus-specific hyperacetylation (*Cis*, *Osm*, *c-Fos* and *p21* | Pinz *et al.*, 2014b, Figure 7 and Pinz *et al.*, 2015, Figures 7 and 8), predicted to result in increased chromatin accessibility for the transcription machinery. Agreeing with results in parental Ba/F3 cells (Figure 34B), STAT5 DNA binding activity was detected upon IL-3 stimulation at the STAT5 binding sites of *Cis*, *Osm*, *Spi2.1*, *Id-1* and *TNFRSF13b*, but not of *IL2Ra* (Figure 35B). STAT5 occupancy was reduced to varying degrees – but not abrogated - in the presence of TSA (Figure 35B), as observed before for *Cis* and *Osm* (Rascle *et al.*, 2003).

With the exception of *c-Fos*, the investigated sites exhibited a clearly lowered histone H3 occupancy in the presence of TSA (Figure 35C) possibly due to genome-wide hyperacetylation (Pinz *et al.*, 2014b, Figure 6 and Pinz *et al.*, 2015, Figure 5). No decrease in histone H3 occupancy was observed at control sites in the proximal promoter

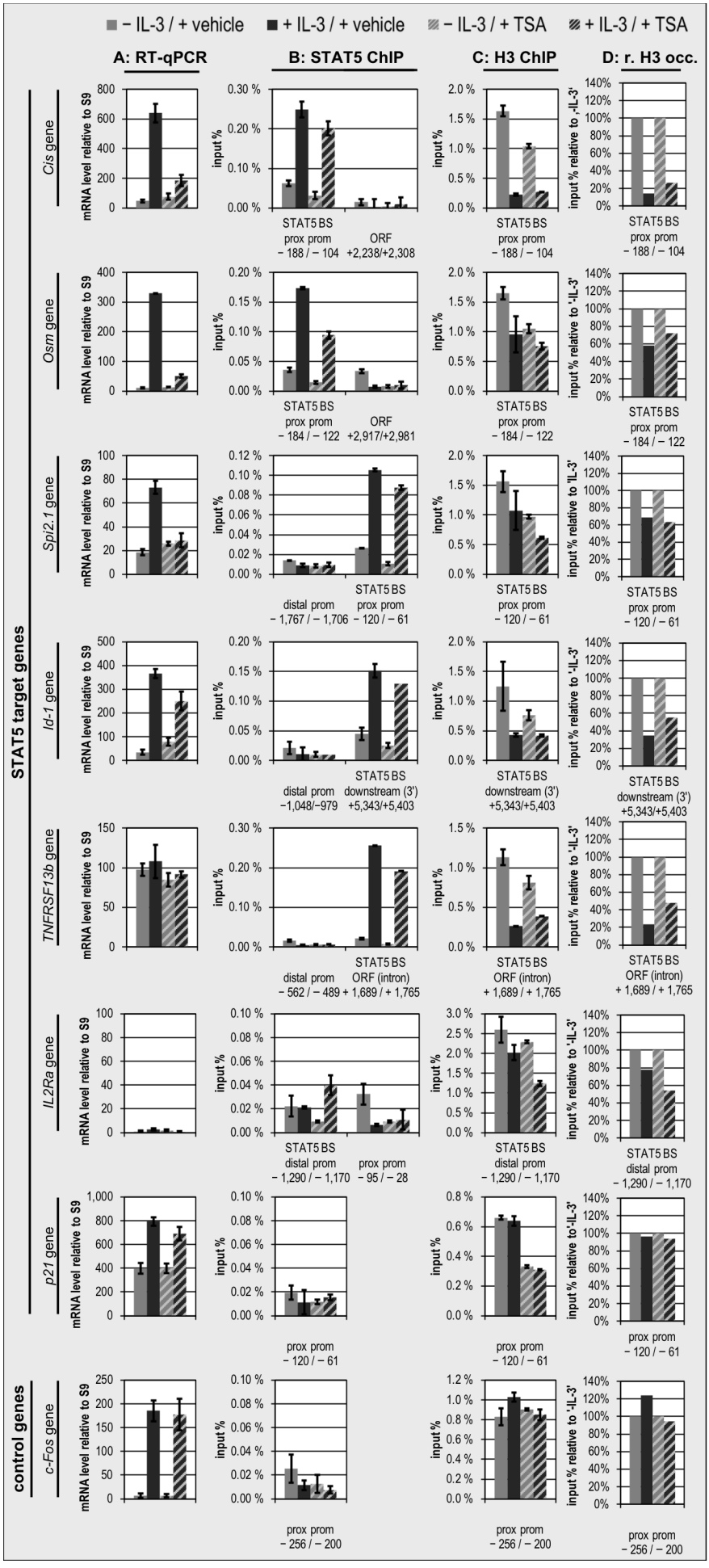
− IL-3 / + vehicle
+ IL-3 / + vehicle
− IL-3 / + TSA
+ IL-3 / + TSA
A: RT-qPCR
B: STAT5 ChIP
C: H3 ChIP
D: r. H3 occ.
STAT5 target genes
control genes
Cis gene
Osm gene
Spi2.1 gene
Id-1 gene
TNFRSF13b gene
IL2Ra gene
p21 gene
c-Fos gene
mRNA level relative to S9
input %
input % relative to -IL-3'
STAT5 BS
prox prom
− 188 / − 104
ORF
+2,238/+2,308
− 184 / − 122
+2,917/+2,981
distal prom
− 1,767 / − 1,706
− 120 / − 61
downstream (3')
−1,048/−979
+5,343/+5,403
ORF (intron)
− 562 / − 489
+ 1,689 / + 1,765
− 1,290 / − 1,170
− 95 / − 28
− 256 / − 200

Figure 35 (previous page): STAT5A/B-associated histone H3 decrease does not depend on transcriptional activation

Ba/F3-wt cells were rested for 10 h without IL-3 and stimulated for 30 min with IL-3 to turn STAT5A/B activation off/on. Before IL-3 stimulation, cells were pre-treated for 45 min with trichostatin A (TSA) to inhibit STAT5 target gene transactivation, with empty vehicle serving as negative control. Cells were harvested and processed for RT-qPCR or chromatin immunoprecipitation (ChIP) as described in the Material and Methods section.

A: RNA was extracted and reverse transcribed into cDNA. cDNA was analyzed by RT-qPCR using primers specific for the transcripts of the STAT5 target genes *Cis*, *Osm*, *Spi2.1*, *Id-1*, *TNFRSF13b*, *IL2Ra* and *p21* as well as the IL-3-inducible STAT5-independent gene *c-Fos* as control.

B–D: ChIP was performed using antibodies directed against STAT5A/B **(B)** and total histone H3 **(C)**. Input and co-precipitated genomic DNA were analyzed by quantitative PCR using primers specific for the STAT5 binding sites of the *Cis*, *Osm*, *Spi2.1*, *Id-1*, *TNFRSF13b* and *IL2Ra* genes (STAT5, H3) as well as control sites in the latter genes (STAT5) and in the *c-Fos* and *p21* genes (STAT5, H3), as specified further in the figure. The relative quantity of co-precipitated genomic DNA is expressed as percentage of input genomic DNA (input %), denoting chromatin occupancy. Histone H3 occupancy relative to '−IL-3' was calculated **(D)**. Structures of the studied genes as well as amplicon positions are illustrated in Figure 33.

A–D: The error bars depict standard deviation among (RT-)qPCR replicates. Nucleotide positions are relative to the transcription start site.

Abbreviations: BS = binding site, ChIP = chromatin immunoprecipitation, occ. = occupancy, ORF = open reading frame, prom = promoter, prox = proximal, r. = relative, TSA = trichostatin A, TSS = transcription start site.

region of *c-Fos* and *p21* in response to IL-3 (Figure 35C and D). This disagrees with the decrease in histone H3 occupancy observed in parental Ba/F3 cells (Figures 31, 34C and 34D). This discrepancy might be due to the very low histone H3 occupancy detected at these sites, making an accurate determination of % of input DNA difficult. In accordance with parental Ba/F3 cells (Figure 34C and D), the *IL2Ra* STAT5 binding site exhibited a low histone H3 decrease associated with an absence of detectable STAT5 DNA binding activity (Figure 35B–D). Strikingly, elevated STAT5 occupancy at *Cis*, *Osm*, *Spi2.1*, *Id-1* and *TNFRSF13b* correlated with a strong decrease in histone H3 occupancy, both in the absence and presence of TSA (Figure 35C and D). Hence, the decrease in histone H3 occupancy was not affected by TSA-induced inhibition of transcription of these STAT5 target genes, demonstrating that the decrease in histone H3 occupancy was associated with STAT5 binding, independently of transcriptional activation. This further supports a – causal or consequential – link between DNA binding of STAT5 and nucleosome loss. In addition, these results demonstrate that STAT5 binding to DNA and histone H3 loss precede the recruitment of RNA Polymerase II and transcriptional activation.

3.5.4 STAT5A-1*6 DNA binding correlates with histone H3 decrease in Ba/F3-tet-on-1*6 cells

3.5.4.1 *De novo* STAT5A-1*6 binding to *Cis* and *Id-1* correlates with IL-3-independent histone H3 decrease

The previous findings indicate that the binding of wild-type STAT5 (endogenous STAT5A/B and STAT5A-wt) to DNA is associated with chromatin remodeling (i.e. nucleosome loss) at STAT5 binding sites in response to IL-3. Whether histone H3 loss is the cause or the consequence of STAT5 binding remains to be demonstrated. In the

IL-3-dependent cell line Ba/F3, it is conceivable that IL-3-inducible third factors may contribute to or even solely mediate the observed STAT5A/B-associated histone H3 decrease, considering that IL-3 has been found to additionally activate the MAPK and PI3K pathways in Ba/F3 cells (Kinoshita *et al.*, 1997, Rosa Santos *et al.*, 2000). Therefore, the IL-3-independent STAT5A-1*6 model was used to address whether constitutive binding of STAT5 to DNA (in the absence of IL-3) is sufficient to trigger a nucleosome loss at its binding site.

Ba/F3-tet-on-1*6 cells were treated for 11h with dox in the absence of IL-3. The previously investigated STAT5 target genes *(Cis*, *Osm*, *Spi2.1*, *Id-1*, *TNFRSF13b*, *Bcl-x*, *MKP-1*, *IL2Ra* and *p21*) and IL-3-inducible STAT5A/B-independent control gene *c-Fos* were analyzed for their mRNA level by RT-qPCR, and for their STAT5 and histone H3 occupancy by ChIP, as before.

As expected from Ba/F3-1*6 cells (Nosaka *et al.*, 1999), and as shown in the present study (Figure 10C), *c-Fos* mRNA levels were not upregulated upon dox treatment in the absence of IL-3 (Figure 36A). mRNA levels of the STAT5 target genes *Cis*, *Id-1*, and to a lesser extent *TNFRSF13b*, *Bcl-x*, *MKP-1* and *p21* were upregulated upon dox treatment (Figure 36A). The STAT5 target genes *Spi2.1*, *Osm* and *IL2Ra*, on the other hand, exhibited mRNA levels near or at the detection limit both in the presence and absence of dox (Figure 36A), opposing any transactivation of these genes following 11h of dox induction. The absence of *IL2Ra* induction by STAT5A-1*6 is in line with the absence of induction of this gene by endogenous STAT5A/B in response to IL-3 in parental Ba/F3 cells (Figure 34A). The low or absent induction of *Spi2.1*, *Osm* and *Bcl-x* is in line with the delayed or low induction of these genes described above (Figure 25C, F and G). STAT5 occupancy strongly increased upon dox treatment at the *Cis*, *Osm*, *Id-1* and *TNFRSF13b* STAT5 binding sites (Figure 36B), showing STAT5A-1*6 DNA binding activity. STAT5 binding at these sites correlated with increased mRNA levels for *Cis*, *Id-1* and *TNFRSF13b,* but not *Osm,* which remained low (Figure 36A). This suggests *Osm*-specific differences, possibly in the chromatin context, preventing its transactivation despite the proper recruitment of STAT5. On the other hand, STAT5 occupancy weakly increased or remained at background levels at the STAT5 binding sites of the *Spi2.1*, *MKP-1*, *Bcl-x* and *IL2Ra* genes (Figure 36B), in line with their low mRNA levels.

Dox treatment did not impact histone H3 occupancy at the *c-Fos* and *p21* proximal promoters (Figure 36C and D). Likewise, *Spi2.1*, *Bcl-x*, *MKP-1* and *IL2Ra* STAT5 binding sites did not exhibit a change in histone H3 occupancy, correlating with the absence of STAT5 binding (Figure 36C and D). By contrast, histone H3 occupancy decreased by 60 % (relative to the level observed before dox treatment) at the *Cis* STAT5 binding site, by 40 % at the *Id-1* STAT5 binding site and by 20 % at the *Cis* TSS (Figure 36C and D),

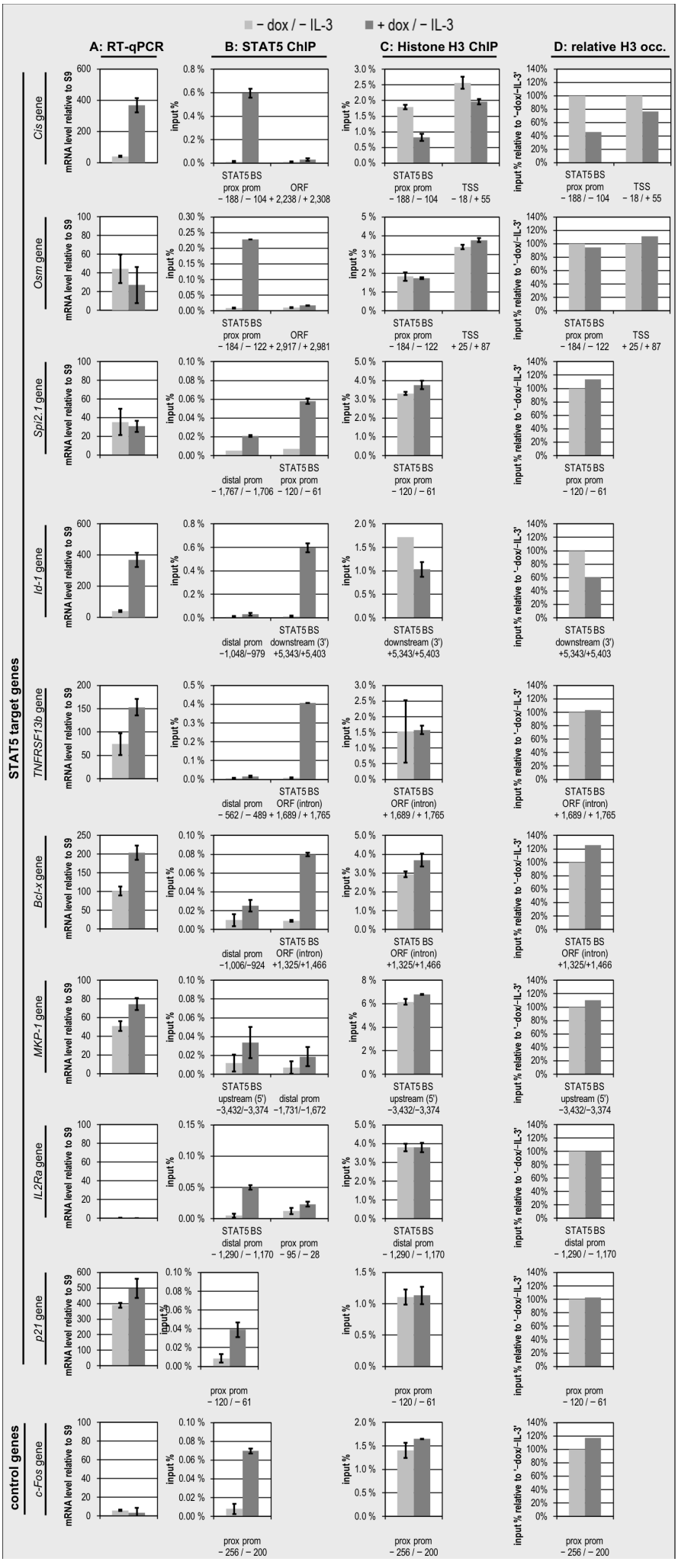
− dox / − IL-3
+ dox / − IL-3
A: RT-qPCR
B: STAT5 ChIP
C: Histone H3 ChIP
D: relative H3 occ.
STAT5 target genes
control genes
Cis gene
Osm gene
Spi2.1 gene
Id-1 gene
TNFRSF13b gene
Bcl-x gene
MKP-1 gene
IL2Ra gene
p21 gene
c-Fos gene
mRNA level relative to S9
input %
input % relative to '−dox/−IL-3'
STAT5 BS
prox prom
− 188 / − 104
ORF
+ 2,238 / + 2,308
TSS
− 18 / + 55
− 184 / − 122
+ 2,917 / + 2,981
+ 25 / + 87
distal prom
− 1,767 / − 1,706
− 120 / − 61
downstream (3')
+5,343/+5,403
−1,048/−979
ORF (intron)
− 562 / − 489
+ 1,689 / + 1,765
−1,006/−924
+1,325/+1,466
upstream (5')
−3,432/−3,374
−1,731/−1,672
− 1,290 / − 1,170
− 95 / − 28
− 256 / − 200

Figure 36 (previous page): *De novo* STAT5A-1*6 binding to *Cis* and *Id-1* correlates with IL-3-independent histone H3 decrease

Ba/F3-tet-on-1*6 cells were deprived of IL-3 and supplemented for 11 h with dox(doxycycline) to induce STAT5A-1*6 production and study the effect of IL-3-independent constitutive STAT5A-1*6 activation. Non-induced cells were rested for 11 h without IL-3 as negative control for STAT5A/B activation. Cells were harvested and processed for RT-qPCR or chromatin immunoprecipitation (ChIP) as described in the Material and Methods section.

A: RNA was extracted and reverse transcribed into cDNA. cDNA was analyzed by RT-qPCR using primers specific for the transcripts of the STAT5 target genes *Cis*, *Osm*, *Spi2.1*, *Id-1*, *TNFRSF13b*, *Bcl-x*, *MKP-1*, *IL2Ra* and *p21*, and for the IL-3-inducible STAT5-independent gene *c-Fos*.

B–D: ChIP was performed using antibodies directed against STAT5A/B **(B)** and total histone H3 **(C)**. Input and co-precipitated genomic DNA were analyzed by quantitative PCR using primers specific for the STAT5 binding sites of the *Cis*, *Osm*, *Spi2.1*, *Id-1*, *TNFRSF13b*, *Bcl-x*, *MKP-1* and *IL2Ra* genes (STAT5, H3) and for control sites in the *Cis*, *Osm*, *c-Fos* and *p21* genes (STAT5, H3), as specified further in the figure. The relative quantity of co-precipitated genomic DNA is expressed as percentage of input genomic DNA (input %), denoting chromatin occupancy. Histone H3 occupancy relative to '−dox' was calculated **(D)**. Structures of the studied genes as well as amplicon positions are illustrated in Figure 33.

A–D: The error bars depict standard deviation among (RT-)qPCR replicates. Nucleotide positions are relative to the transcription start site.

Abbreviations: BS = binding site, ChIP = chromatin immunoprecipitation, dox = doxycycline, occ. = occupancy, ORF = open reading frame, prom = promoter, prox = proximal, TSS = transcription start site

confirming the correlation observed in IL-3-stimulated Ba/F3 cells between a strong STAT5 binding and a decrease in histone H3 occupancy, and suggesting a STAT5-dependent nucleosome loss. Surprisingly however, histone H3 occupancy at the *Osm* and *TNFRSF13b* STAT5 binding sites did not change (Figure 36C and D), despite STAT5 binding activity (Figure 36B), correlating with low transcriptional activity (Figure 36A). This suggests that IL-3-inducible STAT5-independent factors might be essential for nucleosome loss following STAT5 binding to allow transcriptional activation of *Osm* and *TNFRSF13b*. Alternatively, it might suggest that the treatment duration of 11 h was too short to observe an effect of STAT5 DNA binding on histone H3 occupancy and transcriptional activation. In fact, experiments presented in the next section based on a long-term time course of dox treatment support this proposition (Figure 37). Thus, these observations on *Osm* and *TNFRSF13b* cannot totally rule out a mechanism of STAT5-mediated nucleosome loss. Anyhow, these data demonstrate that STAT5 binding can occur in the absence of decreased histone H3 occupancy, further supporting the idea that nucleosome loss is a consequence of rather than a prerequisite for STAT5 binding.

3.5.4.2 Sustained STAT5A-1*6 binding to *Cis*, *Osm* and *Spi2.1* is associated with persistent long-term histone H3 decrease

The observed histone H3 decrease suggests chromatin remodeling and correlated with binding of transiently active endogenous STAT5A/B and of constitutively active STAT5A-1*6 in several genes independently of IL-3 supplementation (Figure 36B–D) and independently of the location of the STAT5 binding site relative to the ORF (Figure 34B–D). These findings strongly suggest a causal link between STAT5 DNA binding and chromatin remodeling, proposing an interaction of STAT5A/B with ATP-dependent chromatin-remodeling complexes. Given this, sustained constitutive STAT5A-1*6 activation was hypothesized to correlate with a sustained decrease in

histone H3 occupancy. Besides, such putative sustained chromatin alterations at STAT5 binding sites were hypothesized to constitute 'passenger' and/or 'driver' alterations and to contribute to the oncogenicity of STAT5A-1*6.

To investigate the effects of constitutive STAT5A-1*6 activation, the previously studied samples from Induction-4 (Figure 17A) were analyzed by ChIP using antibodies against histone H3. *Cis*, *Spi2.1* and *Osm* mRNA levels and STAT5 occupancy have been described before (Figures 25B, 25C, 25G, 27A, 27C and 27D) and are shown again in Figure 37 for easier reference. Histone H3 occupancy was analyzed by qPCR for the previously investigated *Cis*, *Spi2.1* and *Osm* STAT5 binding sites in addition to the *Cis* and *Osm* TSS. As controls, histone H3 occupancy was analyzed at sites in the *c-Fos* proximal promoter, at the TSS of the housekeeping gene *S16* and in the *Id-1* distal promoter.

Both in non-induced and in dox-induced cells, histone H3 occupancy was stable at the control *S16* TSS throughout Induction-4 (Figure 37G). This suggests no global (genome-wide) or *S16* locus-specific 'passenger' chromatin alterations involving nucleosome density. On the other hand, histone H3 occupancy fluctuated in a random manner at the control *Id-1* distal promoter, exhibiting a downward tendency in dox-induced and non-induced cells (Figure 37H). Similarly, histone H3 occupancy at the control *c-Fos* proximal promoter halved in dox-induced cells within one week of dox induction and remained around that lower level throughout dox induction, mirrored by a similar decrease in non-induced cells (Figure 37F). These decreases suggest a locus-specific time-dependent decrease in nucleosome density and putatively locus-specific 'passenger' and/or 'driver' chromatin alterations during Induction-4. Interestingly, histone H3 occupancy also decreased considerably during Induction-4 in non-induced cells at the *Cis* and *Osm* TSS (Figure 37B and E) and at the STAT5 binding sites in the *Spi2.1* and *Osm* proximal promoters (Figure 37C and E), suggesting locus-specific time-dependent decreases in nucleosome density putatively involving STAT5 DNA binding activity.

Within the first week of dox induction, histone H3 occupancy decreased down to 10 % of the initial level at the investigated sites in *Cis*, *Osm* and *Spi2.1* (Figure 37A–E), strongly correlating with *Spi2.1* and *Osm* STAT5 occupancy (Figure 27C and D), but not so much with *Cis* STAT5 occupancy, which showed little fluctuation over time (Figure 27A). This was particularly striking for *Spi2.1*, at which a downward peak of histone H3 occupancy at day 7 of induction (Figure 37C) concurred with an upward peak in *Spi2.1* STAT5 occupancy (Figure 27C) and in mRNA levels (Figure 25C). Following the first week of induction, histone H3 occupancy at the *Cis, Osm* and *Spi2.1* STAT5 binding sites remained low (Figure 37A, C and D), exhibiting a moderate correlation with STAT5

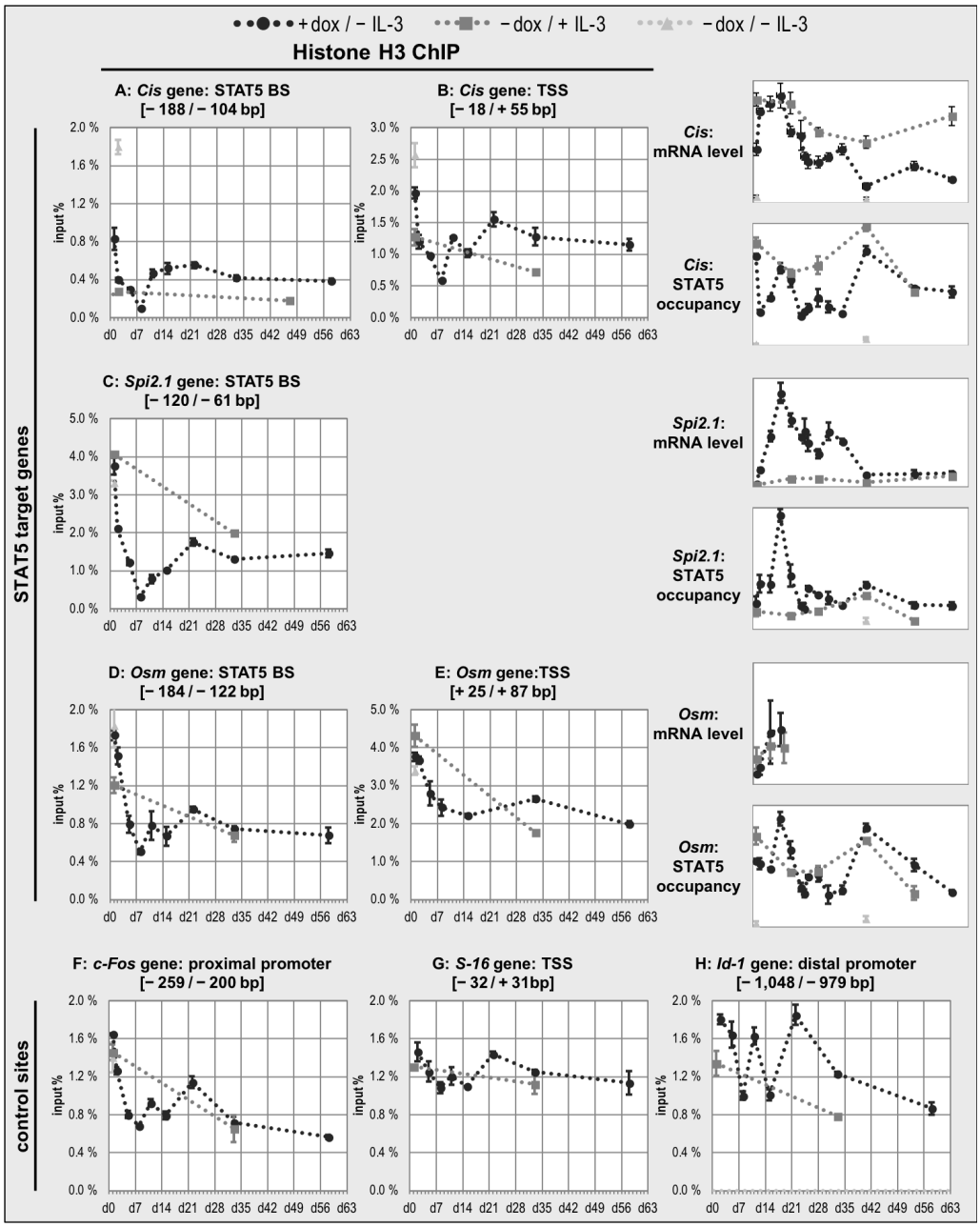

Figure 37: Sustained STAT5A-1*6 binding to *Cis*, *Osm* and *Spi2.1* was associated with persistent long-term histone H3 decrease

Ba/F3-tet-on-1*6 cells were grown in the absence of IL-3 and supplemented with doxycycline to induce STAT5A-1*6 production. Cells were kept for nine weeks as part of the 'Induction-4' experiment to study the effects of sustained constitutive STAT5A-1*6 activation. Non-induced cells were grown in the presence of IL-3 as control for the effects of endogenous STAT5A/B activation or rested without IL-3 for 11 h as baseline control for the absence of STAT5A/B activation. Cells were harvested at the indicated time-points and processed for chromatin immunoprecipitation (ChIP) as described in the Material and Methods section. ChIP was performed using an antibody directed against histone H3. Input and co-precipitated genomic DNA were analyzed by quantitative PCR using primers specific for sites in the STAT5 target genes *Cis*, *Spi2.1*, *Osm* and *Id-1* as well as in the STAT5-independent control genes *c-Fos* and *S16*. Primers were specific for the *Cis*, *Spi2.1*, *Osm* and *c-Fos* proximal promoter regions **(A, C, D, F)**, the *Cis*, *Osm* and *S16* transcription start sites **(B, E, G)** and the *Id-1* distal promoter region **(H)**, as specified further in the figure. *Cis*, *Spi2.1* and *Osm* proximal promoter amplicons overlap their respective STA5 binding sites. *S16* and *Id-1* amplicons were not analyzed for rested non-induced cells. The relative quantity of co-precipitated genomic DNA is expressed as percentage of input genomic DNA (input %), denoting H3 occupancy. Structures of the studied genes as well as amplicon positions are illustrated in Figure 33.The error bars depict standard deviation among qPCR replicates. Nucleotide positions are relative to the transcription start site. The dotted lines connect single data points for dox-induced cells and non-induced cells, growing in the presence of IL-3. *Cis*, *Spi2.1* and *Osm* mRNA level and STAT5 occupancy profiles from Figures 25B, 25C, 25G, 27A, 27C and 27D are shown on the side for easier reference.

Abbreviations: BS = binding site, ChIP = chromatin immunoprecipitation, dox = doxycycline, TSS = transcription start site.

occupancy (Figure 27A, C and D). Of note, histone H3 occupancy had only decreased considerably by day 2 of dox induction for *Spi2.1* and by day 3 for *Osm* (Figure 37C and D), suggesting that the lack of detectable histone H3 decrease despite STAT5 binding in *Osm* and *TNFRSF13b* (Figure 36B–D) was linked to the short treatment duration of 11 h.

Altogether, the correlation of STAT5A-1*6 DNA binding with histone H3 decrease in *Cis*, *Osm* and *Spi2.1* despite the absence of IL-3 strongly supports a causal link between STAT5A-1*6 DNA binding and nucleosome loss, leading to transcriptional activation, and opposes the participation of third IL-3-inducible factors in STAT5A/B-mediated nucleosome loss. In addition, the maintained low histone H3 occupancy in long-term dox induction at *Cis*, *Osm* and *Spi2.1* STAT5 binding sites strongly suggests sustained chromatin alterations, involving nucleosome loss, mediated by STAT5A-1*6 and, thus, proposes STAT5A-1*6-mediated ‘passenger’ and/or ‘driver’ chromatin alterations as contributing factors to STAT5A-1*6 oncogenicity.

4 Discussion

Constitutive, as opposed to transient, STAT5A/B activity has been shown to be oncogenic in amongst others hematopoietic cells. Therefore, the present study aimed to elucidate effects specific to constitutive STAT5A/B activity as opposed to transient STAT5A/B activity – in particular upon sustained DNA binding on chromatin – underlying its oncogenicity. A stable Ba/F3 cell line inducibly expressing constitutively active STAT5A-1*6 (Ba/F3-tet-on-1*6) was generated as an experimental model system and shown to mirror *in vivo* oncogenesis in the acquisition of cancer hallmarks upon STAT5A-1*6 induction and in the misregulation of oncogenes.

Using the Ba/F3-tet-on-1*6 cell line and other Ba/F3-derived cell lines, STAT5 DNA binding was correlated with nucleosome loss. Several lines of evidence suggested a causal link between STAT5 DNA binding and nucleosome loss. Strikingly, persistent nucleosome loss was correlated with sustained STAT5A-1*6 DNA binding in transformed (dox-induced) Ba/F3-tet-on-1*6 cells, leading me to propose a new molecular mechanism for 'driver' and 'passenger' chromatin alterations mediated by oncogenic constitutive STAT5 activity.

4.1 Correlative evidence suggests that STAT5A/B causes nucleosome loss in Ba/F3 cells upon DNA binding

4.1.1 The STAT5A/B-mediated *Cis* and *Osm* transactivation mechanisms might involve HAT and H3K4 methyltransferase recruitment

Distribution of the histone modifications investigated in parental Ba/F3 cells (acH3, acH4, H3K4me1/3, H3K9me1/3 and H3K27me1/3) along the STAT5 target genes *Cis*, *Osm* and the control gene *c-Fos* (Figures 28, 30 and 32) mostly agreed with their reported distributions for active euchromatic genes with an expected increase in active marks upon IL-3-induced transactivation (Table 1 and 1.2.2.2), as well as with previous reports and with the predominant function of STAT5A/B as transactivator (1.3.3). Surprisingly, this excepted the unchanged acH3 and acH4 enrichment at the *Cis* STAT5 binding site (upon IL-3 stimulation in parental Ba/F3 cells | Figures 28 and 30). This might be explained by the concurrent histone H3 decrease at this site, which was much stronger than at the *Osm* STAT5 binding site (Figure 30), or by gene-specific differences in the STAT5A/B-mediated transactivation mechanisms (discussed in 4.1.2). Besides, (i) above-background signals of the repressive heterochromatic marks H3K9me3 (*Osm* ORF) and H3K27me3 (*c-Fos* ORF | Figure 28 and Table 1) and (ii) negative *Osm* and *c-Fos* mRNA signals compared with the low positive *Cis* mRNA signals (Figure 10) were observed upon IL-3 deprivation, raising the possibility of heterochromatic silencing of *Osm* and *c-Fos*, but not *Cis*, in the absence of IL-3.

The increase in acH3, acH4 and H3K4me3 enrichment along *Cis*, *Osm* and *c-Fos* (Figures 30 and 32) suggests IL-3-induced recruitment of HATs and H3K4 methyltransferases, whereas the loss of above-background H3K9me3 and H3K27me3 signals at DNA sites in *Osm* and *c-Fos* (Figure 28) might point to IL-3-induced recruitment of H3K9 and K27 demethylases (provided that the loss of signals is not caused by histone H3 loss *per se*). Reversely, the observed pattern opposes the IL-3-induced recruitment of antagonistic HDACs and H3K4 demethylases, in accordance with recently reported negative HDAC3 and LSD1 signals at these three loci (Nanou *et al.*, 2017, GEO accession number GSE79520). It remains to be determined, whether these chromatin modifiers are recruited to *Cis* and *Osm* by DNA-bound STAT5 and/or other IL-3-inducible factors, e.g. by experiments based on the ones conducted for histone H3 decrease in the present study (3.5). STAT5A/B-mediated HAT recruitment is strongly supported by the existent evidence (Table 2). Although no STAT5A/B-histone lysine methyltransferase interaction has been described so far, Wagatsuma *et al.* (2015) has recently shown that GAS motif disruption in a *TCRG-Jγ1* STAT5 binding site abrogated (amongst other things) enrichment of H3K4me1/2/3, supporting STAT5A/B-mediated H3K4 methyltransferase recruitment. Identifying the chromatin modifiers responsible for the observed chromatin alterations, for instance by screening available transcriptome data of Ba/F3 cells (Basham *et al.*, 2008, GEO accession number GSE10389; Nanou *et al.*, 2017, GEO accession number GSE79520) for candidates and confirming their recruitment using ChIP assay (with specific antibodies), might offer novel insights into the STAT5A/B transactivation mechanism.

STAT5 DNA binding to the *Cis* proximal promoter has been correlated with increased acH3 enrichment in a human breast cancer cell line (Schauwecker *et al.*, 2017), in contrast to the unchanged acH3 enrichment observed in the present study (Figure 32). This disagreement might be explained by the fact that the *Cis* proximal promoter site investigated by Schauwecker *et al.* (2017) is located more closely to the *Cis* TSS, where increased acH3 enrichment was also detected in the present study (Figure 32). In accordance with my findings (Figure 28), Schauwecker *et al.* (2017) detected negative H3K9me3 and H3K27me3 ChIP signals at this site both in the absence and presence of STAT5 DNA binding. Interestingly, Chia and Rotwein (2010) observed decreased H3K4me1 and H3K4me3 and unchanged acH3 and acH4 ChIP signals (not normalized to histone H3 occupancy) in hepatocytes at the *Cis* STAT5 binding site upon STAT5 DNA binding. While the H3K4 methylation pattern is in agreement with my findings (Figure 30), the acH3 and acH4 pattern is not (Figure 32). The comparability of these patterns is, however, unclear, given that ChIP signals of histone modifications changed dramatically after normalization to histone H3 occupancy in the present study (Figures 30 and 32). Overall, these findings raise the possibility of cell type-specific differences in

H3K4me1/3, acH3 and acH4 enrichment and/or histone H3 occupancies, i.e. the overall chromatin landscape, at the *Cis* locus among B cells, mammary epithelial cells and hepatocytes despite *Cis* being a common STAT5 target gene (compare 1.3.3.3).

4.1.2 Chromatin decondensation mechanisms at the investigated sites might exhibit gene-specific differences

The present study investigated mRNA levels, STAT5 and histone H3 occupancy at the STAT5 binding sites of *Cis*, *Osm*, *Spi2.1*, *Id-1*, *TNFRSF13b*, *Bcl-x*, *MKP-1* and *IL2Ra*, with additional chromatin components investigated for *Cis* and *Osm* (3.5). In doing so, the observed differences among STAT5 target genes suggest gene-specific differences in the STAT5A/B transactivation and STAT5A/B-associated nucleosome loss mechanism, as further detailed below. Such differences agree with the information of STAT5A/B DNA binding and transcriptional regulation patterns by the pre-existent chromatin landscape (amongst other things | 1.3.3.4) and have been confirmed by recent genome-wide ChIP-seq data of Ba/F3 cells (Nanou *et al.*, 2017, GEO accession number GSE79520). Specifically, LSD1 was co-recruited to the *Bcl-x* STAT5 binding site upon IL-3 stimulation and HDAC3 and LSD1 co-occupied the *Id-1* STAT5 binding site independently of IL-3 stimulation, proposing a role for LSD1 in *Bcl-x* and for both HDAC3 and LSD1 in *Id-1* transactivation. By contrast, no positive HDAC3 and LSD1 ChIP signals were detected among all other investigated STAT5 target genes, opposing a role for HDAC3 or LSD1 there.

4.1.2.1 Short doxycycline treatment duration might explain the absence of detectable nucleosome loss in the presence of STAT5A-1*6 DNA binding

DNA binding of wild-type STAT5 (i.e. endogenous STAT5A/B and STAT5A-wt) consistently correlated with histone H3 decrease at the *Cis*, *Osm*, *Spi2.1*, *Id-1* and *TNFRSF13b* STAT5 binding sites (Figures 30, 31, 34 and 35). Unexpectedly, STAT5A-1*6 DNA binding in dox-induced Ba/F3-tet-on-1*6 cells did so only for *Cis*, *Id-1* and *Spi2.1*, but not for *TNFRSF13b* and only in a time-delayed manner for *Osm* starting after day 3 of induction (Figures 36 and 37). This suggests the contribution of third factors late-responsive to STAT5A-1*6 activity for *Osm* and putatively *TNFRSF13b* (given investigation of only the 11 h of dox induction time-point | discussed in 4.1.3), although a technical problem in the ChIP assay, interfering with the proper detection of histone H3 loss cannot be excluded.

Indeed, two of my findings support the latter possibility, considering that the applied ChIP assay measures average chromatin occupancies across the entire cell population: On the one hand, nucleosome positioning and overall density has been shown to change during the cell cycle along protein-coding genes (in yeast | Deniz *et al.*, 2016, Hogan *et al.*, 2006, Ma *et al.*, 2015) and chromatin condensation and DNA fragmentation are

hallmarks of apoptosis (Kerr *et al.*, 1972, Prokhorova *et al.*, 2015, Taylor *et al.*, 2008 | compare 4.2.2). Therefore, the presence of dead/dying cells and the absence of dividing cells (most pronounced in the first three days of induction | Figures 20–22) might have skewed average histone H3 occupancy and precluded the detection of a histone H3 decrease observed under different conditions. On the other hand, STAT5A-1*6 production was not fully induced until day 3 of dox induction with undetectable production in ~50 % of the cells after 12 h of induction (Figure 18). While the absence of STAT5A-1*6 activity in ~50 % of cells might not have affected the detectability of STAT5 DNA binding in ChIP assay, the putatively concurrent decrease in histone H3 occupancy might have been less pronounced and therefore not detectable in ChIP assay. These two issues could be addressed by (i) increasing the duration of dox treatment to 3 days and/or (ii) by flow cytometric cell sorting prior to the ChIP assay to isolate GFP-positive (i.e. STAT5A-1*6-expressing) cells and/or living cells of a given cell cycle phase (among dox-induced and non-induced control cells to ensure comparability).

4.1.2.2 The nucleosome loss mechanism at the *Cis* STAT5 binding site might not involve a BRG1-containing SWI/SNF complex and HAT activity

Given multiple STAT5A/B-HAT interactions (Table 2), the absence of IL-3-induced acH3 and acH4 enrichment at the *Cis* and the weak increase at the *Osm* STAT5 binding site (Figure 32) was unexpected and suggested that STAT5A/B does not recruit HATs to its *Cis* STAT5 binding site, while it might at the *Osm* STAT5 binding site. This, in turn, proposes that HATs contributed to the STAT5A/B-associated chromatin remodeling in *Osm*, but not *Cis*. Interestingly, this *Cis* and *Osm* gene-specific difference is in agreement with the proposal that two different BET family members participate in *Cis* (Brd2) and *Osm* (unidentified) transactivation in Ba/F3 cells, respectively (1.3.3.5 | Liu *et al.*, 2014, Pinz *et al.*, 2015). Though, my findings cannot entirely refute the participation of HATs in the nucleosome loss mechanism at the *Cis* STAT5 binding site, considering the (i) acH3 and acH4 enrichment in proximity (Figure 32), that (ii) nucleosomes containing acH3 and acH4 (acetylated *de novo* in response to IL-3) might be selectively lost or deacetylated and that (iii) HATs regulate activity of numerous non-histone substrates (e.g. Choudhary *et al.*, 2009, Iwabata *et al.*, 2005, Shankaranarayanan *et al.*, 2001, Spange *et al.*, 2009). Overall, the role of HATs in STAT5A/B-associated nucleosome loss remains to be determined and could be uncovered by investigating the effects of pan-HAT inhibitor treatment (e.g. anacardic acid | Balasubramanyam *et al.*, 2003, Sun *et al.*, 2006, Wapenaar and Dekker, 2016) or the specific recruitment of HAT proteins by ChIP.

So far, the catalytic SWI/SNF-family subunit BRG1 is the only constituent subunit of ATP-dependent chromatin remodeling complexes shown to physically and functionally interact with STAT5A/B (Wagatsuma *et al.*, 2015, Xu *et al.*, 2007 | Table 2), proposing a role in the STAT5A/B-associated nucleosome loss mechanism in Ba/F3 cells. Therefore,

the negative BRG1 ChIP signal detected at the *Cis* STAT5 binding site and TSS (in absence and presence of IL-3 | data not shown) was surprising, especially given the demonstrated expression of *Brg1* in Ba/F3 cells (Basham *et al.*, 2008, GEO accession number GSE10389). We cannot exclude that this negative signal is due to a technical issue linked to the application of a non-verified antibody. The present study, hence, cannot refute the hypothesized recruitment of BRG1 to the aforementioned sites. Investigating STAT5A/B-associated chromatin condensation upon *Brg1* knock-down and/or forced expression of dominant-negative BRG1 (compare Xu *et al.*, 2007) could uncover its possible implication. Though, it is conceivable that another chromatin remodeling enzyme catalyzes nucleosome loss along *Cis*.

4.1.2.3 The absence of detectable STAT5 DNA binding at its *Bcl-x*, *MKP-1* and *IL2Ra* binding sites might be due to a technical issue

The STAT5 target genes *Bcl-x*, *MKP-1* and *IL2Ra* have been shown to be bound and transactivated by STAT5A/B in response to IL-3 in Ba/F3 cells (Basham *et al.*, 2008, Dumon *et al.*, 1999, Lecine *et al.*, 1996, Nelson *et al.*, 2004). Therefore, the absence of detectable STAT5 DNA binding at the *Bcl-x*, *MKP-1* and *IL2Ra* STAT5 binding sites was unexpected (Figures 34–36). Nevertheless, both IL-3-dependent and -independent STAT5 activity correlated with *Bcl-x* and *MKP-1* transactivation (Figures 34–36) and IL-3-dependent STAT5 activity correlated with histone H3 decrease at *Bcl-x*, *MKP-1* and *IL2Ra* (Figures 34 and 35), suggesting STAT5A/B-mediated mechanisms. These contradictory findings could be explained (i) by false negative STAT5 ChIP signals for technical reasons or (ii) by differences between the Ba/F3 cells employed by Basham *et al.* (2008) and the ones employed in the present study in case of *bona fide* negative signals.

In support of possibility (i), STAT5 occupancy levels in IL-3 stimulated parental Ba/F3 cells, as detected using ChIP assay (Basham *et al.*, 2008, not *Bcl-x*) and ChIP-seq assay (Nanou *et al.*, 2017, GEO accession number GSE79520), were lower at the *Bcl-x*, *MKP-1*, *IL2Ra* and *Spi2.1* STAT5 binding sites than at the other STAT5 binding sites (*Cis*, *Osm*, *Id-1* and *TNFRSF13b*) investigated in the present study (~5–15 % of the level at the *Cis* STAT5 binding site with the exception of the level observed a the *IL2Ra* STAT5 binding site by Basham *et al.*, 2008 [~40 %]). In case of similar ratios in the present study, the expected values for STAT5 chromatin occupancy (~0.02–0.05 % of input DNA) would be below the detection limit of the ChIP assay ($\lesssim$0.10 % of input DNA), with the exception of the expected values for *IL2Ra* according to Basham *et al.* (2008 | ~0.14 %). This agrees with the values detected in the present study (Figure 34). This, in turn, suggests a lower sensitivity of the applied ChIP assay for technical reasons and proposes STAT5 DNA binding to *Bcl-x*, *MKP-1* and *IL2Ra* below the detection limit in the present study.

Technical improvements to the STAT5 ChIP assay (e.g. based on Pinz and Rascle, 2017) might allow detection of STAT5 DNA binding to these genes.

In support of possibility (ii), the striking difference in STAT5 occupancy at *IL2Ra* (relative to the *Cis* and the other investigated STAT5 binding sites) between, on the one hand, the Basham *et al.* (2008) study and, on the other hand, the Nanou *et al.* (2017 | GEO accession number GSE79520) and the present studies suggests molecular differences between the employed parental Ba/F3 cell lines. Moreover, the IL-3-independent upregulation of *Bcl-x* and *MKP-1* in the presence of STAT5A-1*6 suggests a STAT5A/B-dependent transactivation mechanism in the present study. In case of *bona fide* negative STAT5 ChIP signals, this proposes that STAT5A-1*6 mediated *Bcl-x* and *MKP-1* transactivation (a) by a mechanism independent of its DNA binding and transcriptional activity, (b) by transactivation of third *Bcl-x*- and *MKP-1*-regulating factors and/or (c) through occupation of other than the investigated *Bcl-x* and *MKP-1* promoter/enhancer elements. Previous and recent findings propose molecular mechanisms for possibilities (a) and (c): (a) IL-3-independent cross-activation of the PI3K and MAPK pathways by STAT5A-1*6 (via GAB2 | Nyga *et al.*, 2005) might transactivate *Bcl-x* and *MKP-1*, given the reported (partially) PI3K pathway-dependent upregulation of *Bcl-x* in Ba/F3 cells (Gesbert and Griffin, 2000). (c) ChIP-seq data of Ba/F3 cells (Nanou *et al.*, 2017, GEO accession number GSE79520) have revealed four additional STAT5 binding sites in its second intron both outside and within the *Bcl-x* super-enhancer (two sites respectively | Katerndahl *et al.*, 2017, Loven *et al.*, 2013) as well as one additional STAT5 binding site ~7 kb upstream the *MKP-1* ORF, suggesting alternative candidate *Bcl-x* and *MKP-1*-regulating STAT5 binding sites. These three possibilities could be investigated in dox-induced Ba/F3-tet-on-1*6 cells by (a) forced expression of a dominant negative GAB2 form to abrogate PI3K pathway cross-activation (compare Nyga *et al.*, 2005), by (b) treatment with a protein synthesis inhibitor (e.g. cycloheximide | compare Thiel *et al.*, 2000) and by (c) GAS motif disruption (using e.g. CRISPR/Cas9-mediated gene editing) in the candidate alternative *Bcl-x* and *MKP-1*-regulating STAT5 binding sites.

4.1.2.4 Differences at the *IL2Ra* locus among parental Ba/F3 cell lines might explain negative *IL2Ra* mRNA signals

In accordance with its previously reported late-responsiveness (Basham *et al.*, 2008), *IL2Ra* transactivation was not detectable after 30-minute IL-3 stimulation of parental Ba/F3 cells in the present study (Figure 34). Though unexpectedly, *IL2Ra* mRNA levels were at the detection limit in contrast to the *IL2Ra* mRNA levels slightly above the detection limit detected by Basham *et al.*, 2008 (despite application of the same RT-qPCR primers). Surprisingly, my negative *IL2Ra* mRNA signals agree with recent RNA-seq data (Nanou *et al.*, 2017, GEO accession number GSE79520). This fact, in turn, agrees with the difference in STAT5 occupancy described above and, thus, further

supports molecular differences between the employed parental Ba/F3 cell lines. It is conceivable that a more condensed chromatin state impeded both STAT5 DNA binding and transcriptional activity. Though, other possibilities such as DNA alterations (affecting STAT5 DNA binding and/or the detectability of the *IL2Ra* mRNA by the applied RT-qPCR primers) cannot be excluded. Extending the duration of IL-3 stimulation to 2 h (based on Basham *et al.*, 2008) might allow detection of late-responsive *IL2Ra* transactivation and exclude the possibility of false negative *IL2Ra* mRNA signals in the present study.

4.1.3 STAT5A/B DNA binding activity might be a cause of, rather than a consequence of, nucleosome loss at the *Cis*, *Osm*, *Spi2.1* and *Id-1* STAT5 binding sites

The correlative evidence of the present study strongly suggests a causal link between STAT5 DNA binding and histone H3 decrease (i.e. STAT5A/B-mediated recruitment of ATP-dependent chromatin remodeling complexes catalyzing nucleosome translocation and/or eviction) for its *Cis*, *Osm*, *Spi2.1* and *Id-1* binding sites in Ba/F3 cells. This evidence is based on the positive correlation of STAT5 DNA binding with histone H3 decrease, while being independent of (i) STAT5 binding site location within the gene locus, (ii) transactivation and (iii) IL-3 supplementation (Figures 30, 31 and 34–37). Future studies might reveal a similar link at the *TNFRSF13b*, *Bcl-x*, *MKP-1* and *IL2Ra* STAT5 binding sites for the reasons detailed above (4.1.2). My findings are in agreement with an abundance of correlative evidence linking STAT5 DNA binding with high chromatin accessibility (1.3.3.2). This includes the *Cis* STAT5 binding site in the Ba/F3 cell line (Rascle and Lees, 2003) as well as in a human breast cancer cell line (Schauwecker *et al.*, 2017), where prolactin-induced STAT5 DNA binding has been correlated with the eviction of the −1 nucleosome overlapping the *Cis* STAT5 binding sites and upstream translocation of the −2 nucleosome. This mirrors the tremendous decrease (by up to 90 %) in histone H3 occupancy observed at this site in the present study in response to STAT5A/B activation (Figures 30, 31 and 35–37). Interestingly, STAT5 DNA binding has been found to be a prerequisite for chromatin decondensation at one of two of its binding sites in the *Wap* super-enhancer using GAS motif disruption (Shin *et al.*, 2016), again supporting a STAT5A/B-mediated chromatin decondensation mechanism in accordance with my findings.

As detailed in the introduction section (1.3.3.4.2), the Clevenger's research group has recently shown that HMGN2-dependent linker histone H1 displacement in response to prolactin is a prerequisite for (likewise prolactin-induced) full STAT5 DNA binding to *Cis* and full STAT5A/B-mediated transactivation of *Cis* and other genes in two human breast cancer cell lines (Fiorillo *et al.*, 2011, Medler *et al.*, 2016, Schauwecker *et al.*, 2017). They, therefore, proposed that STAT5 DNA binding is a consequence of concurrent STAT5A/B-independent chromatin decondensation in this cellular context, i.e. both the

HMGN2-independent nucleosome loss described above and the HMGN2-dependent linker histone H1 displacement (Schauwecker *et al.*, 2017). This disagrees with my findings in Ba/F3 cells, which suggest that STAT5A/B binding is a cause of, not a consequence of, concurrent nucleosome loss. Of note, STAT5 DNA binding to *Cis* is decreased, but not fully abrogated, in response to prolactin upon complete inhibition of prolactin-inducible HMGN2 recruitment to *Cis* (Medler *et al.*, 2016). Considering this and my findings, Schauwecker *et al.* (2017) cannot exclude the possibility that the prolactin-induced (decreased) HMGN2 (recruitment)-independent STAT5 DNA binding is a cause, rather than a consequence of, the concurrent HMGN2-independent nucleosome loss in *Cis*. In addition, considering this argument and that Schauwecker *et al.* (2017) did not investigate (i) prolactin-independent effects of STAT5 DNA binding and/or (ii) STAT5A/B-independent effects of prolactin on *Cis* linker histone H1 occupancy, their findings can neither exclude the possibility that the (decreased) HMGN2 (recruitment)-independent STAT5 DNA binding to *Cis* is a prerequisite for the concurrent recruitment of HMGN2, proposing a STAT5A/B-dependent mechanism for HMGN2-dependent histone H1 displacement and its consequential events described above. The availability of active HMGN2 molecules might be the rate-limiting factor for these consequential events, given that HMGN2 inhibition impedes them and that *Hdac6* overexpression (increasing HMGN2 activation) augments them (Fiorillo *et al.*, 2011, Medler *et al.*, 2016, Schauwecker *et al.*, 2017). Overall, for these reasons the findings of the Clevenger's research group might not be in disagreement with my findings despite different cellular contexts.

This raises the possibility of a similar mechanism involving HDAC6/HMGN2-dependent histone H1 displacement in Ba/F3 cells (given the presence of HGMN2 expression; Basham *et al.*, 2008, GEO accession number GSE10389). This is opposed by the fact that *Hdac6* knock-down has been found to not impede STAT5A/B-dependent *Cis* transactivation in Ba/F3 cells (Pinz *et al.*, 2015). Interestingly, pre-treatment with TSA decreased both STAT5 occupancy (upon IL-3 stimulation) to varying degrees and histone H3 occupancy slightly (independently of IL-3, putatively due to hyperacetylation; compare 3.5.3) at the investigated STAT5 binding sites (*Cis*, *Osm*, *Spi2.1*, *Id-1* and *TNFRSF13b* | Figure 35 in accordance with Rascle *et al.*, 2003, Rascle and Lees, 2003 for *Cis* and *Osm*). This is an unexpected finding, as (i) increased chromatin accessibility has been argued to facilitate DNA binding of transcription factors (1.2.1.2), including STAT5A/B (1.3.3.4.2), and that (ii) TSA has been argued to inhibit STAT5A/B-mediated transactivation of *Cis* and other genes at a step following STAT5 DNA binding by an indirect mechanism (involving the displacement of BET family proteins) in Ba/F3 cells (Pinz *et al.*, 2015 | 1.3.3.5). By contrast, Bufexamac and, accordingly, TSA have been argued to do this at a step preceding full (HMGN2-dependent) STAT5 DNA binding by

impeding HDAC6-mediated HMGN2 activation in two human breast cancer cell lines (Medler *et al.*, 2016 | 1.3.3.5). Taken together, this raises the possibility of an additional molecular mechanism for TSA-inhibited STAT5A/B-mediated transactivation at a step preceding (full) STAT5 DNA binding. It is conceivable that this involves inhibition of IL-3-inducible HDAC-dependent activation of histone H1 displacement activity of HMGN2 or another HMGN family member (by deacetylation | compare Bergel *et al.*, 2000, Herrera *et al.*, 1999, Medler *et al.*, 2016). It remains to be determined, whether the aforementioned findings in two human breast cancer cell lines are transferrable to the murine pro-B cell line Ba/F3 e.g. by (single and combined) knock-down experiments of HMGN family members, considering the cell type-specific DNA binding and transcriptional regulation patterns of STAT5A/B (1.3.3).

The putative causal link between STAT5 binding and nucleosome loss, suggested in the present study, rests on its IL-3 independence. My findings, however, cannot exclude the possibility that STAT5A-1*6, but not wild-type STAT5A/B, mediates nucleosome loss independently of IL-3 due to molecular differences (including the disrupted interaction with the co-repressor NCoR2/SMRT, Nakajima *et al.*, 2001 | 1.3.4.3). In addition, nucleosome loss at *Cis* and *Id-1* was less pronounced upon *de novo* STAT5A-1*6 DNA binding than upon wild-type STAT5 DNA binding and time-delayed at *Osm* and putatively *TNFRSF13b* (Figures 36 and 37 | 4.1.2.1). (Disregarding the technical issues discussed in 4.1.2.1), this suggests (i) the possible necessity of third IL-3-inducible factors for full histone H3 decrease at *Cis* and *Id-1* and (ii) the participation of third (putatively IL-3-dependent) factors late-responsive to STAT5A-1*6 activity in histone H3 decrease at least at *Osm*. Mirroring these findings, Lau-Corona *et al.* (2017) have reported temporal differences in chromatin decondensation following forced sustained STAT5A/B activation in hepatocytes. Taken together, the aforementioned possibility should be addressed by further experiments to consolidate a causal link between STAT5 DNA binding and nucleosome loss in Ba/F3 cells. For instance, the abrogation of IL-3-inducible STAT5 DNA binding by GAS motif disruption in parental Ba/F3 cells would be expected to impede IL-3-inducible nucleosome loss. In addition, gain and loss of both (i) IL-3-dependent and (ii) IL-3-independent STAT5 DNA binding would be expected to tightly correlate with chromatin decondensation and condensation, respectively, in a temporal manner. This could be investigated in time-courses of (i) IL-3 stimulation and withdrawal of parental Ba/F3 cells and (ii) dox induction and removal of Ba/F3-tet-on-1*6 cells. Besides, chromatin co-precipitated with STAT5 in ChIP-ChIP assays would be expected to have a lower histone H3 occupancy than overall chromatin.

4.1.3.1 STAT5A/B might cause a nucleosome loss at its binding sites globally in Ba/F3 cells

The STAT5A/B-mediated chromatin remodeling suggested for *Cis*, *Osm*, *Spi2.1* and *Id-1* and proposed for *TNFRSF13b*, *Bcl-x*, *MKP-1* and *IL2Ra* in the present study raises the possibility that STAT5A/B-mediated chromatin remodeling is not restricted to this small set of STAT5 binding sites, but might be a global mechanism in Ba/F3 cells and other cellular contexts. Besides, the fact that histone H3 decrease was observed all along the *Cis* gene (Figure 31) and at control sites in other genes (Figures 30, 34, 35 and 37) raises the possibility that STAT5A/B also mediated nucleosome loss at DNA sites in proximity to its binding sites. On the other hand, my results suggest HAT-dependent nucleosome loss at upstream and downstream regions, thus suggesting a different mechanism of nucleosome eviction at these regions compared to that at STAT5 binding sites, whether STAT5A/B-independent or -dependent. Besides, the gene-specific differences observed in the present study (4.1.2) and the fact, that abrogated STAT5 DNA binding (upon GAS motif disruption) only partially correlated with the absence of chromatin decondensation (Shin *et al.*, 2016), proposes information of STAT5A/B-mediated chromatin decondensation by the pre-existent cellular context (i.e. the chromatin landscape and interactions with other factors) in accordance with previous findings (1.3.3.4). Therefore, it remains to be determined whether the correlation of STAT5 DNA binding and chromatin decondensation in the present and other studies (1.3.3.2) have a causal, consequential or another relationship. Notably, this pattern is mirrored by STAT3 (the STAT family member most closely related to STAT5A/B | Copeland *et al.*, 1995, Wang and Levy, 2012), as STAT3 DNA binding and transcriptional regulation patterns have likewise been proposed/shown to be informed by the pre-existent cellular context (e.g. Fleming *et al.*, 2015, Ho *et al.*, 2011, Oestreich *et al.*, 2012, Urayama *et al.*, 2013), and STAT3 has likewise been proposed/shown to mediate chromatin alterations by functional and physical interaction with chromatin modifiers (reviewed by Wingelhofer *et al.*, 2018) including BRG1 (e.g. Fan *et al.*, 2017, Giraud *et al.*, 2004, Ito *et al.*, 2018, Wu *et al.*, 2016). This raises the possibility of a general association of chromatin remodeling with STAT family transcription factors.

Expanding the locus/transcript-specific assays applied in the present study and the ones proposed above using genome-wide/transcriptome assays would allow investigating global correlations of STAT5 DNA binding (using STAT5A/B ChIP-seq) and STAT5A/B-mediated transcriptional regulation (using RNA-seq) and nucleosome loss (see below) as well as co-occupancies with ATP-dependent chromatin remodeling complexes such as the SWI/SNF subunit BRG1 (using BRG1 ChIP-seq), further elucidating causal or consequential relationships between STAT5 DNA binding and chromatin remodeling. After all, recently available STAT5A ChIP-seq data of parental Ba/F3 cells has identified

overall ~15,500 STAT5A binding sites in parental Ba/F3 cells (Nanou *et al.*, 2017, GEO accession number GSE79520). Of note, histone H3 ChIP assays indicate the (core) nucleosome density at a given DNA site, but cannot indicate chromatin accessibility *per se* (i.e. the degree of DNA exposure) given its information by other parameters in addition to nucleosome positioning (e.g. the presence of linker histone H1 | Tsompana and Buck, 2014). Several techniques are now available for locus-specific and genome-wide analyses of both nucleosome positioning (e.g. micrococcal nuclease digest followed by high-throughput sequencing [MNase-seq]) and chromatin accessibility (e.g. DNase-seq I DNase I digest followed by high-throughput sequencing [DNase-seq] | reviewed by Tsompana and Buck, 2014).

It is tempting to speculate about the far-reaching implications of a STAT5A/B-mediated chromatin decondensation mechanism. For instance, previously reported negative correlations of STAT5A/B DNA binding with ChIP signals of active marks (without normalization to histone occupancy | Chia and Rotwein, 2010, Chia *et al.*, 2010a, Chia *et al.*, 2010b, Eilon *et al.*, 2007, Xu *et al.*, 2003) might not suggest an unexpected depletion of active marks despite concurrent transactivation, but rather nucleosome loss. In addition, STAT5A/B functioning as an anchor for other transcription factors similarly to pioneer factors (Girardot *et al.*, 2015, Ogawa *et al.*, 2014, Shi *et al.*, 2008, Shin *et al.*, 2016) might depend on the exposure of their binding motifs by STAT5A/B-mediated chromatin remodeling. Besides, misregulated STAT5A/B-mediated chromatin remodeling upon sustained DNA binding of constitutively active STAT5 proposes potentially oncogenic 'driver' chromatin alterations, as further detailed below.

4.2 Ba/F3-tet-on-1*6 cells mirror *in vivo* oncogenesis upon STAT5A-1*6 induction

4.2.1 The Ba/F3-tet-on-1*6 experimental system might reflect the clonal evolution of *in vivo* tumorigenesis and its heterogeneity

The mutability of cancer cells is their defining characteristic and underlies the clonal evolution process among them, which leads to the stochastic acquisition of cancer hallmark traits defining the disease cancer (1.1.1). Circumstantial evidence suggests such a clonal evolution process in long-term dox induction experiments of Ba/F3-tet-on-1*6 cells, mirroring *in vivo* cancers. Specifically, the detected pattern in singe-cell GFP fluorescence levels (co-expressed with the STAT5A-1*6 transgene) during Induction-1 (Figure 18) suggested outgrowth of a single cell with a selective growth advantage, which eventually supplanted all other cells. Similarly, a dividing subpopulation of cells with tetraploid G_1 phase DNA content was detected at day 54 of Induction-3, suggesting outgrowth of a single cell after a tetraploidization event (Figure 23). In addition, the temporal differences in survival of dox removal between

Induction-2 and -3 (Table 9) suggest that they were caused by stochastic rather than deterministic events. Besides, the detection of an aberrant STAT5A-1*6 form during Induction-3 (Figure 18) suggests a stochastically acquired 'driver' or 'passenger' alteration.

4.2.2 Ba/F3-tet-on-1*6 cells acquired the 'resisting cell death' and 'sustaining proliferative signaling' cancer hallmarks in a stochastic manner

The reproducible changes in cell cycle distribution, doubling times and the percentage of dead/dying cells during long-term dox induction (Figures 19–23) indicated severely impaired cell viability and proliferation (i.e. a growth arrest) directly following dox induction, which gradually increased reaching the level observed in control cells after 1 and 4–5 weeks of induction, respectively. Given only ~50 % GFP-positive (Figure 18) and G_1 phase accumulation (Figures 18 and 19) after 12–14 h of induction, Ba/F3-tet-on-1*6 cells with late-onset STAT5A-1*6 production and/or in S and G_2/M phase might have died disproportionately directly following IL-3 deprivation. In addition, this pattern suggests that surviving cells could not transition through the G_1 cell cycle check-point, proposing that STAT5A-1*6 activity *per se* constituted a sufficient survival, but yet a weak growth signal upon IL-3 deprivation, likely due to suboptimal STAT5A-1*6 expression levels.

Given the circumstantial evidence for clonal evolution (4.2.1), the gradual increase in cell viability and proliferation (Figures 20–22) suggests the acquisition of 'driver' alterations in a stochastic manner rather than time-dependent deterministic effects of STAT5A-1*6. This is supported by the enormous selective growth advantage for single cells upon acquisition of higher viability or proliferation rate. Ba/F3-tet-on-1*6 relied on STAT5A-1*6 as survival and growth signal until week 4–5 of induction (Table 9). This suggests that 'driver' alterations invigorated the pre-existent pro-survival effect of STAT5A-1*6 and enabled and/or invigorated a pro-growth effect of STAT5A-1*6, rather than having STAT5A-1*6-independent effects. This proposes that STAT5A-1*6 activity *per se* effected the initial cell survival and growth despite IL-3 deprivation in a deterministic manner, possibly by transactivating pro-survival oncogenes. Later on (4–5 weeks of dox induction), STAT5A-1*6-independent Ba/F3-tet-on-1*6 cell survival and growth (upon dox removal | Table 9) suggests that accumulated 'driver' alterations enabled an independence of external growth and survival signaling (both IL-3 and STAT5A-1*6), suggesting the acquisition of the 'resisting cell death' and 'sustaining proliferative signaling' cancer hallmarks (Figure 1). Strikingly, immunocompromised mice injected with Ba/F3 cells producing STAT5A-1*6 *de novo* developed Ba/F3-cell-based-leukemia after around six weeks (Gesbert and Griffin, 2000), suggesting a similar time-frame for the acquisition of these two cancer hallmarks *in vivo*, in accordance with my findings.

Of note, the applied methods (trypan blue staining-based cell counting, cell cycle analysis) together are indicative of cell viability and proliferation. Though, they cannot exclude the possibility that high rates of cell proliferation mask low cell viability, considering that this is a feature present in early stages of *in vivo* cancers (e.g. Bergers *et al.*, 1999, Hanahan and Weinberg, 2000, Kim *et al.*, 2014, Symonds *et al.*, 1994). Although parental Ba/F3 cells have been shown to undergo apoptosis upon IL-3 deprivation in numerous studies (e.g. Ahmed *et al.*, 1998, Ariyoshi *et al.*, 2000, Funakoshi-Tago *et al.*, 2010, Gesbert and Griffin, 2000) and the observed pattern (lower size cellular bodies with sub-G_1 DNA content | Figures 24 and 25) agreed with apoptotic cell death (Kerr *et al.*, 1972, Prokhorova *et al.*, 2015, Taylor *et al.*, 2008), the applied methods can neither distinguish between different forms of cell death. Terminal deoxynucleotidyl transferase dUTP nick end labeling (TUNEL) assay (Gorczyca *et al.*, 1992) could (i) confirm apoptotic cell death of IL-3-deprived Ba/F3-tet-on-1*6 cells and (ii) uncover whether S or G_2/M phase cells disproportionately undergo apoptosis. *Bona fide* cell proliferation could be investigated using a dye dilute assay (Lyons and Parish, 1994).

4.2.3 Ba/F3-tet-on-1*6 cells exhibited leaky expression of STAT5A-1*6 upon doxycycline removal

Of note, positive pSTAT5 and STAT5A-1*6 transgene mRNA signals persisted after dox removal (Figures 24 and 26), suggesting the continued presence of active STAT5A-1*6 molecules – albeit only at a very low level – and thus of associated pSTAT5 signals. On the other hand, pSTAT5 signals might also be explained by autocrine IL-3-induced endogenous STAT5A/B activity, considering that some Ba/F3 cells acquired independence of IL-3 supplementation by producing IL-3 themselves in the aforementioned mutagenesis study (Guo *et al.*, 2016). The persistence of STAT5A-1*6 mRNA and protein (provided *bona fide* positive signals) could be due to (i) a long mRNA and protein half-life or (ii) continued transcription of the STAT5A-1*6 transgene mRNA. Given the short half-life of dox (Agwuh and MacGowan, 2006), possibility (ii) cannot be explained by the continued presence of dox intracellularly or by insufficient cell washing. This proposes transcriptional activity at the integrated STAT5A-1*6 transgene loci despite the absence of dox-dependent rtTA Advanced-mediated transactivation (i.e. leaky expression), putatively due to DNA or chromatin alterations at these loci preventing the re-establishment of heterochromatic silencing.

The slight increase in above-background in STAT5A-1*6 transgene mRNA signals upon dox removal (from day 42/49 compared with from day 7 | Figure 26) raises the possibility that the presence of more STAT5A-1*6 molecules contributed to the survival of Ba/F3-tet-on-1*6 cells at these time-points. This is supported by the fact that a stable Ba/F3 cell

line with BCR-ABL expression slightly above background level exhibited higher spontaneous oncogenicity than its parental BCR-ABL-free Ba/F3 cell line (Klucher *et al.*, 1998). Though, in line with the effects of dox removal in the present study, incomplete knock-down of constitutively activated endogenous STAT5A (and/or STAT5B) negatively impacted survival and growth of an IL-3-independent Ba/F3 cell line expressing BCR-ABL (Schaller-Schönitz *et al.*, 2014). To exclude the aforementioned possibility in the future, complete STAT5A/B inhibition e.g. by treatment with CAS 285986-31-4 (Muller *et al.*, 2008) could be applied in lieu of dox removal experiments.

4.2.4 Ba/F3-tet-on-1*6 cells acquired the 'genomic instability' cancer hallmark

Given that mutability *per se* constitutes a selective growth advantage for individual cancer cells, Hanahan and Weinberg (2011) proposed 'genomic instability' as an enabling cancer hallmark (Figure 1). Thus, the proposed clonal evolution in all four long-term dox induction experiments (4.2.1) suggests a positive selection pressure on 'genomic instability'. This is supported by the fact that parental Ba/F3 cells have been shown to not survive IL-3 deprivation spontaneously and only in 20 % of cases in the aforementioned mutagenesis study (Guo *et al.*, 2016), suggesting low mutability of parental Ba/F3 and, accordingly, non-induced Ba/F3-tet-on-1*6 cells. Thus, the detection of a tetraploid DNA content during Induction-3 (Figure 23) was an expected finding. It suggests a tetraploidization event in at least one cell conferring a selective growth advantage, which is indicative of misregulated cell division and cell cycle check-point evasion, and, thus, 'genomic instability'.

The applied cell cycle analysis method *a priori* can only detect large deviations in overall DNA content, but not other DNA alterations indicative of 'genomic instability'. Specifically, increased DNA sequence mutations and balanced chromosomal aberrations due to double-strand breaks (e.g. translocations) are indicative of disrupted DNA repair mechanisms, likewise causing 'genomic instability'. Thus, the present study could not determine the presence or absence of such DNA alterations indicative of 'genomic instability' in the other three long-term dox induction experiments. Though, the acquisition of 'genomic instability' conferring increased mutability *per se* might underlie the STAT5A-1*6-independent survival and growth (upon dox removal | Table 9) of Ba/F3-tet-on-1*6 cells after 4–5 weeks of induction (Induction-2 and -3), rather than or in addition to other accumulated 'driver' alterations. In this case, STAT5A-1*6-independent survival and growth of Ba/F3-tet-on-1*6 cells mirror acquisition of the 'evading growth suppressors' cancer hallmark. Next-generation sequencing of Ba/F3-tet-on-1*6 cells, preferably at the single-cell level, during long-term dox induction experiments could

elucidate the emergence and spread of DNA alterations indicative of 'genomic instability' during long-term dox induction (reviewed by Wang and Navin, 2015).

Although it is conceivable that the (putative) acquisition of the 'genomic instability' cancer hallmark is solely a result of 'driver' alterations functioning independently of STAT5A-1*6 activity, several molecular mechanisms have been described by which STAT5A-1*6 activity *per se* could contribute to 'genomic instability', as detailed below (4.6).

4.3 STAT5A-1*6 overexpression might have adverse effects on oncogenesis

The reproducible negative correlation of STAT5A-1*6 protein levels (Figure 18) with increasing cell viability and proliferation rates (Figures 20–22 | 4.2.2) in three of the four long-term dox induction experiments at later time points and the selective growth advantage observed for a 'lower-GFP' (i.e. STAT5A-1*6) subpopulation during Induction-1 (Figure 18) raise the possibility of dose-dependent adverse effects of STAT5A-1*6 on cell survival and growth over time. This proposes a negative selective pressure on STAT5A-1*6 three-fold overexpression (relative to endogenous STAT5A/B | Figure 18). Of note, seven-fold overexpression of wild-type STAT5A has been found to have neither positive nor negative effects on parental Ba/F3 cell survival and growth (Royer *et al.*, 2004). Surprisingly, increased doses of constitutively activated wild-type STAT5A (upon ectopic *Stat5a* overexpression to levels even higher than in the present study) have likewise been found to have no such effects in a Ba/F3 cell line expressing BCR-ABL (Schaller-Schönitz *et al.*, 2014). This is in disagreement with the description of both negative and positive dose-dependent effects of constitutively active wild-type STAT5A on cell survival and growth in models of hematologic cancers (Chen *et al.*, 2013, Hoelbl *et al.*, 2006, Tsuruyama *et al.*, 2002, Wang *et al.*, 2015, Warsch *et al.*, 2011) and of STAT5A-1*6 and wild-type STAT5A in normal hematopoietic cells (Wierenga *et al.*, 2008).

This proposes that (i) the (putative) effects adverse to cell survival and growth are specific to STAT5A-1*6 in Ba/F3-tet-on-1*6 cells, either due to unique molecular properties not shared by constitutively activated wild-type STAT5A or due to differences between the employed Ba/F3 cell lines, or that (ii) the detected dose differences were caused by 'passenger' alterations and have no effect on cell survival and growth. Given the reproducibility of the STAT5A-1*6 decrease, possibility (ii) proposes that certain 'driver' alterations selected by clonal evolution entailed such 'passenger' alterations. STAT5A-1*6 transgene overexpression, for instance by increasing the dox concentration during long-term dox induction, might help elucidating whether STAT5A-1*6 has dose-dependent effects on cell survival and growth. Flow cytometric cell sorting could allow investigation of potential differences in cell survival and growth phenotype between

'lower-GFP' and 'higher-GFP' subpopulations. Investigation of the integration loci of the STAT5A-1*6 transgene on the DNA and chromatin level could also reveal the acquisition of 'passenger' or 'driver' alterations.

4.3.1 Aberrant STAT5A-1*6 forms might reflect a loss of constitutive activity function

Interestingly, co-production of at least one aberrant STAT5A-1*6 protein form with enhanced migration speed was identified by FLAG signals throughout Induction-3 (Figure 18). The detectability of the aberrant STAT5A-1*6 form(s) by the anti-total STAT5A/B and anti-pSTAT5A/B antibodies remains to be determined and could be investigated by Western blot analysis following co-immunoprecipitation of normal and aberrant STAT5A-1*6 using the anti-FLAG antibody. The second positive pSTAT5 signal below the normal signal at day 49 of Induction-3 (Figure 18) suggests (a) undetectability by the anti-pSTAT5A/B antibody for the first seven weeks of induction in case of one aberrant STAT5A-1*6 form or (b) the acquisition of another new aberrant STAT5A-1*6 form at day 49. Importantly, this raises the possibility that the aberrant STAT5A-1*6 form(s) was not phosphorylated at the key Tyr^{694} residue (until day 49), in turn offering an explanation for the enhanced migration speed. The enhanced migration speed could also be explained by (i) a lower molecular weight due to a deletion of some amino acids and/or the exchange of amino acids with higher molecular weight into ones with lower molecular weight and/or by (ii) the gain or loss of one or more charged posttranslational modifications impacting migration speed (e.g. Ser^{725}, Ser^{779} and Tyr^{682} phosphorylation | Cooper *et al.*, 2006, Friedbichler *et al.*, 2010, Haq *et al.*, 2002, Schaller-Schönitz *et al.*, 2014). Taken together, it is thinkable that the co-production of at least one loss-of-function aberrant STAT5A-1*6 form masked the decreasing protein levels of normal STAT5A-1*6 in Western blot analysis, opposing differences between Induction-3 and the other three induction experiments and supporting the aforementioned negative selection pressure hypothesis.

4.4 STAT5A-1*6 might mediate 'driver' chromatin alterations in some of its target genes

4.4.1 Continuous dose-dependent STAT5A-1*6-mediated *Cis* transactivation opposes tumor suppressive effects of CIS

The reproducibly tight correlation of STAT5A-1*6 transgene and *Cis* mRNA levels (in the absence and presence of dox | Figures 25 and 26) suggested dose-dependent STAT5A-*6-mediated transactivation during long-term dox induction experiments. Given similar mRNA levels in control cells grown with IL-3 (Figure 25), this opposes any negative or positive selection pressures on *Cis* expression level upon IL-3 deprivation. In line with this, *Cis* forced (over)expression has been found to maximally slightly impact

IL-3-dependent parental Ba/F3 cell survival and growth (Cohney *et al.*, 1999, Nosaka *et al.*, 1999, Yoshimura *et al.*, 1995) despite CIS inhibiting STAT5A/B activation (Matsumoto *et al.*, 1997, Yoshimura *et al.*, 1995). In addition, *Cis* was not a target in the aforementioned mutagenesis study (Guo *et al.*, 2016). Thus, CIS might not have any tumor suppressive effects on IL-3-independent Ba/F3-tet-on-1*6 cell survival and growth. It is tempting to speculate that CIS does not inhibit IL-3-independent STAT5A-1*6 activation, or that its tumor suppressive effects require a higher dose. Such dose-dependent tumor suppressive effects of STAT5 target genes might offer an explanation for the proposed negative selective pressure on STAT5A-1*6 overexpression (see 4.3). Ectopic forced *Cis* overexpression (e.g. using transient transfection) could elucidate its effects on IL-3-independent Ba/F3-tet-on-1*6 cell survival and growth as well as STAT5A-1*6 activation by phosphorylation.

4.4.2 STAT5A-1*6-associated nucleosome loss at *Cis* and *Osm* does not correlate with STAT5 occupancy level

Although histone H3 loss was detected in STAT5A-1*6-expressing cells at the *Cis* and *Osm* STAT5 binding sites and adjacent TSS (Figure 37), and although STAT5 was bound to these sites, STAT5 occupancy level over time, as detected by ChIP, followed a random pattern (Figure 27). This is to be opposed to *Spi2.1*, which exhibited a perfect correlation between the kinetics of STAT5 DNA binding, histone H3 loss and mRNA levels (Figures 25, 27 and 37). It is possible that the occlusion of the STAT5 ChIP antibody epitope by other chromatin components might explain an impaired detection of STAT5 binding at the *Cis* and *Osm* STAT5 binding sites. Alternatively, the recent identification of other candidate *Cis* and *Osm*-regulating STAT5 binding sites (Nanou *et al.*, 2017, GEO accession number GSE79520) raises the possibility that STAT5A-1*6 mediated the detected nucleosome loss in a dose-dependent manner through these sites or even new STAT5 binding sites, given the possibility of broadened DNA binding patterns (compare 4.5). Overall, it remains to be verified whether STAT5A-1*6 DNA binding is a cause of or a consequence of the concurrent chromatin remodeling at the *Cis* and *Osm* STAT5 binding site and TSS (e.g. by GAS motif disruption and other experiments proposed in 4.1.3).

4.4.3 *Spi2.1* might function as an oncogene in response to STAT5A-1*6

In accordance with *Cis*, the reproducibly tight correlation of STAT5A-1*6 transgene and *Spi2.1* mRNA levels (exempting the first week of induction | Figures 25 and 26) suggested dose-dependent STAT5A-1*6-mediated *Spi2.1* transactivation. Contrary to *Cis* however, *Spi2.1* mRNA levels were reproducibly tremendously upregulated during the first two weeks of induction compared with control cells (grown in the presence of IL-3 | Figure 25). This strong upregulation correlated perfectly with a strong STAT5A-1*6

binding to *Spi2.1* STAT5 binding sites (Figure 27) and with a strong histone H3 loss (Figure 37), indicating a direct dose-dependent effect of STAT5A-1*6. STAT5A-1*6-mediated chromatin remodeling in *Spi2.1* remains to confirmed following GAS motif disruption and other experiments proposed in 4.1.3. Additionally, it remains to be determined, why sustained STAT5A-1*6 DNA binding correlated with *Spi2.1*, but not *Cis* and *Osm* overexpression (Figures 25 and 27). The pre-existent chromatin context at the *Spi2.1* locus might render *Spi2.1* more responsive to STAT5A-1*6. This is in line with the observation that IL-3-induced *Spi2.1* transactivation in Ba/F3 cells is more susceptible to *Stat5a* than to *Stat5b* knock-down, in contrast to *Cis* and *Osm* (Basham *et al.*, 2008). Of note, the absence of additional candidate *Spi2.1*-regulating STAT5 binding sites in parental Ba/F3 cells further disagrees with *Cis* and *Osm* (Nanou *et al.*, 2017, GEO accession number GSE79520), although STAT5A-1*6 might have occupied other *Spi2.1*-regulating sites (given the possibility of broadened DNA binding patterns, compare 4.5).

Spi2.1 has been shown to promote cell survival of hematopoietic cells (Byrne *et al.*, 2012, Dev *et al.*, 2013, Li *et al.*, 2014, Liu *et al.*, 2004a, Liu *et al.*, 2003, Liu *et al.*, 2004b, Shamji *et al.*, 2018), amongst other things by protection from oxidative stress (Dev *et al.*, 2013, Li *et al.*, 2014, Liu *et al.*, 2004b). In addition, *Spi.2.1* has been shown to be upregulated in response to forced oxidative stress in leukemia cells (Liu *et al.*, 2016), suggesting that *Spi2.1* promoted leukemia cell survival there and functioned as an oncogene. Given that Ba/F3 cells expressing STAT5A-1*6 have been shown to exhibit increased oxidative stress (Bourgeais *et al.*, 2017), it is therefore possible that overexpression of *Spi2.1* by STAT5A-1*6 in Ba/F3-tet-on-1*6 cells plays a role in protection from oxidative stress, contributing to the cell survival effect mediated by STAT5A-1*6. The role of *Spi2.1* in IL-3-independent Ba/F3-tet-on-1*6 cell survival and growth could be elucidated using *Spi2.1* knock-down and forced overexpression experiments. Taken together, the possibility of *Spi2.1* functioning as an oncogene in Ba/F3-tet-on-1*6 cells proposes that the (putatively) STAT5A-1*6-mediated nucleosome loss in *Spi2.1* might underlie *Spi2.1* overexpression and, thus, constitutes a ‘driver’ chromatin alteration.

4.4.4 The oncogenes *c-Myc* and *Pim-1*, but not *Bcl-x*, might be targeted by ‘driver’ alterations

Forced overexpression of *Pim-1* (or of a dominant positive c-MYC form | Funakoshi-Tago *et al.*, 2013) alone or of at least two genes among *Pim-1*, *c-Myc* and *Bcl-x*, have been shown to enable IL-3-independent survival and growth of Ba/F3 cells, with a growth phenotype similar to that of STAT5A-1*6 expression (Nosaka *et al.*, 1999, Nosaka and Kitamura, 2002). This suggests that *Pim-1*, *c-Myc* and *Bcl-x* are among the main effectors of IL-3-independent survival and growth of Ba/F3 cells. This is in agreement

with the reproducible correlation of *Pim-1* and *c-Myc* mRNA levels (Figures 25 and 26) with IL-3-independent cell survival and growth both in the presence and absence of dox (i.e. STAT5A-1*6 | Figures 20–22) during long-term dox induction. This suggests that *Pim-1* and *c-Myc* might function as oncogenes in the Ba/F3-tet-on-1*6 experimental system, in accordance with various other models of hematologic cancers (Cuypers *et al.*, 1984, Gabay *et al.*, 2014, Hayward *et al.*, 1981, Narlik-Grassow *et al.*, 2014). Interestingly, their correlation with STAT5A-1*6 mRNA levels was reproducibly restricted to the first few weeks of induction in contrast to *Cis* and *Spi2.1* (Figures 25 and 26), suggesting STAT5A-1*6-dependent *Pim-1* and *c-Myc* transactivation in the first few weeks of induction and (at least partially) STAT5A-1*6-independent transactivation afterwards. This proposes that the hypothesized deterministic effects of STAT5A-1*6, enabling Ba/F3-tet-on-1*6 survival directly after IL-3 deprivation, involved *Pim-1* and *c-Myc* transactivation. Of note, the present study cannot exclude the possibility that low levels of STAT5A-1*6 persisting after dox removal contributed to *Pim-1* and *c-Myc* transactivation. This is supported by the low sensitivity of IL-3-induced STAT5A/B-mediated *Pim-1* and *c-Myc* transactivation to ~50 % *Stat5a/b* knock-down in parental Ba/F3 cells (~35 % and ~0 % inhibition, respectively | Basham *et al.*, 2008). The experiments proposed in 4.2.3 could elucidate this issue. The contribution of *c-Myc* and *Pim-1* to IL-3-independent survival and growth during long-term dox induction could be investigated by knock-down experiments.

STAT5A-1*6-independent transactivation of *Pim-1* and *c-Myc* suggests the reproducible stochastic acquisition of ‘driver’ alterations effecting *Pim-1* and *c-Myc* transactivation (Figure 37). The recent identification of (candidate) *Pim-1*- and *c-Myc*-regulating STAT5 binding sites in parental Ba/F3 cells amongst others in the *c-Myc* super-enhancer (Katerndahl *et al.*, 2017; Kieffer-Kwon *et al.*, 2013; Matikainen *et al.*, 1999; Nanou *et al.*, 2017, GEO accession number GSE79520; Pinz *et al.*, 2016) will allow the investigation of such STAT5A-1*6-associated chromatin remodeling and other chromatin alterations in the future. Of note, HDAC3 and LSD1 co-occupied the STAT5 binding sites in the *c-Myc* super-enhancer in Ba/F3 cells, with a decrease in occupancy upon IL-3 stimulation (Nanou *et al.*, 2017, GEO accession number GSE79520). This suggests a co-repressive function for HDAC3 and LSD1 in *c-Myc* transactivation, proposing their displacement in response STAT5 DNA binding. As detailed in the introduction section (1.3.4.5), STAT5A/B-1*6 might mediate histone acetylation and specifically recruit Brd2 to the *c-Myc* super-enhancer, proposing a STAT5A/B-1*6-specific *c-Myc* transactivation mechanism due to ‘driver’ alterations. Overall, this might involve recruitment of additional BET family members due to increased histone acetylation in response to sustained HDAC3 displacement.

Despite its identification as effector of IL-3-independent Ba/F3 cell survival and growth, *Bcl-x* was reproducibly not or maximally slightly upregulated in the presence and absence of STAT5A-1*6 throughout long-term dox induction compared with rested control cells (lacking STAT5A/B activity | Figures 25 and 26). This suggests that *Bcl-x* did not participate in IL-3-independent Ba/F3 cell survival and growth, opposing any function as oncogene. This agrees with a B-ALL mouse model, where *Bcl-x* has been found to be dispensable for oncogenesis (Harb *et al.*, 2008). Notably, *Bcl-x* was upregulated in non-induced control cells in the presence of IL-3-induced endogenous STAT5A/B activity (compared with rested control cells | Figure 25). This pattern is in agreement with the fact that *Bcl-x* transactivation is sensitive to paralog-specific *Stat5b*, but not *Stat5a* knock-down in parental Ba/F3 cells (upon IL-3 stimulation | Basham *et al.*, 2008) and in a Ba/F3 cell line expressing BCR-ABL (Schaller-Schönitz *et al.*, 2014), suggesting paralog-specific STAT5B-mediated *Bcl-x* transactivation in Ba/F3 cells. Therefore, the slight *Bcl-x* upregulation in dox-induced cells (Figures 25 and 26) might be explained by STAT5A-1*6-mediated PI3K pathway cross-activation, as detailed above (4.1.2.3).

4.5 STAT5A-1*6-mediated chromatin remodeling might misregulate nucleosome positioning globally

I proposed that wild-type STAT5A/B might mediate nucleosome loss at and in proximity of its binding sites in Ba/F3 cells (4.1.3.1). The correlation of histone H3 decrease (Figure 37) and STAT5A-1*6 DNA binding in *Cis*, *Osm* and *Spi2.1* (Figure 27) during long-term dox-induction likewise raises the possibility of STAT5A-1*6-mediated nucleosome loss as a conserved mechanism among all STAT5 target genes. Surprisingly, histone H3 decrease was not restricted to STAT5 binding sites (*Cis*, *Osm* and *Spi2.1*) and sites nearby (*Cis* and *Osm* TSS), but was also detected at controls sites (*c-Fos* proximal promoter and *Id-1* distal promoter | Figure 37), lacking STAT5 DNA binding in parental Ba/F3 cells (Basham *et al.*, 2008; Nanou *et al.*, 2017, GEO accession number GSE79520; Rascle and Lees, 2003), to varying degrees. Although the present study cannot exclude a chromatin remodeling mechanism independent of STAT5A-1*6 at the control sites given a similar histone H3 decrease in non-induced controls (Figure 37), STAT5A-1*6 activity might have contributed to it. On the one hand, sustained STAT5A-1*6 DNA binding might have long-range effects on these two control sites. On the other hand, STAT5A-1*6 might have occupied new DNA sites in proximity given the dose-dependent broadening of STAT5 DNA binding patterns upon STAT5A overexpression (Zhu *et al.*, 2012) and the higher affinity of STAT5A-1*6 to low-affinity GAS motifs (Moucadel and Constantinescu, 2005). In support of this, chromatin recruitment of Ezh2 has been shown to be broadened in Ba/F3 cells expressing

JAK2^{V617F} (Chen *et al.*, 2017), raising the possibility that broadened DNA binding of constitutively activated STAT5A/B recruited Ezh2 to these sites. Besides, the putative leakiness at the loci of integrated STAT5A-1*6 transgenes upon dox removal (compare 4.2.3) might be explained by STAT5A-1*6-mediated chromatin remodeling preventing the re-establishment of heterochromatic silencing. In further support of this, STAT5B-1*6 has been shown to enable binding of the transcription factor p53 globally in contrast to wild-type STAT5A/B (Girardot *et al.*, 2015), proposing that STAT5A-1*6-specific chromatin remodeling exposed occluded p53 binding motifs. On the other hand, histone acetylation patterns differed at STAT5 binding sites and distal sites affected by histone H3 loss (Figures 30 and 32), favoring the implication of HAT-dependent mechanisms at distal sites, as opposed to HAT-independent mechanisms at STAT5 binding sites. This suggests the action of different mechanisms of chromatin remodeling along STAT5 target gene loci, whether regulated by STAT5A-1*6 or not.

In summary, broadened and sustained DNA binding patterns of STAT5A-1*6 and, accordingly, broadened and sustained STAT5A-1*6 chromatin remodeling patterns might have caused global misregulation of nucleosome positioning, in particular nucleosome loss, during long-term dox induction. This might contribute to STAT5A-1*6 oncogenicity, given the essential role of chromatin dynamics for pivotal cellular processes.

4.6 STAT5A-1*6 activity *per se* might effect acquisition of the 'genomic instability' cancer hallmark

Several previous findings suggest that STAT5A-1*6 activity *per se* participates in the acquisition of the 'genomic instability' cancer hallmark in Ba/F3-tet-on-1*6 cells during long-term dox induction (compare 4.2.4). The misregulated chromatin dynamics due to the hypothesized global STAT5A-1*6-mediated nucleosome loss complements existent and proposes additional molecular mechanisms:

Transcriptional misregulation:

The hypothesized STAT5A-1*6-mediated global nucleosome loss might effect transcriptional misregulation, in line with reports of forced nucleosome loss (Booth and Brunet, 2016, Celona *et al.*, 2011, Hu *et al.*, 2014, Zahn *et al.*, 2005). This might involve downregulation of genes adverse to DNA damage and, reversely, upregulation of genes conducive to it, promoting 'genomic instability'. In fact, *c-Myc* overexpression in Ba/F3 cells has been shown to cause chromosomal aberrations (Fest *et al.*, 2002) indicative of 'genomic instability'. Although average *c-Myc* mRNA levels were not increased during long-term dox induction in the presence of constitutive STAT5A-1*6 activity (compared to control cells with transient endogenous STAT5A/B activity | Figure 25), the temporal patterns of *c-Myc* expression might have differed at the single-cell level, with sustained

c-Myc transactivation (as opposed to cycles of transient *c-Myc* transactivation) promoting 'genomic instability'.

Oxidative stress:

As detailed in the introduction section (1.3.4.4), STAT5A-1*6 activity *per se* might mediate oxidative stress through transcriptional misregulation and by non-canonical mechanisms in mitochondria in Ba/F3 cells. This is supported by the tremendous upregulation of *Spi2.1* in dox-induced cells in the first two weeks of induction (compare 4.4.3). Given that linker / euchromatic DNA has been found to be more susceptible to mutagenic agents, putatively including reactive oxygen species, than nucleosomal / heterochromatic DNA (Falk *et al.*, 2008 Cowell *et al.*, 2007, Han *et al.*, 2016, Kim *et al.*, 2007, Lan *et al.*, 2014), the hypothesized STAT5A-1*6-mediated global nucleosome loss might increase DNA damage and promote 'genomic instability'.

Misregulated recruitment of chromatin modifiers:

Broadened and sustained STAT5A-1*6 DNA binding proposes misregulated STAT5A-1*6 recruitment of chromatin modifiers as argued above for Ezh2, which could contribute to 'genomic instability'. For instance, the STAT5A/B-interacting chromatin modifier Tet2 (Yang *et al.*, 2015 | Table 2) has been linked to 'genomic instability' in Ba/F3 cells (Mahfoudhi *et al.*, 2016), raising the possibility of misregulated Tet2 chromatin recruitment in dox-induced cells.

Misregulated chromatin dynamics interferes with DNA damage repair:

DNA damage repair has been found to require accessible DNA, i.e. decondensed euchromatin (Lemaitre and Soutoglou, 2014, Murga *et al.*, 2007, Nair *et al.*, 2017, Schuster-Bockler and Lehner, 2012). Although the hypothesized STAT5A-1*6-mediated global nucleosome loss would render the DNA more accessible, it might nonetheless interfere with DNA damage repair directly, as chromatin condensation mechanisms have been argued to be as essential as chromatin decondensation mechanisms for DNA damage repair (Burgess *et al.*, 2014). In addition, global nucleosome loss has been proposed to cause DNA damage and chromosomal aberrations (Celona *et al.*, 2011, Hu *et al.*, 2014, O'Sullivan *et al.*, 2010, Oberdoerffer, 2010). This raises the possibility that STAT5A-1*6-mediated global nucleosome loss impedes DNA damage repair and, thus, contributes to 'genomic instability'.

In summary, STAT5A-1*6 activity *per se* might have induced the acquisition of the 'genomic instability' cancer hallmark during long-term dox induction. Accordingly, 'genomic instability' has been reported for a Ba/F3 cell line in response to $JAK2^{V617F}$ (Plo *et al.*, 2008), raising the possibility of an effect mediated by constitutively activated endogenous STAT5A/B. Thus, the hypothesized STAT5A-1*6-mediated global

nucleosome loss might not only effect ‘driver’ chromatin alterations, but also promote ‘driver’ DNA alterations. In support of this hypothesis, Katerndahl *et al.*, 2017 recently argued that STAT5B-1*6 functioning as survival and growth signal was not underlying its oncogenicity, given that another survival and growth signal failed to induce oncogenesis in a B-ALL mouse model. Besides, this offers an additional explanation for the hypothesized negative selection pressure on STAT5A-1*6 overexpression (4.3), as too severe misregulation of the aforementioned dynamics might be adverse to cell survival and growth. Expanding the locus- and transcript-specific assays of the present study with the genome-wide and transcriptome analyses proposed in 4.1.3.1 might elucidate the extent of the hypothesized broadened STAT5A-1*6 DNA binding patterns, STAT5A-1*6-associated chromatin remodeling and transcriptional misregulation during long-term dox induction. The next generation sequencing experiments proposed in 4.2.4 might elucidate their relation to DNA damage indicative of ‘genomic instability’.

4.7 Model of STAT5A-1*6-induced oncogenesis in the Ba/F3-tet-on-1*6 experimental system

Based on the findings of the present study, I propose the following model of STAT5A-1*6-mediated oncogenesis during long-term dox induction of the Ba/F3-tet-on-1*6 cells:

Upon IL-3 deprivation, STAT5A-1*6 enables IL-3-independent survival deterministically by transactivating effectors of cell survival, in particular *c-Myc* and *Pim-1*. Broadened and sustained STAT5A-1*6 DNA binding and, accordingly, global STAT5A-1*6-mediated chromatin remodeling (i.e. nucleosome loss) likely causes transcriptional misregulation, constituting ‘driver’ and ‘passenger’ chromatin alterations. This might include the strong STAT5A-1*6-mediated *Spi2.1* overexpression. In addition, STAT5A-1*6 might mediate transcriptional misregulation by cross-activating the PI3K and MAPK pathways (via GAB2) and augment oxidative stress (putatively by non-canonical activities in mitochondria in addition to transcriptional misregulation). Oxidative stress negatively impacts cell viability and might be antagonized by *Spi2.1* overexpression. It might also induce DNA damage, in particular at linker DNA exposed by global STAT5A-1*6-mediated chromatin remodeling. The selective pressures favoring increased (i) cell viability, (ii) cell proliferation and (iii) mutability *per se* might lead to the stochastic acquisition of corresponding ‘driver’ DNA alterations in single cells. These single cells might outgrow and supplant other cells (i.e. clonal evolution) leading to gradual changes in cell survival and growth phenotype. At this stage (1–2 weeks of induction), ‘driver’ alterations conferring IL-3-independent cell survival and growth depend on STAT5A-1*6 activity and, accordingly, cells did not survive dox removal.

STAT5A-1*6 three-fold overexpression (over endogenous STAT5A/B) was under negative selection pressure, putatively because of STAT5A-1*6-mediated oxidative

stress and/or the dose-dependent transactivation of STAT5A-1*6 inhibitors such as *Cis*. This might have led to a decrease in active STAT5A-1*6 protein levels due to 'driver' alterations and, in turn, subjected effectors of cell survival and growth to a positive selection pressure, in particular *c-Myc* and *Pim-1*, given mostly STAT5A-1*6-mediated transactivation. This and the aforementioned three selection pressures might have led to the accumulation of further 'driver' alterations effecting STAT5A-1*6-independent *c-Myc* and *Pim-1* transactivation and increased (i) cell viability, (ii) cell proliferation and (iii) mutability *per se*. At this stage (4–5 weeks of induction), cells managed to survive dox removal because of accumulated 'driver' alterations and/or their increased mutability and had acquired the 'resisting cell death', 'sustaining proliferative signaling', 'genomic instability' and 'evading growth suppressors' cancer hallmarks (Figure 1).

4.8 Outlook

The present study aimed to elucidate effects specific to constitutive STAT5A/B activity as opposed to transient STAT5A/B activity – in particular upon sustained DNA binding on chromatin – underlying its oncogenicity. For this, I established a cellular experimental model system: the stable Ba/F3-tet-on-1*6 cell line. This experimental system was shown to mirror *in vivo* oncogenesis induced by constitutive STAT5A/B activity in the acquisition of cancer hallmarks and in the misregulation of oncogenes. It could be employed as pre-clinical model for both early and late stages of STAT5A/B-associated hematologic cancers in future research. Analogous Ba/F3 cell-based experimental systems inducibly expressing STAT5B-1*6 or other gain-of-function STAT5A/B forms could allow the investigation of paralog-specific and mutation-specific differences in oncogenicity.

Using the Ba/F3-tet-on-1*6 cell line and other Ba/F3 cell lines, STAT5 DNA binding was correlated with nucleosome loss. Several lines of evidence strongly suggest a causal link between STAT5 DNA binding and nucleosome loss and raise the possibility of global STAT5A/B-mediated chromatin remodeling. The correlative evidence of the present study remains be to consolidated by further experiments at a genome-wide level, considering that STAT5A/B DNA binding and transcriptional activity can be both a cause and a consequence of chromatin alterations. Nonetheless, this possibility offers an explanation for STAT5A/B functioning as an anchor for other transcription factors and its instructive biological role in cell differentiation, namely enabling DNA access to other transcription factors similarly to pioneer factors. Strikingly, nucleosome loss was correlated with sustained DNA binding of a constitutively active STAT5A form, proposing a new molecular mechanism for 'driver' and 'passenger' chromatin alterations mediated by oncogenic constitutive STAT5A/B activity. The possibility of broadened and sustained DNA binding patterns of constitutively active STAT5A and, accordingly, globally

misregulated STAT5A-mediated chromatin remodeling likewise remains to be confirmed by genome-wide analyses. It proposes novel molecular mechanisms underlying the oncogenicity of constitutively active STAT5A/B. Specifically, STAT5A/B-mediated global ‘driver’ and ‘passenger’ chromatin alterations might promote ‘driver’ and ‘passenger’ DNA alterations.

Ultimately, elucidating such molecular mechanisms might provide novel molecular targets for cancer therapy and allow the identification of early-stage molecular markers for the early detection and management of cancer.

Publications

Part of the data described and discussed in the present study have been published. In addition, I contributed to a number of studies conducted in PD Dr. Anne Rascle's research group:

Pinz S.*, **Unser S.***, Rascle A. (2016): Signal transducer and activator of transcription STAT5 is recruited to c-Myc super-enhancer. *BMC Mol Biol*,17:10

Pinz S., **Unser S.**, Buob D., Fischer P., Jobst B., Rascle A. (2015): Deacetylase inhibitors repress STAT5-mediated transcription by interfering with bromodomain and extra-terminal (BET) protein function. *Nucleic Acids Res*, *43(7)*:3524-45

Pinz S.*, **Unser S.***, Rascle A. (2014): The natural chemopreventive agent sulforaphane inhibits STAT5 activity. *PLoS One*, 9;9(6):e99391

Pinz S.*, **Unser S.***, Brueggemann S. Besl E., Al-Rifai N., Petkes H., Amslinger S., Rascle A. (2014): The synthetic α-bromo- 2',3,4,4'-tetramethoxychalcone (α-Br-TMC) inhibits the JAK/STAT signaling pathway. *PLoS One*, 9(3):e90275

***shared first authorship**

List of figures

List of tables

Abbreviations

SI units and SI prefixes were abbreviated in the standardized manner. Amino acids and nucleotides were abbreviated by their standardized three- and/or one-letter codes.

Å	Ångström (= 100 pm)
ATP	adenosine triphosphate
B-ALL	B cell acute lymphoblastic leukemia
β_c	common β chain (of interleukin 3 receptor family)
BET	bromodomain and extra-terminal domain protein
bp	base pairs (of DNA/RNA) [used with SI prefixes]
Brd2	bromodomain and extra-terminal domain (BET) protein Brd2
BRG1	brahma-related gene-1 protein
BSA	bovine serum albumin
CA#	catalogue number
C/EBPβ	CCAAT/enhancer-binding protein β
ChIP	chromatin immunoprecipitation
ChIP-seq	ChIP followed by high-throughput sequencing
CIS	cytokine-inducible SH2(Src Homology 2)-containing protein
c-MYC	cellular avian myelocytomatosis viral oncogene protein
C-terminus	COOH-terminus / carboxyl-terminus
C_t-value	threshold cycle value
DAPI	4′,6-diamidino-2-phenylindole dihydrochloride
DMSO	dimethyl sulfoxide
DNA	deoxyribonucleic acid
cDNA	complementary DNA
dsDNA	double-stranded DNA
gDNA	genomic DNA
dox	doxycycline
DPF3	double plant homeodomain(PHD) fingers 3 protein
dUTP	deoxyuridine triphosphate
E. coli	*Escherichia coli*
e.g.	*exempli gratia* (for example)
EMSA	electronic mobility shift assay
et al.	*et alii* (and others)
Ezh2	enhancer of zeste homolog 2 protein
Fc	crystallisable fragment
FCS	fetal calf serum
FSC	forward scatter
G_1 phase	gab 1 phase
G_2 phase	gab 2 phase
GAB2	GRB2(growth factor receptor-bound protein 2)-associated binding protein 2
GAS	interferon γ-activated sequence
GFP	green fluorescent protein
GR	glucocorticoid receptor
HAT	histone acetyltransferase
HDAC	histone deacetylase
HMGN	high-mobility group nucleosome-binding chromosomal protein
HRP	horseradish peroxidase
i.e.	*id est* (this means)
IgG	immunoglobulin G
IL-3	interleukin 3

IL-3R	IL-3 receptor
JAK	Janus kinase
λ	wavelength
LSD1	lysine-specific demethylase 1
M phase	mitosis phase
MAPK	mitogene-activated protein kinase
NCoR2	nuclear receptor co-repressor 2
NFR	nucleosome-free region
N-terminus	NH_2-terminus / amino-terminus
ORF	open reading frame
p.	page
PAGE	polyacrylamide gel electrophoresis
PBS	phosphate-buffered saline
PBST	PBS with Tween20
PCR	polymerase chain reaction
qPCR	quantitative PCR
RT-qPCR	reverse transcription quantitative PCR
PI3K	phosphatidylinositol-4,5-bisphosphate 3-kinase
PIAS	protein inhibitor of activated STAT
PIC	pre-initiation complex
PIPES	piperazine-N,N′-bis(2-ethanesulfonic acid)
PMSF	phenylmethylsulfonyl fluoride
PTP	protein tyrosine phosphatase
PVDF	polyvinylidene difluoride
RNA	ribonucleic acid
pre-mRNA	precursor messenger RNA
mRNA	messenger RNA
RNA-Seq	RNA high-throughput sequencing
rtTA Advanced	reverse tetracycline-controlled transactivator protein Advanced
S phase	DNA synthesis and replication phase
SDS	sodium dodecyl sulfate
SSC	sideward scatter
SH2	Src Homology 2
SHP-1	Src Homology 2(SH2) domain-containing phosphatase 1
SMRT	silencing mediator for retinoic acid receptor and thyroid hormone receptor
SOCS	suppressor of cytokine signaling
STAT	signal transducer and activator of transcription
SUMO	small ubiquitin-like modifier
SWI/SNF	switching defective/sucrose non-fermenting
wt	wild-type
TAD	transactivation domain
Taq	*Thermus aquaticus*
TBST	Tris-buffered saline with Tween20
TE	Tris-EDTA(ethylenediaminetetraacetic acid)
Tet2	ten-eleven translocation 1 protein 2
Tet-on Advanced	Tetracycline-on Advanced
TRE	tetracycline responsive element
TSA	trichostatin A
TSS	transcription start site
TTS	transcription termination site
U	unit
UV	ultraviolet

References

http://www.ensembl.org/Homo_sapiens/Info/Annotation, 27.01.2018

http://www.ensembl.org/Mus_musculus/Info/Annotation, 27.01.2018

Acevedo, A.,Gonzalez-Billault, C. (2018): Crosstalk between Rac1-mediated actin regulation and ROS production. *Free Radic Biol Med*, **116:** 101-113

Adamaki, M., Tsotra, M., Vlahopoulos, S., Zampogiannis, A., Papavassiliou, A. G.,Moschovi, M. (2015): STAT transcript levels in childhood acute lymphoblastic leukemia: STAT1 and STAT3 transcript correlations. *Leuk Res*,

Adams, C. C.,Workman, J. L. (1995): Binding of disparate transcriptional activators to nucleosomal DNA is inherently cooperative. *Mol Cell Biol*, **15: 3**, 1405-1421

Agwuh, K. N.,MacGowan, A. (2006): Pharmacokinetics and pharmacodynamics of the tetracyclines including glycylcyclines. *J Antimicrob Chemother*, **58: 2**, 256-265

Ahmed, M., Dusanter-Fourt, I., Bernard, M., Mayeux, P., Hawley, R. G., Bennardo, T., Novault, S., Bonnet, M. L., Gisselbrecht, S., Varet, B.,Turhan, A. G. (1998): BCR-ABL and constitutively active erythropoietin receptor (cEpoR) activate distinct mechanisms for growth factor-independence and inhibition of apoptosis in Ba/F3 cell line. *Oncogene*, **16: 4**, 489-496

Ariyoshi, K., Nosaka, T., Yamada, K., Onishi, M., Oka, Y., Miyajima, A.,Kitamura, T. (2000): Constitutive activation of STAT5 by a point mutation in the SH2 domain. *J Biol Chem*, **275: 32**, 24407-24413

Atak, Z. K., Gianfelici, V., Hulselmans, G., De Keersmaecker, K., Devasia, A. G., Geerdens, E., Mentens, N., Chiaretti, S., Durinck, K., Uyttebroeck, A., Vandenberghe, P., Wlodarska, I., Cloos, J., Foa, R., Speleman, F., Cools, J.,Aerts, S. (2013): Comprehensive analysis of transcriptome variation uncovers known and novel driver events in T-cell acute lymphoblastic leukemia. *PLoS Genet*, **9: 12**, e1003997

Azam, M., Erdjument-Bromage, H., Kreider, B. L., Xia, M., Quelle, F., Basu, R., Saris, C., Tempst, P., Ihle, J. N.,Schindler, C. (1995): Interleukin-3 signals through multiple isoforms of Stat5. *EMBO J*, **14: 7**, 1402-1411

Bai, L., Charvin, G., Siggia, E. D.,Cross, F. R. (2010): Nucleosome-depleted regions in cell-cycle-regulated promoters ensure reliable gene expression in every cell cycle. *Dev Cell*, **18: 4**, 544-555

Bai, L.,Morozov, A. V. (2010): Gene regulation by nucleosome positioning. *Trends Genet*, **26: 11**, 476-483

Balasubramanyam, K., Swaminathan, V., Ranganathan, A.,Kundu, T. K. (2003): Small molecule modulators of histone acetyltransferase p300. *J Biol Chem*, **278: 21**, 19134-19140

Bandapalli, O. R., Schuessele, S., Kunz, J. B., Rausch, T., Stutz, A. M., Tal, N., Geron, I., Gershman, N., Izraeli, S., Eilers, J., Vaezipour, N., Kirschner-Schwabe, R., Hof, J., von Stackelberg, A., Schrappe, M., Stanulla, M., Zimmermann, M., Koehler, R., Avigad, S., Handgretinger, R., Frismantas, V., Bourquin, J. P., Bornhauser, B., Korbel, J. O., Muckenthaler, M. U.,Kulozik, A. E. (2014): The activating STAT5B N642H mutation is a common abnormality in pediatric T-cell acute lymphoblastic leukemia and confers a higher risk of relapse. *Haematologica*, **99: 10**, e188-192

Bannister, A. J.,Kouzarides, T. (2011): Regulation of chromatin by histone modifications. *Cell Res*, **21: 3**, 381-395

Bantscheff, M., Hopf, C., Savitski, M. M., Dittmann, A., Grandi, P., Michon, A. M., Schlegl, J., Abraham, Y., Becher, I., Bergamini, G., Boesche, M., Delling, M., Dumpelfeld, B., Eberhard, D., Huthmacher, C., Mathieson, T., Poeckel, D., Reader, V., Strunk, K., Sweetman, G., Kruse, U., Neubauer, G., Ramsden, N. G.,Drewes, G. (2011): Chemoproteomics profiling of HDAC inhibitors reveals selective targeting of HDAC complexes. *Nat Biotechnol*, **29: 3**, 255-265

Barclay, J. L., Nelson, C. N., Ishikawa, M., Murray, L. A., Kerr, L. M., McPhee, T. R., Powell, E. E.,Waters, M. J. (2011): GH-dependent STAT5 signaling plays an important role in hepatic lipid metabolism. *Endocrinology*, **152: 1**, 181-192

Basham, B., Sathe, M., Grein, J., McClanahan, T., D'Andrea, A., Lees, E.,Rascle, A. (2008): In vivo identification of novel STAT5 target genes. *Nucleic Acids Res*, **36: 11**, 3802-3818

Baugh, J. E., Jr., Floyd, Z. E.,Stephens, J. M. (2007): The modulation of STAT5A/GR complexes during fat cell differentiation and in mature adipocytes. *Obesity (Silver Spring)*, **15: 3**, 583-590

Beier, U. H., Wang, L., Han, R., Akimova, T., Liu, Y.,Hancock, W. W. (2012): Histone deacetylases 6 and 9 and sirtuin-1 control Foxp3+ regulatory T cell function through shared and isoform-specific mechanisms. *Sci Signal*, **5: 229**, ra45

Bergel, M., Herrera, J. E., Thatcher, B. J., Prymakowska-Bosak, M., Vassilev, A., Nakatani, Y., Martin, B.,Bustin, M. (2000): Acetylation of novel sites in the nucleosomal binding domain of chromosomal protein HMG-14 by p300 alters its interaction with nucleosomes. *J Biol Chem*, **275: 15**, 11514-11520

Berger, A., Hoelbl-Kovacic, A., Bourgeais, J., Hoefling, L., Warsch, W., Grundschober, E., Uras, I. Z., Menzl, I., Putz, E. M., Hoermann, G., Schuster, C., Fajmann, S., Leitner, E., Kubicek, S., Moriggl, R., Gouilleux, F.,Sexl, V. (2014): PAK-dependent STAT5 serine phosphorylation is required for BCR-ABL-induced leukemogenesis. *Leukemia*, **28: 3**, 629-641

Bergers, G., Javaherian, K., Lo, K. M., Folkman, J.,Hanahan, D. (1999): Effects of angiogenesis inhibitors on multistage carcinogenesis in mice. *Science*, **284: 5415**, 808-812

Bertolino, E., Reddy, K., Medina, K. L., Parganas, E., Ihle, J.,Singh, H. (2005): Regulation of interleukin 7-dependent immunoglobulin heavy-chain variable gene rearrangements by transcription factor STAT5. *Nat Immunol*, **6: 8**, 836-843

Beuvink, I., Hess, D., Flotow, H., Hofsteenge, J., Groner, B.,Hynes, N. E. (2000): Stat5a serine phosphorylation. Serine 779 is constitutively phosphorylated in the mammary gland, and serine 725 phosphorylation influences prolactin-stimulated in vitro DNA binding activity. *J Biol Chem*, **275: 14**, 10247-10255

Black, J. C., Van Rechem, C.,Whetstine, J. R. (2012): Histone lysine methylation dynamics: establishment, regulation, and biological impact. *Mol Cell*, **48: 4**, 491-507

Boehm, M. E., Adlung, L., Schilling, M., Roth, S., Klingmuller, U.,Lehmann, W. D. (2014): Identification of isoform-specific dynamics in phosphorylation-dependent STAT5 dimerization by quantitative mass spectrometry and mathematical modeling. *J Proteome Res*, **13: 12**, 5685-5694

Boer, A. K., Drayer, A. L., Rui, H.,Vellenga, E. (2002): Prostaglandin-E2 enhances EPO-mediated STAT5 transcriptional activity by serine phosphorylation of CREB. *Blood*, **100: 2**, 467-473

Boer, A. K., Drayer, A. L.,Vellenga, E. (2003): Stem cell factor enhances erythropoietin-mediated transactivation of signal transducer and activator of transcription 5 (STAT5) via the PKA/CREB pathway. *Exp Hematol*, **31: 6**, 512-520

Bone, H., Dechert, U., Jirik, F., Schrader, J. W.,Welham, M. J. (1997): SHP1 and SHP2 protein-tyrosine phosphatases associate with betac after interleukin-3-induced receptor tyrosine phosphorylation. Identification of potential binding sites and substrates. *J Biol Chem*, **272: 22**, 14470-14476

Booth, Lauren N.,Brunet, A. (2016): The Aging Epigenome. *Molecular Cell*, **62: 5**, 728-744

Bourgeais, J., Ishac, N., Medrzycki, M., Brachet-Botineau, M., Desbourdes, L., Gouilleux-Gruart, V., Pecnard, E., Rouleux-Bonnin, F., Gyan, E., Domenech, J., Mazurier, F., Moriggl, R., Bunting, K. D., Herault, O.,Gouilleux, F. (2017): Oncogenic STAT5 signaling promotes oxidative stress in chronic myeloid leukemia cells by repressing antioxidant defenses. *Oncotarget*, **8: 26**, 41876-41889

Bradford, M. M. (1976): A rapid and sensitive method for the quantitation of microgram quantities of protein utilizing the principle of protein-dye binding. *Anal Biochem*, **72:** 248-254

Brady, A., Gibson, S., Rybicki, L., Hsi, E., Saunthararajah, Y., Sekeres, M. A., Tiu, R., Copelan, E., Kalaycio, M., Sobecks, R., Bates, J.,Advani, A. S. (2012): Expression of phosphorylated signal transducer and activator of transcription 5 is associated with an increased risk of death in acute myeloid leukemia. *Eur J Haematol*, **89: 4**, 288-293

Brault, L., Menter, T., Obermann, E. C., Knapp, S., Thommen, S., Schwaller, J.,Tzankov, A. (2012): PIM kinases are progression markers and emerging therapeutic targets in diffuse large B-cell lymphoma. *Br J Cancer*, **107: 3**, 491-500

Broughton, S. E., Dhagat, U., Hercus, T. R., Nero, T. L., Grimbaldeston, M. A., Bonder, C. S., Lopez, A. F.,Parker, M. W. (2012): The GM-CSF/IL-3/IL-5 cytokine receptor family: from ligand recognition to initiation of signaling. *Immunol Rev*, **250: 1**, 277-302

Brownell, J. E., Zhou, J., Ranalli, T., Kobayashi, R., Edmondson, D. G., Roth, S. Y.,Allis, C. D. (1996): Tetrahymena histone acetyltransferase A: a homolog to yeast Gcn5p linking histone acetylation to gene activation. *Cell*, **84: 6**, 843-851

Buchdunger, E., Zimmermann, J., Mett, H., Meyer, T., Muller, M., Druker, B. J.,Lydon, N. B. (1996): Inhibition of the Abl protein-tyrosine kinase in vitro and in vivo by a 2-phenylaminopyrimidine derivative. *Cancer Res*, **56: 1**, 100-104

Bunda, S., Kommaraju, K., Heir, P.,Ohh, M. (2013): SOCS-1 mediates ubiquitylation and degradation of GM-CSF receptor. *PLoS One*, **8: 9**, e76370

Burgess, R. C., Burman, B., Kruhlak, M. J.,Misteli, T. (2014): Activation of DNA damage response signaling by condensed chromatin. *Cell Rep*, **9: 5**, 1703-1717

Buser, A. C., Obr, A. E., Kabotyanski, E. B., Grimm, S. L., Rosen, J. M.,Edwards, D. P. (2011): Progesterone receptor directly inhibits beta-casein gene transcription in mammary epithelial cells through promoting promoter and enhancer repressive chromatin modifications. *Mol Endocrinol*, **25: 6**, 955-968

Byrne, S. M., Aucher, A., Alyahya, S., Elder, M., Olson, S. T., Davis, D. M.,Ashton-Rickardt, P. G. (2012): Cathepsin B controls the persistence of memory CD8+ T lymphocytes. *J Immunol*, **189: 3**, 1133-1143

Callus, B. A.,Mathey-Prevot, B. (1998): Interleukin-3-induced activation of the JAK/STAT pathway is prolonged by proteasome inhibitors. *Blood*, **91: 9**, 3182-3192

Campbell, M. J.,Turner, B. M. (2013): Altered histone modifications in cancer. *Adv Exp Med Biol*, **754:** 81-107

Capello, D., Gloghini, A., Baldanzi, G., Martini, M., Deambrogi, C., Lucioni, M., Piranda, D., Fama, R., Graziani, A., Spina, M., Tirelli, U., Paulli, M., Larocca, L. M., Gaidano, G., Carbone, A.,Sinigaglia, F. (2013): Alterations of negative regulators of cytokine signalling in immunodeficiency-related non-Hodgkin lymphoma. *Hematol Oncol*, **31: 1**, 22-28

Carr, A.,Biggin, M. D. (1999): A comparison of in vivo and in vitro DNA-binding specificities suggests a new model for homeoprotein DNA binding in Drosophila embryos. *EMBO J*, **18: 6**, 1598-1608

Carter, D., Chakalova, L., Osborne, C. S., Dai, Y. F.,Fraser, P. (2002): Long-range chromatin regulatory interactions in vivo. *Nat Genet*, **32: 4**, 623-626

Casetti, L., Martin-Lanneree, S., Najjar, I., Plo, I., Auge, S., Roy, L., Chomel, J. C., Lauret, E., Turhan, A. G.,Dusanter-Fourt, I. (2013): Differential contributions of STAT5A and STAT5B to stress protection and tyrosine kinase inhibitor resistance of chronic myeloid leukemia stem/progenitor cells. *Cancer Res*, **73: 7**, 2052-2058

Catez, F., Brown, D. T., Misteli, T.,Bustin, M. (2002): Competition between histone H1 and HMGN proteins for chromatin binding sites. *EMBO Rep*, **3: 8**, 760-766

Celona, B., Weiner, A., Di Felice, F., Mancuso, F. M., Cesarini, E., Rossi, R. L., Gregory, L., Baban, D., Rossetti, G., Grianti, P., Pagani, M., Bonaldi, T., Ragoussis, J., Friedman, N., Camilloni, G., Bianchi, M. E.,Agresti, A. (2011): Substantial histone reduction modulates genomewide nucleosomal occupancy and global transcriptional output. *PLoS Biol*, **9: 6**, e1001086

Chen, B., Yi, B., Mao, R., Liu, H., Wang, J., Sharma, A., Peiper, S., Leonard, W. J.,She, J. X. (2013): Enhanced T cell lymphoma in NOD.Stat5b transgenic mice is caused by hyperactivation of Stat5b in CD8+ thymocytes. *PLoS One*, **8: 2**, e56600

Chen, C. C., Chiu, C. C., Lee, K. D., Hsu, C. C., Chen, H. C., Huang, T. H., Hsiao, S. H.,Leu, Y. W. (2017): JAK2V617F influences epigenomic changes in myeloproliferative neoplasms. *Biochem Biophys Res Commun*, **494: 3-4**, 470-476

Chen, W., Daines, M. O.,Khurana Hershey, G. K. (2004): Turning off signal transducer and activator of transcription (STAT): the negative regulation of STAT signaling. *J Allergy Clin Immunol*, **114: 3**, 476-489; quiz 490

Chia, D. J.,Rotwein, P. (2010): Defining the epigenetic actions of growth hormone: acute chromatin changes accompany GH-activated gene transcription. *Mol Endocrinol*, **24: 10**, 2038-2049

Chia, D. J., Varco-Merth, B.,Rotwein, P. (2010a): Dispersed Chromosomal Stat5b-binding elements mediate growth hormone-activated insulin-like growth factor-I gene transcription. *J Biol Chem*, **285: 23**, 17636-17647

Chia, D. J., Young, J. J., Mertens, A. R.,Rotwein, P. (2010b): Distinct alterations in chromatin organization of the two IGF-I promoters precede growth hormone-induced activation of IGF-I gene transcription. *Mol Endocrinol*, **24: 4**, 779-789

Chim, C. S., Fung, T. K., Cheung, W. C., Liang, R.,Kwong, Y. L. (2004a): SOCS1 and SHP1 hypermethylation in multiple myeloma: implications for epigenetic activation of the Jak/STAT pathway. *Blood*, **103: 12**, 4630-4635

Chim, C. S., Wong, K. Y., Loong, F.,Srivastava, G. (2004b): SOCS1 and SHP1 hypermethylation in mantle cell lymphoma and follicular lymphoma: implications for epigenetic activation of the Jak/STAT pathway. *Leukemia*, **18: 2**, 356-358

Chin, H., Wakao, H., Miyajima, A., Kamiyama, R., Miyasaka, N.,Miura, O. (1997): Erythropoietin induces tyrosine phosphorylation of the interleukin-3 receptor beta subunit (betaIL3) and recruitment of Stat5 to possible Stat5-docking sites in betaIL3. *Blood*, **89: 12**, 4327-4336

Choi, H. K.,Waxman, D. J. (1999): Growth hormone, but not prolactin, maintains, low-level activation of STAT5a and STAT5b in female rat liver. *Endocrinology*, **140: 11**, 5126-5135

Cholez, E., Debuysscher, V., Bourgeais, J., Boudot, C., Leprince, J., Tron, F., Brassart, B., Regnier, A., Bissac, E., Pecnard, E., Gouilleux, F., Lassoued, K.,Gouilleux-Gruart, V. (2012): Evidence for a protective role of the STAT5 transcription factor against oxidative stress in human leukemic pre-B cells. *Leukemia*, **26: 11**, 2390-2397

Choudhary, C., Kumar, C., Gnad, F., Nielsen, M. L., Rehman, M., Walther, T. C., Olsen, J. V.,Mann, M. (2009): Lysine acetylation targets protein complexes and co-regulates major cellular functions. *Science*, **325: 5942**, 834-840

Chueh, F.-Y., Leong, K.-F.,Yu, C.-L. (2010): Mitochondrial translocation of signal transducer and activator of transcription 5 (STAT5) in leukemic T cells and cytokine-stimulated cells. *Biochemical and Biophysical Research Communications*, **402: 4**, 778-783

Chueh, F. Y., Leong, K. F., Cronk, R. J., Venkitachalam, S., Pabich, S.,Yu, C. L. (2011): Nuclear localization of pyruvate dehydrogenase complex-E2 (PDC-E2), a mitochondrial enzyme, and its role in signal transducer and activator of transcription 5 (STAT5)-dependent gene transcription. *Cell Signal*, **23: 7**, 1170-1178

Cirillo, L. A., Lin, F. R., Cuesta, I., Friedman, D., Jarnik, M.,Zaret, K. S. (2002): Opening of compacted chromatin by early developmental transcription factors HNF3 (FoxA) and GATA-4. *Mol Cell*, **9: 2**, 279-289

Clark, D. E., Williams, C. C., Duplessis, T. T., Moring, K. L., Notwick, A. R., Long, W., Lane, W. S., Beuvink, I., Hynes, N. E.,Jones, F. E. (2005): ERBB4/HER4 potentiates STAT5A transcriptional activity by regulating novel STAT5A serine phosphorylation events. *J Biol Chem*, **280: 25**, 24175-24180

Clodfelter, K. H., Holloway, M. G., Hodor, P., Park, S. H., Ray, W. J.,Waxman, D. J. (2006): Sex-dependent liver gene expression is extensive and largely dependent upon signal transducer and activator of transcription 5b (STAT5b): STAT5b-dependent activation of male genes and repression of female genes revealed by microarray analysis. *Mol Endocrinol*, **20: 6**, 1333-1351

Clodfelter, K. H., Miles, G. D., Wauthier, V., Holloway, M. G., Zhang, X., Hodor, P., Ray, W. J.,Waxman, D. J. (2007): Role of STAT5a in regulation of sex-specific gene expression in female but not male mouse liver revealed by microarray analysis. *Physiol Genomics*, **31: 1**, 63-74

Cohney, S. J., Sanden, D., Cacalano, N. A., Yoshimura, A., Mui, A., Migone, T. S.,Johnston, J. A. (1999): SOCS-3 is tyrosine phosphorylated in response to interleukin-2 and suppresses STAT5 phosphorylation and lymphocyte proliferation. *Mol Cell Biol*, **19: 7**, 4980-4988

Conaway, J. W., Reines, D.,Conaway, R. C. (1990): Transcription initiated by RNA polymerase II and purified transcription factors from liver. Cooperative action of transcription factors tau and epsilon in initial complex formation. *J Biol Chem*, **265: 13**, 7552-7558

Connerney, J., Lau-Corona, D., Rampersaud, A.,Waxman, D. J. (2017): Activation of Male Liver Chromatin Accessibility and STAT5-Dependent Gene Transcription by Plasma Growth Hormone Pulses. *Endocrinology*, **158: 5**, 1386-1405

Constantinescu, S. N., Girardot, M.,Pecquet, C. (2008): Mining for JAK-STAT mutations in cancer. *Trends Biochem Sci*, **33: 3**, 122-131

Cooper, J. C., Boustead, J. N.,Yu, C. L. (2006): Characterization of STAT5B phosphorylation correlating with expression of cytokine-inducible SH2-containing protein (CIS). *Cell Signal*, **18: 6**, 851-860

Copeland, N. G., Gilbert, D. J., Schindler, C., Zhong, Z., Wen, Z., Darnell, J. E., Jr., Mui, A. L., Miyajima, A., Quelle, F. W., Ihle, J. N.,et al. (1995): Distribution of the mammalian Stat gene family in mouse chromosomes. *Genomics*, **29: 1**, 225-228

Cowell, I. G., Sunter, N. J., Singh, P. B., Austin, C. A., Durkacz, B. W.,Tilby, M. J. (2007): gammaH2AX foci form preferentially in euchromatin after ionising-radiation. *PLoS One*, **2: 10**, e1057

Crowley, T. E., Kaine, E. M., Yoshida, M., Nandi, A.,Wolgemuth, D. J. (2002): Reproductive cycle regulation of nuclear import, euchromatic localization, and association with components of Pol II mediator of a mammalian double-bromodomain protein. *Mol Endocrinol*, **16: 8**, 1727-1737

Cuypers, H. T., Selten, G., Quint, W., Zijlstra, M., Maandag, E. R., Boelens, W., van Wezenbeek, P., Melief, C.,Berns, A. (1984): Murine leukemia virus-induced T-cell lymphomagenesis: integration of proviruses in a distinct chromosomal region. *Cell*, **37: 1**, 141-150

Dai, X., Chen, Y., Di, L., Podd, A., Li, G., Bunting, K. D., Hennighausen, L., Wen, R.,Wang, D. (2007): Stat5 is essential for early B cell development but not for B cell maturation and function. *J Immunol*, **179: 2**, 1068-1079

Dang, W., Kagalwala, M. N.,Bartholomew, B. (2007): The Dpb4 subunit of ISW2 is anchored to extranucleosomal DNA. *J Biol Chem*, **282: 27**, 19418-19425

de Groot, R. P., Coffer, P. J.,Koenderman, L. (1998): Regulation of proliferation, differentiation and survival by the IL-3/IL-5/GM-CSF receptor family. *Cell Signal*, **10: 9**, 619-628

de Klein, A., van Kessel, A. G., Grosveld, G., Bartram, C. R., Hagemeijer, A., Bootsma, D., Spurr, N. K., Heisterkamp, N., Groffen, J.,Stephenson, J. R. (1982): A cellular oncogene is translocated to the Philadelphia chromosome in chronic myelocytic leukaemia. *Nature*, **300: 5894**, 765-767

Demosthenous, C., Han, J. J., Hu, G., Stenson, M.,Gupta, M. (2015): Loss of function mutations in PTPN6 promote STAT3 deregulation via JAK3 kinase in diffuse large B-cell lymphoma. *Oncotarget*, **6: 42**, 44703-44713

Deniz, O., Flores, O., Aldea, M., Soler-Lopez, M.,Orozco, M. (2016): Nucleosome architecture throughout the cell cycle. *Sci Rep*, **6:** 19729

Dev, A., Byrne, S. M., Verma, R., Ashton-Rickardt, P. G.,Wojchowski, D. M. (2013): Erythropoietin-directed erythropoiesis depends on serpin inhibition of erythroblast lysosomal cathepsins. *J Exp Med*, **210: 2**, 225-232

Dey, A., Chitsaz, F., Abbasi, A., Misteli, T.,Ozato, K. (2003): The double bromodomain protein Brd4 binds to acetylated chromatin during interphase and mitosis. *Proc Natl Acad Sci U S A*, **100: 15**, 8758-8763

Dey, R., Ji, K., Liu, Z.,Chen, L. (2009): A cytokine-cytokine interaction in the assembly of higher-order structure and activation of the interleukine-3:receptor complex. *PLoS One*, **4: 4**, e5188

Di Lorenzo, A.,Bedford, M. T. (2011): Histone arginine methylation. *FEBS Lett*, **585: 13**, 2024-2031

Disibio, G.,French, S. W. (2008): Metastatic patterns of cancers: results from a large autopsy study. *Arch Pathol Lab Med*, **132: 6**, 931-939

Dumon, S., Santos, S. C., Debierre-Grockiego, F., Gouilleux-Gruart, V., Cocault, L., Boucheron, C., Mollat, P., Gisselbrecht, S.,Gouilleux, F. (1999): IL-3 dependent regulation of Bcl-xL gene expression by STAT5 in a bone marrow derived cell line. *Oncogene*, **18: 29**, 4191-4199

Ehret, G. B., Reichenbach, P., Schindler, U., Horvath, C. M., Fritz, S., Nabholz, M.,Bucher, P. (2001): DNA binding specificity of different STAT proteins. Comparison of in vitro specificity with natural target sites. *J Biol Chem*, **276: 9**, 6675-6688

Eilon, T., Groner, B.,Barash, I. (2007): Tumors caused by overexpression and forced activation of Stat5 in mammary epithelial cells of transgenic mice are parity-dependent and developed in aged, postestropausal females. *Int J Cancer*, **121: 9**, 1892-1902

Engblom, D., Kornfeld, J. W., Schwake, L., Tronche, F., Reimann, A., Beug, H., Hennighausen, L., Moriggl, R.,Schutz, G. (2007): Direct glucocorticoid receptor-Stat5 interaction in hepatocytes controls body size and maturation-related gene expression. *Genes Dev*, **21: 10**, 1157-1162

Ernst, J.,Kellis, M. (2010): Discovery and characterization of chromatin states for systematic annotation of the human genome. *Nat Biotechnol*, **28: 8**, 817-825

Fahrenkamp, D., Li, J., Ernst, S., Schmitz-Van de Leur, H., Chatain, N., Kuster, A., Koschmieder, S., Luscher, B., Rossetti, G.,Muller-Newen, G. (2016): Intramolecular hydrophobic interactions are critical mediators of STAT5 dimerization. *Sci Rep*, **6:** 35454

Falk, M., Lukasova, E.,Kozubek, S. (2008): Chromatin structure influences the sensitivity of DNA to gamma-radiation. *Biochim Biophys Acta*, **1783: 12**, 2398-2414

Fan, H., Cui, Z., Zhang, H., Mani, S. K., Diab, A., Lefrancois, L., Fares, N., Merle, P.,Andrisani, O. (2017): DNA demethylation induces SALL4 gene re-expression in subgroups of hepatocellular carcinoma associated with Hepatitis B or C virus infection. *Oncogene*, **36: 17**, 2435-2445

Feinberg, A. P. (2007): Phenotypic plasticity and the epigenetics of human disease. *Nature*, **447: 7143**, 433-440

Feng, J., Witthuhn, B. A., Matsuda, T., Kohlhuber, F., Kerr, I. M.,Ihle, J. N. (1997): Activation of Jak2 catalytic activity requires phosphorylation of Y1007 in the kinase activation loop. *Mol Cell Biol*, **17: 5**, 2497-2501

Feng, Y., Arvey, A., Chinen, T., van der Veeken, J., Gasteiger, G.,Rudensky, A. Y. (2014): Control of the inheritance of regulatory T cell identity by a cis element in the Foxp3 locus. *Cell*, **158: 4**, 749-763

Fest, T., Mougey, V., Dalstein, V., Hagerty, M., Milette, D., Silva, S.,Mai, S. (2002): c-MYC overexpression in Ba/F3 cells simultaneously elicits genomic instability and apoptosis. *Oncogene*, **21: 19**, 2981-2990

Fiorillo, A. A., Medler, T. R., Feeney, Y. B., Liu, Y., Tommerdahl, K. L.,Clevenger, C. V. (2011): HMGN2 inducibly binds a novel transactivation domain in nuclear PRLr to coordinate Stat5a-mediated transcription. *Mol Endocrinol*, **25: 9**, 1550-1564

Fleming, J. D., Giresi, P. G., Lindahl-Allen, M., Krall, E. B., Lieb, J. D.,Struhl, K. (2015): STAT3 acts through pre-existing nucleosome-depleted regions bound by FOS during an epigenetic switch linking inflammation to cancer. *Epigenetics Chromatin*, **8:** 7

Fraga, M. F., Ballestar, E., Villar-Garea, A., Boix-Chornet, M., Espada, J., Schotta, G., Bonaldi, T., Haydon, C., Ropero, S., Petrie, K., Iyer, N. G., Perez-Rosado, A., Calvo, E., Lopez, J. A., Cano, A., Calasanz, M. J., Colomer, D., Piris, M. A., Ahn, N., Imhof, A., Caldas, C., Jenuwein, T.,Esteller, M. (2005): Loss of acetylation at Lys16 and trimethylation at Lys20 of histone H4 is a common hallmark of human cancer. *Nat Genet*, **37: 4**, 391-400

Freund, P., Kerenyi, M. A., Hager, M., Wagner, T., Wingelhofer, B., Pham, H. T. T., Elabd, M., Han, X., Valent, P., Gouilleux, F., Sexl, V., Kramer, O. H., Groner, B.,Moriggl, R. (2017): O-GlcNAcylation of STAT5 controls tyrosine phosphorylation and oncogenic transcription in STAT5-dependent malignancies. *Leukemia*, **31: 10**, 2132-2142

Friedbichler, K., Kerenyi, M. A., Kovacic, B., Li, G., Hoelbl, A., Yahiaoui, S., Sexl, V., Mullner, E. W., Fajmann, S., Cerny-Reiterer, S., Valent, P., Beug, H., Gouilleux, F., Bunting, K. D.,Moriggl, R. (2010): Stat5a serine 725 and 779 phosphorylation is a prerequisite for hematopoietic transformation. *Blood*, **116: 9**, 1548-1558

Fu, X. Y., Schindler, C., Improta, T., Aebersold, R.,Darnell, J. E., Jr. (1992): The proteins of ISGF-3, the interferon alpha-induced transcriptional activator, define a gene family involved in signal transduction. *Proc Natl Acad Sci U S A*, **89: 16**, 7840-7843

Funakoshi-Tago, M., Sumi, K., Kasahara, T.,Tago, K. (2013): Critical roles of Myc-ODC axis in the cellular transformation induced by myeloproliferative neoplasm-associated JAK2 V617F mutant. *PLoS One*, **8: 1**, e52844

Funakoshi-Tago, M., Tago, K., Abe, M., Sonoda, Y.,Kasahara, T. (2010): STAT5 activation is critical for the transformation mediated by myeloproliferative disorder-associated JAK2 V617F mutant. *J Biol Chem*, **285: 8**, 5296-5307

Furney, S. J., Higgins, D. G., Ouzounis, C. A.,Lopez-Bigas, N. (2006): Structural and functional properties of genes involved in human cancer. *BMC Genomics*, **7:** 3

Gabay, M., Li, Y.,Felsher, D. W. (2014): MYC activation is a hallmark of cancer initiation and maintenance. *Cold Spring Harb Perspect Med*, **4: 6**,

Gama-Sosa, M. A., Slagel, V. A., Trewyn, R. W., Oxenhandler, R., Kuo, K. C., Gehrke, C. W.,Ehrlich, M. (1983): The 5-methylcytosine content of DNA from human tumors. *Nucleic Acids Res*, **11: 19**, 6883-6894

Garrigan, E., Belkin, N. S., Alexander, J. J., Han, Z., Seydel, F., Carter, J., Atkinson, M., Wasserfall, C., Clare-Salzler, M. J., Amick, M. A.,Litherland, S. A. (2013): Persistent STAT5 Phosphorylation and Epigenetic Dysregulation of GM-CSF and PGS2/COX2 Expression in Type 1 Diabetic Human Monocytes. *PLoS One*, **8: 10**, e76919

Gass, S., Harris, J., Ormandy, C.,Brisken, C. (2003): Using gene expression arrays to elucidate transcriptional profiles underlying prolactin function. *J Mammary Gland Biol Neoplasia*, **8: 3**, 269-285

Gesbert, F.,Griffin, J. D. (2000): Bcr/Abl activates transcription of the Bcl-X gene through STAT5. *Blood*, **96: 6**, 2269-2276

Gewinner, C., Hart, G., Zachara, N., Cole, R., Beisenherz-Huss, C.,Groner, B. (2004): The coactivator of transcription CREB-binding protein interacts preferentially with the glycosylated form of Stat5. *J Biol Chem*, **279: 5**, 3563-3572

Gianti, E.,Zauhar, R. J. (2015): An SH2 domain model of STAT5 in complex with phospho-peptides define "STAT5 Binding Signatures". *J Comput Aided Mol Des*, **29: 5**, 451-470

Gillinder, K. R., Tuckey, H., Bell, C. C., Magor, G. W., Huang, S., Ilsley, M. D.,Perkins, A. C. (2017): Direct targets of pSTAT5 signalling in erythropoiesis. *PLoS One*, **12: 7**, e0180922

Giordanetto, F.,Kroemer, R. T. (2003): A three-dimensional model of Suppressor Of Cytokine Signalling 1 (SOCS-1). *Protein Eng*, **16: 2**, 115-124

Girardot, M., Pecquet, C., Boukour, S., Knoops, L., Ferrant, A., Vainchenker, W., Giraudier, S.,Constantinescu, S. N. (2010): miR-28 is a thrombopoietin receptor targeting microRNA detected in a fraction of myeloproliferative neoplasm patient platelets. *Blood*, **116: 3**, 437-445

Girardot, M., Pecquet, C., Chachoua, I., Van Hees, J., Guibert, S., Ferrant, A., Knoops, L., Baxter, E. J., Beer, P. A., Giraudier, S., Moriggl, R., Vainchenker, W., Green, A. R.,Constantinescu, S. N. (2015): Persistent STAT5 activation in myeloid neoplasms recruits p53 into gene regulation. *Oncogene*, **34: 10**, 1323-1332

Giraud, S., Hurlstone, A., Avril, S.,Coqueret, O. (2004): Implication of BRG1 and cdk9 in the STAT3-mediated activation of the p21waf1 gene. *Oncogene*, **23: 44**, 7391-7398

Gorczyca, W., Bruno, S., Darzynkiewicz, R., Gong, J.,Darzynkiewicz, Z. (1992): DNA strand breaks occurring during apoptosis - their early insitu detection by the terminal deoxynucleotidyl transferase and nick translation assays and prevention by serine protease inhibitors. *Int J Oncol*, **1: 6**, 639-648

Gorman, D. M., Itoh, N., Kitamura, T., Schreurs, J., Yonehara, S., Yahara, I., Arai, K.,Miyajima, A. (1990): Cloning and expression of a gene encoding an interleukin 3 receptor-like protein: identification of another member of the cytokine receptor gene family. *Proc Natl Acad Sci U S A*, **87: 14**, 5459-5463

Gossen, M.,Bujard, H. (1992): Tight control of gene expression in mammalian cells by tetracycline-responsive promoters. *Proc Natl Acad Sci U S A*, **89: 12**, 5547-5551

Gouilleux, F., Wakao, H., Mundt, M.,Groner, B. (1994): Prolactin induces phosphorylation of Tyr694 of Stat5 (MGF), a prerequisite for DNA binding and induction of transcription. *EMBO J*, **13: 18**, 4361-4369

Gouilleux-Gruart, V., Debierre-Grockiego, F., Gouilleux, F., Capiod, J. C., Claisse, J. F., Delobel, J.,Prin, L. (1997): Activated Stat related transcription factors in acute leukemia. *Leuk Lymphoma*, **28: 1-2**, 83-88

Grimley, P. M., Dong, F.,Rui, H. (1999): Stat5a and Stat5b: fraternal twins of signal transduction and transcriptional activation. *Cytokine Growth Factor Rev*, **10: 2**, 131-157

Groffen, J., Voncken, J. W., Kaartinen, V., Morris, C.,Heisterkamp, N. (1993): Ph-positive leukemia: a transgenic mouse model. *Leuk Lymphoma*, **11 Suppl 1:** 19-24

Guo, Y., Updegraff, B. L., Park, S., Durakoglugil, D., Cruz, V. H., Maddux, S., Hwang, T. H.,O'Donnell, K. A. (2016): Comprehensive Ex Vivo Transposon Mutagenesis Identifies Genes That Promote Growth Factor Independence and Leukemogenesis. *Cancer Res*, **76: 4**, 773-786

Hall, T., Emmons, T. L., Chrencik, J. E., Gormley, J. A., Weinberg, R. A., Leone, J. W., Hirsch, J. L., Saabye, M. J., Schindler, J. F., Day, J. E., Williams, J. M., Kiefer, J. R., Lightle, S. A., Harris, M. S., Guru, S., Fischer, H. D.,Tomasselli, A. G. (2010): Expression, purification, characterization and crystallization of non- and phosphorylated states of JAK2 and JAK3 kinase domain. *Protein Expr Purif*, **69: 1**, 54-63

Han, C., Srivastava, A. K., Cui, T., Wang, Q. E.,Wani, A. A. (2016): Differential DNA lesion formation and repair in heterochromatin and euchromatin. *Carcinogenesis*, **37: 2**, 129-138

Han, M.,Grunstein, M. (1988): Nucleosome loss activates yeast downstream promoters in vivo. *Cell*, **55: 6**, 1137-1145

Hanahan, D.,Weinberg, R. A. (2000): The hallmarks of cancer. *Cell*, **100: 1**, 57-70

Hanahan, D.,Weinberg, R. A. (2011): Hallmarks of cancer: the next generation. *Cell*, **144: 5**, 646-674

Hansen, G., Hercus, T. R., McClure, B. J., Stomski, F. C., Dottore, M., Powell, J., Ramshaw, H., Woodcock, J. M., Xu, Y., Guthridge, M., McKinstry, W. J., Lopez, A. F.,Parker, M. W. (2008): The structure of the GM-CSF receptor complex reveals a distinct mode of cytokine receptor activation. *Cell*, **134: 3**, 496-507

Haq, R., Halupa, A., Beattie, B. K., Mason, J. M., Zanke, B. W.,Barber, D. L. (2002): Regulation of erythropoietin-induced STAT serine phosphorylation by distinct mitogen-activated protein kinases. *J Biol Chem*, **277: 19**, 17359-17366

Hara, T.,Miyajima, A. (1992): Two distinct functional high affinity receptors for mouse interleukin-3 (IL-3). *EMBO J*, **11: 5**, 1875-1884

Harb, J. G., Chyla, B. I.,Huettner, C. S. (2008): Loss of Bcl-x in Ph+ B-ALL increases cellular proliferation and does not inhibit leukemogenesis. *Blood*, **111: 7**, 3760-3769

Hargreaves, D. C.,Crabtree, G. R. (2011): ATP-dependent chromatin remodeling: genetics, genomics and mechanisms. *Cell Res*, **21: 3**, 396-420

Harir, N., Boudot, C., Friedbichler, K., Sonneck, K., Kondo, R., Martin-Lanneree, S., Kenner, L., Kerenyi, M., Yahiaoui, S., Gouilleux-Gruart, V., Gondry, J., Benit, L., Dusanter-Fourt, I., Lassoued, K., Valent, P., Moriggl, R.,Gouilleux, F. (2008): Oncogenic Kit controls neoplastic mast cell growth through a Stat5/PI3-kinase signaling cascade. *Blood*, **112: 6**, 2463-2473

Harir, N., Pecquet, C., Kerenyi, M., Sonneck, K., Kovacic, B., Nyga, R., Brevet, M., Dhennin, I., Gouilleux-Gruart, V., Beug, H., Valent, P., Lassoued, K., Moriggl, R.,Gouilleux, F. (2007): Constitutive activation of Stat5 promotes its cytoplasmic localization and association with PI3-kinase in myeloid leukemias. *Blood*, **109: 4**, 1678-1686

Hayward, W. S., Neel, B. G.,Astrin, S. M. (1981): Activation of a cellular onc gene by promoter insertion in ALV-induced lymphoid leukosis. *Nature*, **290: 5806**, 475-480

He, Y., Fang, J., Taatjes, D. J.,Nogales, E. (2013): Structural visualization of key steps in human transcription initiation. *Nature*, **495: 7442**, 481-486

Heath, C.,Cross, N. C. (2004): Critical role of STAT5 activation in transformation mediated by ZNF198-FGFR1. *J Biol Chem*, **279: 8**, 6666-6673

Hedrich, C. M., Rauen, T., Apostolidis, S. A., Grammatikos, A. P., Rodriguez Rodriguez, N., Ioannidis, C., Kyttaris, V. C., Crispin, J. C.,Tsokos, G. C. (2014): Stat3 promotes IL-10 expression in lupus T cells through trans-activation and chromatin remodeling. *Proc Natl Acad Sci U S A*, **111: 37**, 13457-13462

Heltemes-Harris, L. M., Willette, M. J., Ramsey, L. B., Qiu, Y. H., Neeley, E. S., Zhang, N., Thomas, D. A., Koeuth, T., Baechler, E. C., Kornblau, S. M.,Farrar, M. A. (2011): Ebf1 or Pax5 haploinsufficiency synergizes with STAT5 activation to initiate acute lymphoblastic leukemia. *J Exp Med*, **208: 6**, 1135-1149

Hercus, T. R., Broughton, S. E., Ekert, P. G., Ramshaw, H. S., Perugini, M., Grimbaldeston, M., Woodcock, J. M., Thomas, D., Pitson, S., Hughes, T., D'Andrea, R. J., Parker, M. W.,Lopez, A. F. (2012): The GM-CSF receptor family: mechanism of activation and implications for disease. *Growth Factors*, **30: 2**, 63-75

Hernández-Sánchez, M., Rodríguez, A. E., Kohlmann, A., Benito, R., García, J. L., Risueño, A., Fermiñán, E., De Las Rivas, J., González, M.,Hernández-Rivas, J.-M. (2014): TET2Overexpression in Chronic Lymphocytic Leukemia Is Unrelated to the Presence ofTET2Variations. *BioMed Research International*, **2014:** 1-6

Herrera, J. E., Sakaguchi, K., Bergel, M., Trieschmann, L., Nakatani, Y.,Bustin, M. (1999): Specific acetylation of chromosomal protein HMG-17 by PCAF alters its interaction with nucleosomes. *Mol Cell Biol*, **19: 5**, 3466-3473

Herrington, J., Rui, L., Luo, G., Yu-Lee, L. Y.,Carter-Su, C. (1999): A functional DNA binding domain is required for growth hormone-induced nuclear accumulation of Stat5B. *J Biol Chem*, **274: 8**, 5138-5145

Hnisz, D., Abraham, B. J., Lee, T. I., Lau, A., Saint-Andre, V., Sigova, A. A., Hoke, H. A.,Young, R. A. (2013): Super-enhancers in the control of cell identity and disease. *Cell*, **155: 4**, 934-947

Ho, L., Miller, E. L., Ronan, J. L., Ho, W. Q., Jothi, R.,Crabtree, G. R. (2011): esBAF facilitates pluripotency by conditioning the genome for LIF/STAT3 signalling and by regulating polycomb function. *Nat Cell Biol*, **13: 8**, 903-913

Hoelbl, A., Kovacic, B., Kerenyi, M. A., Simma, O., Warsch, W., Cui, Y., Beug, H., Hennighausen, L., Moriggl, R.,Sexl, V. (2006): Clarifying the role of Stat5 in lymphoid development and Abelson-induced transformation. *Blood*, **107: 12**, 4898-4906

Hoelbl, A., Schuster, C., Kovacic, B., Zhu, B., Wickre, M., Hoelzl, M. A., Fajmann, S., Grebien, F., Warsch, W., Stengl, G., Hennighausen, L., Poli, V., Beug, H., Moriggl, R.,Sexl, V. (2010): Stat5 is indispensable for the maintenance of bcr/abl-positive leukaemia. *EMBO Mol Med*, **2: 3**, 98-110

Hogan, G. J., Lee, C. K.,Lieb, J. D. (2006): Cell cycle-specified fluctuation of nucleosome occupancy at gene promoters. *PLoS Genet*, **2: 9**, e158

Hong, L., Schroth, G. P., Matthews, H. R., Yau, P.,Bradbury, E. M. (1993): Studies of the DNA binding properties of histone H4 amino terminus. Thermal denaturation studies reveal that acetylation markedly reduces the binding constant of the H4 "tail" to DNA. *J Biol Chem*, **268: 1**, 305-314

Hopp, T. P., Prickett, K. S., Price, V. L., Libby, R. T., March, C. J., Pat Cerretti, D., Urdal, D. L.,Conlon, P. J. (1988): A Short Polypeptide Marker Sequence Useful for Recombinant Protein Identification and Purification. *Bio/Technology*, **6:** 1204

Hou, H. A., Lin, C. C., Chou, W. C., Liu, C. Y., Chen, C. Y., Tang, J. L., Lai, Y. J., Tseng, M. H., Huang, C. F., Chiang, Y. C., Lee, F. Y., Kuo, Y. Y., Lee, M. C., Liu, M. C., Liu, C. W., Lin, L. I., Yao, M., Huang, S. Y., Ko, B. S., Hsu, S. C., Wu, S. J., Tsay, W., Chen, Y. C.,Tien, H. F. (2014): Integration of cytogenetic and molecular alterations in risk stratification of 318 patients with de novo non-M3 acute myeloid leukemia. *Leukemia*, **28: 1**, 50-58

Hu, X., Dutta, P., Tsurumi, A., Li, J., Wang, J., Land, H.,Li, W. X. (2013): Unphosphorylated STAT5A stabilizes heterochromatin and suppresses tumor growth. *Proc Natl Acad Sci U S A*, **110: 25**, 10213-10218

Hu, Z., Chen, K., Xia, Z., Chavez, M., Pal, S., Seol, J. H., Chen, C. C., Li, W.,Tyler, J. K. (2014): Nucleosome loss leads to global transcriptional up-regulation and genomic instability during yeast aging. *Genes Dev*, **28: 4**, 396-408

Huang, C., Xu, M.,Zhu, B. (2013): Epigenetic inheritance mediated by histone lysine methylation: maintaining transcriptional states without the precise restoration of marks? *Philos Trans R Soc Lond B Biol Sci*, **368: 1609**, 20110332

Iavnilovitch, E., Cardiff, R. D., Groner, B.,Barash, I. (2004): Deregulation of Stat5 expression and activation causes mammary tumors in transgenic mice. *Int J Cancer*, **112: 4**, 607-619

Ilaria, R. L., Jr.,Van Etten, R. A. (1996): P210 and P190(BCR/ABL) induce the tyrosine phosphorylation and DNA binding activity of multiple specific STAT family members. *J Biol Chem*, **271: 49**, 31704-31710

Imada, K., Bloom, E. T., Nakajima, H., Horvath-Arcidiacono, J. A., Udy, G. B., Davey, H. W.,Leonard, W. J. (1998): Stat5b is essential for natural killer cell-mediated proliferation and cytolytic activity. *J Exp Med*, **188: 11**, 2067-2074

Isfort, R. J., Stevens, D., May, W. S.,Ihle, J. N. (1988): Interleukin 3 binds to a 140-kDa phosphotyrosine-containing cell surface protein. *Proc Natl Acad Sci U S A*, **85: 21**, 7982-7986

Ito, K., Noguchi, A., Uosaki, Y., Taga, T., Arakawa, H.,Takizawa, T. (2018): Gfap and Osmr regulation by BRG1 and STAT3 via interchromosomal gene clustering in astrocytes. *Mol Biol Cell*, **29: 2**, 209-219

Itoh, N., Yonehara, S., Schreurs, J., Gorman, D. M., Maruyama, K., Ishii, A., Yahara, I., Arai, K.,Miyajima, A. (1990): Cloning of an interleukin-3 receptor gene: a member of a distinct receptor gene family. *Science*, **247: 4940**, 324-327

Iwabata, H., Yoshida, M.,Komatsu, Y. (2005): Proteomic analysis of organ-specific post-translational lysine-acetylation and -methylation in mice by use of anti-acetyllysine and -methyllysine mouse monoclonal antibodies. *Proteomics*, **5: 18**, 4653-4664

Iyer, J.,Reich, N. C. (2008): Constitutive nuclear import of latent and activated STAT5a by its coiled coil domain. *FASEB J*, **22: 2**, 391-400

Iyer, V. R. (2012): Nucleosome positioning: bringing order to the eukaryotic genome. *Trends Cell Biol*, **22: 5**, 250-256

Jain, D., Baldi, S., Zabel, A., Straub, T.,Becker, P. B. (2015): Active promoters give rise to false positive 'Phantom Peaks' in ChIP-seq experiments. *Nucleic Acids Res*, **43: 14**, 6959-6968

James, C., Ugo, V., Le Couedic, J. P., Staerk, J., Delhommeau, F., Lacout, C., Garcon, L., Raslova, H., Berger, R., Bennaceur-Griscelli, A., Villeval, J. L., Constantinescu, S. N., Casadevall, N.,Vainchenker, W. (2005): A unique clonal JAK2 mutation leading to constitutive signalling causes polycythaemia vera. *Nature*, **434: 7037**, 1144-1148

Jegalian, A. G.,Wu, H. (2002): Regulation of Socs gene expression by the proto-oncoprotein GFI-1B: two routes for STAT5 target gene induction by erythropoietin. *J Biol Chem*, **277: 3**, 2345-2352

Jemal, A., Bray, F., Center, M. M., Ferlay, J., Ward, E.,Forman, D. (2011): Global cancer statistics. *CA Cancer J Clin*, **61: 2**, 69-90

Jenuwein, T.,Allis, C. D. (2001): Translating the histone code. *Science*, **293: 5532**, 1074-1080

Jiang, C.,Pugh, B. F. (2009): Nucleosome positioning and gene regulation: advances through genomics. *Nat Rev Genet*, **10: 3**, 161-172

Jobst, B., Weigl, J., Michl, C., Vivarelli, F., Pinz, S., Amslinger, S.,Rascle, A. (2016): Inhibition of interleukin-3- and interferon- alpha-induced JAK/STAT signaling by the synthetic alpha-X-2',3,4,4'-tetramethoxychalcones alpha-Br-TMC and alpha-CF3-TMC. *Biol Chem*, **397: 11**, 1187-1204

John, S., Robbins, C. M.,Leonard, W. J. (1996): An IL-2 response element in the human IL-2 receptor alpha chain promoter is a composite element that binds Stat5, Elf-1, HMG-I(Y) and a GATA family protein. *Embo j*, **15: 20**, 5627-5635

John, S., Vinkemeier, U., Soldaini, E., Darnell, J. E., Jr.,Leonard, W. J. (1999): The significance of tetramerization in promoter recruitment by Stat5. *Mol Cell Biol*, **19: 3**, 1910-1918

Jolivet, G., Pantano, T.,Houdebine, L. M. (2005): Regulation by the extracellular matrix (ECM) of prolactin-induced alpha s1-casein gene expression in rabbit primary mammary cells: role of STAT5, C/EBP, and chromatin structure. *J Cell Biochem*, **95: 2**, 313-327

Kabotyanski, E. B., Huetter, M., Xian, W., Rijnkels, M.,Rosen, J. M. (2006): Integration of prolactin and glucocorticoid signaling at the beta-casein promoter and enhancer by ordered recruitment of specific transcription factors and chromatin modifiers. *Mol Endocrinol*, **20: 10**, 2355-2368

Kabotyanski, E. B., Rijnkels, M., Freeman-Zadrowski, C., Buser, A. C., Edwards, D. P.,Rosen, J. M. (2009): Lactogenic hormonal induction of long distance interactions between beta-casein gene regulatory elements. *J Biol Chem*, **284: 34**, 22815-22824

Kabotyanski, E. B.,Rosen, J. M. (2003): Signal transduction pathways regulated by prolactin and Src result in different conformations of activated Stat5b. *J Biol Chem*, **278: 19**, 17218-17227

Kanai, T., Seki, S., Jenks, J. A., Kohli, A., Kawli, T., Martin, D. P., Snyder, M., Bacchetta, R.,Nadeau, K. C. (2014): Identification of STAT5A and STAT5B target genes in human T cells. *PLoS One*, **9: 1**, e86790

Kang, K.,Hennighausen, L. (2012): Genomic and bioinformatics tools to understand the biology of signal transducers and activators of transcription. *Horm Mol Biol Clin Investig*, **10: 1**, 207-210

Kang, K., Robinson, G. W.,Hennighausen, L. (2013): Comprehensive meta-analysis of Signal Transducers and Activators of Transcription (STAT) genomic binding patterns discerns cell-specific cis-regulatory modules. *BMC Genomics*, **14:** 4

Kang, K., Yamaji, D., Yoo, K. H., Robinson, G. W.,Hennighausen, L. (2014): Mammary-specific gene activation is defined by progressive recruitment of STAT5 during pregnancy and the establishment of H3K4me3 marks. *Mol Cell Biol*, **34: 3**, 464-473

Katerndahl, C. D. S., Heltemes-Harris, L. M., Willette, M. J. L., Henzler, C. M., Frietze, S., Yang, R., Schjerven, H., Silverstein, K. A. T., Ramsey, L. B., Hubbard, G., Wells, A. D., Kuiper, R. P., Scheijen, B., van Leeuwen, F. N., Muschen, M., Kornblau, S. M.,Farrar, M. A. (2017): Antagonism of B cell enhancer networks by STAT5 drives leukemia and poor patient survival. *Nat Immunol*, **18: 6**, 694-704

Kawai, M., Namba, N., Mushiake, S., Etani, Y., Nishimura, R., Makishima, M.,Ozono, K. (2007): Growth hormone stimulates adipogenesis of 3T3-L1 cells through activation of the Stat5A/5B-PPARgamma pathway. *J Mol Endocrinol*, **38: 1-2**, 19-34

Kawashima, T., Bao, Y. C., Nomura, Y., Moon, Y., Tonozuka, Y., Minoshima, Y., Hatori, T., Tsuchiya, A., Kiyono, M., Nosaka, T., Nakajima, H., Williams, D. A.,Kitamura, T. (2006): Rac1 and a GTPase-activating protein, MgcRacGAP, are required for nuclear translocation of STAT transcription factors. *J Cell Biol*, **175: 6**, 937-946

Kerenyi, M. A., Grebien, F., Gehart, H., Schifrer, M., Artaker, M., Kovacic, B., Beug, H., Moriggl, R.,Mullner, E. W. (2008): Stat5 regulates cellular iron uptake of erythroid cells via IRP-2 and TfR-1. *Blood*, **112: 9**, 3878-3888

Kerr, J. F., Wyllie, A. H.,Currie, A. R. (1972): Apoptosis: a basic biological phenomenon with wide-ranging implications in tissue kinetics. *Br J Cancer*, **26: 4**, 239-257

Kieffer-Kwon, K. R., Tang, Z., Mathe, E., Qian, J., Sung, M. H., Li, G., Resch, W., Baek, S., Pruett, N., Grontved, L., Vian, L., Nelson, S., Zare, H., Hakim, O., Reyon, D., Yamane, A., Nakahashi, H., Kovalchuk, A. L., Zou, J., Joung, J. K., Sartorelli, V., Wei, C. L., Ruan, X., Hager, G. L., Ruan, Y.,Casellas, R. (2013): Interactome maps of mouse gene regulatory domains reveal basic principles of transcriptional regulation. *Cell*, **155: 7**, 1507-1520

Kiel, M. J., Sahasrabuddhe, A. A., Rolland, D. C., Velusamy, T., Chung, F., Schaller, M., Bailey, N. G., Betz, B. L., Miranda, R. N., Porcu, P., Byrd, J. C., Medeiros, L. J., Kunkel, S. L., Bahler, D. W., Lim, M. S.,Elenitoba-Johnson, K. S. (2015): Genomic analyses reveal recurrent mutations in epigenetic modifiers and the JAK-STAT pathway in Sezary syndrome. *Nat Commun*, **6:** 8470

Kiel, M. J., Velusamy, T., Rolland, D., Sahasrabuddhe, A. A., Chung, F., Bailey, N. G., Schrader, A., Li, B., Li, J. Z., Ozel, A. B., Betz, B. L., Miranda, R. N., Medeiros, L. J., Zhao, L., Herling, M., Lim, M. S.,Elenitoba-Johnson, K. S. (2014): Integrated genomic sequencing reveals mutational landscape of T-cell prolymphocytic leukemia. *Blood*,

Kim, J. A., Kruhlak, M., Dotiwala, F., Nussenzweig, A.,Haber, J. E. (2007): Heterochromatin is refractory to gamma-H2AX modification in yeast and mammals. *J Cell Biol*, **178: 2**, 209-218

Kim, W. T., Kim, J., Yan, C., Jeong, P., Choi, S. Y., Lee, O. J., Chae, Y. B., Yun, S. J., Lee, S. C.,Kim, W. J. (2014): S100A9 and EGFR gene signatures predict disease progression in muscle invasive bladder cancer patients after chemotherapy. *Ann Oncol*, **25: 5**, 974-979

Kim, Y. J., Bjorklund, S., Li, Y., Sayre, M. H.,Kornberg, R. D. (1994): A multiprotein mediator of transcriptional activation and its interaction with the C-terminal repeat domain of RNA polymerase II. *Cell*, **77: 4**, 599-608

Kinoshita, T., Shirouzu, M., Kamiya, A., Hashimoto, K., Yokoyama, S.,Miyajima, A. (1997): Raf/MAPK and rapamycin-sensitive pathways mediate the anti-apoptotic function of p21Ras in IL-3-dependent hematopoietic cells. *Oncogene*, **15: 6**, 619-627

Kiu, H.,Nicholson, S. E. (2012): Biology and significance of the JAK/STAT signalling pathways. *Growth Factors*, **30: 2**, 88-106

Kleinschmidt, M. A., Streubel, G., Samans, B., Krause, M.,Bauer, U. M. (2008): The protein arginine methyltransferases CARM1 and PRMT1 cooperate in gene regulation. *Nucleic Acids Res*, **36: 10**, 3202-3213

Kloth, M. T., Catling, A. D.,Silva, C. M. (2002): Novel activation of STAT5b in response to epidermal growth factor. *J Biol Chem*, **277: 10**, 8693-8701

Klucher, K. M., Lopez, D. V.,Daley, G. Q. (1998): Secondary mutation maintains the transformed state in BaF3 cells with inducible BCR/ABL expression. *Blood*, **91: 10**, 3927-3934

Knezetic, J. A.,Luse, D. S. (1986): The presence of nucleosomes on a DNA template prevents initiation by RNA polymerase II in vitro. *Cell*, **45: 1**, 95-104

Kontro, M., Kuusanmaki, H., Eldfors, S., Burmeister, T., Andersson, E. I., Bruserud, O., Brummendorf, T. H., Edgren, H., Gjertsen, B. T., Itala-Remes, M., Lagstrom, S., Lohi, O., Lundan, T., Marti, J. M., Majumder, M. M., Parsons, A., Pemovska, T., Rajala, H., Vettenranta, K., Kallioniemi, O., Mustjoki, S., Porkka, K.,Heckman, C. A. (2014): Novel activating STAT5B mutations as putative drivers of T-cell acute lymphoblastic leukemia. *Leukemia*, **28: 8**, 1738-1742

Kornberg, R. D.,Thomas, J. O. (1974): Chromatin structure; oligomers of the histones. *Science*, **184: 4139**, 865-868

Küçük, C., Jiang, B., Hu, X., Zhang, W., Chan, J. K., Xiao, W., Lack, N., Alkan, C., Williams, J. C., Avery, K. N., Kavak, P., Scuto, A., Sen, E., Gaulard, P., Staudt, L., Iqbal, J., Zhang, W., Cornish, A., Gong, Q., Yang, Q., Sun, H., d'Amore, F., Leppa, S., Liu, W., Fu, K., de Leval, L., McKeithan, T.,Chan, W. C. (2015): Activating mutations of STAT5B and STAT3 in lymphomas derived from gammadelta-T or NK cells. *Nat Commun*, **6:** 6025

Kuzmichev, A., Nishioka, K., Erdjument-Bromage, H., Tempst, P.,Reinberg, D. (2002): Histone methyltransferase activity associated with a human multiprotein complex containing the Enhancer of Zeste protein. *Genes Dev*, **16: 22**, 2893-2905

Kwon, S. H.,Workman, J. L. (2011): The changing faces of HP1: From heterochromatin formation and gene silencing to euchromatic gene expression: HP1 acts as a positive regulator of transcription. *Bioessays*, **33: 4**, 280-289

Laemmli, U. K. (1970): Cleavage of structural proteins during the assembly of the head of bacteriophage T4. *Nature*, **227: 5259**, 680-685

Lan, L., Nakajima, S., Wei, L., Sun, L., Hsieh, C. L., Sobol, R. W., Bruchez, M., Van Houten, B., Yasui, A.,Levine, A. S. (2014): Novel method for site-specific induction of oxidative DNA damage reveals differences in recruitment of repair proteins to heterochromatin and euchromatin. *Nucleic Acids Res*, **42: 4**, 2330-2345

Langenfeld, F., Guarracino, Y., Arock, M., Trouve, A.,Tchertanov, L. (2015): How Intrinsic Molecular Dynamics Control Intramolecular Communication in Signal Transducers and Activators of Transcription Factor STAT5. *PLoS One*, **10: 12**, e0145142

Laszlo, G. S., Ries, R. E., Gudgeon, C. J., Harrington, K. H., Alonzo, T. A., Gerbing, R. B., Raimondi, S. C., Hirsch, B. A., Gamis, A. S., Meshinchi, S.,Walter, R. B. (2014): High expression of suppressor of cytokine signaling-2 predicts poor outcome in pediatric acute myeloid leukemia: a report from the Children's Oncology Group. *Leuk Lymphoma*, **55: 12**, 2817-2821

Latchman, D. S. (1997): Transcription factors: an overview. *Int J Biochem Cell Biol*, **29: 12**, 1305-1312

Lau-Corona, D., Suvorov, A.,Waxman, D. J. (2017): Feminization of male mouse liver by persistent growth hormone stimulation: Activation of sex-biased transcriptional networks and dynamic changes in chromatin states. *Mol Cell Biol*,

Lecine, P., Algarte, M., Rameil, P., Beadling, C., Bucher, P., Nabholz, M.,Imbert, J. (1996): Elf-1 and Stat5 bind to a critical element in a new enhancer of the human interleukin-2 receptor alpha gene. *Mol Cell Biol*, **16: 12**, 6829-6840

Legrand, J. M., Roy, E., Ellis, J. J., Francois, M., Brooks, A. J.,Khosrotehrani, K. (2016): STAT5 Activation in the Dermal Papilla Is Important for Hair Follicle Growth Phase Induction. *J Invest Dermatol*, **136: 9**, 1781-1791

Lemaitre, C.,Soutoglou, E. (2014): Double strand break (DSB) repair in heterochromatin and heterochromatin proteins in DSB repair. *DNA Repair (Amst)*, **19:** 163-168

LeRoy, G., Rickards, B.,Flint, S. J. (2008): The double bromodomain proteins Brd2 and Brd3 couple histone acetylation to transcription. *Mol Cell*, **30: 1**, 51-60

Levine, R. L., Wadleigh, M., Cools, J., Ebert, B. L., Wernig, G., Huntly, B. J., Boggon, T. J., Wlodarska, I., Clark, J. J., Moore, S., Adelsperger, J., Koo, S., Lee, J. C., Gabriel, S., Mercher, T., D'Andrea, A., Frohling, S., Dohner, K., Marynen, P., Vandenberghe, P., Mesa, R. A., Tefferi, A., Griffin, J. D., Eck, M. J., Sellers, W. R., Meyerson, M., Golub, T. R., Lee, S. J.,Gilliland, D. G. (2005): Activating mutation in the tyrosine kinase JAK2 in polycythemia vera, essential thrombocythemia, and myeloid metaplasia with myelofibrosis. *Cancer Cell*, **7: 4**, 387-397

Li, B., Carey, M.,Workman, J. L. (2007): The role of chromatin during transcription. *Cell*, **128: 4**, 707-719

Li, L., Byrne, S. M., Rainville, N., Su, S., Jachimowicz, E., Aucher, A., Davis, D. M., Ashton-Rickardt, P. G.,Wojchowski, D. M. (2014): Brief Report: Serpin Spi2A as a Novel Modulator of Hematopoietic Progenitor Cell Formation. *Stem Cells*, **32: 9**, 2550-2556

Li, P., Mitra, S., Spolski, R., Oh, J., Liao, W., Tang, Z., Mo, F., Li, X., West, E. E., Gromer, D., Lin, J. X., Liu, C., Ruan, Y.,Leonard, W. J. (2017): STAT5-mediated chromatin interactions in superenhancers activate IL-2 highly inducible genes: Functional dissection of the Il2ra gene locus. *Proc Natl Acad Sci U S A*, **114: 46**, 12111-12119

Li, X. Y., MacArthur, S., Bourgon, R., Nix, D., Pollard, D. A., Iyer, V. N., Hechmer, A., Simirenko, L., Stapleton, M., Luengo Hendriks, C. L., Chu, H. C., Ogawa, N., Inwood, W., Sementchenko, V., Beaton, A., Weiszmann, R., Celniker, S. E., Knowles, D. W., Gingeras, T., Speed, T. P., Eisen, M. B.,Biggin, M. D. (2008): Transcription factors bind thousands of active and inactive regions in the Drosophila blastoderm. *PLoS Biol*, **6: 2**, e27

Liao, W., Schones, D. E., Oh, J., Cui, Y., Cui, K., Roh, T. Y., Zhao, K.,Leonard, W. J. (2008): Priming for T helper type 2 differentiation by interleukin 2-mediated induction of interleukin 4 receptor alpha-chain expression. *Nat Immunol*, **9: 11**, 1288-1296

Liao, W., Spolski, R., Li, P., Du, N., West, E. E., Ren, M., Mitra, S.,Leonard, W. J. (2014): Opposing actions of IL-2 and IL-21 on Th9 differentiation correlate with their differential regulation of BCL6 expression. *Proc Natl Acad Sci U S A*, **111: 9**, 3508-3513

Lim, C. P.,Cao, X. (2006): Structure, function, and regulation of STAT proteins. *Mol Biosyst*, **2: 11**, 536-550

Lin, G., LaPensee, C. R., Qin, Z. S.,Schwartz, J. (2014): Reciprocal occupancy of BCL6 and STAT5 on Growth Hormone target genes: contrasting transcriptional outcomes and promoter-specific roles of p300 and HDAC3. *Mol Cell Endocrinol*, **395: 1-2**, 19-31

Lin, J. X., Li, P., Liu, D., Jin, H. T., He, J., Rasheed, M. A., Rochman, Y., Wang, L., Cui, K., Liu, C., Kelsall, B. L., Ahmed, R.,Leonard, W. J. (2012): Critical Role of STAT5 Transcription Factor Tetramerization for Cytokine Responses and Normal Immune Function. *Immunity*, **36: 4**, 586-599

Ling, G., Sugathan, A., Mazor, T., Fraenkel, E.,Waxman, D. J. (2010): Unbiased, genome-wide in vivo mapping of transcriptional regulatory elements reveals sex differences in chromatin structure associated with sex-specific liver gene expression. *Mol Cell Biol*, **30: 23**, 5531-5544

Ling, L.,Lobie, P. E. (2004): RhoA/ROCK activation by growth hormone abrogates p300/histone deacetylase 6 repression of Stat5-mediated transcription. *J Biol Chem*, **279: 31**, 32737-32750

Litterst, C. M., Kliem, S., Marilley, D.,Pfitzner, E. (2003): NCoA-1/SRC-1 is an essential coactivator of STAT5 that binds to the FDL motif in the alpha-helical region of the STAT5 transactivation domain. *J Biol Chem*, **278: 46**, 45340-45351

Liu, J., Peng, L., Niu, T., Wu, Y., Li, J., Wang, F., Zheng, Y.,Liu, T. (2016): PIG7 promotes leukemia cell chemosensitivity via lysosomal membrane permeabilization. *Oncotarget*, **7: 4**, 4841-4859

Liu, N., Phillips, T., Zhang, M., Wang, Y., Opferman, J. T., Shah, R.,Ashton-Rickardt, P. G. (2004a): Serine protease inhibitor 2A is a protective factor for memory T cell development. *Nat Immunol*, **5: 9**, 919-926

Liu, N., Raja, S. M., Zazzeroni, F., Metkar, S. S., Shah, R., Zhang, M., Wang, Y., Bromme, D., Russin, W. A., Lee, J. C., Peter, M. E., Froelich, C. J., Franzoso, G.,Ashton-Rickardt, P. G. (2003): NF-kappaB protects from the lysosomal pathway of cell death. *EMBO J*, **22: 19**, 5313-5322

Liu, N., Wang, Y.,Ashton-Rickardt, P. G. (2004b): Serine protease inhibitor 2A inhibits caspase-independent cell death. *FEBS Lett*, **569: 1-3**, 49-53

Liu, S., Walker, S. R., Nelson, E. A., Cerulli, R., Xiang, M., Toniolo, P. A., Qi, J., Stone, R. M., Wadleigh, M., Bradner, J. E.,Frank, D. A. (2014): Targeting STAT5 in hematologic malignancies through inhibition of the bromodomain and extra-terminal (BET) bromodomain protein BRD2. *Mol Cancer Ther*, **13: 5**, 1194-1205

Liu, X., Robinson, G. W., Gouilleux, F., Groner, B.,Hennighausen, L. (1995): Cloning and expression of Stat5 and an additional homologue (Stat5b) involved in prolactin signal transduction in mouse mammary tissue. *Proc Natl Acad Sci U S A*, **92: 19**, 8831-8835

Liu, X., Robinson, G. W.,Hennighausen, L. (1996): Activation of Stat5a and Stat5b by tyrosine phosphorylation is tightly linked to mammary gland differentiation. *Mol Endocrinol*, **10: 12**, 1496-1506

Liu, X., Robinson, G. W., Wagner, K. U., Garrett, L., Wynshaw-Boris, A.,Hennighausen, L. (1997): Stat5a is mandatory for adult mammary gland development and lactogenesis. *Genes Dev*, **11: 2**, 179-186

Lopez, C., Bergmann, A. K., Paul, U., Murga Penas, E. M., Nagel, I., Betts, M. J., Johansson, P., Ritgen, M., Baumann, T., Aymerich, M., Jayne, S., Russell, R. B., Campo, E., Dyer, M. J., Durig, J.,Siebert, R. (2016): Genes encoding members of the JAK-STAT pathway or epigenetic regulators are recurrently mutated in T-cell prolymphocytic leukaemia. *Br J Haematol*, **173: 2**, 265-273

Loven, J., Hoke, H. A., Lin, C. Y., Lau, A., Orlando, D. A., Vakoc, C. R., Bradner, J. E., Lee, T. I.,Young, R. A. (2013): Selective inhibition of tumor oncogenes by disruption of super-enhancers. *Cell*, **153: 2**, 320-334

Luger, K., Mader, A. W., Richmond, R. K., Sargent, D. F.,Richmond, T. J. (1997): Crystal structure of the nucleosome core particle at 2.8 A resolution. *Nature*, **389: 6648**, 251-260

Lyons, A. B.,Parish, C. R. (1994): Determination of lymphocyte division by flow cytometry. *J Immunol Methods*, **171: 1**, 131-137

Ma, L., Gao, J. S., Guan, Y., Shi, X., Zhang, H., Ayrapetov, M. K., Zhang, Z., Xu, L., Hyun, Y. M., Kim, M., Zhuang, S.,Chin, Y. E. (2010): Acetylation modulates prolactin receptor dimerization. *Proc Natl Acad Sci U S A*, **107: 45**, 19314-19319

Ma, Y., Kanakousaki, K.,Buttitta, L. (2015): How the cell cycle impacts chromatin architecture and influences cell fate. *Frontiers in Genetics*, **6:**

Mahfoudhi, E., Talhaoui, I., Cabagnols, X., Della Valle, V., Secardin, L., Rameau, P., Bernard, O. A., Ishchenko, A. A., Abbes, S., Vainchenker, W., Saparbaev, M.,Plo, I. (2016): TET2-mediated 5-hydroxymethylcytosine induces genetic instability and mutagenesis. *DNA Repair (Amst)*, **43:** 78-88

Malin, S., McManus, S.,Busslinger, M. (2010): STAT5 in B cell development and leukemia. *Curr Opin Immunol*, **22: 2**, 168-176

Malumbres, M.,Barbacid, M. (2009): Cell cycle, CDKs and cancer: a changing paradigm. *Nat Rev Cancer*, **9: 3**, 153-166

Malumbres, M.,Barbacid, M. (2001): To cycle or not to cycle: a critical decision in cancer. *Nat Rev Cancer*, **1: 3**, 222-231

Mandal, M., Powers, S. E., Maienschein-Cline, M., Bartom, E. T., Hamel, K. M., Kee, B. L., Dinner, A. R.,Clark, M. R. (2011): Epigenetic repression of the Igk locus by STAT5-mediated recruitment of the histone methyltransferase Ezh2. *Nat Immunol*,

Marsman, J.,Horsfield, J. A. (2012): Long distance relationships: enhancer-promoter communication and dynamic gene transcription. *Biochim Biophys Acta*, **1819: 11-12**, 1217-1227

Martinez de Paz, A.,Ausio, J. (2016): HMGNs: The enhancer charmers. *Bioessays*, **38: 3**, 226-231

Martinez-Moczygemba, M.,Huston, D. P. (2003): Biology of common beta receptor-signaling cytokines: IL-3, IL-5, and GM-CSF. *J Allergy Clin Immunol*, **112: 4**, 653-665; quiz 666

Martinez-Moczygemba, M.,Huston, D. P. (2001): Proteasomal regulation of betac signaling reveals a novel mechanism for cytokine receptor heterotypic desensitization. *J Clin Invest*, **108: 12**, 1797-1806

Maston, G. A., Evans, S. K.,Green, M. R. (2006): Transcriptional regulatory elements in the human genome. *Annu Rev Genomics Hum Genet*, **7:** 29-59

Masui, N., Tani-ichi, S., Maki, K.,Ikuta, K. (2008): Transcriptional activation of mouse TCR Jgamma4 germline promoter by STAT5. *Mol Immunol*, **45: 3**, 849-855

Matikainen, S., Sareneva, T., Ronni, T., Lehtonen, A., Koskinen, P. J.,Julkunen, I. (1999): Interferon-alpha activates multiple STAT proteins and upregulates proliferation-associated IL-2Ralpha, c-myc, and pim-1 genes in human T cells. *Blood*, **93: 6**, 1980-1991

Medler, T. R., Craig, J. M., Fiorillo, A. A., Feeney, Y. B., Harrell, J. C.,Clevenger, C. V. (2016): HDAC6 Deacetylates HMGN2 to Regulate Stat5a Activity and Breast Cancer Growth. *Mol Cancer Res*, **14: 10**, 994-1008

Melzner, I., Bucur, A. J., Bruderlein, S., Dorsch, K., Hasel, C., Barth, T. F., Leithauser, F.,Moller, P. (2005): Biallelic mutation of SOCS-1 impairs JAK2 degradation and sustains phospho-JAK2 action in the MedB-1 mediastinal lymphoma line. *Blood*, **105: 6**, 2535-2542

Merkenschlager, M.,Nora, E. P. (2016): CTCF and Cohesin in Genome Folding and Transcriptional Gene Regulation. *Annu Rev Genomics Hum Genet*, **17:** 17-43

Merlo, L. M., Pepper, J. W., Reid, B. J.,Maley, C. C. (2006): Cancer as an evolutionary and ecological process. *Nat Rev Cancer*, **6: 12**, 924-935

Metser, G., Shin, H. Y., Wang, C., Yoo, K. H., Oh, S., Villarino, A. V., O'Shea, J. J., Kang, K.,Hennighausen, L. (2016): An autoregulatory enhancer controls mammary-specific STAT5 functions. *Nucleic Acids Res*, **44: 3**, 1052-1063

Meyer, T., Hendry, L., Begitt, A., John, S.,Vinkemeier, U. (2004): A single residue modulates tyrosine dephosphorylation, oligomerization, and nuclear accumulation of stat transcription factors. *J Biol Chem*, **279: 18**, 18998-19007

Meyer, W. K., Reichenbach, P., Schindler, U., Soldaini, E.,Nabholz, M. (1997): Interaction of STAT5 dimers on two low affinity binding sites mediates interleukin 2 (IL-2) stimulation of IL-2 receptor alpha gene transcription. *J Biol Chem*, **272: 50**, 31821-31828

Misteli, T.,Soutoglou, E. (2009): The emerging role of nuclear architecture in DNA repair and genome maintenance. *Nat Rev Mol Cell Biol*, **10: 4**, 243-254

Mitra, A., Ross, J. A., Rodriguez, G., Nagy, Z. S., Wilson, H. L.,Kirken, R. A. (2012): Signal transducer and activator of transcription 5b (Stat5b) serine 193 is a novel cytokine-induced phospho-regulatory site that is constitutively activated in primary hematopoietic malignancies. *J Biol Chem*, **287: 20**, 16596-16608

Mizuguchi, G., Shen, X., Landry, J., Wu, W. H., Sen, S.,Wu, C. (2004): ATP-driven exchange of histone H2AZ variant catalyzed by SWR1 chromatin remodeling complex. *Science*, **303: 5656**, 343-348

Mohr, A., Chatain, N., Domoszlai, T., Rinis, N., Sommerauer, M., Vogt, M.,Muller-Newen, G. (2012): Dynamics and non-canonical aspects of JAK/STAT signalling. *Eur J Cell Biol*, **91: 6-7**, 524-532

Moloney, J. N., Jayavelu, A. K., Stanicka, J., Roche, S. L., O'Brien, R. L., Scholl, S., Bohmer, F. D.,Cotter, T. G. (2017): Nuclear membrane-localised NOX4D generates pro-survival ROS in FLT3-ITD-expressing AML. *Oncotarget*, **8: 62**, 105440-105457

Moriggl, R., Sexl, V., Kenner, L., Duntsch, C., Stangl, K., Gingras, S., Hoffmeyer, A., Bauer, A., Piekorz, R., Wang, D., Bunting, K. D., Wagner, E. F., Sonneck, K., Valent, P., Ihle, J. N.,Beug, H. (2005): Stat5 tetramer formation is associated with leukemogenesis. *Cancer Cell*, **7: 1**, 87-99

Morin, R. D., Johnson, N. A., Severson, T. M., Mungall, A. J., An, J., Goya, R., Paul, J. E., Boyle, M., Woolcock, B. W., Kuchenbauer, F., Yap, D., Humphries, R. K., Griffith, O. L., Shah, S., Zhu, H., Kimbara, M., Shashkin, P., Charlot, J. F., Tcherpakov, M., Corbett, R., Tam, A., Varhol, R., Smailus, D., Moksa, M., Zhao, Y., Delaney, A., Qian, H., Birol, I., Schein, J., Moore, R., Holt, R., Horsman, D. E., Connors, J. M., Jones, S., Aparicio, S., Hirst, M., Gascoyne, R. D.,Marra, M. A. (2010): Somatic mutations altering EZH2 (Tyr641) in follicular and diffuse large B-cell lymphomas of germinal-center origin. *Nat Genet*, **42: 2**, 181-185

Mostoslavsky, R., Chua, K. F., Lombard, D. B., Pang, W. W., Fischer, M. R., Gellon, L., Liu, P., Mostoslavsky, G., Franco, S., Murphy, M. M., Mills, K. D., Patel, P., Hsu, J. T., Hong, A. L., Ford, E., Cheng, H. L., Kennedy, C., Nunez, N., Bronson, R., Frendewey, D., Auerbach, W., Valenzuela, D., Karow, M., Hottiger, M. O., Hursting, S., Barrett, J. C., Guarente, L., Mulligan, R., Demple, B., Yancopoulos, G. D.,Alt, F. W. (2006): Genomic instability and aging-like phenotype in the absence of mammalian SIRT6. *Cell*, **124: 2**, 315-329

Moucadel, V.,Constantinescu, S. N. (2005): Differential STAT5 signaling by ligand-dependent and constitutively active cytokine receptors. *J Biol Chem*, **280: 14**, 13364-13373

Mowel, W. K., McCright, S. J., Kotzin, J. J., Collet, M. A., Uyar, A., Chen, X., DeLaney, A., Spencer, S. P., Virtue, A. T., Yang, E., Villarino, A., Kurachi, M., Dunagin, M. C., Pritchard, G. H., Stein, J., Hughes, C., Fonseca-Pereira, D., Veiga-Fernandes, H., Raj, A., Kambayashi, T., Brodsky, I. E., O'Shea, J. J., Wherry, E. J., Goff, L. A., Rinn, J. L., Williams, A., Flavell, R. A.,Henao-Mejia, J. (2017): Group 1 Innate Lymphoid Cell Lineage Identity Is Determined by a cis-Regulatory Element Marked by a Long Non-coding RNA. *Immunity*, **47: 3**, 435-449 e438

Mui, A. L., Wakao, H., Harada, N., O'Farrell, A. M.,Miyajima, A. (1995): Interleukin-3, granulocyte-macrophage colony-stimulating factor, and interleukin-5 transduce signals through two forms of STAT5. *J Leukoc Biol*, **57: 5**, 799-803

Muller, J., Sperl, B., Reindl, W., Kiessling, A.,Berg, T. (2008): Discovery of chromone-based inhibitors of the transcription factor STAT5. *Chembiochem*, **9: 5**, 723-727

Murga, M., Jaco, I., Fan, Y., Soria, R., Martinez-Pastor, B., Cuadrado, M., Yang, S. M., Blasco, M. A., Skoultchi, A. I.,Fernandez-Capetillo, O. (2007): Global chromatin compaction limits the strength of the DNA damage response. *J Cell Biol*, **178: 7**, 1101-1108

Nagata, Y.,Todokoro, K. (1996): Interleukin 3 activates not only JAK2 and STAT5, but also Tyk2, STAT1, and STAT3. *Biochem Biophys Res Commun*, **221: 3**, 785-789

Nagy, Z. S., Wang, Y., Erwin-Cohen, R. A., Aradi, J., Monia, B., Wang, L. H., Stepkowski, S. M., Rui, H.,Kirken, R. A. (2002): Interleukin-2 family cytokines stimulate phosphorylation of the Pro-Ser-Pro motif of Stat5 transcription factors in human T cells: resistance to suppression of multiple serine kinase pathways. *J Leukoc Biol*, **72: 4**, 819-828

Nair, N., Shoaib, M.,Sorensen, C. S. (2017): Chromatin Dynamics in Genome Stability: Roles in Suppressing Endogenous DNA Damage and Facilitating DNA Repair. *Int J Mol Sci*, **18: 7**,

Nakajima, H., Brindle, P. K., Handa, M.,Ihle, J. N. (2001): Functional interaction of STAT5 and nuclear receptor co-repressor SMRT: implications in negative regulation of STAT5-dependent transcription. *EMBO J*, **20: 23**, 6836-6844

Nakajima, H., Liu, X. W., Wynshaw-Boris, A., Rosenthal, L. A., Imada, K., Finbloom, D. S., Hennighausen, L.,Leonard, W. J. (1997): An indirect effect of Stat5a in IL-2-induced proliferation: a critical role for Stat5a in IL-2-mediated IL-2 receptor alpha chain induction. *Immunity*, **7: 5**, 691-701

Nakayama, J., Yamamoto, M., Hayashi, K., Satoh, H., Bundo, K., Kubo, M., Goitsuka, R., Farrar, M. A.,Kitamura, D. (2009): BLNK suppresses pre-B-cell leukemogenesis through inhibition of JAK3. *Blood*, **113: 7**, 1483-1492

Nanashima, N., Asano, J., Hayakari, M., Nakamura, T., Nakano, H., Yamada, T., Shimizu, T., Akita, M., Fan, Y.,Tsuchida, S. (2005): Nuclear localization of STAT5A modified with O-linked N-acetylglucosamine and early involution in the mammary gland of Hirosaki hairless rat. *J Biol Chem*, **280: 52**, 43010-43016

Nanou, A., Toumpeki, C., Lavigne, M. D., Lazou, V., Demmers, J., Paparountas, T., Thanos, D.,Katsantoni, E. (2017): The dual role of LSD1 and HDAC3 in STAT5-dependent transcription is determined by protein interactions, binding affinities, motifs and genomic positions. *Nucleic Acids Res*, **45: 1**, 142-154

Narlik-Grassow, M., Blanco-Aparicio, C.,Carnero, A. (2014): The PIM family of serine/threonine kinases in cancer. *Med Res Rev*, **34: 1**, 136-159

Neculai, D., Neculai, A. M., Verrier, S., Straub, K., Klumpp, K., Pfitzner, E.,Becker, S. (2005): Structure of the unphosphorylated STAT5a dimer. *J Biol Chem*, **280: 49**, 40782-40787

Nelson, E. A., Walker, S. R., Alvarez, J. V.,Frank, D. A. (2004): Isolation of unique STAT5 targets by chromatin immunoprecipitation-based gene identification. *J Biol Chem*, **279: 52**, 54724-54730

Nishioka, C., Ikezoe, T., Yang, J.,Yokoyama, A. (2016): BCR/ABL increases EZH2 levels which regulates XIAP expression via miRNA-219 in chronic myeloid leukemia cells. *Leuk Res*, **45:** 24-32

Nosaka, T., Kawashima, T., Misawa, K., Ikuta, K., Mui, A. L.,Kitamura, T. (1999): STAT5 as a molecular regulator of proliferation, differentiation and apoptosis in hematopoietic cells. *EMBO J*, **18: 17**, 4754-4765

Nosaka, T.,Kitamura, T. (2002): Pim-1 expression is sufficient to induce cytokine independence in murine hematopoietic cells, but is dispensable for BCR-ABL-mediated transformation. *Exp Hematol*, **30: 7**, 697-702

Nowell P., H. D. (1960): A minute chromosome in human chronic granulocytic leukemia. *Science*, **132:** 1497

Nusinzon, I.,Horvath, C. M. (2003): Interferon-stimulated transcription and innate antiviral immunity require deacetylase activity and histone deacetylase 1. *Proceedings of the National Academy of Sciences*, **100: 25**, 14742-14747

Nyga, R., Pecquet, C., Harir, N., Gu, H., Dhennin-Duthille, I., Regnier, A., Gouilleux-Gruart, V., Lassoued, K.,Gouilleux, F. (2005): Activated STAT5 proteins induce activation of the PI 3-kinase/Akt and Ras/MAPK pathways via the Gab2 scaffolding adapter. *Biochem J*, **390: Pt 1**, 359-366

O'Connell, A. R.,Stenson-Cox, C. (2007): A more serine way to die: defining the characteristics of serine protease-mediated cell death cascades. *Biochim Biophys Acta*, **1773: 10**, 1491-1499

O'Malley, J. T., Sehra, S., Thieu, V. T., Yu, Q., Chang, H. C., Stritesky, G. L., Nguyen, E. T., Mathur, A. N., Levy, D. E.,Kaplan, M. H. (2009): Signal transducer and activator of transcription 4 limits the development of adaptive regulatory T cells. *Immunology*, **127: 4**, 587-595

O'Shea, J. J., Schwartz, D. M., Villarino, A. V., Gadina, M., McInnes, I. B.,Laurence, A. (2015): The JAK-STAT Pathway: Impact on Human Disease and Therapeutic Intervention. *Annu Rev Med*, **66:** 311-328

O'Sullivan, L. A., Liongue, C., Lewis, R. S., Stephenson, S. E.,Ward, A. C. (2007): Cytokine receptor signaling through the Jak-Stat-Socs pathway in disease. *Mol Immunol*, **44: 10**, 2497-2506

O'Sullivan, R. J., Kubicek, S., Schreiber, S. L.,Karlseder, J. (2010): Reduced histone biosynthesis and chromatin changes arising from a damage signal at telomeres. *Nat Struct Mol Biol*, **17: 10**, 1218-1225

Oberdoerffer, P. (2010): An age of fewer histones. *Nat Cell Biol*, **12: 11**, 1029-1031

Oestreich, K. J., Mohn, S. E.,Weinmann, A. S. (2012): Molecular mechanisms that control the expression and activity of Bcl-6 in TH1 cells to regulate flexibility with a TFH-like gene profile. *Nat Immunol*, **13: 4**, 405-411

Ogawa, C., Tone, Y., Tsuda, M., Peter, C., Waldmann, H.,Tone, M. (2014): TGF-beta-mediated Foxp3 gene expression is cooperatively regulated by Stat5, Creb, and AP-1 through CNS2. *J Immunol*, **192: 1**, 475-483

Oka, T., Ouchida, M., Koyama, M., Ogama, Y., Takada, S., Nakatani, Y., Tanaka, T., Yoshino, T., Hayashi, K., Ohara, N., Kondo, E., Takahashi, K., Tsuchiyama, J., Tanimoto, M., Shimizu, K.,Akagi, T. (2002): Gene silencing of the tyrosine phosphatase SHP1 gene by aberrant methylation in leukemias/lymphomas. *Cancer Res*, **62: 22**, 6390-6394

Ola, M. S., Nawaz, M.,Ahsan, H. (2011): Role of Bcl-2 family proteins and caspases in the regulation of apoptosis. *Mol Cell Biochem*, **351: 1-2**, 41-58

Olayioye, M. A., Beuvink, I., Horsch, K., Daly, J. M.,Hynes, N. E. (1999): ErbB receptor-induced activation of stat transcription factors is mediated by Src tyrosine kinases. *J Biol Chem*, **274: 24**, 17209-17218

Onishi, M., Nosaka, T., Misawa, K., Mui, A. L., Gorman, D., McMahon, M., Miyajima, A.,Kitamura, T. (1998): Identification and characterization of a constitutively active STAT5 mutant that promotes cell proliferation. *Mol Cell Biol*, **18: 7**, 3871-3879

Ono, M., Chia, D. J., Merino-Martinez, R., Flores-Morales, A., Unterman, T. G.,Rotwein, P. (2007): Signal transducer and activator of transcription (Stat) 5b-mediated inhibition of insulin-like growth factor binding protein-1 gene transcription: a mechanism for repression of gene expression by growth hormone. *Mol Endocrinol*, **21: 6**, 1443-1457

Ooi, L., Belyaev, N. D., Miyake, K., Wood, I. C.,Buckley, N. J. (2006): BRG1 chromatin remodeling activity is required for efficient chromatin binding by repressor element 1-silencing transcription factor (REST) and facilitates REST-mediated repression. *J Biol Chem*, **281: 51**, 38974-38980

Palacios, R.,Steinmetz, M. (1985): Il-3-dependent mouse clones that express B-220 surface antigen, contain Ig genes in germ-line configuration, and generate B lymphocytes in vivo. *Cell*, **41: 3**, 727-734

Paling, N. R.,Welham, M. J. (2002): Role of the protein tyrosine phosphatase SHP-1 (Src homology phosphatase-1) in the regulation of interleukin-3-induced survival, proliferation and signalling. *Biochem J*, **368: Pt 3**, 885-894

Panieri, E.,Santoro, M. M. (2016): ROS homeostasis and metabolism: a dangerous liason in cancer cells. *Cell Death Dis*, **7: 6**, e2253

Pao, L. I., Badour, K., Siminovitch, K. A.,Neel, B. G. (2007): Nonreceptor protein-tyrosine phosphatases in immune cell signaling. *Annu Rev Immunol*, **25:** 473-523

Park, H. J., Li, J., Hannah, R., Biddie, S., Leal-Cervantes, A. I., Kirschner, K., Flores Santa Cruz, D., Sexl, V., Gottgens, B.,Green, A. R. (2016): Cytokine-induced megakaryocytic differentiation is regulated by genome-wide loss of a uSTAT transcriptional program. *EMBO J*, **35: 6**, 580-594

Patel, J. P., Gonen, M., Figueroa, M. E., Fernandez, H., Sun, Z., Racevskis, J., Van Vlierberghe, P., Dolgalev, I., Thomas, S., Aminova, O., Huberman, K., Cheng, J., Viale, A., Socci, N. D., Heguy, A., Cherry, A., Vance, G., Higgins, R. R., Ketterling, R. P., Gallagher, R. E., Litzow, M., van den Brink, M. R., Lazarus, H. M., Rowe, J. M., Luger, S., Ferrando, A., Paietta, E., Tallman, M. S., Melnick, A., Abdel-Wahab, O.,Levine, R. L. (2012): Prognostic relevance of integrated genetic profiling in acute myeloid leukemia. *N Engl J Med*, **366: 12**, 1079-1089

Paukku, K.,Silvennoinen, O. (2004): STATs as critical mediators of signal transduction and transcription: lessons learned from STAT5. *Cytokine Growth Factor Rev*, **15: 6**, 435-455

Paukku, K., Yang, J.,Silvennoinen, O. (2003): Tudor and nuclease-like domains containing protein p100 function as coactivators for signal transducer and activator of transcription 5. *Mol Endocrinol*, **17: 9**, 1805-1814

Pawlowska, E.,Blasiak, J. (2015): DNA Repair--A Double-Edged Sword in the Genomic Stability of Cancer Cells--The Case of Chronic Myeloid Leukemia. *Int J Mol Sci*, **16: 11**, 27535-27549

Pei, D., Lorenz, U., Klingmuller, U., Neel, B. G.,Walsh, C. T. (1994): Intramolecular regulation of protein tyrosine phosphatase SH-PTP1: a new function for Src homology 2 domains. *Biochemistry*, **33: 51**, 15483-15493

Peng, B., Sutherland, K. D., Sum, E. Y., Olayioye, M., Wittlin, S., Tang, T. K., Lindeman, G. J.,Visvader, J. E. (2002): CPAP is a novel stat5-interacting cofactor that augments stat5-mediated transcriptional activity. *Mol Endocrinol*, **16: 9**, 2019-2033

Peterson, C. L.,Herskowitz, I. (1992): Characterization of the yeast SWI1, SWI2, and SWI3 genes, which encode a global activator of transcription. *Cell*, **68: 3**, 573-583

Pfitzner, E., Jahne, R., Wissler, M., Stoecklin, E.,Groner, B. (1998): p300/CREB-binding protein enhances the prolactin-mediated transcriptional induction through direct interaction with the transactivation domain of Stat5, but does not participate in the Stat5-mediated suppression of the glucocorticoid response. *Mol Endocrinol*, **12: 10**, 1582-1593

Pham, H. T. T., Maurer, B., Prchal-Murphy, M., Grausenburger, R., Grundschober, E., Javaheri, T., Nivarthi, H., Boersma, A., Kolbe, T., Elabd, M., Halbritter, F., Pencik, J., Kazemi, Z., Grebien, F., Hengstschlager, M., Kenner, L., Kubicek, S., Farlik, M., Bock, C., Valent, P., Muller, M., Rulicke, T., Sexl, V.,Moriggl, R. (2018): STAT5BN642H is a driver mutation for T cell neoplasia. *J Clin Invest*, **128: 1**, 387-401

Phillips, D. M. (1963): The presence of acetyl groups of histones. *Biochem J*, **87:** 258-263

Pinz, S.,Rascle, A. (2017): Assessing HDAC Function in the Regulation of Signal Transducer and Activator of Transcription 5 (STAT5) Activity Using Chromatin Immunoprecipitation (ChIP). *Methods Mol Biol*, **1510:** 257-276

Pinz, S., Unser, S., Brueggemann, S., Besl, E., Al-Rifai, N., Petkes, H., Amslinger, S.,Rascle, A. (2014a): The Synthetic alpha-Bromo-2',3,4,4'-Tetramethoxychalcone (alpha-Br-TMC) Inhibits the JAK/STAT Signaling Pathway. *PLoS One*, **9: 3**, e90275

Pinz, S., Unser, S., Buob, D., Fischer, P., Jobst, B.,Rascle, A. (2015): Deacetylase inhibitors repress STAT5-mediated transcription by interfering with bromodomain and extra-terminal (BET) protein function. *Nucleic Acids Res*, **43: 7**, 3524-3545

Pinz, S., Unser, S.,Rascle, A. (2014b): The Natural Chemopreventive Agent Sulforaphane Inhibits STAT5 Activity. *PLoS One*, **9: 6**, e99391

Pinz, S., Unser, S.,Rascle, A. (2016): Signal transducer and activator of transcription STAT5 is recruited to c-Myc super-enhancer. *BMC Mol Biol*, **17:** 10

Plo, I., Nakatake, M., Malivert, L., de Villartay, J. P., Giraudier, S., Villeval, J. L., Wiesmuller, L.,Vainchenker, W. (2008): JAK2 stimulates homologous recombination and genetic instability: potential implication in the heterogeneity of myeloproliferative disorders. *Blood*, **112: 4**, 1402-1412

Pokholok, D. K., Harbison, C. T., Levine, S., Cole, M., Hannett, N. M., Lee, T. I., Bell, G. W., Walker, K., Rolfe, P. A., Herbolsheimer, E., Zeitlinger, J., Lewitter, F., Gifford, D. K.,Young, R. A. (2005): Genome-wide map of nucleosome acetylation and methylation in yeast. *Cell*, **122: 4**, 517-527

Prokhorova, E. A., Zamaraev, A. V., Kopeina, G. S., Zhivotovsky, B.,Lavrik, I. N. (2015): Role of the nucleus in apoptosis: signaling and execution. *Cell Mol Life Sci*, **72: 23**, 4593-4612

Rabello Ddo, A., Lucena-Araujo, A. R., Alves-Silva, J. C., da Eira, V. B., de Vasconcellos, M. C., de Oliveira, F. M., Rego, E. M., Saldanha-Araujo, F.,Pittella Silva, F. (2015): Overexpression of EZH2 associates with a poor prognosis in chronic lymphocytic leukemia. *Blood Cells Mol Dis*, **54: 1**, 97-102

Rajala, H. L., Eldfors, S., Kuusanmaki, H., van Adrichem, A. J., Olson, T., Lagstrom, S., Andersson, E. I., Jerez, A., Clemente, M. J., Yan, Y., Zhang, D., Awwad, A., Ellonen, P., Kallioniemi, O., Wennerberg, K., Porkka, K., Maciejewski, J. P., Loughran, T. P., Jr., Heckman, C.,Mustjoki, S. (2013): Discovery of somatic STAT5b mutations in large granular lymphocytic leukemia. *Blood*, **121: 22**, 4541-4550

Rani, A.,Murphy, J. J. (2016): STAT5 in Cancer and Immunity. *J Interferon Cytokine Res*, **36: 4**, 226-237

Rascle, A., Johnston, J. A.,Amati, B. (2003): Deacetylase activity is required for recruitment of the basal transcription machinery and transactivation by STAT5. *Mol Cell Biol*, **23: 12**, 4162-4173

Rascle, A.,Lees, E. (2003): Chromatin acetylation and remodeling at the Cis promoter during STAT5-induced transcription. *Nucleic Acids Res*, **31: 23**, 6882-6890

Ravandi, F.,Kebriaei, P. (2009): Philadelphia chromosome-positive acute lymphoblastic leukemia. *Hematol Oncol Clin North Am*, **23: 5**, 1043-1063, vi

Rawlings, J. S., Gatzka, M., Thomas, P. G.,Ihle, J. N. (2011): Chromatin condensation via the condensin II complex is required for peripheral T-cell quiescence. *EMBO J*, **30: 2**, 263-276

Rea, S., Eisenhaber, F., O'Carroll, D., Strahl, B. D., Sun, Z. W., Schmid, M., Opravil, S., Mechtler, K., Ponting, C. P., Allis, C. D.,Jenuwein, T. (2000): Regulation of chromatin structure by site-specific histone H3 methyltransferases. *Nature*, **406: 6796**, 593-599

Reid, J. E., Evans, K. J., Dyer, N., Wernisch, L.,Ott, S. (2010): Variable structure motifs for transcription factor binding sites. *BMC Genomics*, **11:** 30

Rico-Bautista, E., Negrin-Martinez, C., Novoa-Mogollon, J., Fernandez-Perez, L.,Flores-Morales, A. (2004): Downregulation of the growth hormone-induced Janus kinase 2/signal transducer and activator of transcription 5 signaling pathway requires an intact actin cytoskeleton. *Exp Cell Res*, **294: 1**, 269-280

Robinson, G. W., Kang, K., Yoo, K. H., Tang, Y., Zhu, B. M., Yamaji, D., Colditz, V., Jang, S. J., Gronostajski, R. M.,Hennighausen, L. (2014): Coregulation of genetic programs by the transcription factors NFIB and STAT5. *Mol Endocrinol*, **28: 5**, 758-767

Rocha-Viegas, L., Vicent, G. P., Baranao, J. L., Beato, M.,Pecci, A. (2006): Glucocorticoids repress bcl-X expression in lymphoid cells by recruiting STAT5B to the P4 promoter. *J Biol Chem*, **281: 45**, 33959-33970

Rochman, M., Taher, L., Kurahashi, T., Cherukuri, S., Uversky, V. N., Landsman, D., Ovcharenko, I.,Bustin, M. (2011): Effects of HMGN variants on the cellular transcription profile. *Nucleic Acids Research*, **39: 10**, 4076-4087

Rosa Santos, S. C., Dumon, S., Mayeux, P., Gisselbrecht, S.,Gouilleux, F. (2000): Cooperation between STAT5 and phosphatidylinositol 3-kinase in the IL-3-dependent survival of a bone marrow derived cell line. *Oncogene*, **19: 9**, 1164-1172

Rowland, J. E., Lichanska, A. M., Kerr, L. M., White, M., d'Aniello, E. M., Maher, S. L., Brown, R., Teasdale, R. D., Noakes, P. G.,Waters, M. J. (2005): In vivo analysis of growth hormone receptor signaling domains and their associated transcripts. *Mol Cell Biol*, **25: 1**, 66-77

Royer, Y., Menu, C., Liu, X.,Constantinescu, S. N. (2004): High-throughput gateway bicistronic retroviral vectors for stable expression in mammalian cells: exploring the biologic effects of STAT5 overexpression. *DNA Cell Biol*, **23: 6**, 355-365

Rusterholz, C., Henrioud, P. C.,Nabholz, M. (1999): Interleukin-2 (IL-2) regulates the accessibility of the IL-2-responsive enhancer in the IL-2 receptor alpha gene to transcription factors. *Mol Cell Biol*, **19: 4**, 2681-2689

Saha, A., Wittmeyer, J.,Cairns, B. R. (2005): Chromatin remodeling through directional DNA translocation from an internal nucleosomal site. *Nat Struct Mol Biol*, **12: 9**, 747-755

Sakurai, Y., Arai, K.,Watanabe, S. (2000): In vitro analysis of STAT5 activation by granulocyte-macrophage colony-stimulating factor. *Genes Cells*, **5: 11**, 937-947

Sallmyr, A., Fan, J., Datta, K., Kim, K. T., Grosu, D., Shapiro, P., Small, D.,Rassool, F. (2008): Internal tandem duplication of FLT3 (FLT3/ITD) induces increased ROS production, DNA damage, and misrepair: implications for poor prognosis in AML. *Blood*, **111: 6**, 3173-3182

Sattler, M., Verma, S., Byrne, C. H., Shrikhande, G., Winkler, T., Algate, P. A., Rohrschneider, L. R.,Griffin, J. D. (1999): BCR/ABL directly inhibits expression of SHIP, an SH2-containing polyinositol-5-phosphatase involved in the regulation of hematopoiesis. *Mol Cell Biol*, **19: 11**, 7473-7480

Schaller-Schönitz, M., Barzan, D., Williamson, A. J., Griffiths, J. R., Dallmann, I., Battmer, K., Ganser, A., Whetton, A. D., Scherr, M.,Eder, M. (2014): BCR-ABL affects STAT5A and STAT5B differentially. *PLoS One*, **9: 5**, e97243

Schauwecker, S. M., Kim, J. J., Licht, J. D.,Clevenger, C. V. (2017): Histone H1 and Chromosomal Protein HMGN2 Regulate Prolactin-induced STAT5 Transcription Factor Recruitment and Function in Breast Cancer Cells. *J Biol Chem*, **292: 6**, 2237-2254

Scheeren, F. A., Naspetti, M., Diehl, S., Schotte, R., Nagasawa, M., Wijnands, E., Gimeno, R., Vyth-Dreese, F. A., Blom, B.,Spits, H. (2005): STAT5 regulates the self-renewal capacity and differentiation of human memory B cells and controls Bcl-6 expression. *Nat Immunol*, **6: 3**, 303-313

Schmidl, C., Hansmann, L., Lassmann, T., Balwierz, P. J., Kawaji, H., Itoh, M., Kawai, J., Nagao-Sato, S., Suzuki, H., Andreesen, R., Hayashizaki, Y., Forrest, A. R., Carninci, P., Hoffmann, P., Edinger, M.,Rehli, M. (2014): The enhancer and promoter landscape of human regulatory and conventional T-cell subpopulations. *Blood*, **123: 17**, e68-78

Schuster-Bockler, B.,Lehner, B. (2012): Chromatin organization is a major influence on regional mutation rates in human cancer cells. *Nature*, **488: 7412**, 504-507

Schwaller, J., Parganas, E., Wang, D., Cain, D., Aster, J. C., Williams, I. R., Lee, C. K., Gerthner, R., Kitamura, T., Frantsve, J., Anastasiadou, E., Loh, M. L., Levy, D. E., Ihle, J. N.,Gilliland, D. G. (2000): Stat5 is essential for the myelo- and lymphoproliferative disease induced by TEL/JAK2. *Mol Cell*, **6: 3**, 693-704

Schwetz, B. A. (2001): From the Food and Drug Administration. *Jama*, **286: 1**, 35

Sen, S., He, Z., Ghosh, S., Dery, K. J., Yang, L., Zhang, J.,Sun, Z. (2018): PRMT1 Plays a Critical Role in Th17 Differentiation by Regulating Reciprocal Recruitment of STAT3 and STAT5. *J Immunol*,

Shahmarvand, N., Nagy, A., Shahryari, J.,Ohgami, R. S. (2018): Mutations in the signal transducer and activator of transcription family of genes in cancer. *Cancer Sci*, **109: 4**, 926-933

Shamji, M. H., Temblay, J. N., Cheng, W., Byrne, S. M., Macfarlane, E., Switzer, A. R., Francisco, N. D. C., Olexandra, F., Jacubczik, F., Durham, S. R.,Ashton-Rickardt, P. G. (2018): Antiapoptotic serine protease inhibitors contribute to survival of allergenic TH2 cells. *J Allergy Clin Immunol*, **142: 2**, 569-581 e565

Shankaranarayanan, P., Chaitidis, P., Kühn, H.,Nigam, S. (2001): Acetylation by Histone Acetyltransferase CREB-binding Protein/p300 of STAT6 Is Required for Transcriptional Activation of the 15-Lipoxygenase-1 Gene. *Journal of Biological Chemistry*, **276: 46**, 42753-42760

Shen, H.,Laird, P. W. (2013): Interplay between the cancer genome and epigenome. *Cell*, **153: 1**, 38-55

Shi, M., Lin, T. H., Appell, K. C.,Berg, L. J. (2008): Janus-kinase-3-dependent signals induce chromatin remodeling at the Ifng locus during T helper 1 cell differentiation. *Immunity*, **28: 6**, 763-773

Shi, Y., Lan, F., Matson, C., Mulligan, P., Whetstine, J. R., Cole, P. A.,Casero, R. A. (2004): Histone demethylation mediated by the nuclear amine oxidase homolog LSD1. *Cell*, **119: 7**, 941-953

Shin, H. Y.,Reich, N. C. (2013): Dynamic trafficking of STAT5 depends on an unconventional nuclear localization signal. *J Cell Sci*, **126: Pt 15**, 3333-3343

Shin, H. Y., Willi, M., HyunYoo, K., Zeng, X., Wang, C., Metser, G.,Hennighausen, L. (2016): Hierarchy within the mammary STAT5-driven Wap super-enhancer. *Nat Genet*, **48: 8**, 904-911

Shuai, K., Schindler, C., Prezioso, V. R.,Darnell, J. E., Jr. (1992): Activation of transcription by IFN-gamma: tyrosine phosphorylation of a 91-kD DNA binding protein. *Science*, **258: 5089**, 1808-1812

Siersbaek, R., Nielsen, R., John, S., Sung, M. H., Baek, S., Loft, A., Hager, G. L.,Mandrup, S. (2011): Extensive chromatin remodelling and establishment of transcription factor 'hotspots' during early adipogenesis. *EMBO J*, **30: 8**, 1459-1472

Siewert, E., Muller-Esterl, W., Starr, R., Heinrich, P. C.,Schaper, F. (1999): Different protein turnover of interleukin-6-type cytokine signalling components. *Eur J Biochem*, **265: 1**, 251-257

Slupianek, A., Hoser, G., Majsterek, I., Bronisz, A., Malecki, M., Blasiak, J., Fishel, R.,Skorski, T. (2002): Fusion Tyrosine Kinases Induce Drug Resistance by Stimulation of Homology-Dependent Recombination Repair, Prolongation of G2/M Phase, and Protection from Apoptosis. *Molecular and Cellular Biology*, **22: 12**, 4189-4201

Solary, E., Bernard, O. A., Tefferi, A., Fuks, F.,Vainchenker, W. (2014): The Ten-Eleven Translocation-2 (TET2) gene in hematopoiesis and hematopoietic diseases. *Leukemia*, **28: 3**, 485-496

Soldaini, E., John, S., Moro, S., Bollenbacher, J., Schindler, U.,Leonard, W. J. (2000): DNA binding site selection of dimeric and tetrameric Stat5 proteins reveals a large repertoire of divergent tetrameric Stat5a binding sites. *Mol Cell Biol*, **20: 1**, 389-401

Sorensen, P., Mui, A. L.,Krystal, G. (1989): Interleukin-3 stimulates the tyrosine phosphorylation of the 140-kilodalton interleukin-3 receptor. *J Biol Chem*, **264: 32**, 19253-19258

Spange, S., Wagner, T., Heinzel, T.,Kramer, O. H. (2009): Acetylation of non-histone proteins modulates cellular signalling at multiple levels. *Int J Biochem Cell Biol*, **41: 1**, 185-198

Stark, G. R.,Darnell, J. E., Jr. (2012): The JAK-STAT Pathway at Twenty. *Immunity*, **36: 4**, 503-514

Strahl, B. D.,Allis, C. D. (2000): The language of covalent histone modifications. *Nature*, **403: 6765**, 41-45

Stratton, M. R., Campbell, P. J.,Futreal, P. A. (2009): The cancer genome. *Nature*, **458: 7239**, 719-724

Sugathan, A.,Waxman, D. J. (2013): Genome-wide analysis of chromatin states reveals distinct mechanisms of sex-dependent gene regulation in male and female mouse liver. *Mol Cell Biol*, **33: 18**, 3594-3610

Sun, Y., Jiang, X., Chen, S.,Price, B. D. (2006): Inhibition of histone acetyltransferase activity by anacardic acid sensitizes tumor cells to ionizing radiation. *FEBS Lett*, **580: 18**, 4353-4356

Svaren, J.,Horz, W. (1997): Transcription factors vs nucleosomes: regulation of the PHO5 promoter in yeast. *Trends Biochem Sci*, **22: 3**, 93-97

Symonds, H., Krall, L., Remington, L., Saenz-Robles, M., Lowe, S., Jacks, T.,Van Dyke, T. (1994): p53-dependent apoptosis suppresses tumor growth and progression in vivo. *Cell*, **78: 4**, 703-711

Tan, S. H., Dagvadorj, A., Shen, F., Gu, L., Liao, Z., Abdulghani, J., Zhang, Y., Gelmann, E. P., Zellweger, T., Culig, Z., Visakorpi, T., Bubendorf, L., Kirken, R. A., Karras, J.,Nevalainen, M. T. (2008): Transcription factor Stat5 synergizes with androgen receptor in prostate cancer cells. *Cancer Res*, **68: 1**, 236-248

Taniguchi, Y. (2016): The Bromodomain and Extra-Terminal Domain (BET) Family: Functional Anatomy of BET Paralogous Proteins. *Int J Mol Sci*, **17: 11**,

Tannenbaum, G. S., Choi, H. K., Gurd, W.,Waxman, D. J. (2001): Temporal relationship between the sexually dimorphic spontaneous GH secretory profiles and hepatic STAT5 activity. *Endocrinology*, **142: 11**, 4599-4606

Tasian, S. K., Doral, M. Y., Borowitz, M. J., Wood, B. L., Chen, I. M., Harvey, R. C., Gastier-Foster, J. M., Willman, C. L., Hunger, S. P., Mullighan, C. G.,Loh, M. L. (2012): Aberrant STAT5 and PI3K/mTOR pathway signaling occurs in human CRLF2-rearranged B-precursor acute lymphoblastic leukemia. *Blood*, **120: 4**, 833-842

Taskinen, M., Valo, E., Karjalainen-Lindsberg, M. L., Hautaniemi, S., Meri, S.,Leppa, S. (2010): Signal transducers and activators of transcription 5a-dependent cross-talk between follicular lymphoma cells and tumor microenvironment characterizes a group of patients with improved outcome after R-CHOP. *Clin Cancer Res*, **16: 9**, 2615-2623

Taunton, J., Hassig, C. A.,Schreiber, S. L. (1996): A mammalian histone deacetylase related to the yeast transcriptional regulator Rpd3p. *Science*, **272: 5260**, 408-411

Taylor, R. C., Cullen, S. P.,Martin, S. J. (2008): Apoptosis: controlled demolition at the cellular level. *Nat Rev Mol Cell Biol*, **9: 3**, 231-241

Teglund, S., McKay, C., Schuetz, E., van Deursen, J. M., Stravopodis, D., Wang, D., Brown, M., Bodner, S., Grosveld, G.,Ihle, J. N. (1998): Stat5a and Stat5b proteins have essential and nonessential, or redundant, roles in cytokine responses. *Cell*, **93: 5**, 841-850

The ENCODE Project Consortium (2012): An integrated encyclopedia of DNA elements in the human genome. *Nature*, **489: 7414**, 57-74

Theodorou, M., Speletas, M., Mamara, A., Papachristopoulou, G., Lazou, V., Scorilas, A.,Katsantoni, E. (2013): Identification of a STAT5 target gene, Dpf3, provides novel insights in chronic lymphocytic leukemia. *PLoS One*, **8: 10**, e76155

Thiel, S., Sommer, U., Kortylewski, M., Haan, C., Behrmann, I., Heinrich, P. C.,Graeve, L. (2000): Termination of IL-6-induced STAT activation is independent of receptor internalization but requires de novo protein synthesis. *FEBS Lett*, **470: 1**, 15-19

Thoma, F., Koller, T.,Klug, A. (1979): Involvement of histone H1 in the organization of the nucleosome and of the salt-dependent superstructures of chromatin. *J Cell Biol*, **83: 2 Pt 1**, 403-427

Thurman, R. E., Rynes, E., Humbert, R., Vierstra, J., Maurano, M. T., Haugen, E., Sheffield, N. C., Stergachis, A. B., Wang, H., Vernot, B., Garg, K., John, S., Sandstrom, R., Bates, D., Boatman, L., Canfield, T. K., Diegel, M., Dunn, D., Ebersol, A. K., Frum, T., Giste, E., Johnson, A. K., Johnson, E. M., Kutyavin, T., Lajoie, B., Lee, B. K., Lee, K., London, D., Lotakis, D., Neph, S., Neri, F., Nguyen, E. D., Qu, H., Reynolds, A. P., Roach, V., Safi, A., Sanchez, M. E., Sanyal, A., Shafer, A., Simon, J. M., Song, L., Vong, S., Weaver, M., Yan, Y., Zhang, Z., Lenhard, B., Tewari, M., Dorschner, M. O., Hansen, R. S., Navas, P. A., Stamatoyannopoulos, G., Iyer, V. R., Lieb, J. D., Sunyaev, S. R., Akey, J. M., Sabo, P. J., Kaul, R., Furey, T. S., Dekker, J., Crawford, G. E.,Stamatoyannopoulos, J. A. (2012): The accessible chromatin landscape of the human genome. *Nature*, **489: 7414**, 75-82

Tran, T. H., Utama, F. E., Lin, J., Yang, N., Sjolund, A. B., Ryder, A., Johnson, K. J., Neilson, L. M., Liu, C., Brill, K. L., Rosenberg, A. L., Witkiewicz, A. K.,Rui, H. (2010): Prolactin inhibits BCL6 expression in breast cancer through a Stat5a-dependent mechanism. *Cancer Res*, **70: 4**, 1711-1721

Tsompana, M.,Buck, M. J. (2014): Chromatin accessibility: a window into the genome. *Epigenetics Chromatin*, **7: 1**, 33

Tsuruyama, T., Nakamura, T., Jin, G., Ozeki, M., Yamada, Y.,Hiai, H. (2002): Constitutive activation of Stat5a by retrovirus integration in early pre-B lymphomas of SL/Kh strain mice. *Proc Natl Acad Sci U S A*, **99: 12**, 8253-8258

Udy, G. B., Towers, R. P., Snell, R. G., Wilkins, R. J., Park, S. H., Ram, P. A., Waxman, D. J.,Davey, H. W. (1997): Requirement of STAT5b for sexual dimorphism of body growth rates and liver gene expression. *Proc Natl Acad Sci U S A*, **94: 14**, 7239-7244

Ujvari, D., Nagy, N., Madapura, H. S., Kallas, T., Krohnke, M. C. L., Stenke, L., Klein, E.,Salamon, D. (2018): Interferon gamma is a strong, STAT1-dependent direct inducer of BCL6 expression in multiple myeloma cells. *Biochem Biophys Res Commun*, **498: 3**, 502-508

Ungureanu, D., Saharinen, P., Junttila, I., Hilton, D. J.,Silvennoinen, O. (2002): Regulation of Jak2 through the ubiquitin-proteasome pathway involves phosphorylation of Jak2 on Y1007 and interaction with SOCS-1. *Mol Cell Biol*, **22: 10**, 3316-3326

Urayama, S., Semi, K., Sanosaka, T., Hori, Y., Namihira, M., Kohyama, J., Takizawa, T.,Nakashima, K. (2013): Chromatin accessibility at a STAT3 target site is altered prior to astrocyte differentiation. *Cell Struct Funct*, **38: 1**, 55-66

Urlinger, S., Baron, U., Thellmann, M., Hasan, M. T., Bujard, H.,Hillen, W. (2000): Exploring the sequence space for tetracycline-dependent transcriptional activators: novel mutations yield expanded range and sensitivity. *Proc Natl Acad Sci U S A*, **97: 14**, 7963-7968

van der Weyden, L., Giotopoulos, G., Wong, K., Rust, A. G., Robles-Espinoza, C. D., Osaki, H., Huntly, B. J.,Adams, D. J. (2015): Somatic drivers of B-ALL in a model of ETV6-RUNX1; Pax5(+/-) leukemia. *BMC Cancer*, **15:** 585

Van Nguyen, T., Angkasekwinai, P., Dou, H., Lin, F. M., Lu, L. S., Cheng, J., Chin, Y. E., Dong, C.,Yeh, E. T. (2012): SUMO-specific protease 1 is critical for early lymphoid development through regulation of STAT5 activation. *Mol Cell*, **45: 2**, 210-221

Vaquerizas, J. M., Kummerfeld, S. K., Teichmann, S. A.,Luscombe, N. M. (2009): A census of human transcription factors: function, expression and evolution. *Nat Rev Genet*, **10: 4**, 252-263

Verdier, F., Rabionet, R., Gouilleux, F., Beisenherz-Huss, C., Varlet, P., Muller, O., Mayeux, P., Lacombe, C., Gisselbrecht, S.,Chretien, S. (1998): A sequence of the CIS gene promoter interacts preferentially with two associated STAT5A dimers: a distinct biochemical difference between STAT5A and STAT5B. *Mol Cell Biol*, **18: 10**, 5852-5860

Verdone, L., Wu, J., van Riper, K., Kacherovsky, N., Vogelauer, M., Young, E. T., Grunstein, M., Di Mauro, E.,Caserta, M. (2002): Hyperacetylation of chromatin at the ADH2 promoter allows Adr1 to bind in repressed conditions. *EMBO J*, **21: 5**, 1101-1111

Vidal, O. M., Merino, R., Rico-Bautista, E., Fernandez-Perez, L., Chia, D. J., Woelfle, J., Ono, M., Lenhard, B., Norstedt, G., Rotwein, P.,Flores-Morales, A. (2007): In vivo transcript profiling and phylogenetic analysis identifies suppressor of cytokine signaling 2 as a direct signal transducer and activator of transcription 5b target in liver. *Mol Endocrinol*, **21: 1**, 293-311

Villarino, A., Laurence, A., Robinson, G. W., Bonelli, M., Dema, B., Afzali, B., Shih, H. Y., Sun, H. W., Brooks, S. R., Hennighausen, L., Kanno, Y.,O'Shea, J. J. (2016): Signal transducer and activator of transcription 5 (STAT5) paralog dose governs T cell effector and regulatory functions. *Elife*, **5:**

Viny, A. D., Ott, C. J., Spitzer, B., Rivas, M., Meydan, C., Papalexi, E., Yelin, D., Shank, K., Reyes, J., Chiu, A., Romin, Y., Boyko, V., Thota, S., Maciejewski, J. P., Melnick, A., Bradner, J. E.,Levine, R. L. (2015): Dose-dependent role of the cohesin complex in normal and malignant hematopoiesis. *J Exp Med*, **212: 11**, 1819-1832

Vogelstein, B., Papadopoulos, N., Velculescu, V. E., Zhou, S., Diaz, L. A., Jr.,Kinzler, K. W. (2013): Cancer genome landscapes. *Science*, **339: 6127**, 1546-1558

Vollbrecht, C., Mairinger, F. D., Koitzsch, U., Peifer, M., Koenig, K., Heukamp, L. C., Crispatzu, G., Wilden, L., Kreuzer, K. A., Hallek, M., Odenthal, M., Herling, C. D.,Buettner, R. (2015): Comprehensive Analysis of Disease-Related Genes in Chronic Lymphocytic Leukemia by Multiplex PCR-Based Next Generation Sequencing. *PLoS One*, **10: 6**, e0129544

Wagatsuma, K., Tani-ichi, S., Liang, B., Shitara, S., Ishihara, K., Abe, M., Miyachi, H., Kitano, S., Hara, T., Nanno, M., Ishikawa, H., Sakimura, K., Nakao, M., Kimura, H.,Ikuta, K. (2015): STAT5 Orchestrates Local Epigenetic Changes for Chromatin Accessibility and Rearrangements by Direct Binding to the TCRgamma Locus. *J Immunol*, **195: 4**, 1804-1814

Wakao, H., Gouilleux, F.,Groner, B. (1994): Mammary gland factor (MGF) is a novel member of the cytokine regulated transcription factor gene family and confers the prolactin response. *EMBO J*, **13: 9**, 2182-2191

Walker, S. R., Nelson, E. A.,Frank, D. A. (2007): STAT5 represses BCL6 expression by binding to a regulatory region frequently mutated in lymphomas. *Oncogene*, **26: 2**, 224-233

Walz, C., Ahmed, W., Lazarides, K., Betancur, M., Patel, N., Hennighausen, L., Zaleskas, V. M.,Van Etten, R. A. (2012): Essential role for Stat5a/b in myeloproliferative neoplasms induced by BCR-ABL1 and JAK2(V617F) in mice. *Blood*, **119: 15**, 3550-3560

Wan, C. K., Oh, J., Li, P., West, E. E., Wong, E. A., Andraski, A. B., Spolski, R., Yu, Z. X., He, J., Kelsall, B. L.,Leonard, W. J. (2013): The cytokines IL-21 and GM-CSF have opposing regulatory roles in the apoptosis of conventional dendritic cells. *Immunity*, **38: 3**, 514-527

Wang, G. G., Allis, C. D.,Chi, P. (2007a): Chromatin remodeling and cancer, Part I: Covalent histone modifications. *Trends Mol Med*, **13: 9**, 363-372

Wang, G. G., Allis, C. D.,Chi, P. (2007b): Chromatin remodeling and cancer, Part II: ATP-dependent chromatin remodeling. *Trends Mol Med*, **13: 9**, 373-380

Wang, Y.,Levy, D. E. (2012): Comparative evolutionary genomics of the STAT family of transcription factors. *JAKSTAT*, **1: 1**, 23-33

Wang, Y.,Navin, N. E. (2015): Advances and applications of single-cell sequencing technologies. *Mol Cell*, **58: 4**, 598-609

Wang, Z.,Bunting, K. D. (2013): STAT5 in hematopoietic stem cell biology and transplantation. *JAKSTAT*, **2: 4**, e27159

Wang, Z., Medrzycki, M., Bunting, S. T.,Bunting, K. D. (2015): Stat5-deficient hematopoiesis is permissive for Myc-induced B-cell leukemogenesis. *Oncotarget*, **6: 30**, 28961-28972

Wang, Z., Zang, C., Cui, K., Schones, D. E., Barski, A., Peng, W.,Zhao, K. (2009): Genome-wide mapping of HATs and HDACs reveals distinct functions in active and inactive genes. *Cell*, **138: 5**, 1019-1031

Wapenaar, H.,Dekker, F. J. (2016): Histone acetyltransferases: challenges in targeting bi-substrate enzymes. *Clinical Epigenetics*, **8: 1**,

Warsch, W., Grundschober, E., Berger, A., Gille, L., Cerny-Reiterer, S., Tigan, A. S., Hoelbl-Kovacic, A., Valent, P., Moriggl, R.,Sexl, V. (2012): STAT5 triggers BCR-ABL1 mutation by mediating ROS production in chronic myeloid leukaemia. *Oncotarget*, **3: 12**, 1669-1687

Warsch, W., Kollmann, K., Eckelhart, E., Fajmann, S., Cerny-Reiterer, S., Holbl, A., Gleixner, K. V., Dworzak, M., Mayerhofer, M., Hoermann, G., Herrmann, H., Sillaber, C., Egger, G., Valent, P., Moriggl, R.,Sexl, V. (2011): High STAT5 levels mediate imatinib resistance and indicate disease progression in chronic myeloid leukemia. *Blood*, **117: 12**, 3409-3420

Watanabe, S., Itoh, T.,Arai, K. (1996): JAK2 is essential for activation of c-fos and c-myc promoters and cell proliferation through the human granulocyte-macrophage colony-stimulating factor receptor in BA/F3 cells. *J Biol Chem*, **271: 21**, 12681-12686

Watanabe, S., Kubota, H., Sakamoto, K. M.,Arai, K. (1997): Characterization of cis-acting sequences and trans-acting signals regulating early growth response 1 and c-fos promoters through the granulocyte-macrophage colony-stimulating factor receptor in BA/F3 cells. *Blood*, **89: 4**, 1197-1206

Watanabe-Smith, K., Tognon, C., Tyner, J. W., Meijerink, J. P., Druker, B. J.,Agarwal, A. (2016): Discovery and functional characterization of a germline, CSF2RB-activating mutation in leukemia. *Leukemia*, **30: 9**, 1950-1953

Weber-Nordt, R. M., Egen, C., Wehinger, J., Ludwig, W., Gouilleux-Gruart, V., Mertelsmann, R.,Finke, J. (1996): Constitutive activation of STAT proteins in primary lymphoid and myeloid leukemia cells and in Epstein-Barr virus (EBV)-related lymphoma cell lines. *Blood*, **88: 3**, 809-816

Weisbrod, S., Groudine, M.,Weintraub, H. (1980): Interaction of HMG 14 and 17 with actively transcribed genes. *Cell*, **19: 1**, 289-301

Weisenberger, D. J. (2014): Characterizing DNA methylation alterations from The Cancer Genome Atlas. *J Clin Invest*, **124: 1**, 17-23

Weng, Y. R., Yu, Y. N., Ren, L. L., Cui, Y., Lu, Y. Y., Chen, H. Y., Ma, X., Qin, W. X., Cao, W., Hong, J.,Fang, J. Y. (2014): Role of C9orf140 in the promotion of colorectal cancer progression and mechanisms of its upregulation via activation of STAT5, beta-catenin and EZH2. *Carcinogenesis*, **35: 6**, 1389-1398

Wernig, G., Mercher, T., Okabe, R., Levine, R. L., Lee, B. H.,Gilliland, D. G. (2006): Expression of Jak2V617F causes a polycythemia vera-like disease with associated myelofibrosis in a murine bone marrow transplant model. *Blood*, **107: 11**, 4274-4281

Wheadon, H., Paling, N. R.,Welham, M. J. (2002): Molecular interactions of SHP1 and SHP2 in IL-3-signalling. *Cell Signal*, **14: 3**, 219-229

Wierenga, A. T., Schepers, H., Moore, M. A., Vellenga, E.,Schuringa, J. J. (2006): STAT5-induced self-renewal and impaired myelopoiesis of human hematopoietic stem/progenitor cells involves down-modulation of C/EBPalpha. *Blood*, **107: 11**, 4326-4333

Wierenga, A. T., Vellenga, E.,Schuringa, J. J. (2008): Maximal STAT5-induced proliferation and self-renewal at intermediate STAT5 activity levels. *Mol Cell Biol*, **28: 21**, 6668-6680

Willi, M., Yoo, K. H., Wang, C., Trajanoski, Z.,Hennighausen, L. (2016): Differential cytokine sensitivities of STAT5-dependent enhancers rely on Stat5 autoregulation. *Nucleic Acids Res*, **44: 21**, 10277-10291

Wingelhofer, B., Neubauer, H. A., Valent, P., Han, X., Constantinescu, S. N., Gunning, P. T., Muller, M.,Moriggl, R. (2018): Implications of STAT3 and STAT5 signaling on gene regulation and chromatin remodeling in hematopoietic cancer. *Leukemia*,

Wu, A. M., Yang, M., Dalvi, P., Turinsky, A. L., Wang, W., Butcher, D., Egan, S. E., Weksberg, R., Harper, P. A.,Ito, S. (2014): Role of STAT5 and epigenetics in lactation-associated upregulation of multidrug transporter ABCG2 in the mammary gland. *Am J Physiol Endocrinol Metab*, **307: 7**, E596-610

Wu, J., Keng, V. W., Patmore, D. M., Kendall, J. J., Patel, A. V., Jousma, E., Jessen, W. J., Choi, K., Tschida, B. R., Silverstein, K. A., Fan, D., Schwartz, E. B., Fuchs, J. R., Zou, Y., Kim, M. O., Dombi, E., Levy, D. E., Huang, G., Cancelas, J. A., Stemmer-Rachamimov, A. O., Spinner, R. J., Largaespada, D. A.,Ratner, N. (2016): Insertional Mutagenesis Identifies a STAT3/Arid1b/beta-catenin Pathway Driving Neurofibroma Initiation. *Cell Rep*, **14: 8**, 1979-1990

Wu, X.,Zhang, Y. (2017): TET-mediated active DNA demethylation: mechanism, function and beyond. *Nat Rev Genet*, **18: 9**, 517-534

Wyszomierski, S. L.,Rosen, J. M. (2001): Cooperative effects of STAT5 (signal transducer and activator of transcription 5) and C/EBPbeta (CCAAT/enhancer-binding protein-beta) on beta-casein gene transcription are mediated by the glucocorticoid receptor. *Mol Endocrinol*, **15: 2**, 228-240

Xiao, W., Hong, H., Kawakami, Y., Kato, Y., Wu, D., Yasudo, H., Kimura, A., Kubagawa, H., Bertoli, L. F., Davis, R. S., Chau, L. A., Madrenas, J., Hsia, C. C., Xenocostas, A., Kipps, T. J., Hennighausen, L., Iwama, A., Nakauchi, H.,Kawakami, T. (2009): Tumor suppression by phospholipase C-beta3 via SHP-1-mediated dephosphorylation of Stat5. *Cancer Cell*, **16: 2**, 161-171

Xu, M., Nie, L., Kim, S. H.,Sun, X. H. (2003): STAT5-induced Id-1 transcription involves recruitment of HDAC1 and deacetylation of C/EBPbeta. *EMBO J*, **22: 4**, 893-904

Xu, R., Nelson, C. M., Muschler, J. L., Veiseh, M., Vonderhaar, B. K.,Bissell, M. J. (2009): Sustained activation of STAT5 is essential for chromatin remodeling and maintenance of mammary-specific function. *J Cell Biol*, **184: 1**, 57-66

Xu, R., Spencer, V. A.,Bissell, M. J. (2007): Extracellular matrix-regulated gene expression requires cooperation of SWI/SNF and transcription factors. *J Biol Chem*, **282: 20**, 14992-14999

Xue, H. H., Fink, D. W., Jr., Zhang, X., Qin, J., Turck, C. W.,Leonard, W. J. (2002): Serine phosphorylation of Stat5 proteins in lymphocytes stimulated with IL-2. *Int Immunol*, **14: 11**, 1263-1271

Yamaji, D., Kang, K., Robinson, G. W.,Hennighausen, L. (2012): Sequential activation of genetic programs in mouse mammary epithelium during pregnancy depends on STAT5A/B concentration. *Nucleic Acids Res*,

Yamashita, H., Xu, J., Erwin, R. A., Farrar, W. L., Kirken, R. A.,Rui, H. (1998): Differential control of the phosphorylation state of proline-juxtaposed serine residues Ser725 of Stat5a and Ser730 of Stat5b in prolactin-sensitive cells. *J Biol Chem*, **273: 46**, 30218-30224

Yang, J., Liu, L., He, D., Song, X., Liang, X., Zhao, Z. J.,Zhou, G. W. (2003): Crystal structure of human protein-tyrosine phosphatase SHP-1. *J Biol Chem*, **278: 8**, 6516-6520

Yang, R., Qu, C., Zhou, Y., Konkel, J. E., Shi, S., Liu, Y., Chen, C., Liu, S., Liu, D., Chen, Y., Zandi, E., Chen, W., Zhou, Y.,Shi, S. (2015): Hydrogen Sulfide Promotes Tet1- and Tet2-Mediated Foxp3 Demethylation to Drive Regulatory T Cell Differentiation and Maintain Immune Homeostasis. *Immunity*, **43: 2**, 251-263

Yang, W., Tabrizi, M., Berrada, K.,Yi, T. (1998): SHP-1 phosphatase C-terminus interacts with novel substrates p32/p30 during erythropoietin and interleukin-3 mitogenic responses. *Blood*, **91: 10**, 3746-3755

Yang, X. P., Ghoreschi, K., Steward-Tharp, S. M., Rodriguez-Canales, J., Zhu, J., Grainger, J. R., Hirahara, K., Sun, H. W., Wei, L., Vahedi, G., Kanno, Y., O'Shea, J. J.,Laurence, A. (2011): Opposing regulation of the locus encoding IL-17 through direct, reciprocal actions of STAT3 and STAT5. *Nat Immunol*, **12: 3**, 247-254

Yao, Z., Cui, Y., Watford, W. T., Bream, J. H., Yamaoka, K., Hissong, B. D., Li, D., Durum, S. K., Jiang, Q., Bhandoola, A., Hennighausen, L.,O'Shea, J. J. (2006): Stat5a/b are essential for normal lymphoid development and differentiation. *Proc Natl Acad Sci U S A*, **103: 4**, 1000-1005

Yasukawa, H., Misawa, H., Sakamoto, H., Masuhara, M., Sasaki, A., Wakioka, T., Ohtsuka, S., Imaizumi, T., Matsuda, T., Ihle, J. N.,Yoshimura, A. (1999): The JAK-binding protein JAB inhibits Janus tyrosine kinase activity through binding in the activation loop. *EMBO J*, **18: 5**, 1309-1320

Ye, D., Wolff, N., Li, L., Zhang, S.,Ilaria, R. L., Jr. (2006): STAT5 signaling is required for the efficient induction and maintenance of CML in mice. *Blood*, **107: 12**, 4917-4925

Ye, S. K., Agata, Y., Lee, H. C., Kurooka, H., Kitamura, T., Shimizu, A., Honjo, T.,Ikuta, K. (2001): The IL-7 receptor controls the accessibility of the TCRgamma locus by Stat5 and histone acetylation. *Immunity*, **15: 5**, 813-823

Yi, T., Mui, A. L., Krystal, G.,Ihle, J. N. (1993): Hematopoietic cell phosphatase associates with the interleukin-3 (IL-3) receptor beta chain and down-regulates IL-3-induced tyrosine phosphorylation and mitogenesis. *Mol Cell Biol*, **13: 12**, 7577-7586

Yoo, K. H., Oh, S., Kang, K., Hensel, T., Robinson, G. W.,Hennighausen, L. (2015): Loss of EZH2 results in precocious mammary gland development and activation of STAT5-dependent genes. *Nucleic Acids Res*, **43: 18**, 8774-8789

Yoshida, M., Kijima, M., Akita, M.,Beppu, T. (1990): Potent and specific inhibition of mammalian histone deacetylase both in vivo and in vitro by trichostatin A. *J Biol Chem*, **265: 28**, 17174-17179

Yoshimura, A., Ichihara, M., Kinjyo, I., Moriyama, M., Copeland, N. G., Gilbert, D. J., Jenkins, N. A., Hara, T.,Miyajima, A. (1996): Mouse oncostatin M: an immediate early gene induced by multiple cytokines through the JAK-STAT5 pathway. *EMBO J*, **15: 5**, 1055-1063

Yoshimura, A., Ohkubo, T., Kiguchi, T., Jenkins, N. A., Gilbert, D. J., Copeland, N. G., Hara, T.,Miyajima, A. (1995): A novel cytokine-inducible gene CIS encodes an SH2-containing protein that binds to tyrosine-phosphorylated interleukin 3 and erythropoietin receptors. *EMBO J*, **14: 12**, 2816-2826

Yuan, G. C., Liu, Y. J., Dion, M. F., Slack, M. D., Wu, L. F., Altschuler, S. J.,Rando, O. J. (2005): Genome-scale identification of nucleosome positions in S. cerevisiae. *Science*, **309: 5734**, 626-630

Zahn, J. M., Poosala, S., Owen, A. B., Ingram, D., Lustig, A., Carter, A., Weeraratna, A. T., Taub, D. D., Gorospe, M., Mazan-Mamczarz, K., Lakatta, E., Boheler, K. R., Xu, X., Mattson, M. P., Falco, G., Ko, M. S. H., Schlessinger, D., Firman, J., Kummerfeld, S. K., Wood, W., Longo, D. L., Zonderman, A. B., Kim, S. K.,Becker, K. G. (2005): AGEMAP: a gene expression database for aging in mice. *PLoS Genetics*, **preprint: 2007**,

Zaret, K. S.,Carroll, J. S. (2011): Pioneer transcription factors: establishing competence for gene expression. *Genes Dev*, **25: 21**, 2227-2241

Zeng, R., Aoki, Y., Yoshida, M., Arai, K.,Watanabe, S. (2002): Stat5B shuttles between cytoplasm and nucleus in a cytokine-dependent and -independent manner. *J Immunol*, **168: 9**, 4567-4575

Zeng, X., Willi, M., Shin, H. Y., Hennighausen, L.,Wang, C. (2016): Lineage-Specific and Non-specific Cytokine-Sensing Genes Respond Differentially to the Master Regulator STAT5. *Cell Rep*, **17: 12**, 3333-3346

Zhang, Q., Wang, H. Y., Liu, X.,Wasik, M. A. (2007): STAT5A is epigenetically silenced by the tyrosine kinase NPM1-ALK and acts as a tumor suppressor by reciprocally inhibiting NPM1-ALK expression. *Nat Med*, **13: 11**, 1341-1348

Zhang, X., Yang, L., Liu, X., Nie, Z., Wang, X., Pan, Y.,Luo, J. (2017): Research on the epigenetic regulation mechanism of the PTPN6 gene in advanced chronic myeloid leukaemia. *Br J Haematol*, **178: 5**, 728-738

Zhang, Y., Laz, E. V.,Waxman, D. J. (2012): Dynamic, sex-differential STAT5 and BCL6 binding to sex-biased, growth hormone-regulated genes in adult mouse liver. *Mol Cell Biol*, **32: 4**, 880-896

Zhu, B. M., Kang, K., Yu, J. H., Chen, W., Smith, H. E., Lee, D., Sun, H. W., Wei, L.,Hennighausen, L. (2012): Genome-wide analyses reveal the extent of opportunistic STAT5 binding that does not yield transcriptional activation of neighboring genes. *Nucleic Acids Res*, **40: 10**, 4461-4472

Zhu, M., John, S., Berg, M.,Leonard, W. J. (1999): Functional association of Nmi with Stat5 and Stat1 in IL-2- and IFNgamma-mediated signaling. *Cell*, **96: 1**, 121-130

Zupkovitz, G., Tischler, J., Posch, M., Sadzak, I., Ramsauer, K., Egger, G., Grausenburger, R., Schweifer, N., Chiocca, S., Decker, T.,Seiser, C. (2006): Negative and positive regulation of gene expression by mouse histone deacetylase 1. *Mol Cell Biol*, **26: 21**, 7913-7928